Title
Three-Dimensional Polypeptide Architectures Through Tandem Catalysis and Click Chemistry

Author
Rhodes, Allison Jane

Publication Date
2013

Peer reviewed|Thesis/dissertation

UNIVERSITY OF CALIFORNIA

Los Angeles

Three-Dimensional Polypeptide Architectures Through Tandem Catalysis and Click Chemistry

A dissertation submitted in partial satisfaction of the requirements for the degree Doctor of Philosophy in Chemistry

By

Allison Jane Rhodes

2013

ABSTRACT OF THE DISSERTATION

Three-Dimensional Polypeptide Architectures through Tandem Catalysis and Click Chemistry

By

Allison Rhodes

Doctor of Philosophy in Chemistry

University of California, Los Angeles, 2013

Professor Timothy J. Deming, Chair

Rapid renal clearance, liver accumulation, proteolytic degradation and non-specificity are challenges small molecule drugs, peptides, proteins and nucleic acid therapeutics encounter en route to their intended destination within the body. Nanocarriers (i.e. dendritic polymers, vesicles, and micelles) of approximately 100 nm in diameter, shuttle small molecule drugs to their desired location through passive (EPR effect) and active (ligand-mediated) targeting, maximizing therapeutic efficiency.

Polypeptide-based polymers are water-soluble, biocompatible, non-toxic and are therefore excellent candidates for nanocarriers.

Dendritic polymers, including dendrimers, cylindrical brushes, and star polymers, are the newest class of nanomedicine drug delivery vehicles. The synthesis and characterization of dendritic polymers is challenging, with tedious and costly procedures. Dendritic polymers possess peripheral pendent functional groups that can potentially be used in ligand-mediated drug delivery vehicles and bioimaging applications. More specifically, cylindrical brushes are dendritic polymers where a single linear polymer (primary chain) has polymer chains (secondary chains) grafted to it. Recently, research groups have shown that cylindrical brush polymers are capable of nanoparticle and supramolecular structure self-assembly.

The facile preparation of high-density brush copolypeptides by the “grafting from” approach will be discussed. This approach utilizes a novel, tandem catalytic methodology where alloc-α-aminoamide groups are installed within the side-chains of the α-amino-*N*-carboxyanhydride (NCA) monomer serving as masked initiators. These groups are inert during cobalt initiated NCA polymerization, and give alloc-α-aminoamide substituted polypeptide main-chains. The alloc-α-aminoamide groups are activated *in situ* using nickel to generate initiators for growth of side-chain brush segments. This method proves to be efficient, yielding well-defined, high-density brushes for applications in drug delivery and imaging.

Here, we also report a method for the synthesis of soluble, well-defined, azido functionalized polypeptides in a straightforward, 3-step synthesis. Homo and diblock azidopolypeptides were prepared with controlled segment lengths via living

polymerization using $Co(PMe_3)_4$ initiator. Through copper azide alkyne click chemistry (CuAAC) in organic solvent, azidopolypeptides were regioselectively and quantitatively modified with carboxylic acid (pH-responsive), amino acid and sugar functional groups.

Finally, the advances towards well-defined hyperbranched polypeptides through α-amino-acid-N-thiocarboxyanhydrides (NTAs) will be discussed. Within the past 10 years, controlled NCA (α-amino acid-*N*-carboxyanhydride) ring-opening polymerization (ROP) has emerged, expanding the application of copolypeptide polymers in various drug delivery and tissue engineering motifs. Modification of NCA monomers to the corresponding α-amino-acid-N-thiocarboxyanhydride (NTA) will diversify ROP reactions, leading to more complex polypeptides (such as hyperbranched polymers), in addition to the possibility of performing these polymerizations under ambient conditions, which would greatly expand their potential utility. The project focuses on the preparation of hyperbranched polypeptides with well-defined architectures and controlled branching density in a one-pot reaction. This will be accomplished by taking advantage of the different selectivities of $Co(PMe_3)_4$ and depeNi(COD) polymerization initiators, and by exploiting the reactivity difference between NCA and the more stable NTA monomers.

The dissertation of Allison Jane Rhodes is approved

Heather D. Maynard

Daniel Kamei

Timothy J. Deming, Committee Chair

University of California, Los Angeles

2013

This work is dedicated to my parents and sister as well as my best friend in the entire world, Steevens Alconcel. Your unwavering love and support is why I made it this far…

TABLE OF CONTENTS

LIST OF FIGURES AND TABLES

CHAPTER 1.

CHAPTER 2.

CHAPTER 3.

CHAPTER 4.

List of Abbreviations

AA	Amino Acid
Anl	L-azidonorleucine
Anv	L-azidonorvaline
Ala	L-Alanine
AcOH	Acetic Acid
ATRP	Atom Transfer Radical Polymerization
a.u.	Arbitrary Units
Bn	Benzyl
BOC	t-butyloxycarbonyl
CBZ	Carboxybenzyl
CD_3CN	Deuterated Acetonitrile
$CDCl_3$	Deuterated Chloroform
$CHCl_3$	Chloroform
CMC	Critical Micelle Concentration
CNBr	Cyanogen Bromide
CO	Carbon Monoxide
COD	Cyclooctadiene
COS	Carbonyl Sulfide
COSY	Correlation Spectroscopy
CRP	Controlled Radical Polymerization
CS_2	Carbon Disulfide
Cys	Cysteine

CuACC	Copper Assisted Click Chemistry
d	doublet (NMR)
d-DCM	Deuterated Methylene Chloride
Da	Dalton
DCC	*N,N*'-Dicyclohexylcarbodiimide
DCM	Methylene Chloride
DCU	Dicyclohexylurea
dd	doublet of doublets (NMR)
ddd	doublet of doublet of doublets (NMR)
DIPEA	*N,N'*-Diisopropylethylamine
dmpe	1,2-Bis(dimethylphosphino)ethane
DNA	Deoxyribose Nucleic Acid
dt	doublet of triplets (NMR)
DMAP	4-Dimethylaminopyridine
DMF	*N,N*'-Dimethylformamide
DMSO	Dimethyl Sulfoxide
DP	Degree of Polymerization
EDC	1-Ethyl-3-(3-dimethylaminopropyl)carbodiimide
EPR	Enhanced Permeability and Retention
E	Benzyl Glutamate
eq	Equivalents
ESI	Electrospray ionization
EtOAc	Ethyl Acetate

EtOH	Ethyl Alcohol
FT-IR	Fourier Transform Infrared Spectroscopy
Fmoc	Fluorenylmethyloxycarbonyl
GPC	Gel Permeation Chromatography
h	Hour
HCl	Hydrochloric acid
Hex	Hexanes
HPLC	High Performance Liquid Chromatography
HRMS-ESI	High Resolution Mass Spectrometry Electrospray Ionization
HMDS	Hexamethyldisilazane
i-BuOH	Isobutyl Alcohol
J	Coupling Constant (NMR)
K	N_{α}-carboxybenzyl-L-lysine
K^{AM} NCA	N_e-(alloc-L-methionyl)-L-lysine-N-carboxyanhydride
kDa	Kilodalton
Leu	L-Leucine
LiBr	Lithium Bromide
LS	Light Scattering
m	multiplet (NMR)
MALDI	Matrix-Assisted Laser Desorption/Ionization
MeOD	Deuterated Methanol
MeOH	Methanol
MHz	Megahertz (NMR)

mmol	Millimole
M_n	Number Average Molecular Weight
MS	Mass Spectrometry
M_w	Weight Average Molecular Weight
MWCO	Molecular Weight Cut Off
n-BuLi	n-Butyllithium
NCL	Native Chemical Ligation
NCA	α-amino-*N*-carboxyanhydrides
NCO	Isocyanate
NTA	α-amino-*N*-thiocarboxyanhydrides
NHS	*N*-Hydroxysuccinimide
NMR	Nuclear Magnetic Resonance
PB	Phosphate Buffer
PCR	Polymerase Chain Reaction
PDI	Polydispersity Index
PGA	Polyglutamic Acid
PEG	Poly(ethylene glycol)
Phe	L-Phenylalanine
ppm	parts per million (NMR)
PTFE	Polytetrafluoroethylene
q	quartet (NMR)
RAFT	Reverse Addition Fragmentation Chain Transfer
RNA	Ribose Nucleic Acid

ROMP	Ring Opening Metathesis Polymerization
ROP	Ring Opening Polymerization
s	singlet (NMR)
Sar	Sarcosine
SDS-PAGE	Sodium Dodecyl Sulfate Poly(acrylamide) Gel Electrophoresis
SEC	Size Exclusion Chromatography
$SOCl_2$	Thionyl Chloride
SPPS	Solid-Phase Peptide Synthesis
t	triplet (NMR)
TEA	Triethylamine
TEPA	Tetraethylene Pentamine
TEG	Tetra(ethylene glycol)
THF	Tetrahydrofuran
tt	triplet of triplets (NMR)
TLC	Thin Layer Chromatography
TFA	Trifluoroacetic acid
TOF	Time of Flight
Val	L-Valine

ACKNOWLEDGMENTS

I would like to take this opportunity to thank everyone who has made this journey worthwhile. I first would like to thank my advisor Tim Deming for his patience and guidance throughout graduate school. You allowed me to take full responsibility over my research projects, with all the triumphs and failures on no one else but me. Because of this I became proactive as well as independent in my research. Jarrod Hanson, although long gone from UCLA, trained and welcomed me into the lab from the very beginning. More than just a great laboratory manager, Jarrod, you are an awesome human being and a good friend. Thank you April Rodriguez and Ilya Yakovlev for always being entertaining and reminding me life requires balance and that the occasional distraction can be healthy.

I would like to thank my parents and sister who have always been supportive of my education especially during my first year of graduate school. You always reminded me of what was truly important in life when I was bogged down by department requirements and research. You guys are a nice escape on the weekends and I have thoroughly enjoyed the time we've spent together.

While at UCLA I had the opportunity to find balance in my personal life when meeting Steevens Alconcel who, after much persistence and time, became my best friend. Thank goodness first impressions aren't everything because I'd have overlooked someone who's now very important to me. I can't express my gratitude to you for being there for me everyday, which is not easy when research projects are moving slowly. I love you and look forward to our life together.

VITA

EDUCATION

March 2013 **Ph.D. in Chemistry**. University of California, Los Angeles

June 2007 **B.S. in Chemistry**. University of California, Riverside

June 2003 Maranatha High School, Pasadena, California

PUBLICATIONS

- "Soluble, Clickable Polypeptides using Readily Prepared Azido functionalized NCA Monomers." *In preparation*. **Rhodes, A.J**.; Deming, T.J.
- "Tandem Catalysis for the Preparation of Cylindrical Polypeptide Brushes." **Rhodes A.J**.; Deming T.J. *J. Am. Chem. Soc.* **2012**, *134*, 19463-19467.
- Bunnelle, E.; Smith, C.; Lee, S. K.; Singaram, S. W.; **Rhodes, A.J**.; Sarpong, R. *Tetrahedron* **2008**, *64*, 7008- 7014.
- Smith, C.; Bunnelle, E. M.; **Rhodes, A. J**.; Sarpong, R. *Organic Letters* **2007**, *9*, 1169-1171.

HONORS AND AWARDS

- Department of Chemistry and Biochemistry Dissertation Fellowship (UCLA, 2013)
- Academic Excellence Award in Chemistry (UC Riverside)
- UC LEADS Research Scholar (UC Riverside)
- Dean's List (UC Riverside)
- Chancellor's List (requires a minimum 3.9 GPA, UC Riverside)

PRESENTATIONS

March 2012 ACS National Meeting, PMSE Division, San Diego, CA. “Tandem Catalysis for the Preparation of Cylindrical Polypeptide Brushes”

December 2011 California Nanosystems Institute, UCLA. *CNSI 10-Year Review*. “Tandem Catalysis for the Preparation of Cylindrical Polypeptide Brushes”

March 2010 ACS National Meeting, PMSE Division. San Francisco, CA. “α-amino Acid-*N*-thiocarboxyanhydride (NTA) Polymerization Utilizing $Co(PMe_3)_4$ and depeNi(COD) Initiators”

TEACHING EXPERIENCE

08/11-06/12 **Teaching Assistant Consultant, UCLA.**

- Improved undergraduate learning in the chemistry department by teaching new graduate students how to teach
- Organized graduate student orientation in the chemistry department
- Planned and led weekly 1 hour seminars with a multidisciplinary team consisting of graduate students, faculty and lecturers

09/07-06/10 **Laboratory Teaching Assistant, UCLA.**

- Directed 40 undergraduate organic chemistry students in weekly laboratory experiments
- Defined experimental goals and facilitated the assembly of laboratory apparatus’

- Encouraged critical thinking when students encountered experimental problems

Discussion Teaching Assistant, UCLA.

- Facilitated 3 weekly (1 hour) discussions with undergraduate students
- Clarified lecture material, graded exams and prepared carefully selected problems sets

Graduate Level Discussion Teaching Assistant, UCLA.

- Instructed graduate level biomedical engineers discussion sections for 1 academic quarter
- Clarified lecture material during a one-hour weekly discussion with 40-50 students
- Created easy-to-follow answer keys for graded problem sets

ASSOCIATION MEMBERSHIPS

09/11-present	Member of Organization for Cultural Diversity in Chemistry (OCDC) sponsored by Procter & Gamble
06/09-present	American Chemical Society
06/06-06/07	Member of Sigma Xi Research Honors Society
09/03-09/04	Member of Alpha Lambda Delta Honors Society

OUTREACH/ACTIVITIES

09/11-present	Organization for Cultural Diversity in Chemistry (OCDC) at UCLA (sponsored by Procter & Gamble). Invited outstanding scientists (academia/industry) from under-represented groups in science and helped facilitate the launch of an undergraduate mentorship program.
06/11	Boy Scout Chemistry Merit Badge. Demonstration: oxidation of nail in copper sulfate solution at the Boy Scout Expo through Southern California Section of the American Chemical Society (SCSACS).
05/11	Captain of Team Chemistry, Bruin 5K Walk/Run benefiting Mattel Childrens' Hospital at UCLA and Child Life/Child Development Program. Raised over $600 as captain of a team of six chemistry graduate students from the Department of Chemistry and Biochemistry.
05/10	17th Annual EIF Revlon 5K Walk/Run benefitting Jonsson Comprehensive Cancer Center at UCLA. Member of the "UCLA Fights Women's Cancers" Team.

Chapter 1

Introduction to Polypeptides

1.1 Introduction

Proteins, polypeptides, and DNA are biopolymers with specialized functions derived from their precisely controlled biosynthesis.[1] Evolutionary processes have produced enzymes and proteins with controlled sequence and composition that are renowned for their unique properties such as: strength/toughness and longevity. For example, spider silk is tougher than any synthetic fiber having breakage energy per unit weight greater than high tensile steel.[2,3] Mammalian elastin, an extracellular matrix protein in the cartiovascular system, is unmatched by any synthetic protein for longevity and durability.[4] Due to the diversity of polypeptides (both in application and structural features) various methods are available for their preparation.

Polypeptides are conventionally prepared by stepwise solid-phase synthesis (SPPS),[5,6] recombinant DNA techniques,[7] native chemical ligation (NCL),[8] and ring-opening polymerization of α-amino-*N*-carboxyanhydrides (NCAs).[9] Peptides, or short segments of amino acids, are used as therapeutic agents (such as oxytocin to induce labor and calcitonin to treat hypercalcaemia), food additives (like aspartame) and nutritional supplements. Peptides can act as chemical messengers, inhibiting or stimulating multiple processes within the body.[1]

1.2 Solid-Phase Peptide Synthesis (SPPS)

In 1963 R. Merrifield proposed a new process, Solid-Phase Peptide Synthesis (SPPS), for the preparation of short peptides with potential for high molecular weight polypeptide preparation.[5,10] Merrifield covalently attached partially chlorinated chloromethyl polystyrene (200-400 mesh beads) to the first N-protected amino acid

group through a benzyl ester linkage.[5,10] The protecting group was removed and the free amine reacted with the next N-protected amino acid group, and the process is repeated.[11] The polystyrene resin is then removed and the peptide isolated. This method allows for complete control over composition of the peptide, ease of purification at each step and later automation using a peptide synthesizer.[12] Another advantage of SPPS is the incorporation of non-natural amino acids, which allows for new material syntheses.[13,14] 9-fluorenylmethyloxycarbonyl (Fmoc) group is the amino protecting group of choice due to ease of removal with piperidine and safe protocol but t-butyloxycarbonyl (BOC) and carboxybenzylcarbony (CBZ) groups are also used.[15]

During the late 1960s to early 1970s, several naturally occurring proteins were synthesized using SPPS, including: ferredoxin (55 amino acid (AA) residues),[16] ribonuclease A (124 AA residues),[6] cytochrome C (104 AA residues),[17] and lysozyme (129 AA residues).[18] High purity is a criterion for synthetic proteins due to applications in biomaterials. Scientists soon recognized that this criterion was not met using SPPS and the number of synthetic protein publications diminished in the following years.

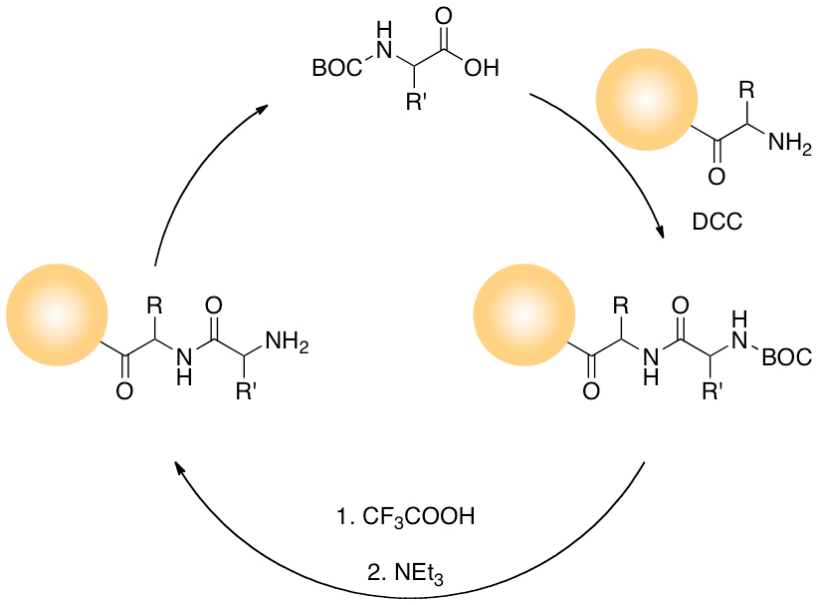

Figure 1-1. Merrifield solid-phase peptide synthesis (SPPS).

Aside from purity issues, SPPS suffers from other serious drawbacks. First, large, complex polypeptides/proteins cannot be prepared as Merrifield had originally envisaged, due to low coupling efficiency as the length of the peptide increases.[19] Another disadvantage is the use of excess amino acid (usually 2-10 equivalents) to ensure maximum coupling efficiency. Since high reaction efficiency cannot be obtained, significant quantities of resin-bound byproducts accumulate. Solubility issues of protected peptide segments, purification and complete deprotection of longer peptides has proven to be quite challenging. Therefore, SPPS is typically used for peptides that are no greater than 50 amino acid residues to ensure purity. Polypeptides prepared through SPPS are traditionally purified and homogeneity evaluated by HPLC techniques.

1.3 Recombinant DNA Expression of Proteins

Over the past 30 years proteins have been expressed through recombinant DNA methods in genetically engineered cells. In 1980 Doel and coworkers synthesized aspartyl-phenylalanie (Asp-Ph), an artificial sweetener, using recombinant DNA techniques.[7] They created a protein with < 150 amino acid repeat units of Asp-Ph that was enzymatically degraded forming the desired dipeptide. Proteins from the recombinant DNA technique have also been used for the synthesis of biomaterials such as: silk, collagen, and elastin.[20]

In recombinant techniques, first a protein target is identified and translated into the corresponding genetic code. The target oligonucleotide is synthesized by Polymerase Chain Reaction (PCR) or chemical synthesis.[21] Bacteria serve as 'protein factories' where plasmid DNA is removed, lysed and the synthetic gene inserted. The non-natural plasmid vector is reintroduced into the cytoplasm of the bacteria. This gene produces large quantities of the desired protein, which is then isolated (Figure 1-2). Typically bacteria (such as Escherichia coli (*E. coli*) or Bacillus subtilis) are utilized due to convenience and low cost.

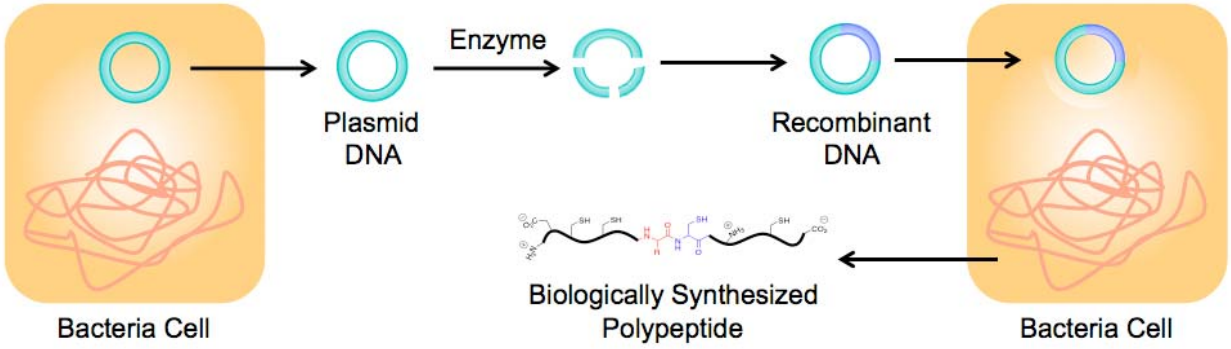

Figure 1-2. Recombinant DNA technique for protein synthesis

The advantages of recombinant DNA is the proteins produced are precise; with control over primary structure, composition and chain length.[20] However, multidomain proteins are much more challenging to express than proteins smaller than 30 kDa. In addition, incompatibility of the protein and bacteria leads to toxicity, lowing protein production.

1.4 Native Chemical Ligation (NCL)

With the inherent limitations of SPPS and recombinant DNA methods, chemical ligation is a valid alternative. Chemical ligation (the chemoselective reaction of unprotected amino acids in solution) incorporates unique functional groups not conventionally found in amino acids. These groups exclusively react with one another minimizing potential byproducts.[22,23] In 1991, the idea of chemical ligation was introduced with such chemistries as: thioester, oxime, thioether, directed disulfide and thiazolidine-forming covalent linkages.[19] Addition of 6 M guanidine HCl solubilized the reactive, unprotected amino acids allowing higher reaction concentration of amino acid, further accelerating the rate of reaction. The introduction of a non-native linker, within the proteins, was tolerated in folded proteins. However to fully mimic natural proteins and enzymes, native linkers are more desirable.

In 1994, Dawson and coworkers introduced conjugation of two peptide segments through an amide linkage at neutral pH in aqueous solution.[8,24] Two peptide segments, one with a thiol group and the other with a thioester bond, undergo a thio- exchange.

The new thioester bond linking the two segments spontaneously rearranges forming the more stable amide bond (Figure 1-3).

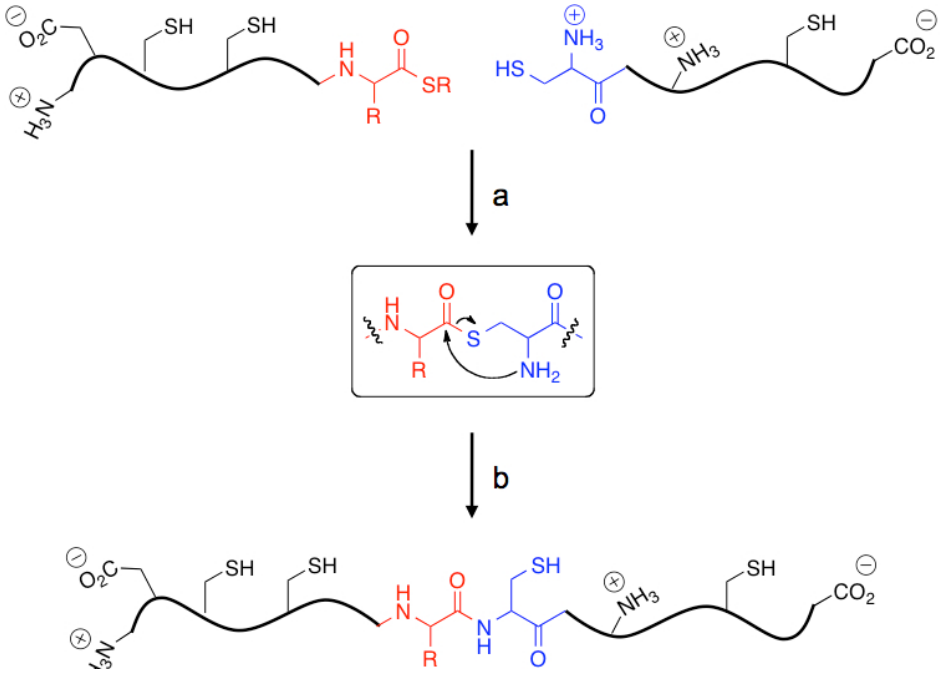

Figure 1-3. Native chemical ligation. a) water, pH = 7, b) rearrangement of thioester intermediate amide linked product.

1.5 Ring-Opening Polymerization (ROP) of NCAs

1.5.1 Introduction

The most facile route to prepare block copolypeptides is through the polymerization of α-amino-*N*-carboxyanhydrides (NCAs). Synthetic polypeptides, due to their similarities to natural proteins, are widely applicable in drug delivery (i.e. vesicles,[25] micelles, and emulsions[26]) and tissue engineering (i.e. hydrogels[27-29]). Synthetic polypeptides are appealing in these applications as they possess complex structures

and functionalities that are hard to obtain in conventional polymers (i.e. secondary structure dictated by hydrogen bonding).[30] The rapid development of copolypeptides for biotechnology is due, in part, to the discovery of efficient initiators for synthesis of these materials.

In 1906 Hermann Leuchs published a paper on the synthesis and characteristic properties of α-amino-N-carboxyanhydrides (NCAs).[9] Initially called Leuchs anhydrides, NCAs were first discovered when Leuchs attempted the distillation of *N*-alkoxycarbonyl amino acid chlorides. In 1921, Curtius and Wessely reacted NCAs with amines and alcohols, determining the product was in fact polymeric in nature.[31-33] Curtius and Wessely's work marked the beginning of organoinitiators for the polymerization of NCAs in the literature.[9,34,35]

1.5.2 Organoinitiators

Organoinitiators are the most common initiators for the ROP of NCAs in the literature. Primary and secondary amines such as hexylamine and diethylamine are the most widely used initiators but primary alcohols and thiols have also been explored. Some advantages of organoinitiators are facile distillation, commercial availability, and ease of reaction setup (no glovebox needed). Organoinitiators suffer from serious drawbacks such as prolonged reaction times (days), require elevated temperatures and incomplete reactions at high monomer-to-initiator ratios. Another challenge with organoinitiators is the polypeptides produced are not monodisperse, having a wide molecular weight distribution or polydispersity index (PDI). This is due to two possible mechanisms of polypeptide formation (shown in Figure 1-4).

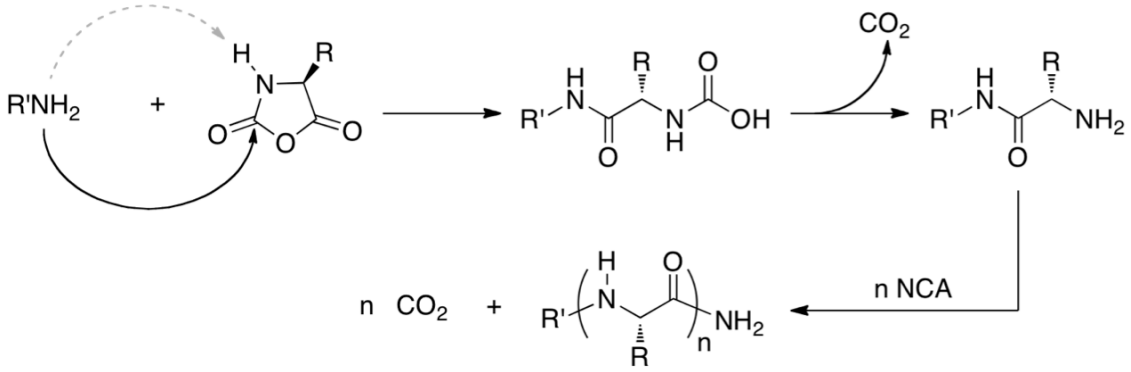

Figure 1-4. Ring-opening polymerization using primary amine initiator

Primary amines react as bases and/or nucleophiles depending on the intrinsic properties of its reaction partner. When a primary amine reacts with a single equivalent of NCA it removes the amino proton (acting as a base) or attacks the electrophilic carbonyl of the NCA (acting as a nucleophile). This produces two different reactive species that then attack the next NCA unit. Often not all monomer is consumed when amines and NCAs react at high monomer-to-initiator ratios due to chain terminating steps. Research in this field dwindled by the mid 1980s since NCA polymerization was uncontrollable using these traditional initiators.

1.5.3 Transition-metal mediated ROP: Co and Ni

In 1997 the Deming lab developed a new methodology for polypeptide preparation, renewing interest in the synthetic polypeptide field.[36] Since then, our group has developed additional zerovalent cobalt and other nickel initiators to control the polymerization of NCAs. For efficient polymerization to occur the transition metal initiator must (I) be a low-valent metal capable of undergoing a 2-electron oxidative addition (II) contain strongly electron-donating ligands and (III) be stable towards the functionalities present in polypeptides (i.e. amides, esters, thioesters, etc.).[37] In 1999,

our group investigated highly reactive zerovalent cobalt initiators and found that $Co(PMe_3)_4$ initiates NCA polymerization faster than bipyNi(COD).[38] Platinum and palladium initiators were also investigated but were found to react at the N-H bond of the NCA rather than regioselective oxidative addition between C-O_5.[39]

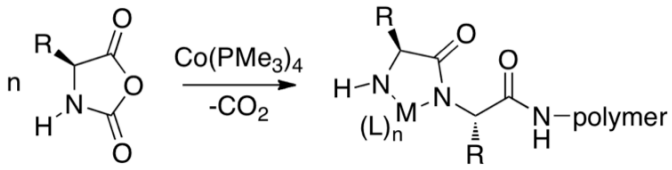

Figure 1-5. Zerovalent cobalt initiator for NCA polymerization

Cobalt and nickel initiators are powerful tools for the polymerization of NCAs yielding polymers with low polydispersity indices and controlled molecular weights.[36,38,40] The controlled mechanism leads to living polymerization where well-defined (narrow chain length distributions) homopolymers and block copolypeptides are prepared.

The mechanism of transition metal initiated polymerization is shown below (Figure 1-6). First, oxidative addition occurs between the C_5 and oxygen of an NCA. Next, a loss of carbon monoxide occurs forming a five-membered alkyl carbamate metellacycle.[38,41] A second monomer unit then adds to this species followed by a loss of carbon dioxide, forming an 8-membered metallocycle. This metallocycle again releases carbon dioxide resulting in an alkyl-amido species. A third NCA unit is incorporated and finally, a proton migration leads to the amido-amidate propagating species. NCA polymerization initiated by transition metal complexes is an example of living polymerization, where there are no significant chain termination or chain transfer steps (where chain lengths are dependent on the monomer-to-initiator ratio). This is advantageous as it allows preparation of well-defined (narrow chain length distribution)

and block copolypeptides.[37] NCA polymerization utilizing zerovalent cobalt and nickel initiators is widely applicable in the preparation of complex synthetic polypeptides (micelles, hydrogels and vesicles).

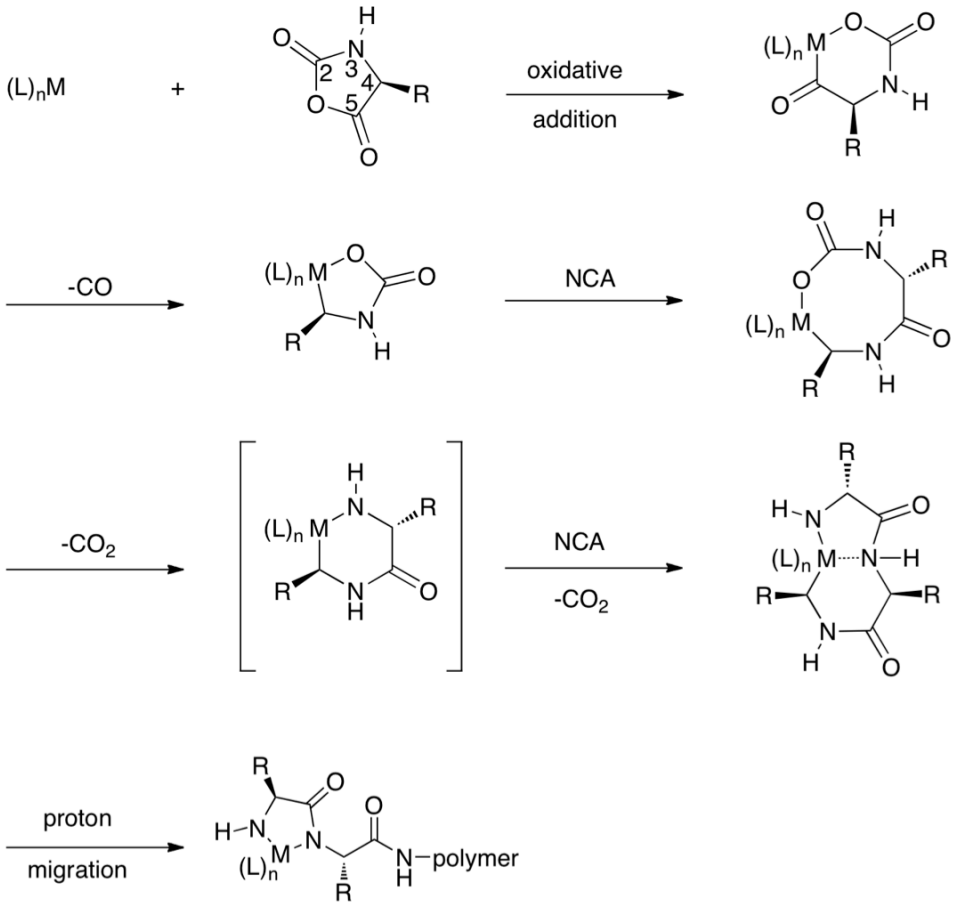

Figure 1-6. Zerovalent cobalt mechanism

Nickel initiators (i.e. dmpeNi(COD) possess additional reactivity as compared to Co initiators, reacting with allyloxycarbonyl (alloc) protected amino groups as well as NCAs.[42] By reacting these complexes with an alloc-protected amino acid, the amino acid is incorporated as the polymer end-group (i.e. one amino acid group per chain). First $Ni(COD)_2$ undergoes a ligand exchange followed by oxidative addition forming an eta 3 (η^3) complex (Figure 1-7). A 5-membered amidoamidate metallocycle is formed and propene is lost along with 2 equivalents of ligand (COD). The metallocycle reacts

further with NCA units with the loss of CO_2 forming the polypeptide. This nickel chemistry is later exploited to prepare diverse end-functionalized polypeptides and brush copolypeptides (Chapter 2).

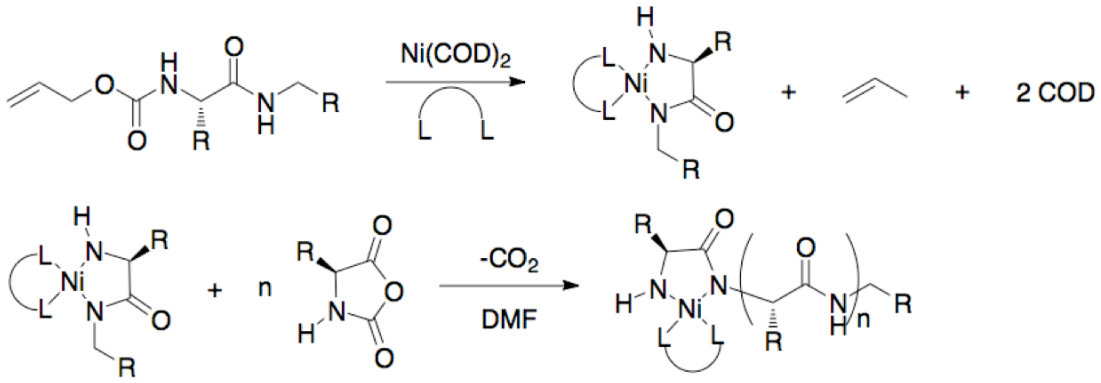

Figure 1-7. Zerovalent nickel initiation of NCA polymerization

1.6 Complex Polypeptide Architectures for Drug Delivery

Rapid renal clearance, liver accumulation, proteolytic degradation, and non-specificity are challenges small molecule drugs, peptides, proteins and nucleic acid therapeutics encounter en route to their intended destination within the body.[43,44] To circumvent these challenges polymer-based therapeutic carriers are of increasing interest. Small molecule drugs encapsulated in nanocarriers (i.e. macromolecules) exhibit longer circulation times requiring lower concentrations of the drug for the same therapeutic affect as compared to small molecule version of the drug. Proteolytic degradation can be minimized by the introduction of stealth functionalities such as polyethylene glycol (i.e. PEG). Polypeptide-based polymers are water-soluble, biocompatible and non-toxic and are therefore excellent candidates for nanocarriers.

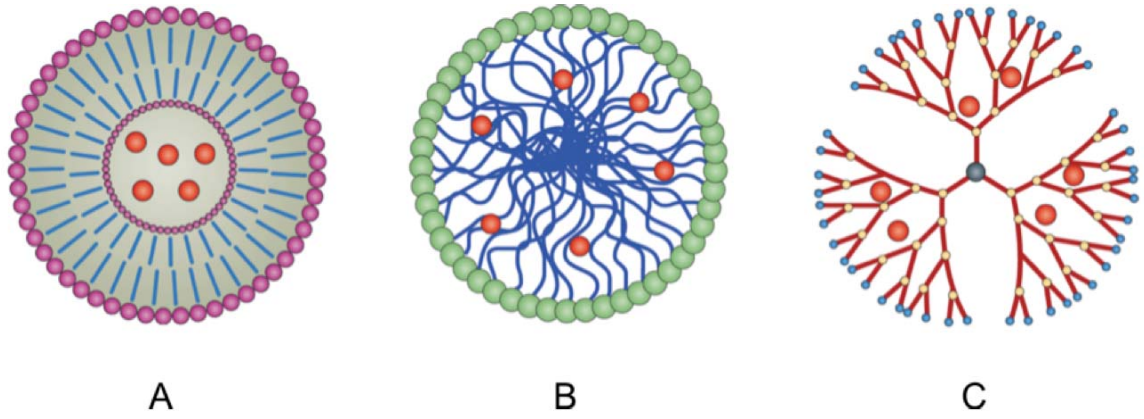

Figure 1-8. Nanomedicine drug delivery systems. a) vesicles/polymersomes, b) micelles and c) dendritic polymers.[45]

Vesicles, micelles, and dendric polymers are just a few nanomedicine drug delivery systems in the literature (Figure 1-8). Vesicles are of particular interest due to their higher stability as compared to natural liposomes. Composed of discrete hydrophobic and hydrophilic segments, vesicles traditionally carry hydrophilic cargoes at their core while the hydrophobic bilayer is potentially available for hydrophobic drugs (this can compromise the integrity/stability of the vesicle structure). Depending on chemical composition, the vesicles can be pH-, thermo- or chemo-responsive, releasing cargoes at their intended destination.

Micelles are comprised of a hydrophobic and a hydrophilic polymer segment shuttling hydrophobic drugs. Micelle stability is highly dependent on polymer composition and lengths of each segment. One disadvantage to micelle drug carriers is the disassembly of the structure at the critical micelle concentration (CMC) (i.e. low concentrations). As a candidate for drug delivery, micelles can release the hydrophobic drug prior to reaching its destination.

Dendritic polymers, including dendrimers, cylindrical brushes, and star polymers, are the newest class of nanomedicine drug delivery vehicles.[46,47] The synthesis and characterization of dendritic polymers is very challenging, with tedious and costly procedures. Dendritic polymers possess peripheral pendent functional groups that can potentially be used in ligand-mediated drug delivery vehicles and bioimaging applications.[48,49] Dendrimers are by far the most popular dendritic polymers due to uniformity and symmetry.

The biological rationale for the development of anti-cancer polymeric therapeutics stems from the non-specificity of small molecule drugs and inherent leaky vasculature of solid tumor tissue.[43,50] The unique pathophysiological tumor vasculature results from rapidly growing cancer cells requiring oxygen, nutrients and the necessary transport system for these nutrients (i.e. blood vessels). Gap junctions occur between endothelial cells lining the blood vessels allowing for diffusion of large particles (< 100 nm) into tumor tissue.[51] This defective vasculature architecture coupled with poor lymphatic drainage allows for passive tumor targeting through the Enhanced Permeability and Retention Effect (EPR).[52] In theory, nanocarriers (i.e. dendritric polymers, vesicles, and micelles) of approximately 100 nm in diameter can shuttle small molecule drugs to their desired tumor tissue through passive targeting.[53] Macromolecules can freely enter tumor tissue while tight endothelial cell junctions prohibit these drug delivery vehicles from entering healthy tissue (Figure 1-9).

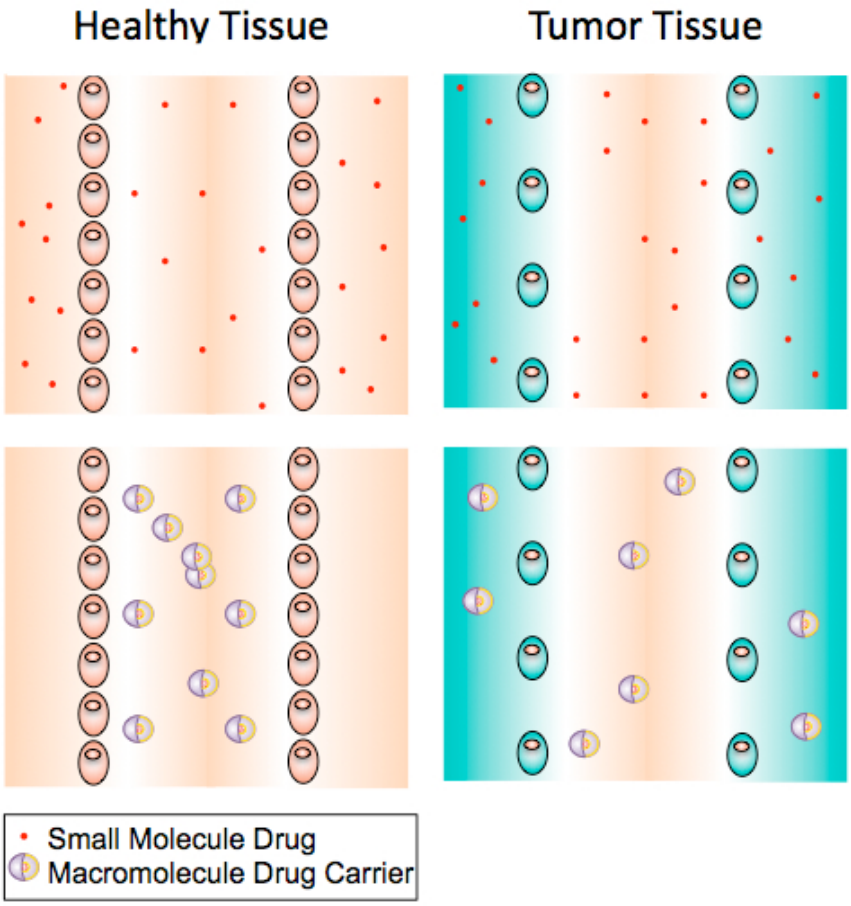

Figure 1-9. Enhanced permeability and retention effect

The attachment of targeting ligands, or small molecule groups (such as folate, DNA, RNA and sugars), can further enhance tumor active targeting through polymer-cell surface interactions. Tumor cells exhibit different cell surface receptor composition than healthy tissue. Folate receptors, found in abundance on tumor cell surfaces, exhibit high binding affinity for vitamin folate and polymer-folate conjugates. After binding to the receptor, the polymer-folate conjugate enters the cell through receptor-mediated endocytosis.

1.7 Cylindrical Brushes

1.7.1 Introduction

Recent progress in controlled radical polymerization (CRP) techniques (namely ATRP and RAFT) have allowed for the preparation of polymers with complex architectures. Similarly, the development of efficient zerovalent nickel and cobalt initiators for the polymerization of NCAs has enabled rapid growth in the development of polypeptide materials for drug delivery.[37,40] Controlled NCA polymerization allows access to polypeptide materials (i.e. vesicles,[25,54,55] hydrogels,[56-58] emulsions,[26,59] and glycopolypeptides[60]) with precisely controlled molecular weights imparting unique functionalities and properties. However, the preparation of highly branched polypeptides (i.e. dendrimers, hyperbranched and cylindrical brushes) is more challenging,[49,61,62] due to increased branching points and level of complexity.

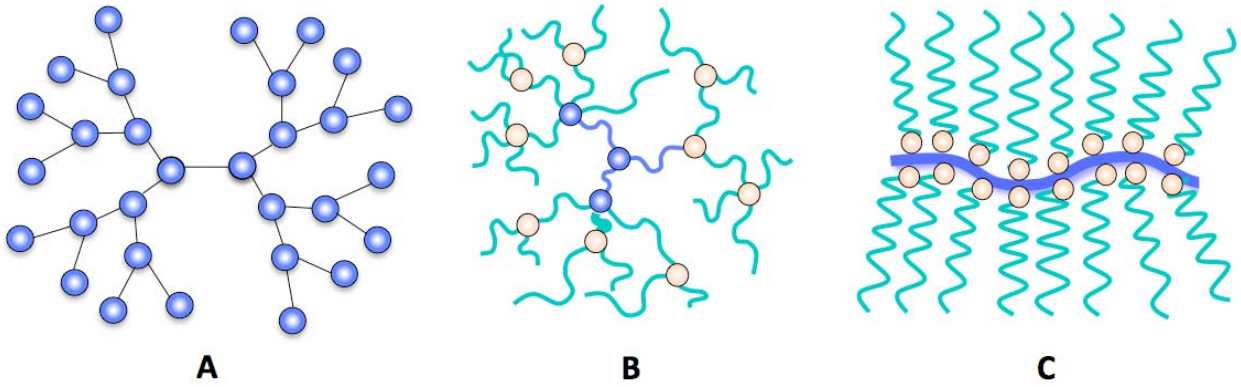

Figure 1-10. Types of branched polymers. a) dendrimer, b) hyperbranched, c) cylindrical brush or bottle brush.

Viable drug delivery vehicle candidates must be non-immunogenic, non-toxic, biocompatible, and must be uniform in size and composition. As the newest class of

potential drug delivery vehicles, branched polymers (dendrimers, hyperbranched and cylindrical brushes) are difficult to prepare with regular size, and composition is difficult to control (Figure 1-10).[46,47] Dendrimers are polymers with uniform branching points and complete control over composition is achieved. Dendrimer preparation is long and tedious with a series of protection and deprotection steps. Hyperbranched materials possess irregular branching points and there are currently no methods available for their controlled synthesis.

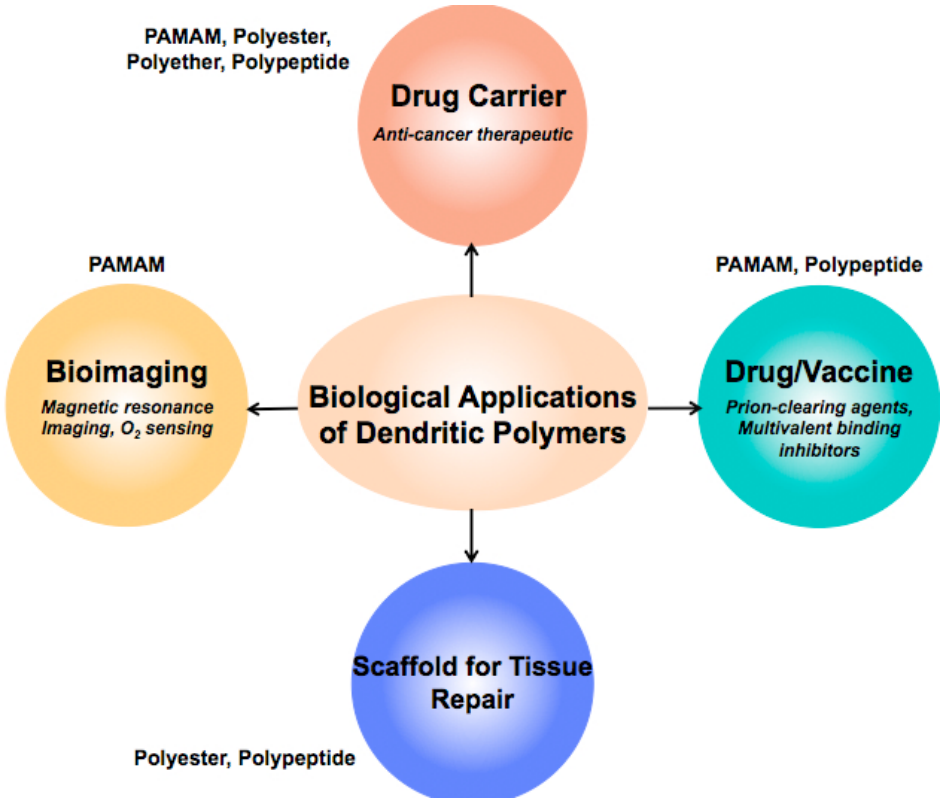

Figure 1-11. Biomaterial applications of dendritic Polymers

More specifically, cylindrical brushes are branched polymers where a single linear polymer (primary chain) has polymer chains (secondary chains) grafted to it (Figure 1-13). Recently, research groups have shown that cylindrical brush polymers are capable of self-assembling into nanoparticles and supramolecular structures.[63,64]

Dentritic polypeptides are attractive candidates for antigen presentation, MRI contrast agent platforms and gene carriers.[65-67]

1.7.2 Natural Cylindrical Brushes

The efficiency of biosynthetic processes within the body surpasses the synthetic tools available for the chemical synthesis of macromolecules. The complexity of biological macromolecular structures, such as multidomain proteins, directly relates to their biological function. Proteoglycans have a cylindrical brush topology with the protein serving as the primary chain and repeats of glycoaminoglycans (GAGs) as the secondary chains (Figure 1-13). Proteoglycans are found in several locations within the human body but the most heavily studied are those found on cell surfaces and within articular cartilage of joints.

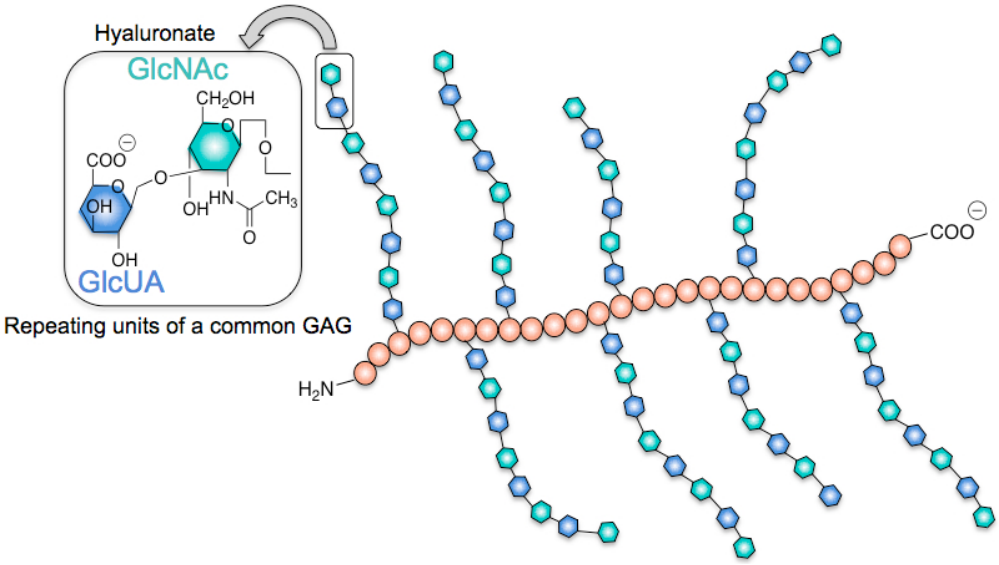

Figure 1-12. Proteoglycan structure

Serving as extracellular ligands, herparan sulfate (HS) proteoglycans mediate recognition events on the cell surface such as cell proliferation, differentiation and migration.[68] The evolutionary motivation behind HS proteoglycans is their ability to entangle a wide variety of biomolecules, mitigating the need for diverse binding proteins.[69] The lack of HS proteogycans on some cell surfaces can be indicative of disease.

Proteogylcans dictate physical properties within the articular cartilage of joints. The secondary chains of proteoglycans provide a high drag force within the fluid, resulting in high osmotic pressure.[70] Due to the high density of the negative charges within the proteoglycan secondary chains, osmotic pressure increases/decreases with proximity of secondary chains, effecting the total swelling pressure.[70] As a result, proteogylcans directly affect skeletal growth and development of arthritis within joints.

1.7.3 Synthesis of Cylindrical Brushes

There are currently three strategies available to prepare cylindrical “bottle” brushes: ‘grafting to’ (or onto), ‘grafting through’, and ‘grafting from’ (Figure 1-13). The common goal of all strategies is to prepare well-defined, densely grafted cylindrical brushes (Figure 1-12). However, each method has its unique advantages and challenges no matter the type of polymerization technique utilized (i.e. ring-opening polymerization (ROP), ring opening metathesis polymerization (ROMP), radical, cationic or anionic polymerization).

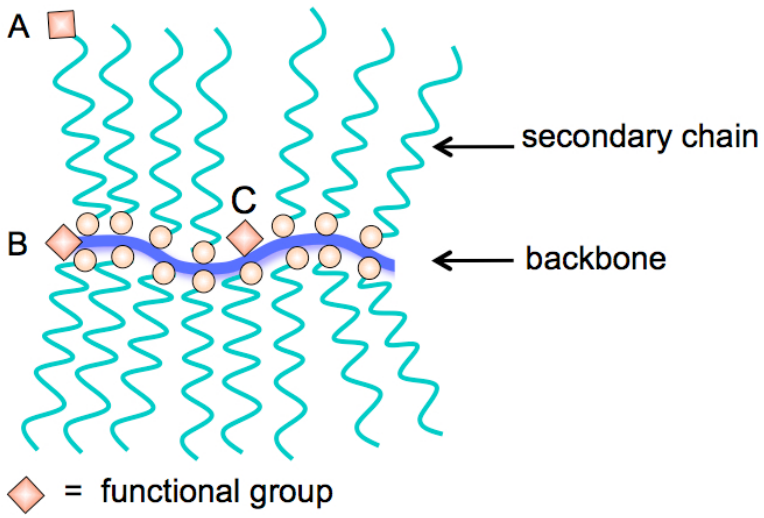

Figure 1-13. Features of cylindrical brushes. Functional groups attached to a) secondary chain end, b) primary chain end and c) primary chain buried within the secondary chains

The 'grafting to' method is the reaction of two polymers (primary chain and secondary chains), usually through click chemistry, forming brushes. The advantage of this strategy is facile characterization of cylindrical brushes since both the primary chain and secondary chain lengths are known prior to brush formation, making it the preferred route to cylindrical brushes. However, low grafting efficiency of secondary chains to the primary chain is problematic as well as separation of un-reacted secondary chains from the brushes. In 2009 Hammond and coworkers prepared cylindrical brushes through grafting azido functionalized PEG (MW = 1000, 2000, and 5000 g/mol) onto a poly(γ-propargyl-glutamate) backbone.[71] First, γ-propargyl-L-glutamate NCA was polymerized using a heptyl amine initiator. Azido functionalized PEG was then grafted to the primary chain through "click chemistry" with efficiencies reported as high as 98.9% (as determined by ^{1}H NMR).

The 'grafting through' approach uses polymeric secondary chains (macromonomer) and upon addition of an initiator, the secondary chains react forming

the primary chain. One advantage to this route is secondary chain length is known prior to brush preparation. However, this route results in low degree of polymerization (DP) of primary chain due to steric repulsion of the secondary chains that results in slow kinetics and low conversion. In 1997, Sheiko and coworkers reported the synthesis of a poly(vinylpyridine) based cylindrical brush prepared by the 'grafting through' method. The methacryloyl-functionalized poly(vinylpyridine) secondary chains were prepared by free radical polymerization of 2-vinyl pyridine monomer. This macromonomer was reacted with AIBN to grow the primary chains forming cylindrical brushes.

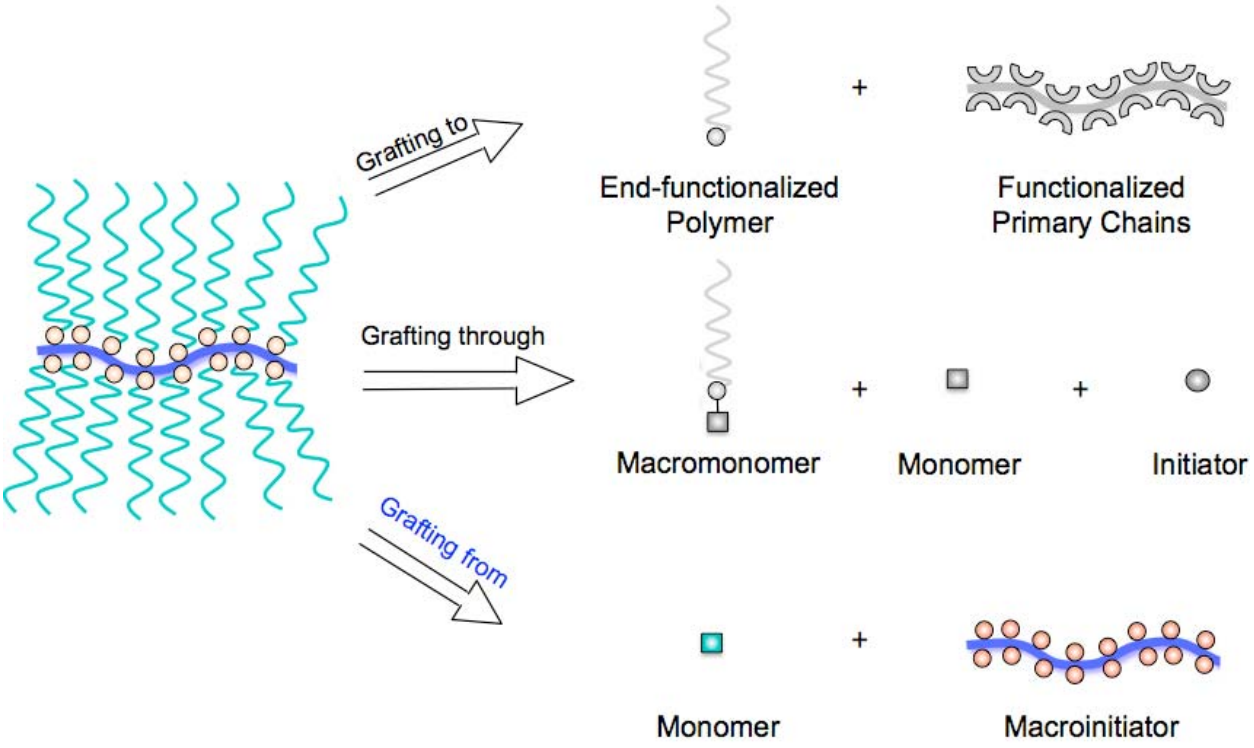

Figure 1.14. Cylindrical brush synthetic strategies

Lastly, 'grafting from' involves a polymer backbone (macro-initiator) where secondary chains grow from the backbone by the addition of a monomer. The gradual growth of secondary chains minimizes steric repulsion resulting in brushes with longer

primary chains and secondary chains (than brushes obtained by ‘grafting through’ or ‘grafting to’). However, control of grafting density and secondary chain length is dependent on the initiator efficiency. Therefore, a robust initiation process is required to control both secondary chain length and grafting density. Characterization of these materials is not trivial; no single technique can be used to determine secondary chain length and polydispersity *within* the cylindrical brushes. In 2009, Cheng et. al.[63] reported a one-pot synthesis of hybrid polypeptide brushes by ring-opening metathesis polymerization (ROMP) of norbornene monomer each containing an *N*-trimethylsilyl group (*N*-TMS).[72] After preparation of the polynorbornene (PN) backbone using Grubb’s catalyst, γ-benzyl-L-glutamate NCA was then added forming PN-*g*-PBLG brushes. More recently, Cheng and coworkers reported that these brushes are capable of forming ‘rope-like’ supramolecular structures in water at pH 7, 4 ^{o}C, and also form 30 μM tubular structures after 7 days.[64]

Chapter 2

Tandem Catalysis for Preparation of Cylindrical Polypeptides

2.1 Introduction

Branched chain copolypeptides have intrigued scientists for many years. Sela performed pioneering studies on what he termed “multi-chain polypeptides” that were evaluated for their immunostimulating properties.[62,73-77] More recently, hyperbranched and dendritic polypeptides with their abundance of functional groups, and three-dimensional globule-like presentation of functionality, have been found valuable for multiple presentation of antigens in vaccines, as imaging agents, and for drug and oligonucleotide delivery.[67] Although the properties of branched polypeptides show great promise, controlled synthesis of these materials remains challenging. Stepwise peptide dendrimer synthesis provides excellent control over polypeptide branching, but is a tedious process that can be difficult to scale. An alternative is the preparation of hyperbranched or dendrigraft polypeptides via polymerization of α-amino acid-N-carboxyanhydrides (NCAs).[78-82] These materials have been prepared via a stepwise sequence of polymerization, side-chain deprotection, and polymerization; as well as by simultaneous polymerization and deprotection.[78-82] Although these methods are more efficient and scalable compared to dendrimer preparation, they tend to give limited control over branch architecture, or provide only low branch density in polymer brushes.[78-82] High density cylindrical copolypeptide brushes are desirable synthetic targets since the potential to control their three-dimensional shape makes them intriguing as components in block copolymers, which can then be used for preparation of self-assembled materials with complex morphologies.[83-85] Although there have been many successes in controlled synthesis of cylindrical hybrid-polypeptide copolymer brushes,[63,86-89] the preparation of entirely polypeptide based cylindrical copolymer

brushes has not been achieved. Here, we report a new method for synthesis of cylindrical copolypeptide brushes via NCA polymerization utilizing a tandem catalysis approach that allows preparation of brushes with controlled segment lengths in a straightforward, one-pot procedure that requires no intermediate isolation or purification steps.

The synthesis of branched polypeptides via NCA polymerization is challenging since protecting groups typically need to be removed from side-chain functionalities (e.g. primary amines of lysine) to generate initiators for branch points.[78-82] Although this can be done *in situ* via hydrogenation to generate hyperbranched polypeptides,[82] this approach is difficult to control and more regular branched structures are typically only obtained when polymers with deprotected side-chains are isolated and purified before resuming polymerization.[78-81] To avoid this need for intermediate purification steps and to obtain high density brush copolypeptides, we pursued a "grafting from" approach where alloc-α-aminoamide groups (alloc = allyloxycarbonyl) were installed onto the side-chains of NCAs to serve as masked initiators. These groups were envisioned to be inert during NCA polymerization to give alloc-α-aminoamide substituted polypeptide main-chains, but then would be activated *in situ* to generate NCA polymerization initiators for side-chain brush growth (Figure 2-1). We have shown previously that alloc-α-aminoamides react quantitatively with $L_2Ni(COD)$ (L = donor ligand, COD = cyclooctadiene) in DMF to generate amido-amidate nickelacycles, which are efficient initiators for living polymerization of NCAs.[90] We have also found (*vide infra*) that this reaction is selective for Ni(0), since Co(0) complexes (i.e. $(PMe_3)_4Co$) do not react with alloc-α-aminoamides under similar conditions. Since $(PMe_3)_4Co$ reacts directly with

NCAs to generate amido-amidate cobaltacycles, which also initiate the living polymerization of NCAs,[38] use of stepwise tandem cobalt and nickel catalysis should enable the facile synthesis of brush copolypeptides from alloc-a-aminoamide substituted NCAs (Figure 2-1). A key feature of this process is the envisioned use of different initiator formation mechanisms for main-chain and side-chain growth,[40] so that these polymerizations can be sequentially controlled in a single pot procedure.

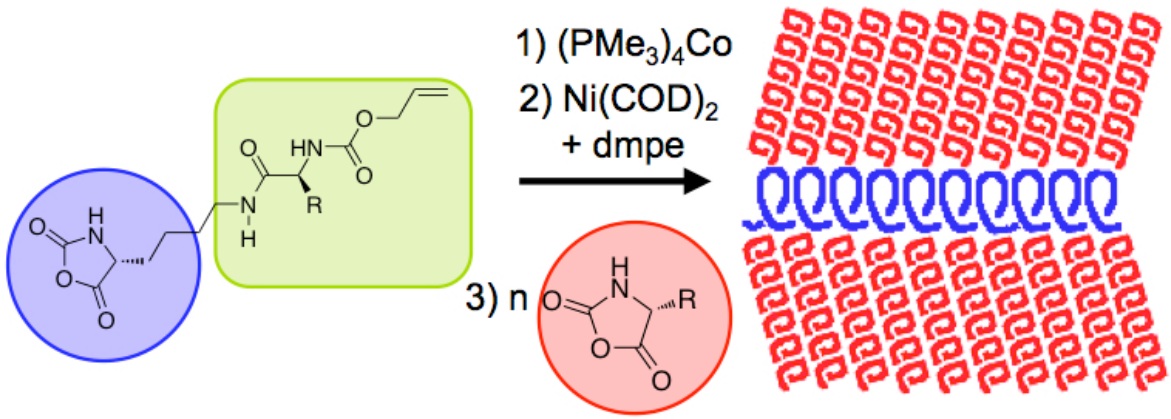

Figure 2-1. Schematic diagram showing two-stage, one-pot synthesis of cylindrical brush copolypeptides. NCA component (blue) of N_e-(alloc-L-methionyl)-L-lysine NCA is first polymerized using $(PMe_3)_4Co$ initiator to give a linear polypeptide that bears pendant initiator precursors (green). Side-chain initiators are then activated using dmpeNi(COD), followed by addition of a second NCA monomer (red) to give the brush copolymers.

2.2 Synthesis of Monomer

For the synthesis of alloc-α-aminoamide substituted NCAs, we chose to use L-lysine as the main-chain forming NCA, as substituted lysine NCAs are readily polymerized and the side-chain amine group is easily functionalized.[60,91,92] We used the hydrophobic amino acids L-isoleucine and L-methionine for construction of the alloc-α-

aminoamide side-chain groups (Figure 2-2) since these required no protecting groups and similar residues had been found to form good initiators in earlier work.[89] Methionine was also chosen since it provides a means for chemoselective, post-polymerization cleavage of side-chain segments by reaction with CNBr.[93] The methionine and isoleucine derivatized lysine NCA monomers were prepared using standard methods (Figure 2-2), and were obtained in reasonable yields after purification using flash column chromatography.[94] Although both monomers were found to be efficiently polymerized using $(PMe_3)_4Co$, we have focused the studies here on the methionine based monomer, N_e-(alloc-L-methionyl)-L-lysine-N-carboxyanhydride (K^{AM} NCA), to take advantage of the side-chain segment cleavability at this residue.

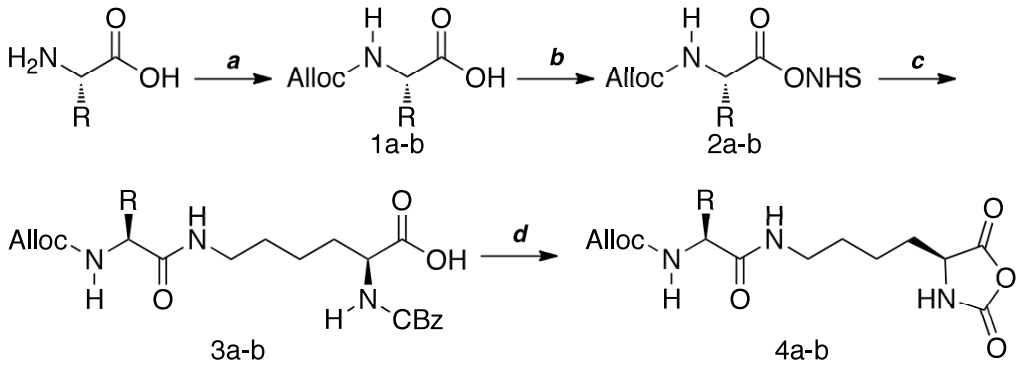

Figure 2-2. Synthesis of allyloxycarbonyl-aminoamide containing NCA monomers. (a) allylchloroformate, Na_2CO_3, β-cyclodextrin, H_2O, 3.5 h (88% yield); (b) DCC, NHS, THF, 0 - 21 ^oC, 1 h (69% yield); (c) Nε-Cbz-L-Lys-OH, Na_2CO_3, 1:1 THF: H_2O, 21 ^oC, 48 h (72% yield); (d) DCMME, DCM, 40 ^oC, 36 h (70% yield). **4a** = *N*ε-(allyloxycarbonyl-L-methionyl)-L-lysine-*N*-carboxyanhydride (R = $-CH_2CH_2SCH_3$), **4b** = *N*ε-(allyloxycarbonyl-L-isoleucyl)-L-lysine-*N*-carboxyanhydride (R = $-CH(CH_3)CH_2CH_3$).

2.3 Synthesis of K^{AM} Homopolymer and Diblocks

Polymerization of K^{AM} NCA using $(PMe_3)_4Co$ in THF proceeded readily at ambient temperature to give poly(N_ε-(alloc-L-methionyl)-L-lysine), poly(K^{AM}), with complete monomer conversion and no reaction at the side-chain alloc groups. To determine chain lengths, K^{AM} NCA was polymerized at different monomer to initiator ratios, and after complete monomer consumption, active chains were end-capped with isocyanate terminated PEG (M_n = 2000 Da).[95] Compositional analysis of purified, end-capped polymers by ^1H NMR gave number average poly(K^{AM}) chain lengths that increased linearly with stoichiometry (Figure 2-3). Chain length distributions of these poly(K^{AM}) samples were obtained by GPC/LS analysis and were found to possess low polydispersity indices (M_w/M_n) between 1.12 and 1.28, indicating the formation of well-defined polypeptides (Figure 2-2). Poly(K^{AM}) was prepared in high yield with precisely controlled chain lengths up to nearly 300 residues long, and could also be prepared as diblock copolymers with other amino acids (Table 2-1).

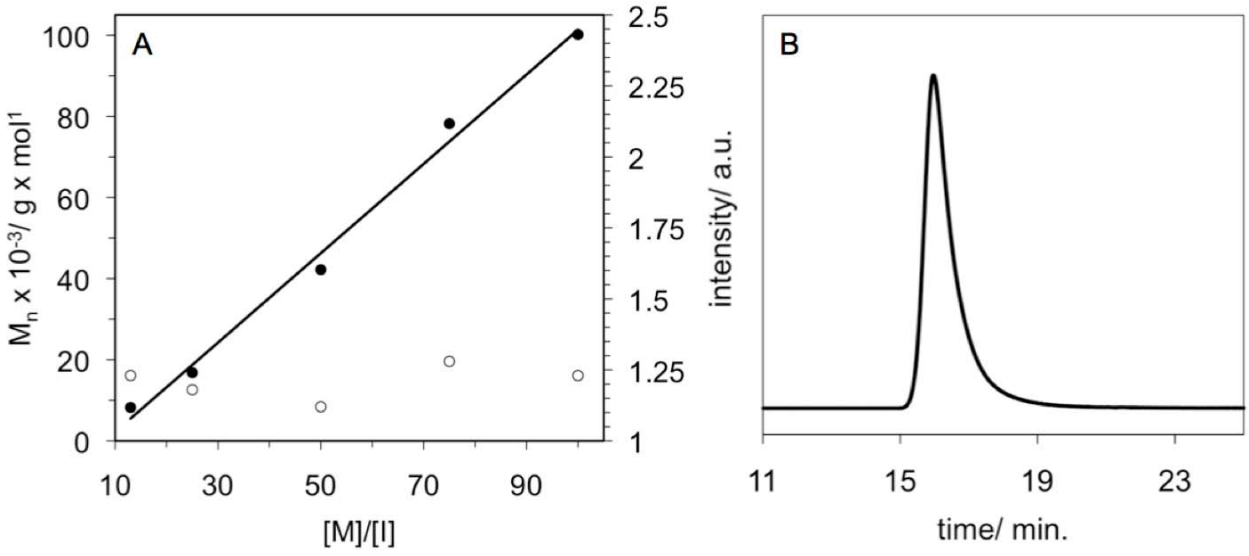

Figure 2-3. (a) Molecular weight (M_n, filled circles) and polydispersity index (M_w/M_n, open circles) of poly(K^{AM}) as a function of monomer to initiator ratio ([M]:[I]) after 100% monomer conversion. M_n and M_w/M_n were determined by ^{1}H NMR and gel permeation chromatography (GPC/LS). (b) GPC chromatogram (normalized LS intensity in arbitrary units (a.u.) versus elution time) of a poly(K^{AM}) sample (Table 2-1, entry 2).

M:I[a]	M_n[b]	M_w/M_n[c]	DP	yield (%)[d]
13	8 230	1.23	25	94
25	16 800	1.18	49	98
50	35 500	1.12	103	99
75	78 200	1.28	228	90
100	100 100	1.23	292	92

Table 2-1. Molecular weight (M_n) of poly(K^{AM}) as a function of monomer to initiator ratio using $(PMe_3)_4Co$ in THF at 20 °C. [a]M:I = monomer to $(PMe_3)_4Co$ initiator ratio, [b] M_n determined by end-capping with PEG-NCO (MW = 2000 Da) and analysis by ^1H NMR. [c]M_w/M_n determined by gel permeation chromatography (GPC/LS), [d]Isolated yields of PEG end-capped polypeptides.

Overall, these data (Figure 2-2 and Table 2-1) show that K^{AM} NCA, similar to other NCAs, is able to undergo living polymerization when initiated with $(PMe_3)_4Co$. Circular dichroism spectroscopy of poly(K^{AM}) in THF revealed this polymer, similar to other poly(L-lysine) derivatives,[60,92,96] is predominantly α-helical (see Figure 2-12), which imparts poly(K^{AM}) with good solubility in organic solvents as well as provides an exposed presentation of the side-chain alloc-α-aminoamide groups.[71]

			First segment[b]			Diblock Copolymer[c]			
Entry	1st monomer[a]	2nd monomer[a]	M_n	M_w/M_n	DP	M_n	M_w/M_n	DP	Yield (%)[d]
1	17 K NCA	17 K^{AM} NCA	18700	1.18	71	43000	1.12	142	99
2	17 K NCA	6 K^{AM} NCA	18700	1.18	71	29300	1.29	102	97
3	50 K^{AM} NCA	50 K NCA	31200	1.11	91	55000	1.12	184	100
4	50 K^{AM} NCA	25 K NCA	31200	1.11	91	45300	1.25	145	100

Table 2-2. Synthesis of diblock copolypeptides using $(PMe_3)_4Co$ in THF at 21 ^oC. [a] First and second monomers added stepwise to the initiator; number indicates equivalents of monomer per $(PMe_3)_4Co$. K NCA = $N\varepsilon$-Cbz-L-lysine-N-carboxyanhydride. K^{AM} NCA = $N\varepsilon$-(alloc-L-methionyl)-L-lysine-N-carboxyanhydride. [b]Molecular weight and polydispersity index after polymerization of the first monomer (determined by GPC/LS for poly(K); determined by GPC/LS and ^1H NMR for poly(K^{AM})). [c]Molecular weight and polydispersity index after polymerization of the second monomer (as determined by GPC/LS and ^1H NMR). [d]Total isolated yield of diblock copolypeptide. DP = degree of polymerization.

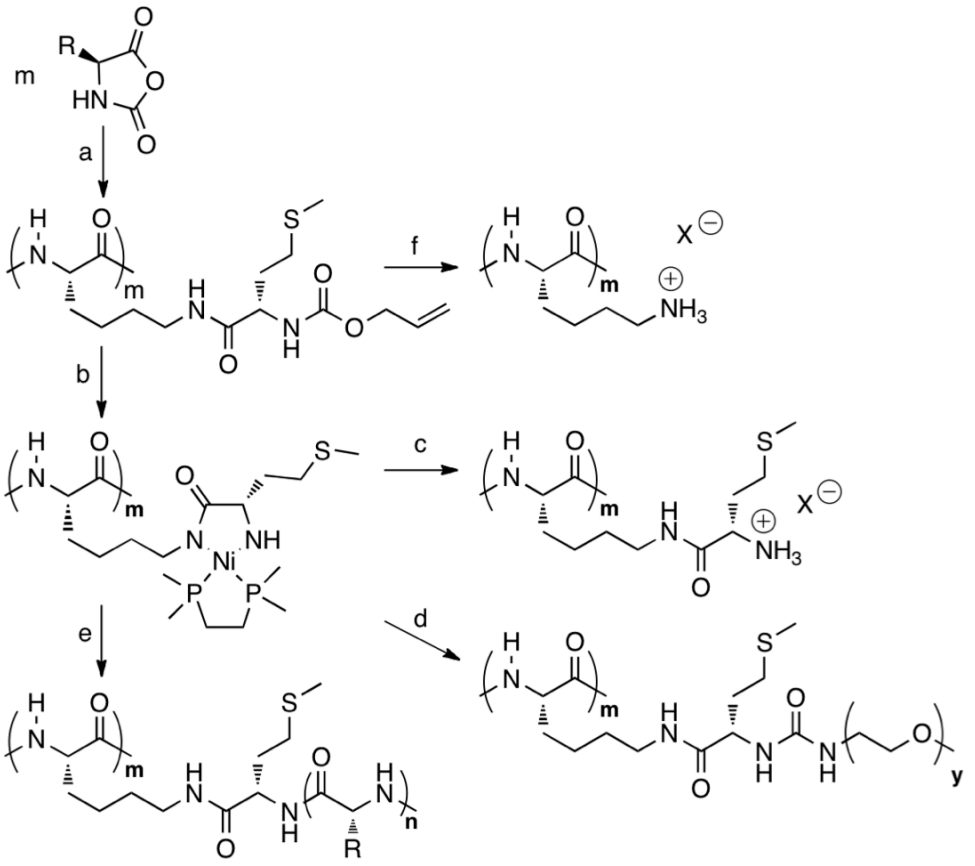

Figure 2-4. Synthesis and reactivity of poly(K^{AM}). (a) $(PMe_3)_4Co$, THF, 21 ^oC, 1 h. (b) dmpeNi(COD), DMF, 80 ^oC, 16 h. (c) 4.0 M HCl, 21 ^oC, 2 h. (d) α-methoxy-ω-isocyanoethyl-poly(ethylene glycol), PEG-NCO (MW = 350 Da), DMF, 21 ^oC, 16h. (e) Bn-Glu NCA, DMF, 21 ^oC, 16 h. (f) 0.25 M cyanogen bromide in 100 mM HCl: THF (1:1), 4 h.

2.4 Activation of Poly(K^{AM})

The key feature of poly(K^{AM}) is the reactivity of its side-chain alloc-L-methionyl groups that will be utilized for cylindrical polypeptide brush growth. To evaluate this chemistry, the side-chains in freshly prepared, unpurified poly(K^{AM}) (Figure 2-4a) were reacted with stoichiometric $Ni(COD)_2$ and bis(dimethylphosphino)ethane (dmpe) at 80 ^oC to generate amido-amidate nickelacycle initiating groups (Figure 2-4b). This reaction,

on small molecules, is known to proceed quantitatively,[90] yet we needed to confirm that active nickelacycle initiators were also formed in high yield on the poly(K^{AM}) side-chains. As a first step, to determine if all alloc-L-methionyl groups react with Ni(0), the product of this reaction was quenched by addition of 4.0M HCl. While alloc-L-methionyl groups are stable to these conditions, the activated nickel complexes are hydrolyzed to give poly(N_{ε}-(L-methionyl)-L-lysine) (Figure 2-4c). Analysis of the polymer product by ^{1}H NMR showed that at least 91% of the alloc groups had reacted when stoichiometric Ni(0) was used (Figure 2-5). It is likely that higher conversion of alloc groups could be obtained by using excess Ni(0), but this was not pursued since free Ni(0) will also react with NCAs and would need to be removed in a subsequent purification step.[40]

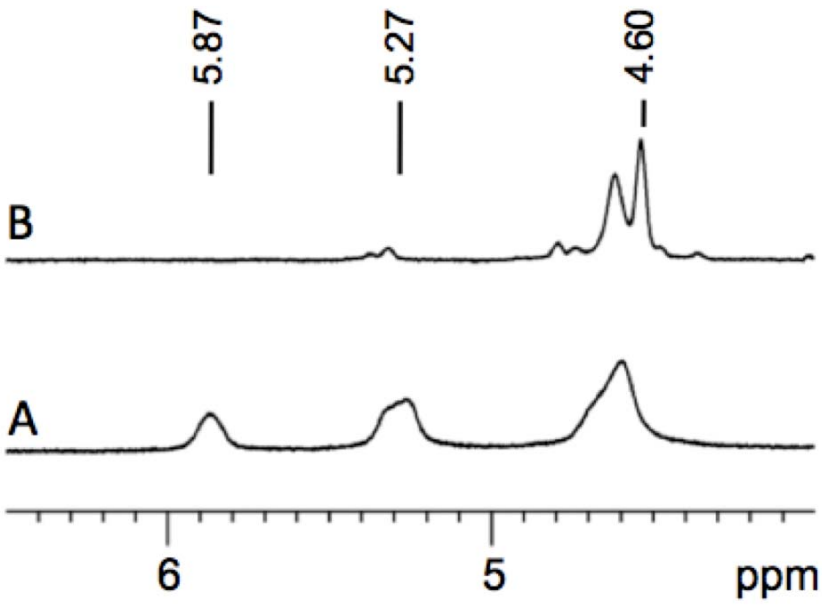

Figure 2-5. Activation and quenching of alloc side-chains in poly(K^{AM}). (a) Partial ^{1}H NMR spectrum in TFA-*d* showing alloc proton resonances of poly(K^{AM}). Resonances: -CH_2CH=CH_2 (5.87 ppm), -CH_2CH=CH_2 (5.27 ppm), and -CH_2CH=CH_2 and α-carbon protons (4.60 ppm). (b) Partial ^{1}H NMR spectrum in TFA-*d* of poly(K^{AM}) after activation with dmpeNi(COD) followed by quenching with 4.0 M HCl to remove nickel complexes. By NMR integrations, 91 to 100% of alloc side chains were activated (see experimental).

2.5 Initiation Efficiency of Activated Poly(K^{AM})

Having verified that the side-chain groups of poly(K^{AM}) can be converted *in situ* to active nickelacycle initiators, we next explored the grafting of cylindrical polypeptide brushes from these activated polymers (Figure 2-4e). To obtain high chain density cylindrical brushes, the initiation efficiency for side-chain initiating groups needs to be very high to ensure that polypeptides grow from each side-chain. We had previously found that initiation efficiency for NCA polymerization using small molecule nickelacycle initiators was low in THF, due to nickelacycle aggregation (Figure 2-6).[40] However,

initiation efficiency was quantitative in DMF, which better solubilizes these complexes. Here, we also found that growth of side-chain brush segments was optimal in DMF, and that nickelacycle aggregation on activated poly(K^{AM}) was further suppressed by use of two equivalents of dmpe per nickel center.

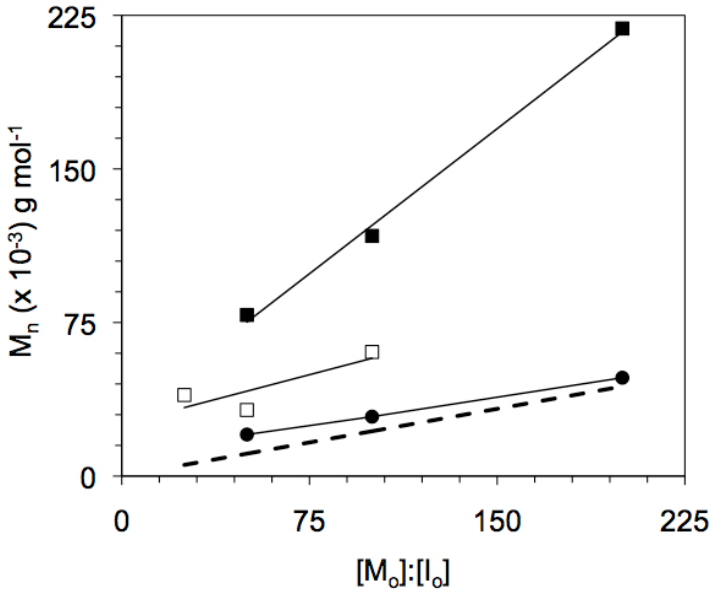

Figure 2-6. Molecular weight (M_n, filled square = THF, open square = nitrobenzene, filled circles = DMF, dashed line = theoretical) of poly(E) as a function of monomer to initiator ratio ([M]:[I]) after 100% monomer conversion. M_n and M_w/M_n were determined gel permeation chromatography (GPC/LS). Initiator is activated nickel amidoamidate poly(K^{AM}) small-molecule analog.

One aspect of activation not previously explored was reaction time. According to the literature, the required time for activation was overnight (~ 12 h) at 80 ^{o}C. A reaction of 25:1 E NCA to active amidoamidate nickelocycle, in DMF, was monitored by SEC with three time points; 0.5 hour, 4 hours and 24 hours. The M_n among these samples

varied at most by 5.7%, showing no significant change in M_n (Figure 2-7). Therefore the activation of polypeptide is likely complete after 0.5 hours.

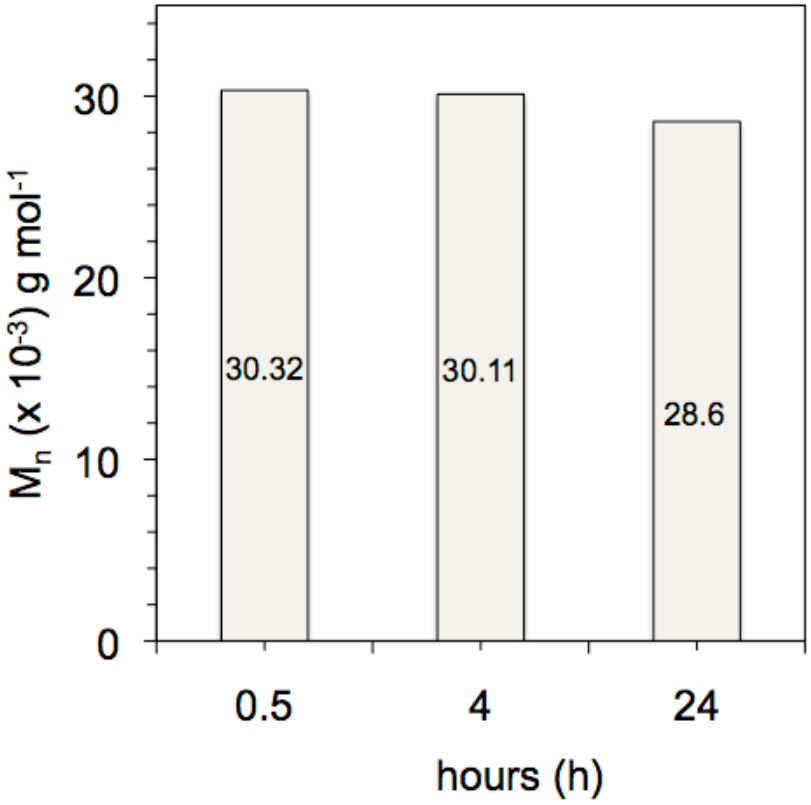

Figure 2-7. Duration of activation step at 80 ^{o}C and the effect on molecular weight (M_n) as determined by gel permeation chromatography

2.6 Cylindrical Polypeptide Brushes

To show that the alloc-L-methionyl groups not only react with Ni(0), but also form active nucleophilic initiators, we reacted them with different lengths of isocyanate terminated PEG (M_n = 350 or 1000 Da), which have been shown to react quantitatively with active nickelacycle chain-ends (Figure 2-4d).[95] Analysis of these products (Table 2-

3) revealed that the Ni-activated side chains of poly(K^{AM}) were capped by PEG chains with 91 to 100% efficiency, showing that the formation of active nickelacycle initiators at each side-chain in poly(K^{AM}) proceeds with high efficiency.

	K Segment	K^{AM} Segment	PEG DP[b]		
entry	DP[a]	DP[a]	Theoretical	Found	% funct.[c]
1	60	15	8	7.7	97
2	60	30	8	7.7	96
3	60	15	23	21	91
4	60	30	23	23	100

Table 2-3. End-capping of activated poly(K)-*b*-poly(K^{AM}) chains with PEG-NCO (MW = 350 and 1000 Da) to determine side-chain activation efficiency. [a]Degrees of polymerization (DP) of K and K^{AM} segments in poly(K)-*b*-poly(K^{AM}) block copolymers. [b]Degrees of polymerization (DP) of PEG-NCO chains used for end-capping experiments. [c]PEG end-capping efficiency (% funct.) defined as 100 x (number of found PEG chains)/(number of theoretical PEG chains for 100% functionalization).

For initial proof of concept, δ-benzyl-L-glutamate NCA (E NCA) was used for side-chain segment growth since it forms soluble, α-helical chains that are readily distinguished from the lysine based main chain. Different amounts of E NCA in DMF were added directly to homopolymer (K^{AM}) macroinitiator solutions resulting in the growth of the secondary chains (Figure 2-8).

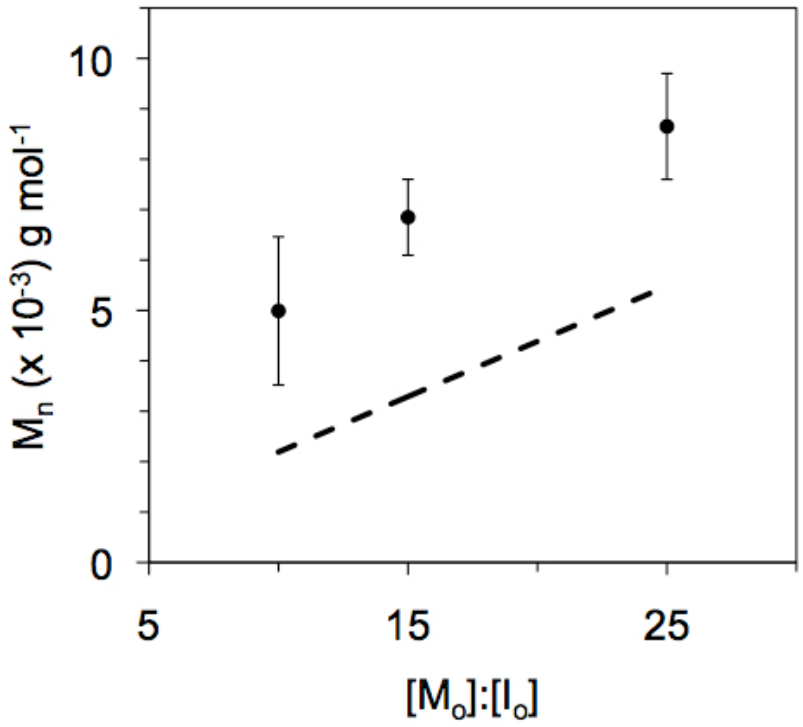

Figure 2-8. Lengths and chain length distributions of poly(E) segments grown from activated poly(K^{AM}) side-chains followed by PEGylation (with PEG-CNO M_w = 2000 g/mol). Number average molecular weight after 100% monomer conversion of poly(E) segments as a function of monomer to activated K^{AM} initiator ratio ([M]:[I]) in poly(K^{AM}) polymers. Values were determined using ^{1}H NMR integrations (filled circles), and each data point represents the average of four repeat experiments (error bars show the range of data obtained). Dotted line represents the expected calculated values.

Once all E NCA is consumed the chain-ends remain active and can be quenched. The chain ends were then quenched with PEG-NCO (MW, 2000 g/mol) allowing for compositional analysis of the PEGylated brushes using ^{1}H NMR. According to Table 2-4 and Figure 2-6**,** inflated values were obtained for PBLG segments. This inflated value could stem from 1) the secondary chain end-groups are dying off (and not PEGyated) or 2) the reaction between active secondary chain end-group and PEG-NCO is inefficient

due to steric hinderance (polymer-polymer reaction), or 3) active nickelocycle initiation species are aggregating, causing only a percentage of initiation species to react. Molecular weight inflation is mostly likely due to inefficient reaction of PEG-NCO with the active secondary chain ends due to steric hinderance.

Poly(K^{AM}) Primary Chain			PBLG segments				
entry	DP[a]	M_w/M_n[c]	M:I[b]	DP[c]	M_w/M_n[c]	M_n[c]	yield (%)[d]
1	38	1.19	10	17	1.02	3.73	81
2	12	1.17	10	28	1.18	6.13	87
3	24	1.17	10	17	1.11	3.7	85
4	44	1.19	10	29	1.06	6.4	87
5	38	1.19	15	29	1.01	6.13	97
6	12	1.17	15	30	1.22	6.57	94
7	24	1.17	15	36	1.19	7.9	92
8	44	1.19	15	31	1.04	6.79	93
9	38	1.19	25	35	1.05	7.67	90
10	12	1.17	25	44	1.19	10.07	99
11	24	1.17	25	40	1.23	8.76	93
12	44	1.19	25	37	1.13	8.1	95

Table 2-4. Molecular weight (M_n and DP) data for PEGylated poly(K^{MPBLG}) brush polypeptides. [a]Degrees of polymerization (DP) K^{AM} segments. [b]M:I = δ-Benzyl-L-glutamate NCA monomer to nickel activated alloc-methionyl initiator ratio. [c]Average degree of polymerization (DP), polydispersity index (M_w/M_n) and molecular weight (M_n) of PBLG chains grown off of poly(K^{AM})

polymers, as determined by ^{1}H NMR and GPC/LS. [d]Isolated yields of PEGylated poly(K^{MPBLG}) brush polypeptides.

To circumvent the challenges of PEGylating cylindrical brush secondary chains, we used a poly(N_{ε}-Cbz-L-lysine)-*b*-poly(K^{AM}), poly(K)-*b*-poly(K^{AM}), block copolymer main-chain, where the poly(K) segment served as a high molecular weight end-group for determination of average side-chain segment lengths by ^{1}H NMR analysis (see experimental). The poly(K)-*b*-poly(K^{AM}) copolymers of different segment lengths (see experimental) were prepared in THF using $(PMe_3)_4Co$ as described above. After concentration of the crude reaction mixtures under vacuum followed by dilution with DMF, the K^{AM} side-chains in the copolymers were activated by reaction with $Ni(COD)_2$ and dmpe at 80 ºC to give macroinitiators that were used directly with no further isolation or purification steps. Different amounts of E NCA in DMF were added directly to the block copolymer macroinitiator solutions, resulting in growth of the brush segments. The polymerizations of E NCA were found to go to completion and the copolypeptide brushes were obtained in high yields (Table 2-5). Compositional analysis of the copolypeptide brushes by ^{1}H NMR showed that average poly(δ-benzyl-L-glutamate), poly(E), segment lengths increased linearly with E NCA monomer to activated K^{AM} initiator ratios and were close to values expected for 100% brush initiation efficiency, indicating controlled polymerization of the side-chain segments (Figure 2-9).

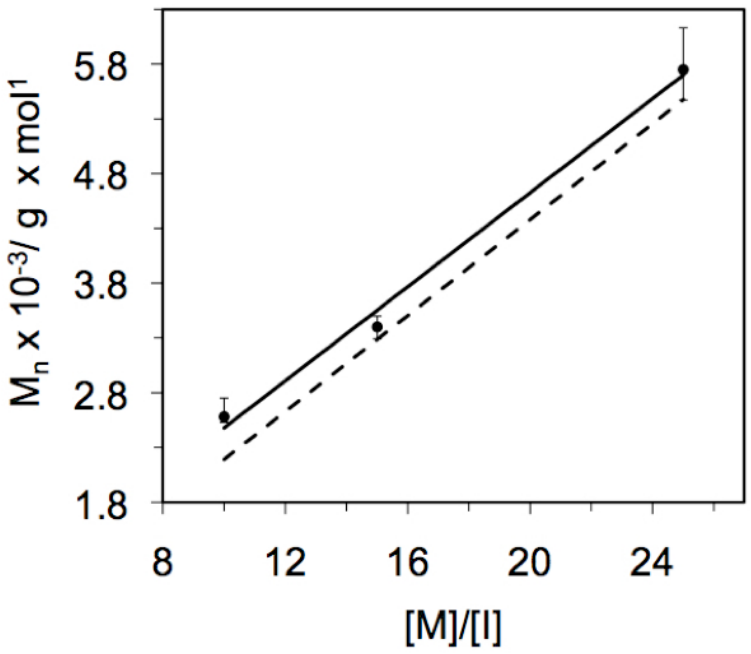

Figure 2-9. Lengths and chain length distributions of poly(E) segments grown from activated poly(K^{AM}) side-chains. Number average molecular weight after 100% monomer conversion of poly(E) segments as a function of monomer to activated K^{AM} initiator ratio ([M]:[I]) in poly(K)-*b*-poly(K^{AM}) block copolymers. Values were determined using ^{1}H NMR integrations (filled circles), and each data point represents the average of four repeat experiments (error bars show the range of data obtained). Dotted line represents the expected calculated values

poly(K)-*b*-poly(K^{AM})			Poly(E) segments				
	K Segment[a]	K^{AM} Segment[a]					
entry	DP	DP	M:I[b]	DP[c]	M_w/M_n[c]	M_n[c]	yield (%)[d]
1	85	9	10	12	1.15	2 630	82
2	60	17	10	12	1.25	2 630	98
3	60	30	10	12	1.23	2 630	96
4	63	16	10	11	1.04	2 410	97
5	85	9	15	15	1.10	3 290	91
6	60	17	15	15	1.13	3 290	89
7	60	30	15	16	1.08	3 500	92
8	63	16	15	16	1.02	3 500	98
9	85	9	25	27	1.10	5 910	87
10	60	17	25	28	1.20	6 130	93
11	60	30	25	25	1.18	5 470	93
12	63	16	25	25	1.13	5 470	94

Table 2-5. Molecular weight (M_n and DP) data for poly(K)-*b*-poly(K^{MPBLG}) brush copolypeptides. [a]Degrees of polymerization (DP) of K and K^{AM} segments in poly(K)-*b*-poly(K^{AM}) precursor block copolymers. [b]M:I = δ-Benzyl-L-glutamate NCA monomer to nickel activated alloc-methionyl initiator ratio. [c]Average degree of polymerization (DP), polydispersity index (M_w/M_n) and

molecular weight (M_n) of poly(E) chains grown off of poly(K)-*b*-poly(K^{AM}) block copolymers, as determined by ^{1}H NMR and GPC/LS. [d]Isolated yields of poly(K)-*b*-poly(K^{MPBLG}) brush copolypeptides.

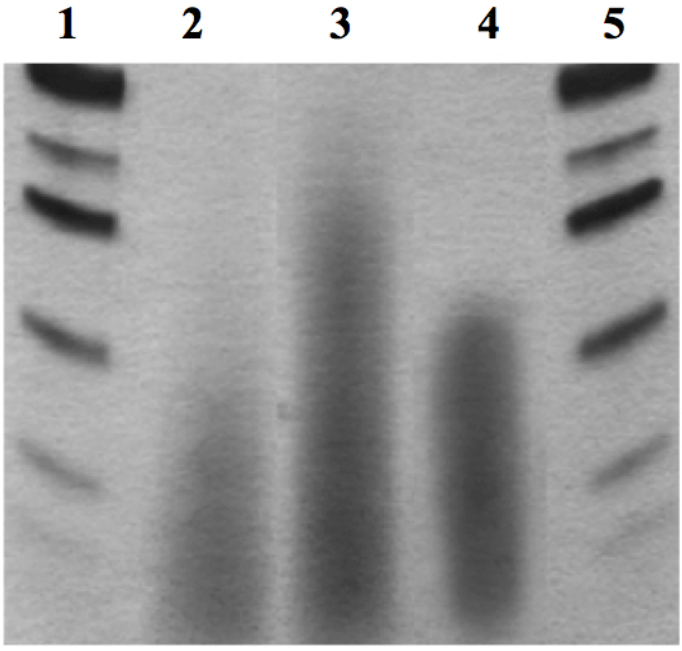

Figure 2-10. Visualization of PGA chain length distributions using SDS-PAGE. Lanes 1 and 5: protein molecular weight standards (from top: 25, 20, 15, 10, 5 and 2 kDa); Lanes 2 and 3: synthetic PGA standards (2: M_n = 5120, M_w/M_n = 1.05, 3: M_n = 18900, M_w/M_n = 1.13); Lane 4: PGA sample (M_n = 3820) cleaved from a brush copolymer using CNBr.

To measure chain length distributions of the poly(E) segments, we utilized the methionine linker to cleave the brush segments from the main-chain. A model reaction was performed by mixing N_e-(alloc-L-methionyl)-N_a-Cbz-L-lysine with CNBr resulting in complete cleavage of the alloc-L-methionyl group from the lysine residue, which confirmed the utility of this reaction for chemoselective peptide cleavage (see experimental). A similar reaction on poly(K^{AM}) showed that CNBr cleavage at the

methionine linkers works equally as well on this polypeptide, and gave the expected alloc-homoserine lactone byproduct (Figure 2-4f). To perform this reaction on the copolypeptide brushes, the poly(E) segments were first deprotected to poly(L-glutamic acid), PGA, to improve their solubility in polar media, and the brushes were then incubated with CNBr in aqueous formic acid (see experimental). The resulting cleaved polypeptide segments were then analyzed using SDS PAGE and compared to narrow molecular weight distribution PGA standards (M_w/M_n = 1.05 – 1.13) (Figure 2-10). We found that the cleaved PGA segments gave bands similar in width and location to the standards, indicating narrow chain length distributions and molecular weights close to expected values, which confirmed the growth of a high density of uniform brush segments.

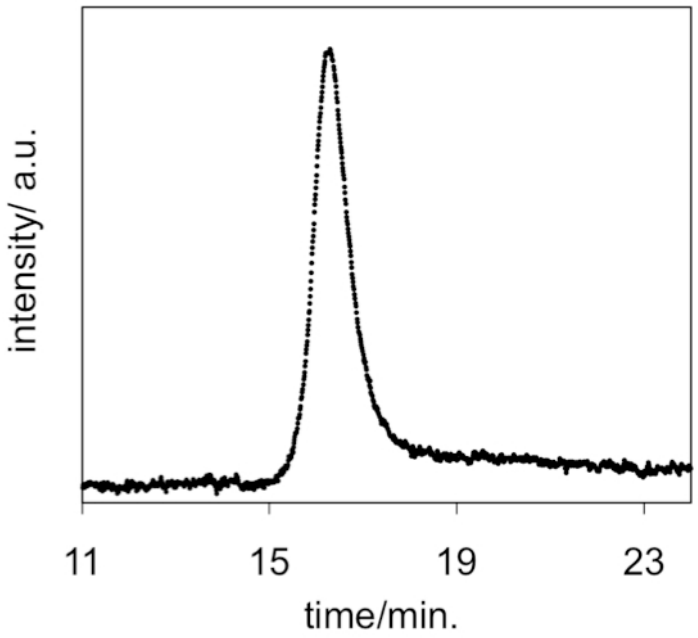

Figure 2-11. Gel Permeation Chromatograph of re-benzylated poly(E) from Cleaved Brush.

To confirm that high density brushes are growth with uniform secondary chain legnth, the PGA secondary chains were benzylated to give linear PBLG segments. These PBLG segments were soluble in 0.1 M LiBr DMF and analyzed by gel-permeation chromatography (Figure 2-11) to give a single, monodisperse peak. This is confirmation that secondary chain growth occurs at the same rate for all growing chains.

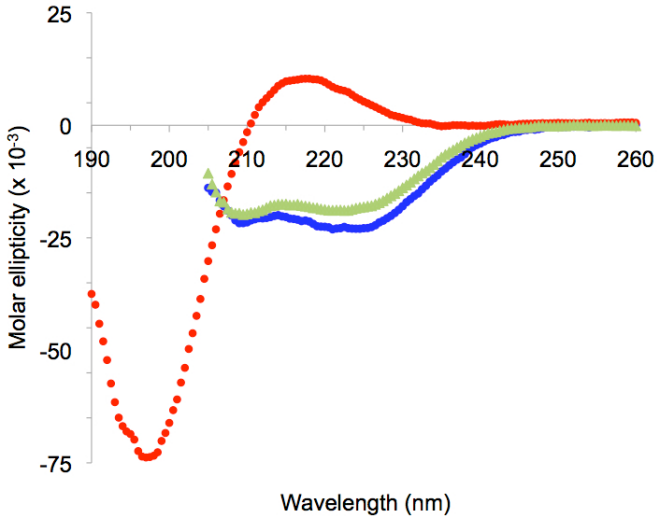

Figure 2-12. Circular dichroism spectra of poly(K^{AM}) in THF (blue data), protected poly(K)-*b*-poly(K^{MPBLG}) brush copolypeptide in THF (green data), and deprotected poly(K)-*b*-poly(K^{MPBLG}) brush copolypeptide in pH 7 H_2O (red data). Concentrations of all samples = 0.5 mg/mL, 20 ^{o}C.

2.7 Conclusion

The use of tandem cobalt and nickel catalysis has been shown to be an efficient method for preparation of high chain density, cylindrical copolypeptide brushes, where both the main-chains and side-chains can be prepared with controlled segment lengths. This new methodology avoids the need for intermediate deprotection and purification steps,

yields well-defined copolymers, and should be valuable for the straightforward preparation of new copolypeptide architectures. We plan to use this chemistry to create three dimensional copolymers, with block segments either along the main-chain or in the side-chains, which should give rise to new self-assemblies that can incorporate the useful properties of branched polypeptides.

2.8 Acknowledgments

The authors acknowledge the valuable contributions of Dr. Zhibo Li and Ilya Yakovlev to the early stages of this project, and Steevens Alconcel for assistance in obtaining the SDS-PAGE data. This work was supported by the NSF under award No. MSN 0956481. Mass spectroscopy data collection was supported by Grant Number S10RR025631 from the National Center for Research Resources. The content is solely the responsibility of the authors and does not necessarily represent the official views of the National Center for Research Resources or the National Institutes of Health.

Supporting Information Available

Experimental procedures and spectral data for all new compounds. Polymerization data, M_n vs. [M]/[I] plots, and CD spectra. This material is available free of charge via the Internet at http://pubs.acs.org.

2.9 Experimental Procedures

Materials and Methods.

Reactions were conducted under an inert atmosphere of N_2, using oven-dried glassware unless otherwise stated. Hexanes and THF were purified by first purging

with dry nitrogen, followed by passage through columns of activated alumina.[97] DMF was purified by drying over 4Å molecular sieves followed by vacuum distillation. Infrared spectra were recorded on a Perkin Elmer 1605 FT-IR Spectrophotometer. Deionized water (18 MΩ-cm) was obtained by passing in-house deionized water through a Millipore Milli-Q Biocel A10 purification unit. Tandem gel permeation chromatography/light scattering (GPC/LS) was performed on a SSI Accuflow Series III liquid chromatograph pump equipped with a Wyatt DAWN EOS light scattering (LS) and Optilab rEX refractive index (RI) detectors. Separations were achieved using 10^5, 10^4, and 10^3Å Phenomenex Phenogel 5 mm columns using 0.10 M LiBr in DMF as the eluent at 60 °C. All GPC/LS samples were prepared at concentrations of 8 mg/mL. ^{1}H NMR spectra were recorded on a DRX500 Bruker spectrometer (500 MHz) and are reported relative to deuterated solvent. Data for ^{1}H NMR are reported as follows: chemical shift (δ ppm), multiplicity, coupling constant (Hz) and integration. Data for ^{13}C NMR spectra are reported in chemical shift. High-resolution mass spectrometry (HRMS) was performed on a Micromass Quatro-LC Electrospray spectrometer with a pump rate of 20 µL/min using electrospray ionization (ESI).

A. Synthesis and polymerization of NCA monomer

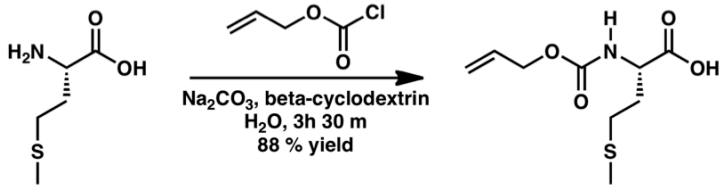

Representative procedure for synthesis of allyloxycarbonyl-L-amino acids: allyloxycarbonyl-L-methionine (1a). L-Methionine (10.0 g, 67.1 mmol) was dissolved

in 1:1 THF/H_2O (350 mL total). Sodium carbonate (Na_2CO_3) (14.2 g, 134 mmol) was added followed by the addition of β-cyclodextrin (1.88 g, 1.7 mmol). Allylchloroformate (7.13 mL, 67.1 mmol) was added and the reaction stirred at 21 ^oC until completion. THF was removed and the reaction was acidified to pH 2 with 10% aqueous HCl (200 mL). The acidified, aqueous mixture was extracted with EtOAc (3 x 100 mL) and the organic layer was dried over sodium sulfate (Na_2SO_4), filtered and evaporated to dryness. The crude product was a clear, colorless oil. No further purification was necessary. Mass isolated: 13.8 g (88% yield). ^1H NMR (500 MHz, $CDCl_3$): δ 5.94 (m, 1H), 5.41 (s, 1 H), 5.34-3.32 (d, J = 10, 1 H), 5.25-5.23 (d, J = 8, 1 H) 4.60 (m, 2 H), 4.12 (m, 1 H), 2.61-2.58 (t, J = 3.5, 2 H), 2.21 (m, 2 H), 2.11 (s, 3 H). ^{13}C NMR (125 MHz, $CDCl_3$): δ 178.44, 157.80, 134.09, 119.83, 67.86, 54.71, 33.25, 31.62, 17.08; FT-IR (THF): 1731, 1654, 1539 cm^{-1}, HRMS-ESI (*m/z*) $[2M + 2Na]^+$ Calcd for $C_{18}H_{28}NO_8S_2$: 511.12; found: 511.12.

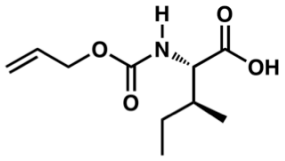

Allyloxycarbonyl-L-isoleucine (1b). No further purification required; 12.6 g isolated as a white solid (77% yield). ^1H NMR (500 MHz, $CDCl_3$): δ 9.73 (b, 1H), 5.91-5.89 (J = 5.1, 1 H), 5.34-5.31 (d, J = 18, 1 H), 5.24-5.21 (d, J = 9, 1 H), 4.59 (m, 2 H), 4.38 (m, 1 H), 1.96 (m, 1 H), 1.48 (m, 1 H), 1.21 (m, 1 H), 0.99-0.94 (m, 6 H). ^{13}C NMR (125 MHz, $CDCl_3$): δ 177.13, 156.28, 132.65, 118.14, 66.15, 58.36, 37.88, 24.95, 15.63, 11.73. Additional characterization data available in the literature.[98]

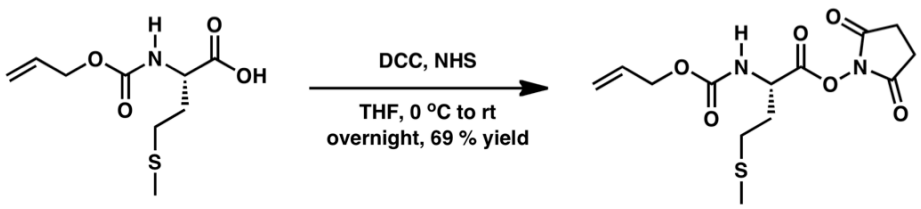

Representative procedure for preparation of allyloxycarbonyl-L-methionine-*N*-hydroxysuccinimide ester (2a). Under an atmosphere of N_2, allyloxycarbonyl-L-methionine (13.8 g, 59.2 mmol) was dissolved in THF (320 mL). *N*-hydroxysuccinimide (8.18 g, 71.1 mmol) was added to the reaction mixture and cooled to 0 ^{o}C. Dicyclohexylcarbodimide (DCC) (12.8 g, 62.2 mmol) was added and the reaction warmed to 21 ^{o}C, with stirring for 1 h. The reaction flask was placed in the freezer overnight where dicyclohexylurea (DCU) precipitated and was removed by vacuum filtration. The crude product was an opaque colorless oil (13.4 g crude isolated, 69% yield). Residual DCU was separated from the product by flash chromatography (crude product was loaded in EtOAc and eluted in 1:1 Hex: EtOAc). Product R_f = 0.32. 7.30 g purified product was isolated as a clear, colorless oil. ^{1}H NMR (500 MHz, $CDCl_3$): δ 5.93 (m, 1 H), 5.66 (s, 1 H), 5.34-5.32 (d, J= 10, 1 H), 5.25-5.23 (d, J= 8, 1 H), 4.9 (s, 1 H), 4.58 (m, 2 H), 2.83 (s, 4 H), 2.65 (m, 2 H), 2.26 (m, 1 H), 2.12 (m, 3 H). ^{13}C NMR (125 MHz, $CDCl_3$): δ 168.48, 167.83, 132.23, 118.04, 66.10, 51.47, 31.82, 29.38, 15.23. FT-IR (THF): 1788, 1741, 1722 cm^{-1}. HRMS-ESI (*m/z*) $[M + Na]^+$ Calcd for $C_{13}H_{18}N_2O_6SNa$: 353.08; found: 353.08.

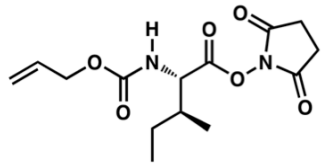

Allyloxycarbonyl-L-isoleucine-*N*-hydroxysuccinimide ester (2b). Purified by flash column chromatography starting with 1:1 Hex: EtOAc (product R_f = 0.43), 3.95 g isolated as a colorless oil (94% yield). ^{1}H NMR (500 MHz, $CDCl_3$): δ 5.91-5.89 (m, 1 H), 5.34-5.33 (d, J = 5, 1 H), 5.25-5.23 (d, J = 8, 1 H), 4.70 (m, 1 H), 4.59 (m, 2 H), 2.84 (s, 4 H), 1.96 (m, 1 H), 1.61-1.58 (m, 1 H), 1.29-1.25 (m, 1 H), 1.06-1.05 (d, J = 2, 3 H), 0.99-0.97 (t, J = 7, 3 H). ^{13}C NMR (125 MHz, $CDCl_3$): δ 169.68, 168.84, 156.66, 133.54, 119.32, 67.34, 58.00, 39.45, 26.73, 25.84, 16.25, 12.65. FT-IR (THF): 2973, 2861, 1816, 1787, and 1745 cm^{-1}. HRMS-ESI (*m/z*) $[M + Na]^+$ Calcd for $C_{14}H_{20}N_2NaO_6$ 335.12; found: 335.12.

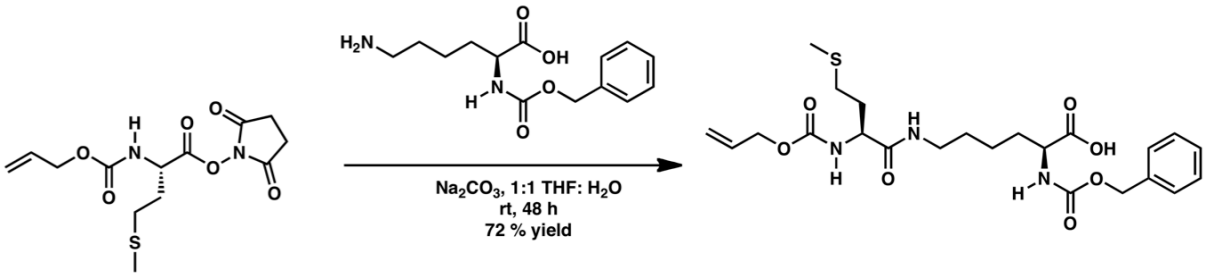

***N*$_\varepsilon$-(allyloxycarbonyl-L-methionyl)-*N*$_\alpha$-carboxybenzyl-L-lysine (3a).** Allyloxycarbonyl-L-methionine-*N*-hydroxysuccinimide ester (7.30 g, 22.1 mmol) was dissolved in THF (73 mL) in a 250 mL round bottom flask equipped with a Teflon stir bar. In a separate 250 mL round bottom flask Na_2CO_3 (2.56 g, 24.2 mmol) was dissolved in water (73 mL). *N*$_\alpha$-carboxybenzyl-L-Lysine (6.78 g, 24.2 mmol) was added to the aqueous flask and dissolved. The allyloxycarbonyl-L-methionine-*N*-hydroxysuccinimide ester solution was

transferred to the aqueous reaction flask and the resulting mixture allowed stirred for 2 days. THF was removed under reduced pressure and the aqueous layer was acidified to pH 2 and extracted with EtOAc (3 x 50 mL). The organic layer was separated, dried using Na_2SO_4, filtered and concentrated. The resulting oil was again dissolved in minimal EtOAc and precipitated into hexanes yielding a white solid. Mass isolated prior to precipitation: 8.41 g. Mass isolated post-precipitation: 7.93 g (72 % yield). ^{1}H NMR (500 MHz, $CDCl_3$): δ 7.33-7.32 (m, 5 H), 6.91 (s, 1H), 6.09 (s, 1H), 5.88-5.82 (2 H), 5.31-5.30 (d, *J* = 10, 1H), 5.19-5.11 (d, *J* = 8, 1H), 5.09 (s, 1H), 4.52 (m, 2H), 4.34 (m, 2H), 3.24-3.17 (m, 2 H) 2.48 (m, 2 H), 2.04 (s, 3H), 1.91-1.89 (m, 2 H), 1.78-1.66 (m, 2 H), 1.49-1.26 (m, 2 H). ^{13}C NMR (125 MHz, $CDCl_3$): 175.00, 172.19, 156.43, 136.07, 132.32, 128.43, 117.88, 66.98, 65.9 9, 53.86, 53.52, 39.00, 31.45, 29.99, 28.48, 25.32, 22.12, 15.13, 14.01, 11.33. FT-IR (THF): 2922, 1704, 1658, 1528 cm^{-1}. HRMS-ESI (*m/z*) $[M + H]^+$ Calcd for $C_{23}H_{34}N_3O_7S$, 496.21; found: 496.21.

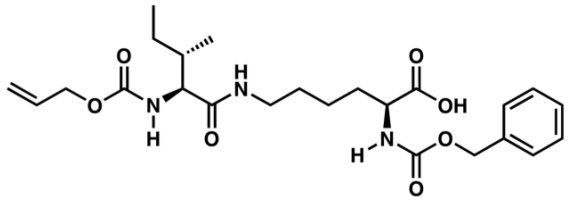

***N*$_\varepsilon$-(allyloxycarbonyl-L-isoleucyl)-*N*$_\alpha$-carboxybenzyl-L-lysine (3b)**. Purified by flash column chromatography using 1:1 Hex:EtOAc; 3.60 g white solid isolated (80% yield). ^{1}H NMR (500 MHz, $CDCl_3$): δ 12.45 (b, 1 H), 7.85 (s, 1 H), 7.26-7.12 (m, 5 H), 7.10-7.08 (s, 1 H), 5.80-5.77 (m, 1 H), 5.30-5.29(d, J = 10, 1 H), 5.25-5.24(d, J = 7, 1 H), 5.18 (m, 2 H), 4.36 (s 2 H), 3.81-3.79 (m, 1 H), 3.68 (m, 1 H), 3.22 (m, 2 H), 1.85 (m, 1 H), 1.76 (m, 2 H), 1.51-1.23 (m, 5 H), 1.08 (m, 1 H), 0.89-0.87 (m, 6 H). ^{13}C NMR (125 MHz,

$CDCl_3$): δ 175.17, 172.52, 156.87, 156.39, 136.31, 132.60, 128.64, 128.31, 118.06, 67.19, 66.16, 59.94, 53.73, 39.02, 36.99, 31.74, 28.75, 24.85, 22.29, 15.57, 22.08. FT-IR (THF): 2958, 2873, 1722, 1691, 1642, 1533 cm^{-1}. HRMS-ESI (*m/z*) [M + H]: Calcd for $C_{24}H_{36}N_3O_7$: 478.26; found: 478.26.

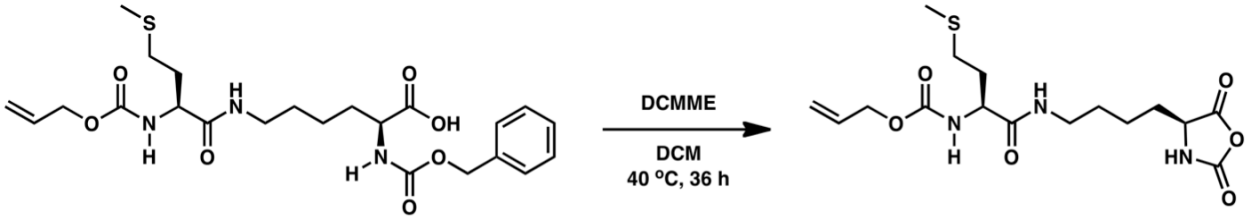

***N*-(allyloxycarbonyl-L-methionyl)-L-lysine-*N*-carboxyanhydride (K^{AM} NCA) (4a).** NCA precursor **3a** (1.0 g, 2.02 mmol) was added to a 125 mL schlenk flask equipped with a Teflon stir bar and then dissolved in anhydrous DCM (70 mL) under N_2. α,α-Dichloromethylmethyl ether (460 μL, 5.0 mmol) was added via syringe to the stirring solution under N_2. The reaction was refluxed for 36 h. The solution was evaporated to dryness under reduced pressure and transferred to a glovebox (N_2 atmosphere) for purification. The crude residue was purified by flash chromatography (10% to 75% THF in hexanes) and collected in 15 x 10 mL fractions. K^{AM} NCA gave an R_f = 0.464 in 1:1 THF:Hex. 547 mg of NCA was isolated as a clear oil after evaporation of the THF and hexanes from the combined fractions (70% yield). ^{1}H NMR (500 MHz, $CDCl_3$): δ 7.35 (s, 1 H), 6.50 (s, 1 H), 5.92-5.89 (m, 1 H), 5.78-5.69 (m, 1 H), 5.34 (dd, J= 1.5, 9.5, 1 H), 5.23 (dd, J =5.5, 1.5, 1 H), 4.31 (s, 2 H), 4.31-4.17 (m, 2 H), 3.64-3.59 (m, 1 H), 3.35 (m, 2 H), 2.57 (m, 1 H), 2.13 (m, 1 H), 2.00 (m, 2 H), 1.76 (m, 2 H), 1.59 (m, 2 H), 1. 48 (m, 2 H). ^{13}C NMR (125 MHz, $CDCl_3$): δ 131.38, 65.54, 55.72, 37.42, 29.74, 27.46, 14.45.

FT-IR (THF): 1853, 1783, 1713, 1622, 1528 cm^{-1}. HRMS-ESI (*m/z*) $[M + H]^+$ Calcd for $C_{16}H_{25}N_3O_6S$: 388.16; found: 388.15.

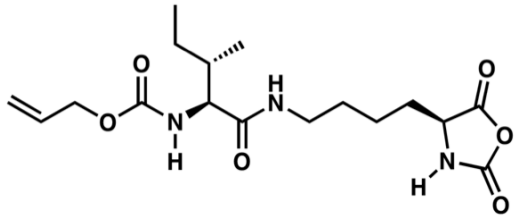

***N*,-(allyloxycarbonyl-L-isoleucyl)-L-lysine-*N*-carboxyanhydride (4b).** Purified by flash column chromatography using gradient elution (10:1 Hex:THF to 1:1 Hex:THF to 2:3 Hex:THF to 1:3 Hex:THF to THF); 240 mg white solid isolated (63 % yield). ^{1}H NMR (500 MHz, $CDCl_3$): δ 7.49 (s, 1 H), 6.17 (s, 1H), 5.92 (m, 1 H), 5.34-5.25 (m, 2 H), 5.25(dd, J = 10, J = 1.3, 1 H), 4.61 (s, 2 H), 4.29-4.27 (dd, J = 15, J= 1.2, 1H), 3.90 (m, 1 H), 3.36-3.34 (m, 1 H), 3.30-3.29 (m, 1 H), 2.05 (m, 1H), 1.66 (m, 1 H), 1.48-1.15 (m, 6 H), 1.18-1.15 (m, 1H), 0.97-0.93 (m, 6 H). ^{13}C NMR (125 MHz, $CDCl_3$): δ 172.22, 170.38, 156.83, 152.43, 132.44, 118.09, 66.37 60.53, 57.43, 38.67, 36.81, 31.28, 28.51, 24.99, 21.84, 15.74, 11.30. FT-IR (THF): 1856, 1789, 1723, 1679, 1652 cm^{-1}. HRMS-ESI (*m/z*) $[M + Na]^+$ Calcd for $C_{17}H_{27}N_3NaO_6$: 392.18; found: 392.18.

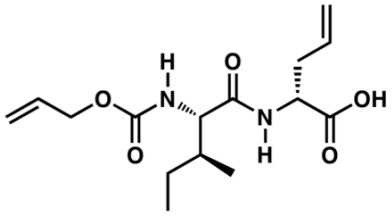

***N*-allyloxycarbonyl-L-isoleucine-L-allylglycine**. No further purification required; 4.10 g isolated as a white solid (74% yield). ^{1}H NMR (500 MHz, DMSO): δ 12.65 (s, 1 H),

8.16-8.11 (dd, 1 H), 7.22-7.16 (dd, 1 H), 5.91 (m, 1 H), 5.87 (s, 1 H), 5.30 (dd, 1 H), 5.17 (dd, 1 H), 5.10-5.03 (m, 3 H), 4.47 (s, 2 H), 4.28 (m, 1 H), 3.91 (m, 1 H), 2.50 (m, 1 H), 2.36 (m, 1 H), 1.75 (m, 1 H), 1.55 (m, 1 H), 1.13 (m, 1 H), 1.96 (d, 3 H), 1.75 (t, 1 H).

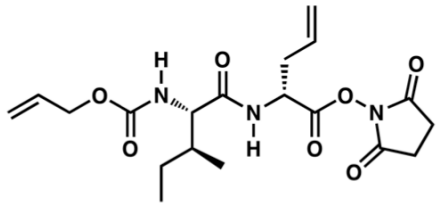

***N*-allyloxycarbonyl-L-isoleucyl-L-allylglycine-*N*-hydroxysuccinimide ester**. Purified by flash column chromatography using 1:1 DCM: EtOAc (R_f = 0.60); 3.02 g isolated of colorless oil (82 % yield). ^{1}H NMR (500 MHz, $CDCl_3$): δ 6.58-6.41 (dd, 1 H), 5.90 (m, 1 H), 5.80 (m, 1 H), 5.32-5.21 (m, 4 H), 5.05 (m, 1 H), 4.57 (s, 2 H), 4.13-4.04 (m, 1 H), 2.85 (s, 4 H), 2.71 (s, 2 H), 1.92 (m, 1 H), 1.87-1.81 (m, 1 H), 1.52-1.16 (m, 2 H) 1.10-0.86 (m, 6 H), FT-IR (THF): 2974, 2858, 1745, 1723, 1687 cm^{-1}; HRMS-ESI (*m/z*) $[M + Na]^+$ Calcd for $C_{19}H_{27}N_3O_7Na$, 432.17; found 432.17.

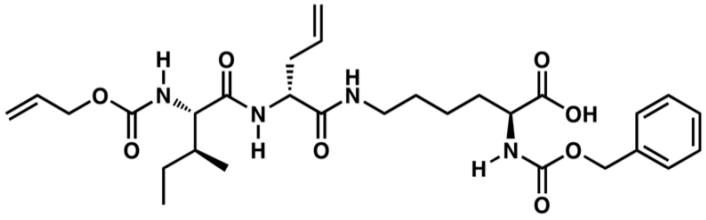

***N*-allyloxycarbonyl-L-isoleucyl-allylglycine-α-carboxybenzyl-L-lysine.** No further purifi-cation necessary. Isolated as a white solid (2.04 g, 53 %). ^{1}H NMR (500 MHz, DMSO: D_2O): δ 5.89 (m, 1 H), 5.68 (m, 1 H), 5.29 (dd, 1 H), 5.17 (dd, 1 H), 5.15-4.97 (m, 4 H), 4.46 (s, 2 H), 3.89-3.84 (m, 2 H), 3.03-2.91 (m, 2 H), 2.43-2.17 (m, 2 H), 1.67-

1.55 (m, 4 H), 1.39-1.08 (m, 5 H), 0.79 (m, 6 H), FT-IR (DCM): 2972, 2862, 1722, 1658, 1538 cm^{-1}HRMS-ESI (*m/z*) $[M + H]^+$ Calcd for $C_{29}H_{43}N_4O_8$, 575.31; found 575.31.

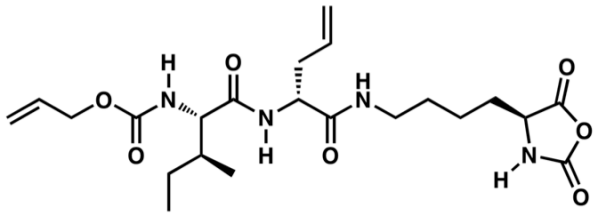

***N*-allyloxycarbonyl-L-isoleucyl-L-allylglycine-L-lysine-*N*-carboxyanhydride.**

Purified by flash column chromatography using the same gradient elution solvents as above. 251 mg obtained, isolated as a white solid (79 % yield).^{1}H NMR (500 MHz, $CDCl_3$): δ 8.18 (s, 1H), 7.86 (s, 1H), 6.73 (s, 1 H), 6.34 (s, 1 H), 5.91-5.89 (m, 1H), 5.74 (m, 1H); FT-IR (THF): 1851, 1780, 1690, 1637, 1534 cm^{-1}. HRMS-ESI (*m/z*) $[M + H]^+$ Calcd for $C_{22}H_{35}N_4O_7$, 467.25; found 467.25.

General procedure for the polymerization of K^{AM} NCA. All polymerization reactions were performed in a dinitrogen filled glove box. To a solution of K^{AM} NCA (15 mg, 38.7 mmol) in dry THF (375 μL) was rapidly added, via syringe, a solution of $(PMe_3)_4Co$ in dry THF (28 μL, 1.55 mmol). The reaction was stirred at room temperature and polymerization progress was monitored by removing small aliquots for analysis by FTIR. Polymerization reactions were generally complete within 1 hour. Reactions were removed from the drybox, all THF was removed, and the polypeptide was washed with 100 mM HCl (2 x 15 mL), centrifuged for 5 minutes at 3000 rpm and the supernatent

was removed. The white polypeptide was washed with 15 mL water and then lyophilized to yield poly(K^{AM}) as a fluffy white solid (12 mg, 94 % yield). ^{1}H NMR (500 MHz, TFA-d): δ 5.87 (s, 1 H), 5.27 (s, 2H), 4.60 (s, 3 H), 3.36 (s, 2 H), 2.70 (s, 2 H), 2.16 (s, 3 H), 1.87-1.63 (s, 2 H), 1.62- 1.48 (s, 3 H). FT-IR (THF): 3095, 2922, 1650,1622, 1541, 1528 cm^{-1}.

General Procedure for Endcapping of poly(K^{AM}) with poly(ethylene glycol) and Molecular Weight Determination by Endgroup Analysis. The general procedure for polymerization of K^{AM} NCA was followed. Upon completion of the reaction, as confirmed by FTIR, a solution of a-methoxy-w-isocyanoethyl-poly(ethylene glycol), PEG-NCO (MW = 2000 Da), in THF (5 equiv per $(PMe_3)_4Co$) was added to the polymerization reaction in a dinitrogen filled glove box. The reaction was stirred overnight at room temperature and then removed from the drybox, all THF was removed, and the polypeptide was washed with 100 mM HCl (2 x 15 mL) to remove unconjugated PEG, centrifuged for 5 minutes at 3000 rpm and the supernatent was removed. The white polypeptide was washed with 15 mL water and then lyophilized to yield PEG-endcapped poly(K^{AM}) as a fluffy white solid (91 % yield). To determine poly(K^{AM}) molecular weights (M_n), ^{1}H NMR spectra were obtained in deuterated trifluoroacetic acid (TFA-*d*). Since it has been shown that end-capping is quantitative for $(PMe_3)_4Co$ initiated NCA polymerizations when excess isocyanate is used,[5] integrations of methioninyl methyl and methylene resonances versus the polyethylene glycol resonance at δ 3.64 could be used to obtain poly(K^{AM}) lengths (see example in spectral data section).

B. Sample diblock copolypeptide syntheses

Poly(γ-carboxybenzyl-L-Lysine)-*block*-poly(*N*$_\varepsilon$-(allyloxycarbonyl-L-methionyl)-L-lysine), Poly(K)-*b*-poly(K^{AM}). All polymerization reactions were performed in a dinitrogen filled glove box. A solution of $(PMe_3)_4Co$ in THF (71 µL, 3.91 mmol) was added to a solution of *N*$_e$-carboxybenzyl-L-Lysine NCA (K NCA) (20 mg, 0.0652 mmol) in THF (1.0 mL). After 1 h, the polymerization reaction was complete as determined by FTIR. An aliquot of poly(Z-L-lysine) was removed and analyzed by GPC/LS (M_n = 18700, M_w/M_n = 1.18, DP = 71). K^{AM} NCA (23 mg, 0.059 mmol) was then added to the stirring solution of poly(K). The reaction was stirred for an additional 1 h after which all NCA was consumed. An aliquot of poly(K)-b-poly(K^{AM}) was removed from the reaction and analyzed by GPC/LS (M_n = 43000, M_w/M_n = 1.12, DP = 142). The reaction mixture was concentrated to dryness and the copolypeptide was removed from the glovebox. The copolypeptide was dissolved in minimal THF (250 µL), and precipitated by the slow addition of 100 mM aqueous HCl (3 x 15 mL) followed by centrifugation (3000 rpm) for 5 minutes. The supernatants were discarded and the residue was lyophilized to remove remaining water, giving the product as a white fluffy solid. (35.2 mg, 99 % yield). ^{1}H NMR (500 MHz, $CDCl_3$): δ 7.24 (m, 5 H), 5.85 (bs, 1 H), 5.28 (m, 2 H), 5.11 (s, 2 H), 4.58 (m, 4 H), 3.61 (s, 1 H), 3.34 (bs, 2 H), 3.14 (bs, 2 H), 2.70 (bs, 2 H), 2.20 (m, 4 H), 1.77-1.35 (m, 11 H) . FT-IR (THF): 3095, 2922, 1741, 1651, 1540 cm^{-1}.

Poly(*N*$_\varepsilon$-(allyloxycarbonyl-L-methionyl)-L-lysine)-*block*-poly(γ-carboxybenzyl-L-Lysine), Poly(K^{AM})-*b*-poly(K). A solution of $(PMe_3)_4Co$ in THF (55 µL, 3.1 mmol) was added to a solution of K^{AM} NCA (60 mg, 0.15 mmol) in THF (1.5 mL). After 1 h, the polymerization reaction was complete as determined by FTIR. The reaction mixture was divided into 6 equal portions (0.025 mmol each) and two aliquots of poly(K^{AM}) was

reacted with excess PEG-NCO (MW = 2000 Da) and analyzed by ^{1}H NMR and GPC/LS (M_n = 31200, M_w/M_n = 1.11, DP = 91). K NCA (8 mg, 0.025 mmol) was then added to the stirring solution of poly(K^{AM}) (0.025 mmol, 1 aliquot). The reaction was stirred for an additional 1 h after which all NCA was consumed and analyzed by GPC/LS (M_n = 55000, M_w/M_n = 1.12, DP = 184). The reaction mixture was concentrated to dryness and the copolypeptide was removed from the glovebox. The polymer was then dissolved in minimal THF (250 μL), and precipitated by the slow addition of 100 mM aqueous HCl (3 x 15 mL) followed by centrifugation (3000 rpm) for 5 minutes. The supernatants were discarded and the residue was lyophilized to remove remaining water, giving the product as a white fluffy solid. (15 mg, 100 % yield). ^{1}H NMR (500 MHz, $CDCl_3$): δ 7.31 (m, 5 H), 5.92 (bs, 1 H), 5.43-5.19 (m, 3 H), 4.64 (m, 4 H), 3.47 (m, 2.4 H), 3.01 (bs, 2 H), 2.91 (bs, 2 H), 2.23 (bs, 4 H), 1.87 (bs, 4 H), 1.55 (bs, 3 H). FT-IR (THF): 3095, 2922, 1741, 1651, 1540 cm^{-1}.

C. Activation and reactivity of poly(K^{AM})

General procedure for activating poly(K^{AM}) using Ni(0).[6] In the glove box, poly(K^{AM}) (0.077 mmol of K^{AM} residues) was freshly prepared, most of the THF then removed under vacuum, and the residue dissolved in DMF (5 mL). In a separate vial $Ni(COD)_2$ (21 mg, 0.077 mmol, 1.0 eq. per K^{AM} residue) was dissolved in minimal THF (500 μL). 1,2-Bis(dimethylphosphino)ethane (dmpe) (26 mL, 0.15 mmol, 2.0 eq. per Ni) was then added to the $Ni(COD)_2$ solution followed by stirring for 10 minutes. The poly(K^{AM}) solution was then combined with the Ni(0) solution, changing it from a yellow to deep orange color. This solution was transferred to a thick walled glass tube that was sealed

with a teflon cap and heated overnight (15 h) at 80 ^{o}C. The resulting activated poly(K^{AM}) solution was cooled to ambient temperature and then used directly for further reactions and polymerizations.

Quenching of activated poly(K^{AM}) with HCl. Excess aqueous 4.0 M HCl (4 mL) was added to a THF (500 μL) and DMF(2.0 mL) solution of activated poly(K^{AM}) (0.103 mmol). The reaction was stirred for 2 h after which the solution was dialyzed (MWCO = 2000) against water and EDTA (0.01 M). After several water changes, the polymer precipitate was dialyzed against HCl (0.02 M), after which the polymer product became fully water soluble. After several water changes the product was dialyzed against pure deionized water. The sample was lyophilized and the product analyzed using ^{1}H NMR, which showed that the resonances from the allyloxycarbonyl groups of poly(K^{AM}) had essentially disappeared, indicating near complete activation of the allyloxycarbonyl side-chains (Figure 3). ^{1}H NMR (500 MHz, D_2O): δ 4.11 (2 H), 3.35 (2 H), 2.59-2.50 (2 H), 2.19 (1 H), 2.14 (3 H), 1.94 (2 H), 1.59 (2 H), 1.43 (2 H).

Stability of allyloxycarbonyl groups to 4.0 M HCl. To ensure any unreacted allyloxycarbonyl groups in the poly(K^{AM}) sample above are stable against hydrolysis by 4.0 M HCl alone, N_e-(allyloxycarbonyl-L-methionyl)-N_α-carboxybenzyl-L-lysine (**3a**) **(**100 mg, 0.20 mmol) was dissolved in 5.0 mL THF. Excess 4.0 M HCl (5.0 mL) was added and the reaction stirred at 21 ^{o}C for 2 h. THF was removed under vacuum and the aqueous layer was then extracted with EtOAc and dried with $MgSO_4$, filtered, and concentrated. ^{1}H NMR analysis showed that resonances of the allyloxycarbonyl group remained intact: 5.88-5.83 ppm (1 H, m) and 5.29-5.10 ppm (2H, dd).

General procedure for quenching of activated poly(K^{AM}) with PEG-NCO (MW = 350 or 1000 Da).[95] PEG-NCO (MW = 1000) (76.0 mg, 0.076 mmol) in DMF (3.0 mL) was added to a stirring solution of activated poly$(K)_{60}$-*b*-poly$(K^{AM})_{17}$ (0.427 mL, 0.015 mmol of activated alloc groups) in DMF. The resulting solution was stirred overnight at room temperature. The reaction mixture was concentrated under vacuum, and the polymer residue was dissolved in Millipore water and dialyzed (MWCO = 6,000-8,000) against aqueous EDTA (0.01 M), followed by Millipore water for 5 days, changing water twice a day. The sample was then lyophilized to give the product as a white solid (32 mg, 98 % yield). ^{1}H NMR analysis of the sample was used to determine the degree of PEG end-capping of activated alloc groups. ^{1}H NMR (500 MHz, d-TFA): δ 7.26 (br s, 5 H), 5.13 (br s, 2 H), 4.55 (br s, 2 H), 3.88 (br s, 59 H), 3.16 (br s, 2 H), 2.14 (br s) 1.79-1.72 (br m), 1.49-1.34 (br m).

D. Growth of cylindrical brush copolypeptides from activated poly(K)-*b*-poly(K^{AM})

Preparation of activated poly$(K)_{60}$-*b*-poly$(K^{AM})_{17}$ for cylindrical brush growth. All polymerization reactions were performed in a dinitrogen filled glove box. A solution of $(PMe_3)_4Co$ in THF (297 μL, 16.1 mmol) was added to a solution of K NCA (100 mg, 0.33 mmol) in THF (2 mL). After 1 h, the polymerization reaction was complete as determined by FTIR. An aliquot of poly(K) was removed and analyzed by GPC/LS (M_n = 15650, M_w/M_n = 1.11, DP = 60). K^{AM} NCA (32 mg, 0.0827 mmol) in THF (527 μL) was then added to the stirring solution of poly(K). The reaction was stirred for an additional

1 h after which all NCA was consumed. An aliquot of poly(K)$_{60}$-*b*-poly(K^{AM})$_{17}$ was removed for analysis by GPC/LS and ^{1}H NMR (K^{AM} segment: M_n = 5800, M_w/M_n = 1.09, DP = 17). Poly(K)$_{60}$-*b*-poly(K^{AM})$_{17}$ (0.077 mmol of K^{AM} residues) in THF was then concentrated under vacuum and then diluted in DMF (2.0 mL). In a separate vial, Ni(COD)$_2$ (21 mg, 0.077 mmol, 1 eq. per K^{AM} residue) was dissolved in minimal THF (500 μL) and dmpe (26 μL, 0.15 mmol, 2 eq. per Ni) was then added. The poly(K)$_{60}$-*b*-poly(K^{AM})$_{17}$ solution was then combined with the Ni(0) solution, changing it from a yellow to deep orange color. This solution was transferred to a thick walled glass tube that was sealed with a teflon cap and heated overnight (15 h) at 80 ^{o}C. The resulting activated poly(K)$_{60}$-*b*-poly(K^{AM})$_{17}$ solution was cooled to ambient temperature and then used directly for polymerizations.

Preparation of cylindrical brush polypeptides: Poly(γ-carboxybenzyl-L-Lysine)$_{60}$-*block*-poly(*N*$_e$-(poly(δ-benzyl-L-glutamate)-*graft*-L-methionyl)-L-lysine)$_{17}$, Poly(K)$_{60}$-*b*-poly(K^{MPBLG})$_{17}$. δ-Benzyl-L-glutamate NCA, E NCA, (68.0 mg, 0.258 mmol) in DMF (1.7 mL) was added to activated poly(K)$_{60}$-*b*-poly(K^{AM})$_{17}$ solution (0.0258 mmol *of activated nickel amidoamidate groups*) resulting in a color change to deep orange. The solution was then stirred overnight (15 h) at 21 ^{o}C to ensure reaction completion. The sample was concentrated under reduced pressure and precipitated by addition to 100 mM HCl (2 x 15 mL) followed by centrifugation. The sample was washed with water (1 x 15 mL), centrifuged and the product isolated by lyophilization as a white solid

(75.6 mg, 87 % yield). ^{1}H NMR (500 MHz, d-TFA): δ 7.20 (m), 5.11 (m), 4.65 (bs), 6.43 (m), 3.15 (bs), 2.43 (bs), 2.14 (bs), 1.93 (bs), 1.47 (bs), 1.33 (bs).

Deprotection of cylindrical brush copolypeptides using TMSI. Poly(N_ε-(poly(δ-benzyl-L-glutamate)$_{44}$-*graft*-L-methionyl)-L-lysine)$_{12}$, poly(K^{MPBLG}), brush copolypeptide (80 mg, 0.673 μmol) was dissolved in 10 mL DCM. An excess of TMSI (222 μL, 1.64 mmol) was added and the reaction was refluxed for 16 h. The deprotected polypeptide was precipitated with 20 mL hexanes and the product was redissolved in water and dialyzed (2000 MWCO dialysis tubing) against EDTA (0.01 M), followed by basic water (NaOH, pH = 8) then Millipore water for 4 days. The product poly(N_ε-(poly(L-glutamatic acid)$_{44}$-*graft*-L-methionyl)-L-lysine)$_{12}$, poly(K^{MPGA}), was isolated by lyophilization as a white solid (31 mg, 65 % yield). ^{1}H NMR (500 MHz, D_2O): δ 4.18-4.17 (m, 1 H), 2.14-2.05 (m, 2 H), 1.95-1.89 (bs, 1 H), 1.79-1.73 (bs, 1 H).

E. Cleavage of polypeptides at methionine residues using cyanogen bromide

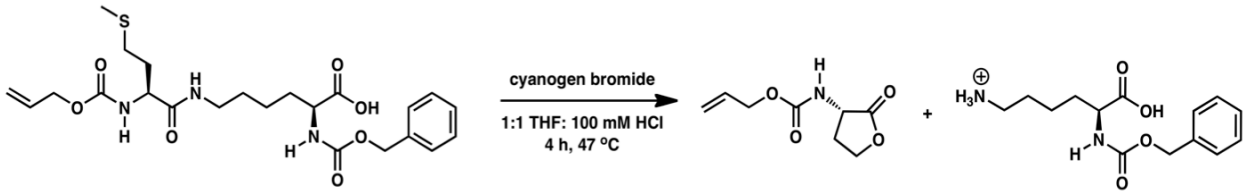

Cleavage of N_e-(allyloxycarbonyl-L-methionyl)-N_α-carboxybenzyl-L-lysine using cyanogen bromide. N_e-(allyloxycarbonyl-L-methionyl)-N_α-carboxybenzyl-L-lysine (114 mg, 0.23 mmol) was dissolved in THF (2.0 mL). Excess cyanogen bromide (6.0 mL, 0.25 M) was added to the solution and the resulting mixture was heated at 47 °C for 4 h.

Next, all THF was removed under reduced pressure and the product homoserine lactone was isolated by extraction of the aqueous layer with EtOAc (3 x 10 mL). The organic layer was separated, dried over $MgSO_4$ and concentrated (42 mg, 99 % yield). The homoserine lactone was purified by flash column chromatography in 1:2 Hex:EtOAc with an R_f = 0.44. After removal of solvents, the homoserine lactone isolated as a white solid (19 mg, 45% yield). ^{1}H NMR (500 MHz, $CDCl_3$): δ 5.91-5.82 (m, 1H), 5.38-5.34 (s, 1H), 5.31-5.25 (d, J = 1.5, 9.5, 1 H), 5.25-5.22 (d, J = 5.5, 1.5, 1 H), 4.61 (d, J = 5.5, 2 H), 4.46 (m, 2 H), 4.27 (m, 1 H). ^{13}C NMR (125 MHz, $CDCl_3$): δ 175.10, 156.10, 132.403, 118.31, 66.31, 65.91, 50.60, 30.53. FT-IR (film in THF): 2924, 1777, 1699, 1527 cm^{-1}. No N_e-(allyloxycarbonyl-L-methionyl)-N_α-carboxybenzyl-L-lysine was observed by TLC or ^{1}H NMR indicating all of the starting material was consumed.

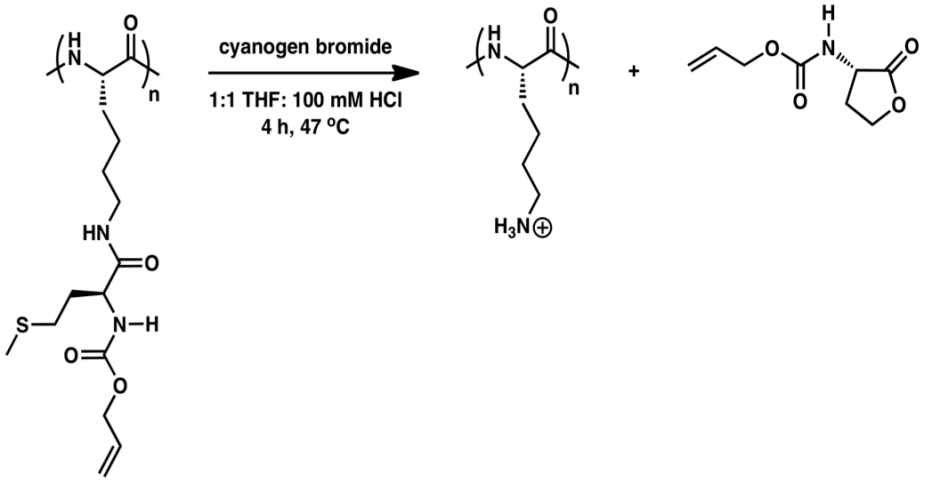

Cleavage of poly(K^{AM}) side-chains using cyanogen bromide. A sample of poly(K^{AM}) (0.145 mmol) was prepared as described above and the resulting polymer solution was further diluted in THF (to a final of volume of 3.5 mL) and removed from the glovebox. Aqueous HCl (7.0 mL, 100 mM) was added to the polymer solution resulting in

precipitation of the polypeptide. Cyanogen bromide solution in THF (4.31 mL , 0.25 M) was added to the polypeptide suspension, which was then heated to 47 ^{o}C for 18 h. After 3 h the initially cloudy reaction mixture became completely clear and colorless. The THF was then removed under reduced pressure. Additional aqueous HCl (10 mL, 100 mM) was added to the reaction mixture followed by EtOAc (7.0 mL). Upon addition of EtOAc, the cloudy aqueous mixture become clear. The homoserine lactone byproduct was isolated and purified using flash column chromatography in 1:2 Hex:EtOAc with an R_f = 0.32 in 1:1 Hex:EtOAc (20 mg, 75 % yield). No poly(K^{AM}) was observed by ^{1}H NMR ($CDCl_3$).

Cleavage of deprotected cylindrical brush polypeptides, poly(K^{MPGA}). A sample of poly(K^{MPGA}) (9.3 mg, 1.1 mmol) was dissolved in 1.90 mL 70% formic acid (aqueous). Cyanogen bromide (88 µL, 0.022 mmol) in 70 % formic acid (0.25 M) was added to the polypeptide solution. The reaction mixture was stirred at 21 ^{o}C for 24 h. Formic acid was removed under reduced pressure and the polypeptide residue was dissolved in freshly prepared PBS buffer (10 mg/ml). The sample, composed primarily of cleaved poly(L-glutamic acid) (PGA) segments, was filtered through a 0.2 µm PTFE filter and analyzed using SDS-PAGE as described below.

Analysis of cleaved PGA segment chain length distributions using SDS-PAGE. Two PGA standards (M_n = 5120, M_w/M_n = 1.05 and M_n = 18900, M_w/M_n = 1.13) were prepared using nickel amidoamidate initiator in DMF, and deprotected using TMSI

following procedures as described above. PGA segments (M_n = 3820, determined by ^1H NMR and GPC/LS as described above) cleaved from a brush copolymer were obtained as described above. Sodium dodecyl sulfate polyacrylamide gel electrophoresis (SDS-PAGE) was carried out on a Mini-PROTEAN Tetra cell electrophoresis system using a 16.5% polyacrylamide Mini-PROTEAN Tris-Tricine Precast Gel to maximize separation of small molecular weight PGA (see Figure 4b) in Tris/Tricine/SDS buffer (100mM Tris, 100mM tricine, 0.1% SDS, pH 8.3, Bio Rad). The PGA samples were visualized using silver staining.

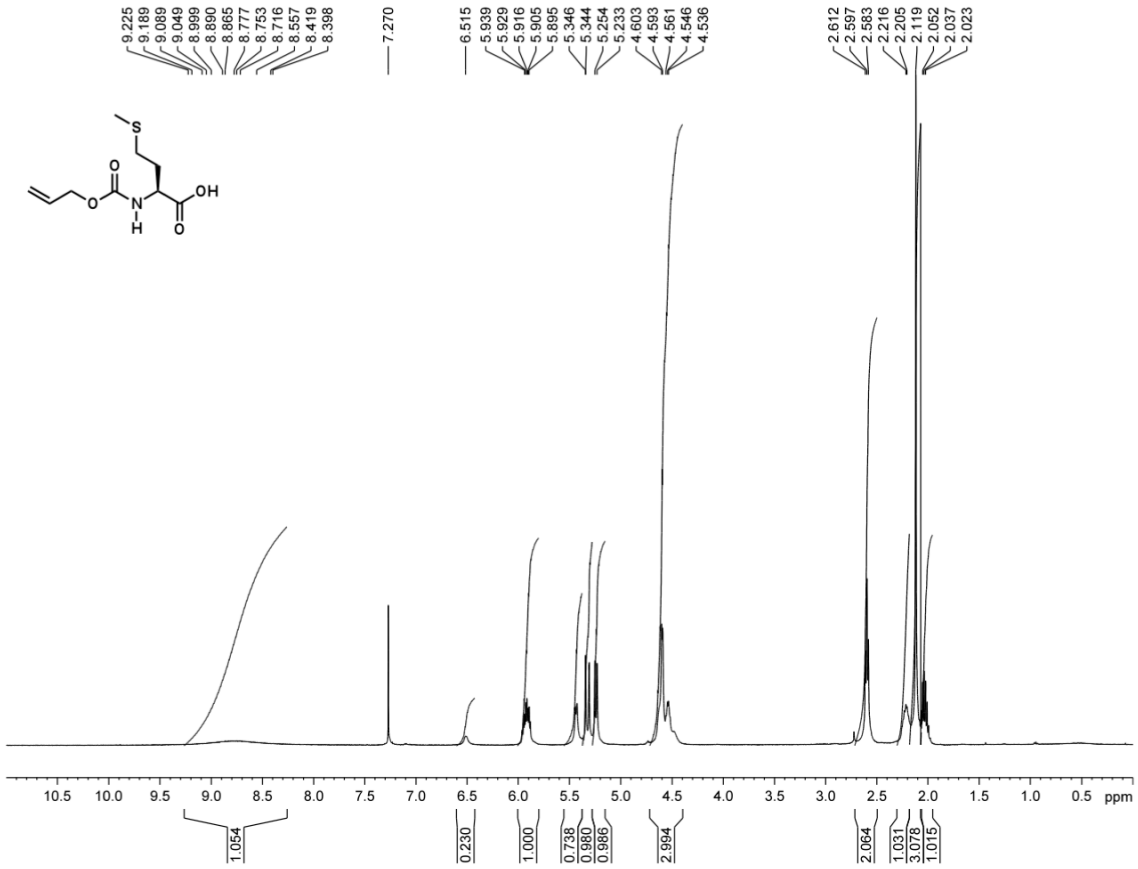
9.225
9.189
9.089
9.049
8.999
8.890
8.865
8.777
8.753
8.716
8.557
8.419
8.398
7.270
6.515
5.939
5.929
5.916
5.905
5.895
5.346
5.344
5.254
5.233
4.603
4.593
4.561
4.546
4.536
2.612
2.597
2.583
2.216
2.205
2.119
2.052
2.037
2.023
S
O
O
N
H
OH
O
10.5 10.0 9.5 9.0 8.5 8.0 7.5 7.0 6.5 6.0 5.5 5.0 4.5 4.0 3.5 3.0 2.5 2.0 1.5 1.0 0.5 ppm
1.054
0.230
1.000
0.738
0.980
0.986
2.994
2.064
1.031
3.078
1.015

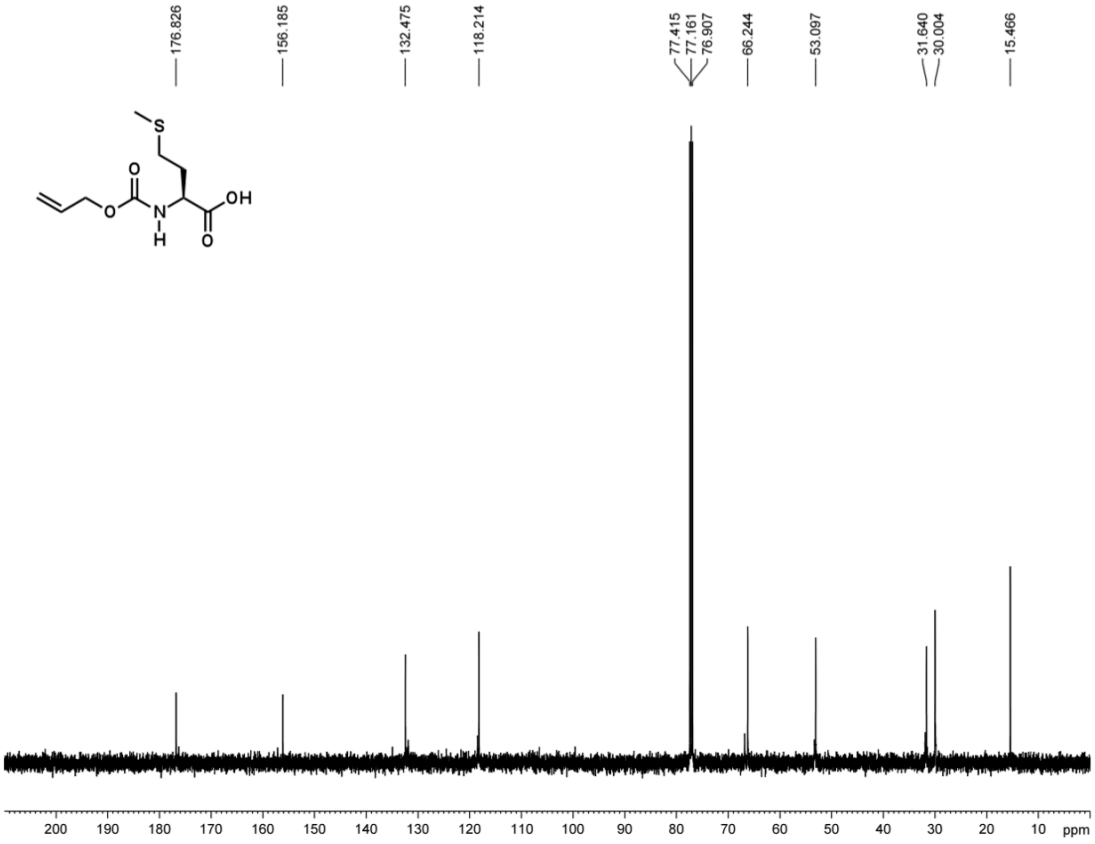
176.826
156.185
132.475
118.214
77.415
77.161
76.907
66.244
53.097
31.640
30.004
15.466
S
O
O
N
H
OH
O
200 190 180 170 160 150 140 130 120 110 100 90 80 70 60 50 40 30 20 10 ppm

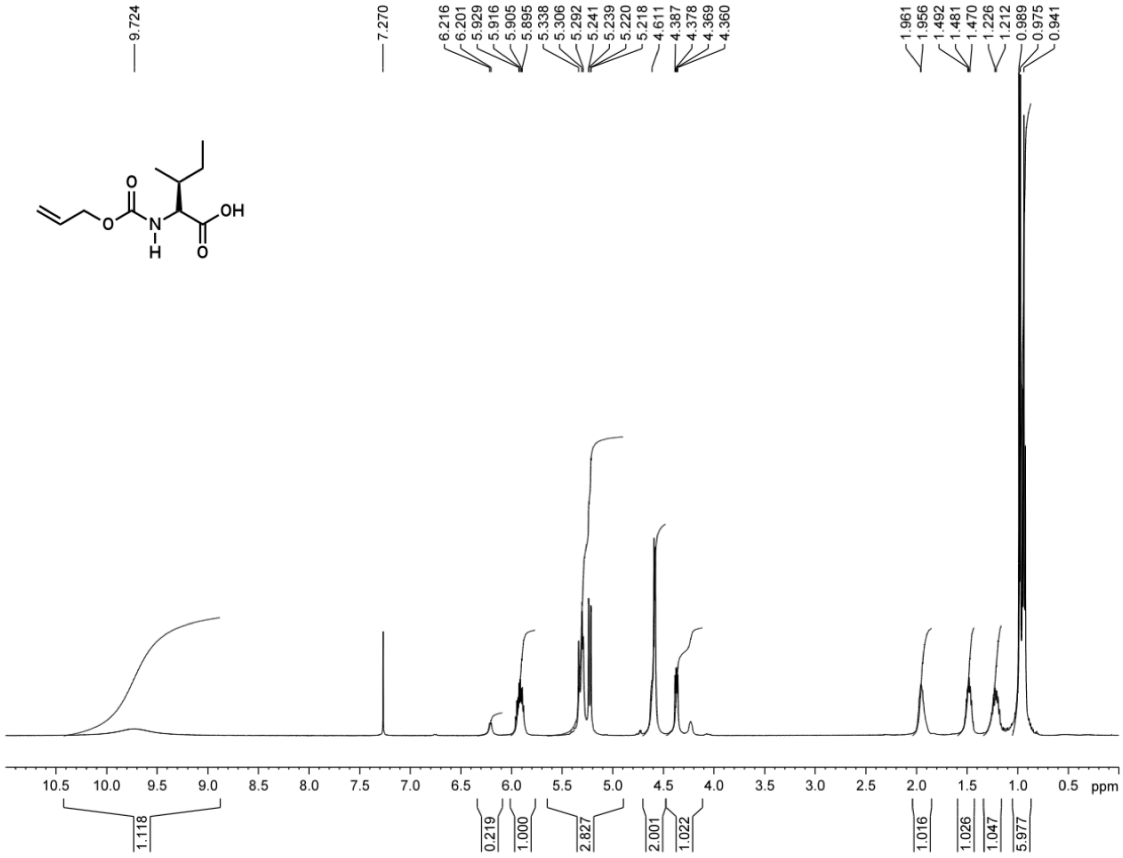
9.724
7.270
6.216
6.201
5.929
5.916
5.905
5.895
5.338
5.306
5.292
5.241
5.239
5.220
5.218
4.611
4.387
4.378
4.369
4.360
1.961
1.956
1.492
1.481
1.470
1.226
1.212
0.989
0.975
0.941
O
O
N
H
O
OH
10.5 10.0 9.5 9.0 8.5 8.0 7.5 7.0 6.5 6.0 5.5 5.0 4.5 4.0 3.5 3.0 2.5 2.0 1.5 1.0 0.5 ppm
1.118
0.219
1.000
2.827
2.001
1.022
1.016
1.026
1.047
5.977

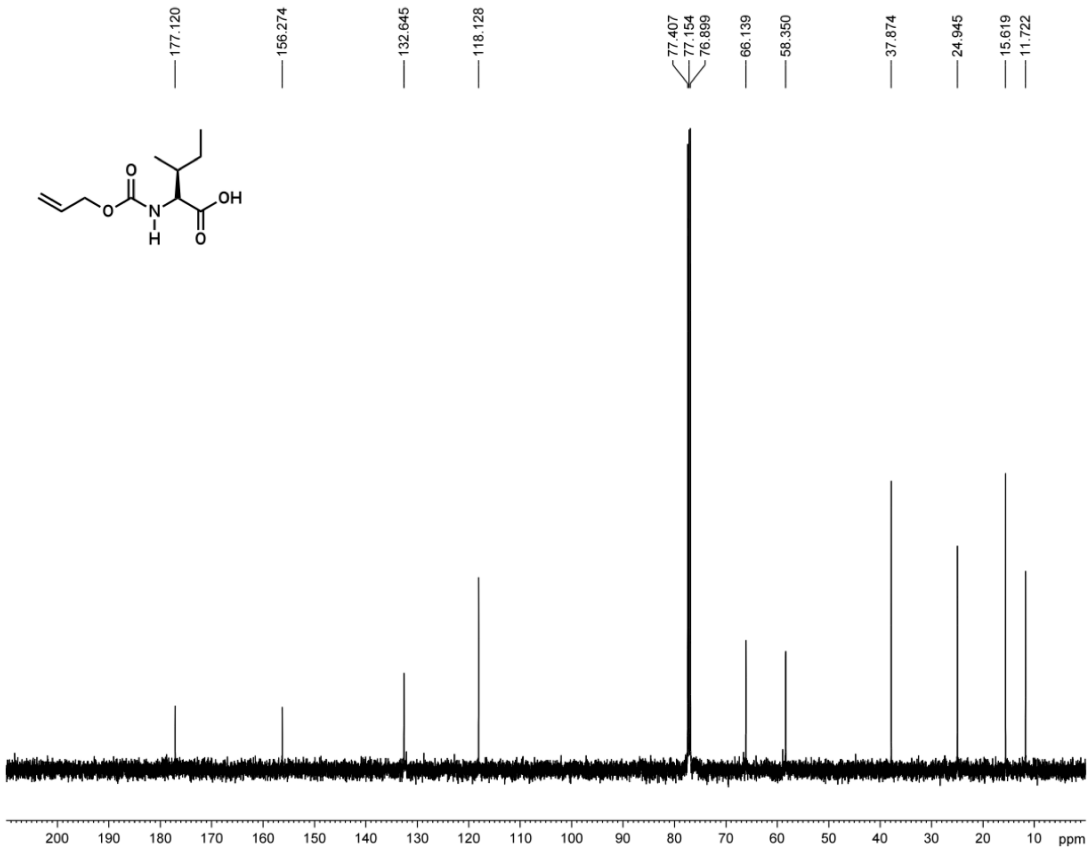
177.120
156.274
132.645
118.128
77.407
77.154
76.899
66.139
58.350
37.874
24.945
15.619
11.722
O
O
N
H
OH
O
200 190 180 170 160 150 140 130 120 110 100 90 80 70 60 50 40 30 20 10 ppm

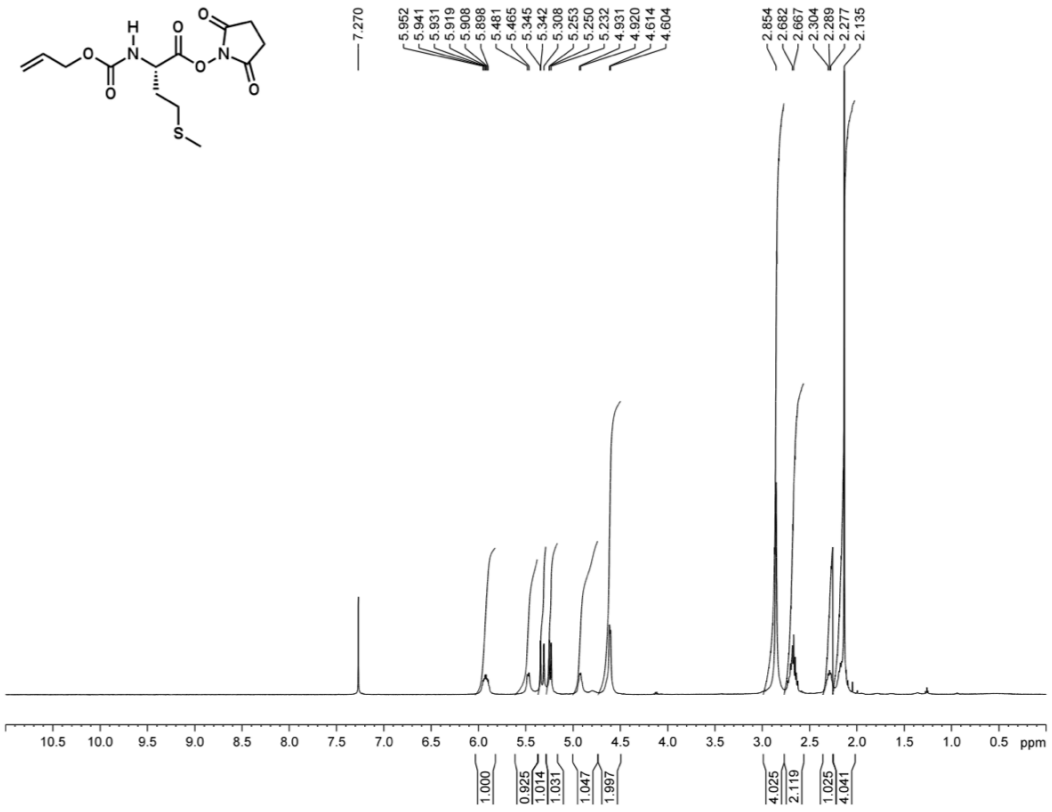
7.270
5.952
5.941
5.931
5.919
5.908
5.898
5.481
5.465
5.345
5.342
5.308
5.253
5.250
5.232
4.931
4.920
4.614
4.604
2.854
2.682
2.667
2.304
2.289
2.277
2.135
10.5 10.0 9.5 9.0 8.5 8.0 7.5 7.0 6.5 6.0 5.5 5.0 4.5 4.0 3.5 3.0 2.5 2.0 1.5 1.0 0.5 ppm
1.000
0.925
1.014
1.031
1.047
1.997
4.025
2.119
1.025
4.041

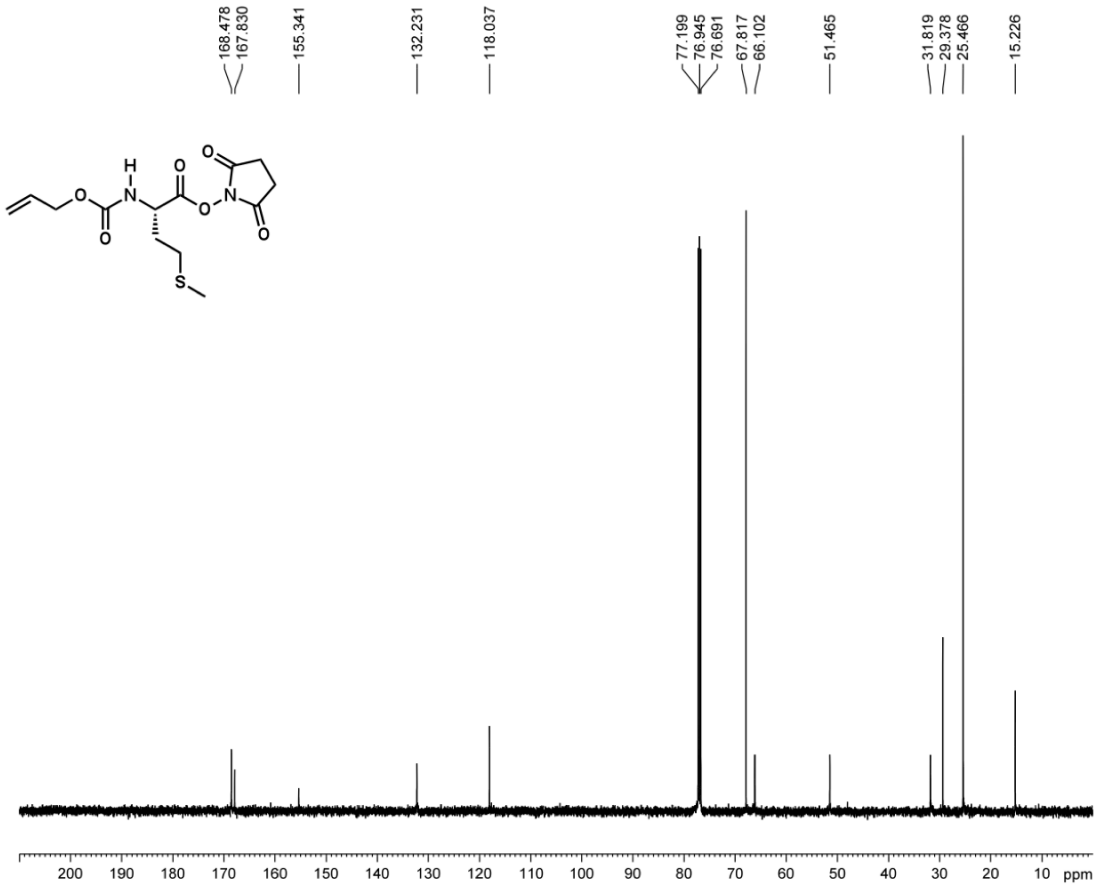
168.478
167.830
155.341
132.231
118.037
77.199
76.945
76.691
67.817
66.102
51.465
31.819
29.378
25.466
15.226
200 190 180 170 160 150 140 130 120 110 100 90 80 70 60 50 40 30 20 10 ppm

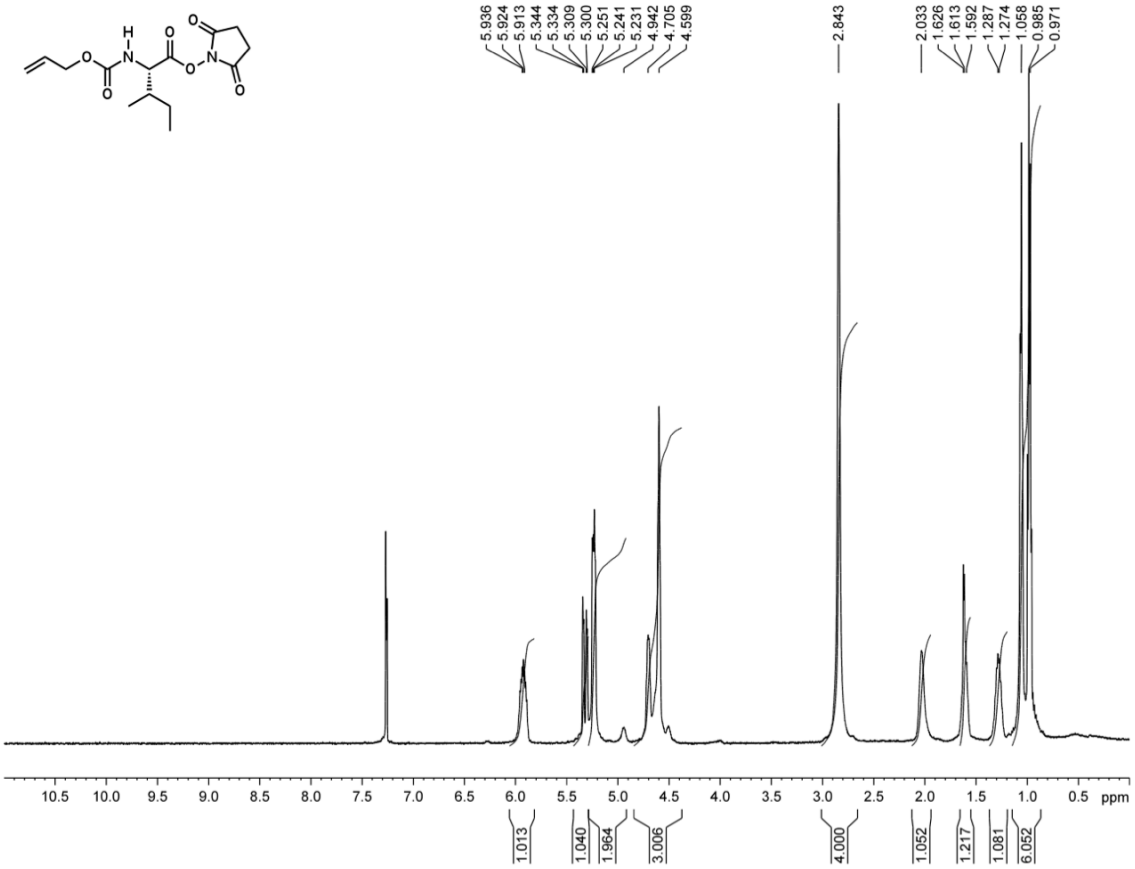
5.936
5.924
5.913
5.344
5.334
5.309
5.300
5.251
5.241
5.231
4.942
4.705
4.599
2.843
2.033
1.626
1.613
1.592
1.287
1.274
1.058
0.985
0.971
10.5 10.0 9.5 9.0 8.5 8.0 7.5 7.0 6.5 6.0 5.5 5.0 4.5 4.0 3.5 3.0 2.5 2.0 1.5 1.0 0.5 ppm
1.013
1.040
1.964
3.006
4.000
1.052
1.217
1.081
6.052

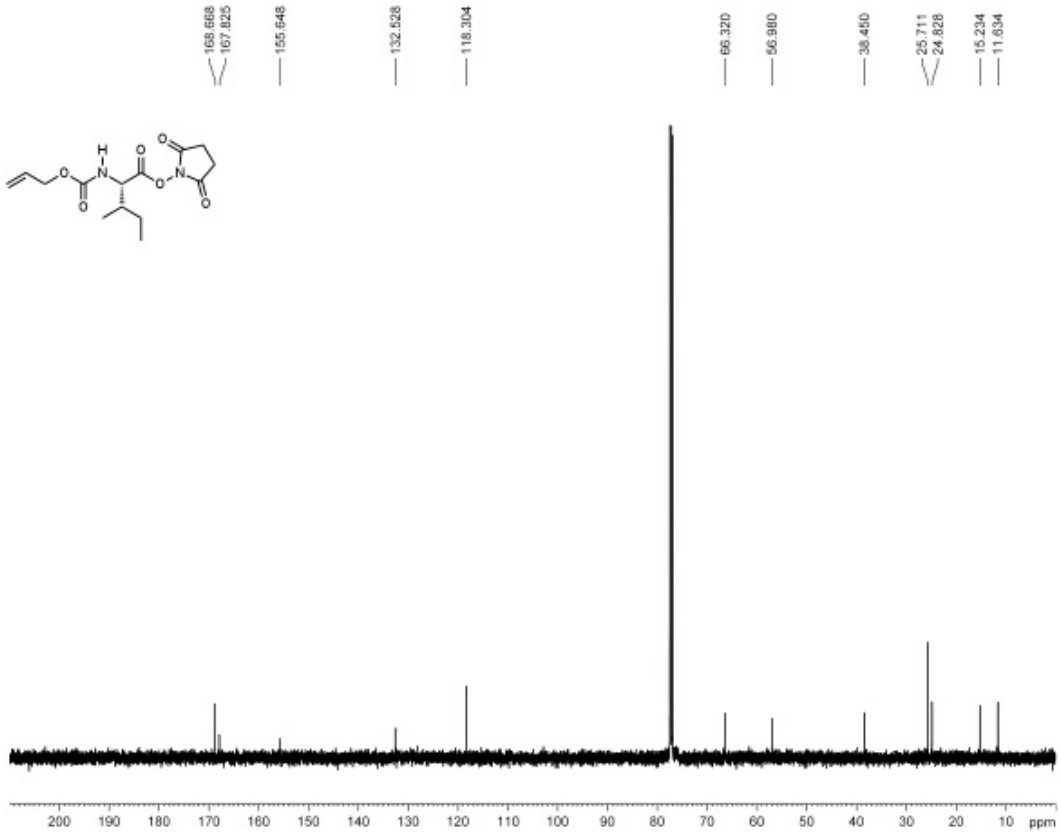
168.668
167.825
155.648
132.528
118.304
66.320
56.980
38.450
25.711
24.828
15.234
11.634
200 190 180 170 160 150 140 130 120 110 100 90 80 70 60 50 40 30 20 10 ppm

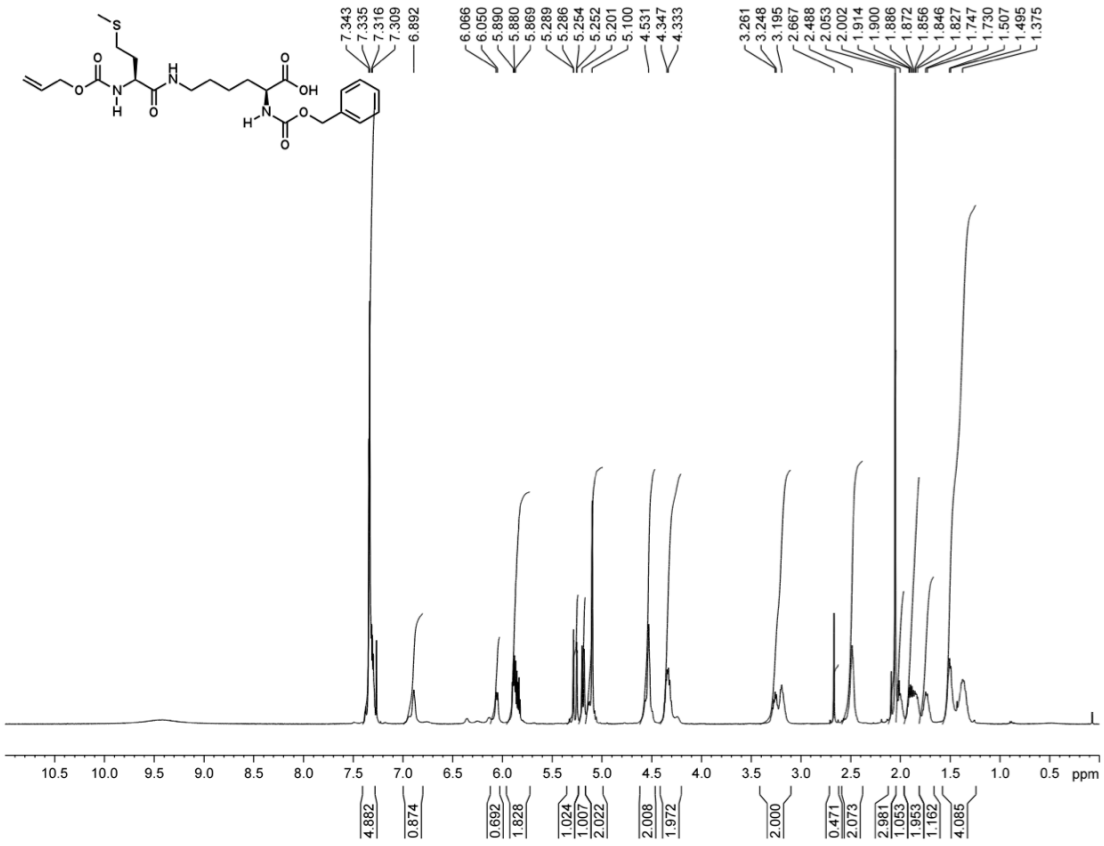
7.343
7.335
7.316
7.309
6.892
6.066
6.050
5.890
5.880
5.869
5.289
5.286
5.254
5.252
5.201
5.100
4.531
4.347
4.333
3.261
3.248
3.195
2.667
2.488
2.053
2.002
1.914
1.900
1.886
1.872
1.856
1.846
1.827
1.747
1.730
1.507
1.495
1.375
10.5 10.0 9.5 9.0 8.5 8.0 7.5 7.0 6.5 6.0 5.5 5.0 4.5 4.0 3.5 3.0 2.5 2.0 1.5 1.0 0.5 ppm
4.882
0.874
0.692
1.828
1.024
1.007
2.022
2.008
1.972
2.000
0.471
2.073
2.981
1.053
1.953
1.162
4.085

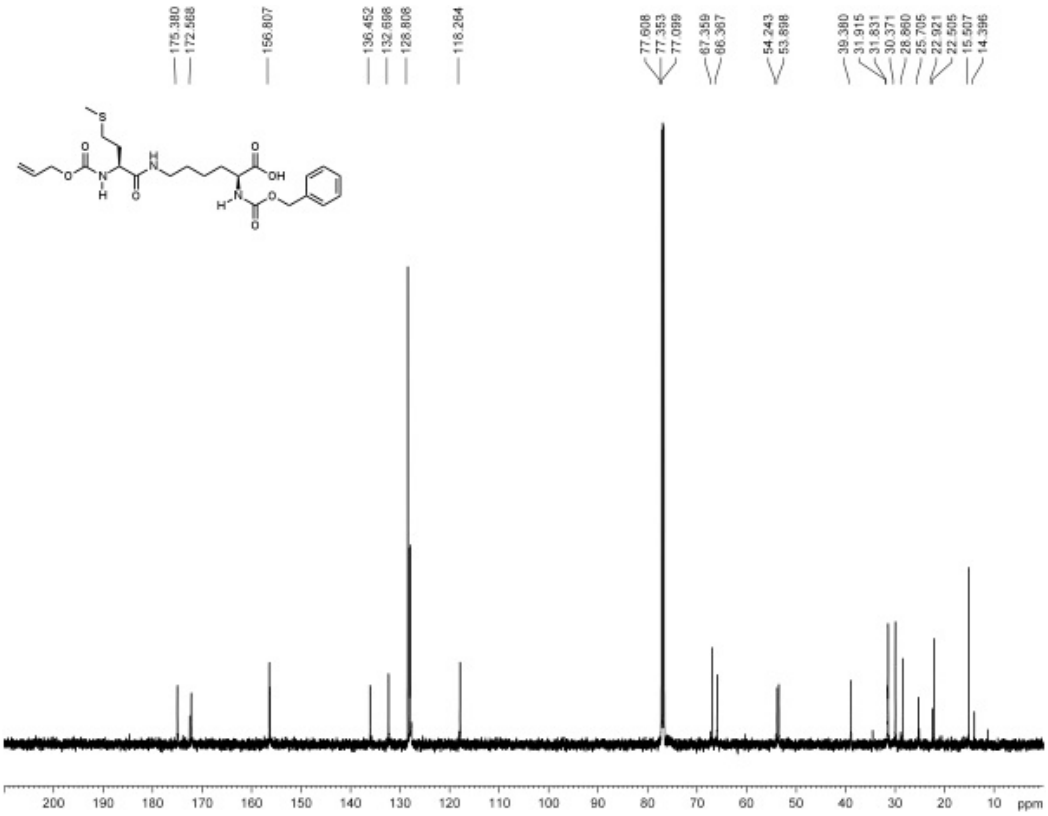
175.380
172.568
156.807
136.452
132.686
128.808
118.264
77.608
77.353
77.099
67.359
66.367
54.243
53.898
39.380
31.915
31.831
30.371
28.860
25.705
22.921
22.505
15.507
14.396
200
190
180
170
160
150
140
130
120
110
100
90
80
70
60
50
40
30
20
10
ppm

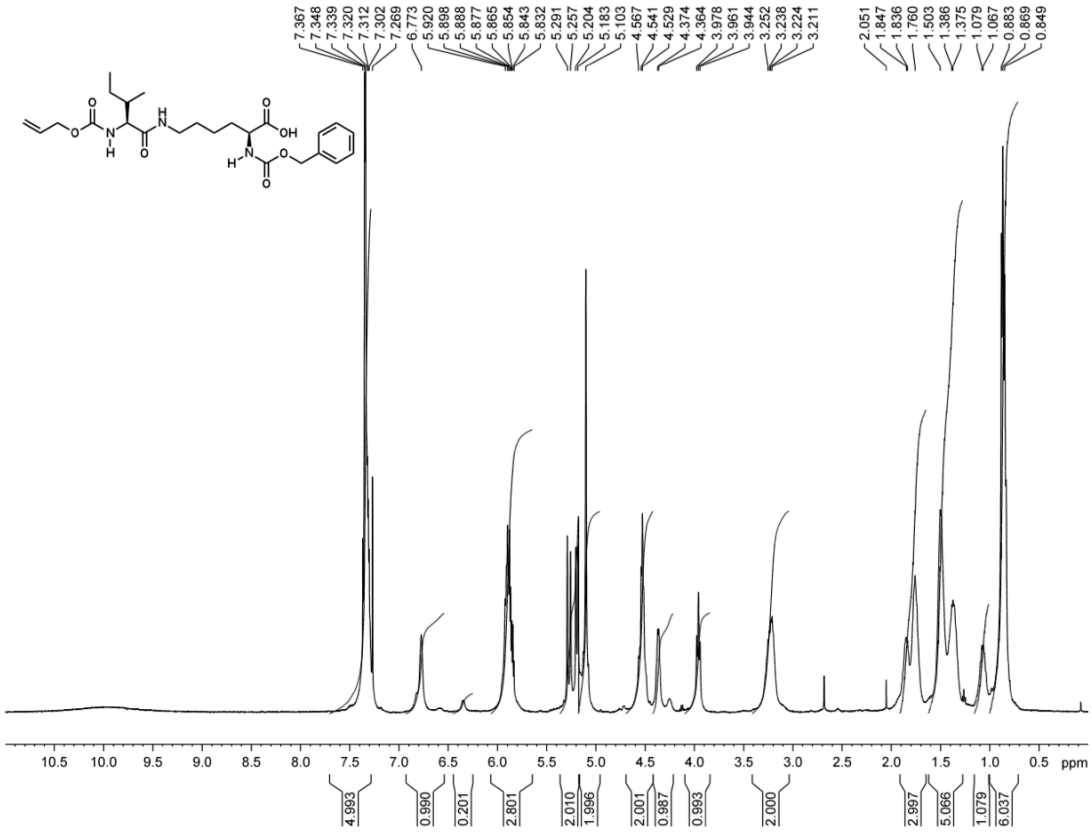
7.367
7.348
7.339
7.320
7.312
7.302
7.269
6.773
5.920
5.898
5.888
5.877
5.865
5.854
5.843
5.832
5.291
5.257
5.204
5.183
5.103
4.567
4.541
4.529
4.374
4.364
3.978
3.961
3.944
3.252
3.238
3.224
3.211
2.051
1.847
1.836
1.760
1.503
1.386
1.375
1.079
1.067
0.883
0.869
0.849
10.5 10.0 9.5 9.0 8.5 8.0 7.5 7.0 6.5 6.0 5.5 5.0 4.5 4.0 3.5 3.0 2.5 2.0 1.5 1.0 0.5 ppm
4.993
0.990
0.201
2.801
2.010
1.996
2.001
0.987
0.993
2.000
2.997
5.066
1.079
6.037

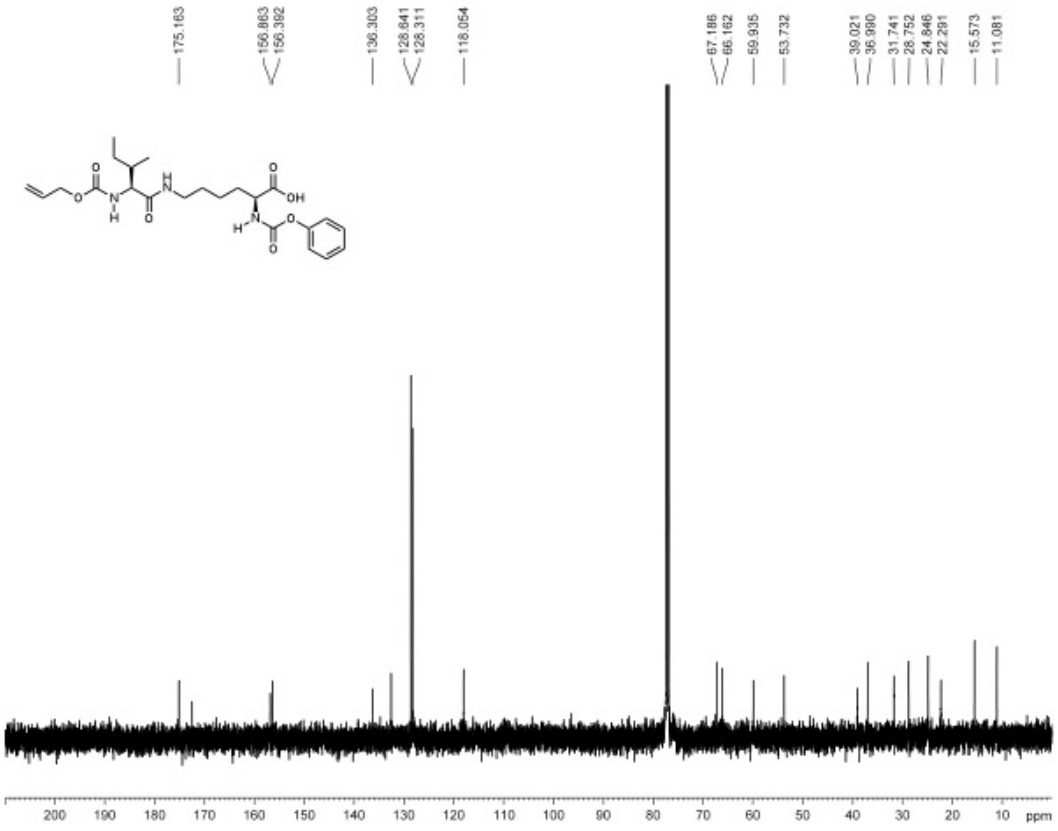
175.163
156.863
156.392
136.303
128.841
128.311
118.054
67.186
66.162
59.935
53.732
39.021
36.990
31.741
28.752
24.846
22.291
15.573
11.081
200 190 180 170 160 150 140 130 120 110 100 90 80 70 60 50 40 30 20 10 ppm

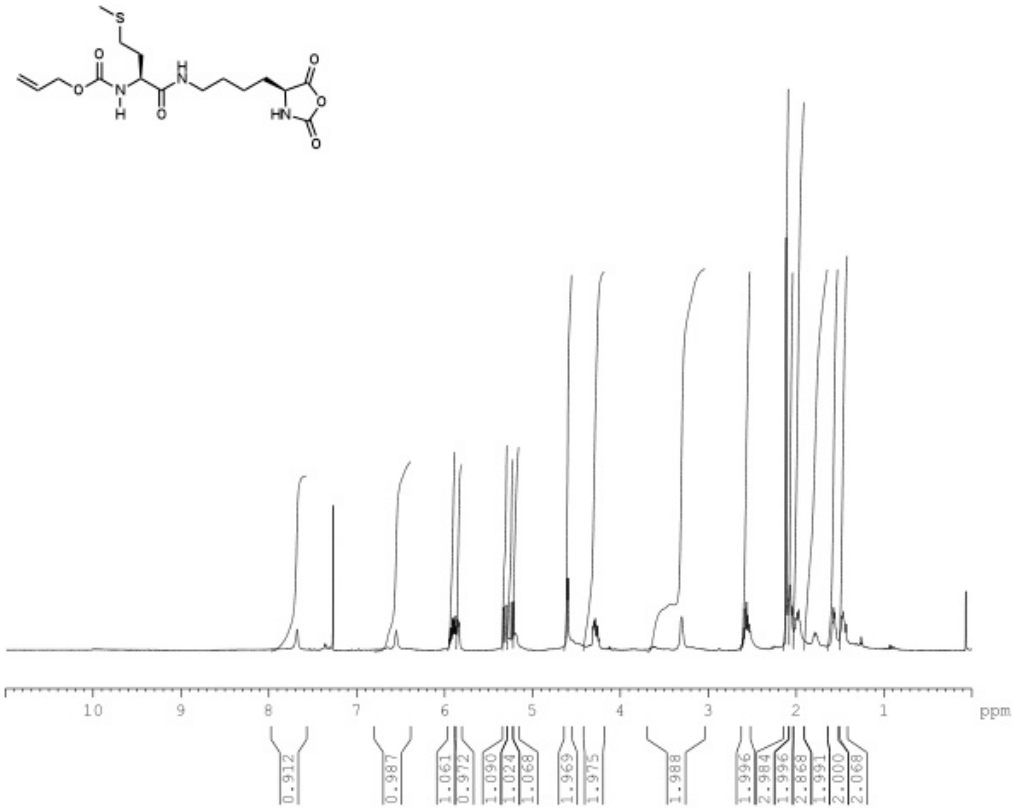
10
9
8
7
6
5
4
3
2
1
ppm
0.912
0.987
1.061
0.972
1.090
1.024
1.068
1.969
1.975
1.988
1.996
2.984
1.996
2.868
1.991
2.000
2.068

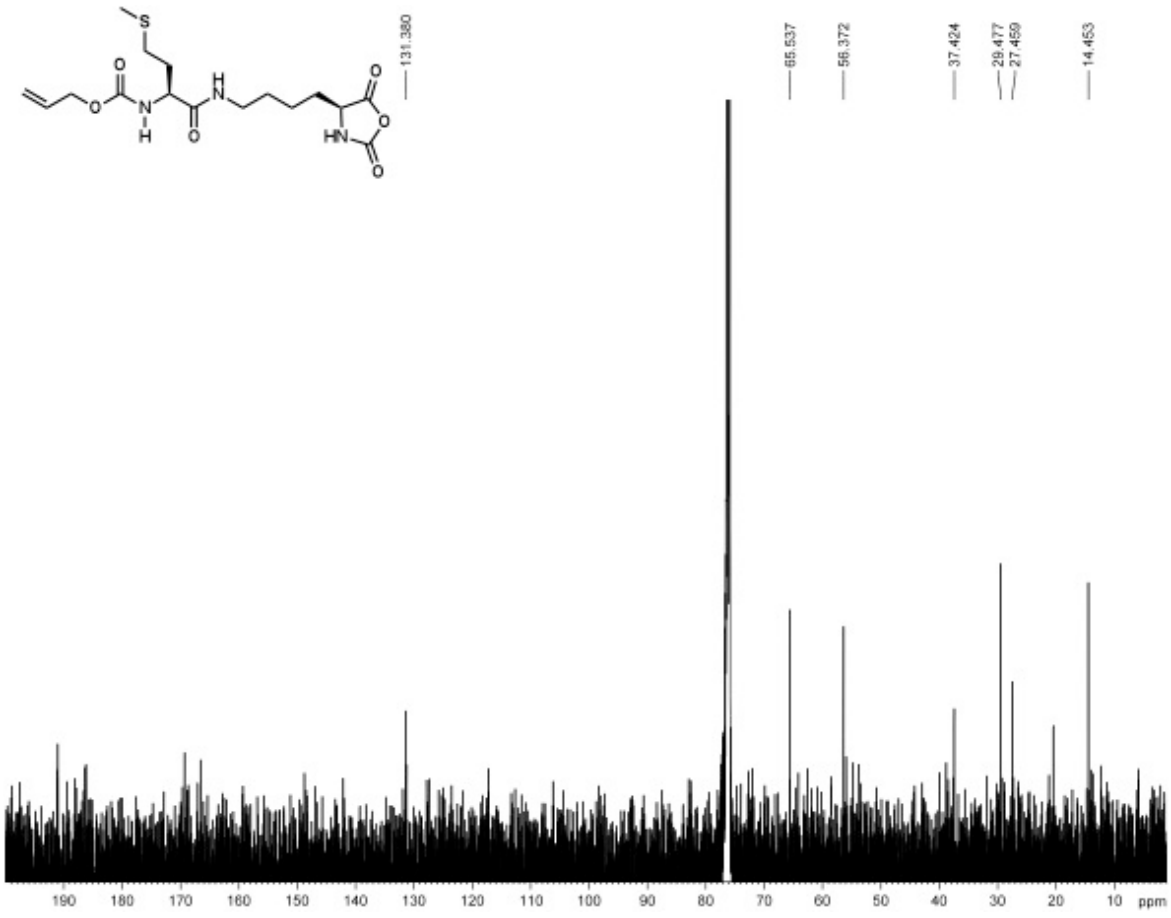
131.380
65.537
56.372
37.424
29.477
27.459
14.453
190 180 170 160 150 140 130 120 110 100 90 80 70 60 50 40 30 20 10 ppm

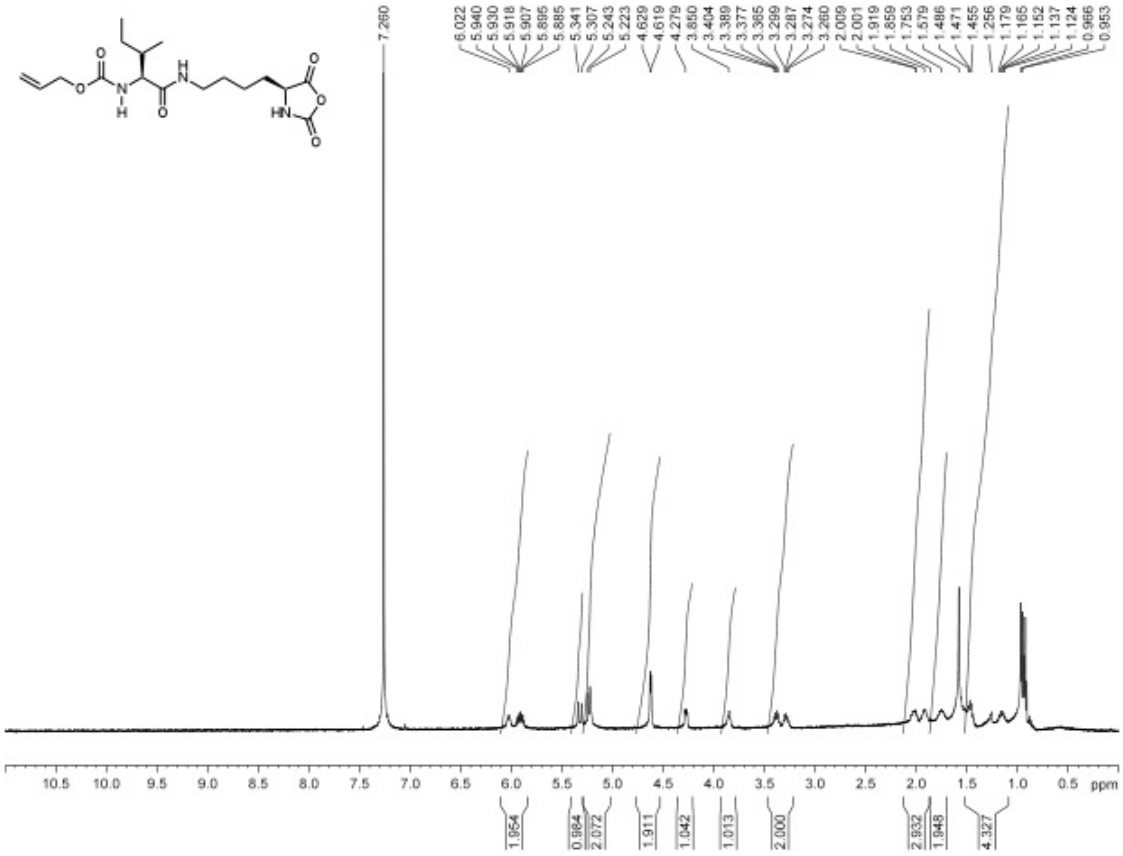
7.260
6.022
5.940
5.930
5.918
5.907
5.895
5.885
5.341
5.307
5.243
5.223
4.629
4.619
4.279
3.850
3.404
3.389
3.377
3.365
3.299
3.287
3.274
3.260
2.009
2.001
1.919
1.859
1.753
1.579
1.486
1.471
1.455
1.256
1.179
1.165
1.152
1.137
1.124
0.966
0.953
10.5 10.0 9.5 9.0 8.5 8.0 7.5 7.0 6.5 6.0 5.5 5.0 4.5 4.0 3.5 3.0 2.5 2.0 1.5 1.0 0.5 ppm
1.864
0.984
2.072
1.911
1.042
1.013
2.000
2.932
1.948
4.327

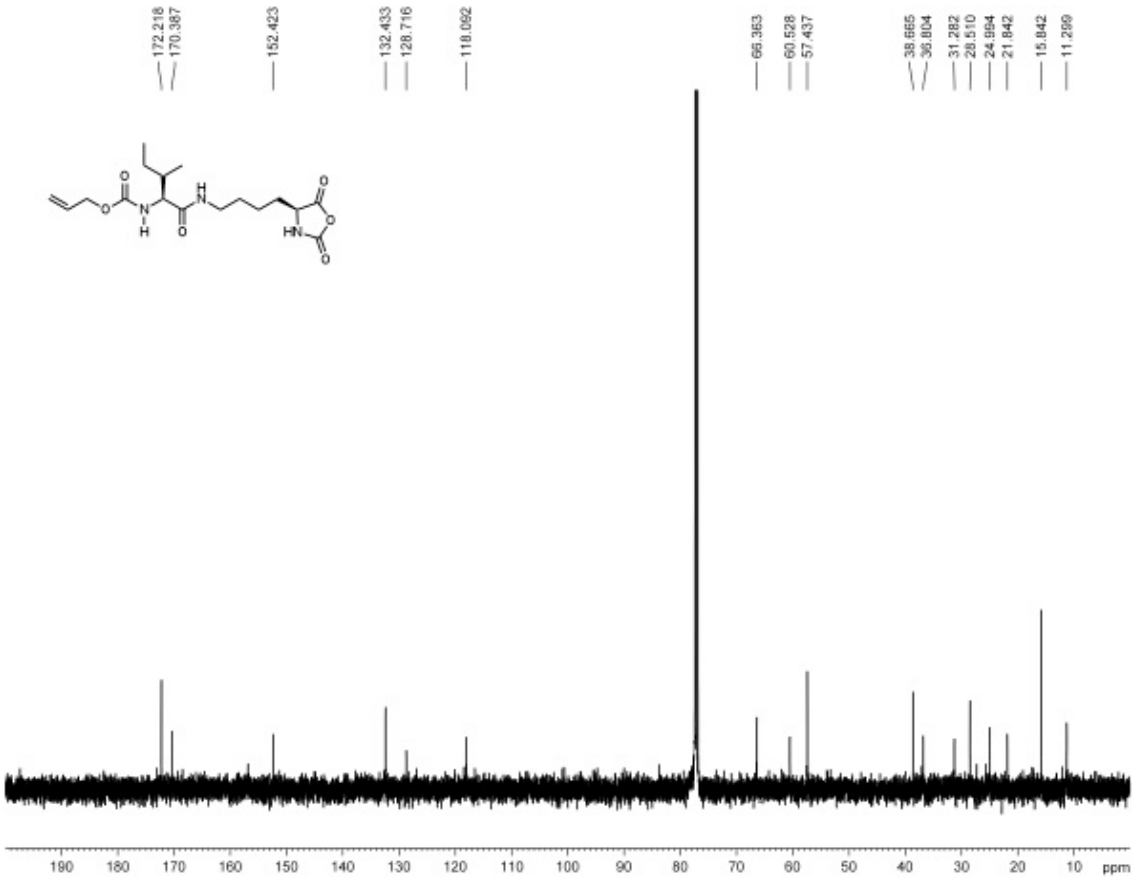
172.218
170.387
152.423
132.433
128.716
118.092
66.363
60.528
57.437
38.665
38.804
31.282
28.510
24.994
21.842
15.842
11.299
190 180 170 160 150 140 130 120 110 100 90 80 70 60 50 40 30 20 10 ppm

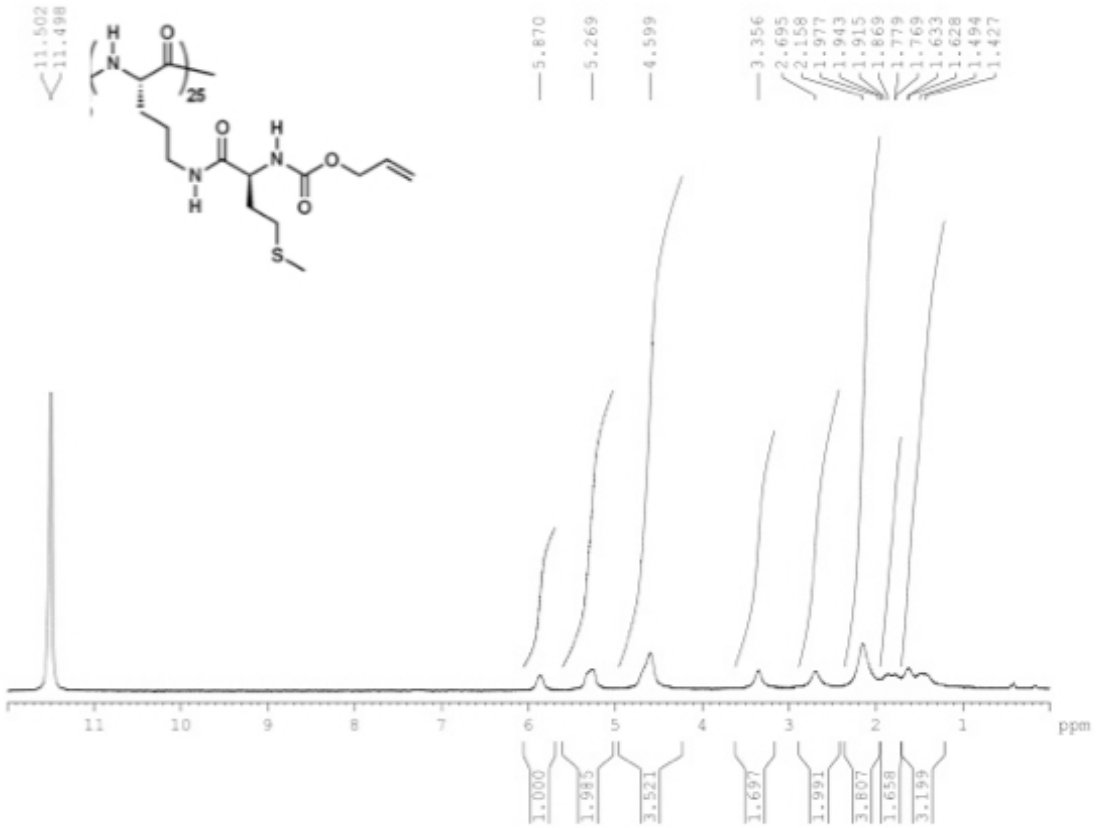
11.502
11.498
5.870
5.269
4.599
3.356
2.695
2.158
1.977
1.943
1.915
1.869
1.779
1.769
1.633
1.628
1.494
1.427
25
11
10
9
8
7
6
5
4
3
2
1
ppm
1.000
1.985
3.521
1.697
1.991
3.807
1.658
3.199

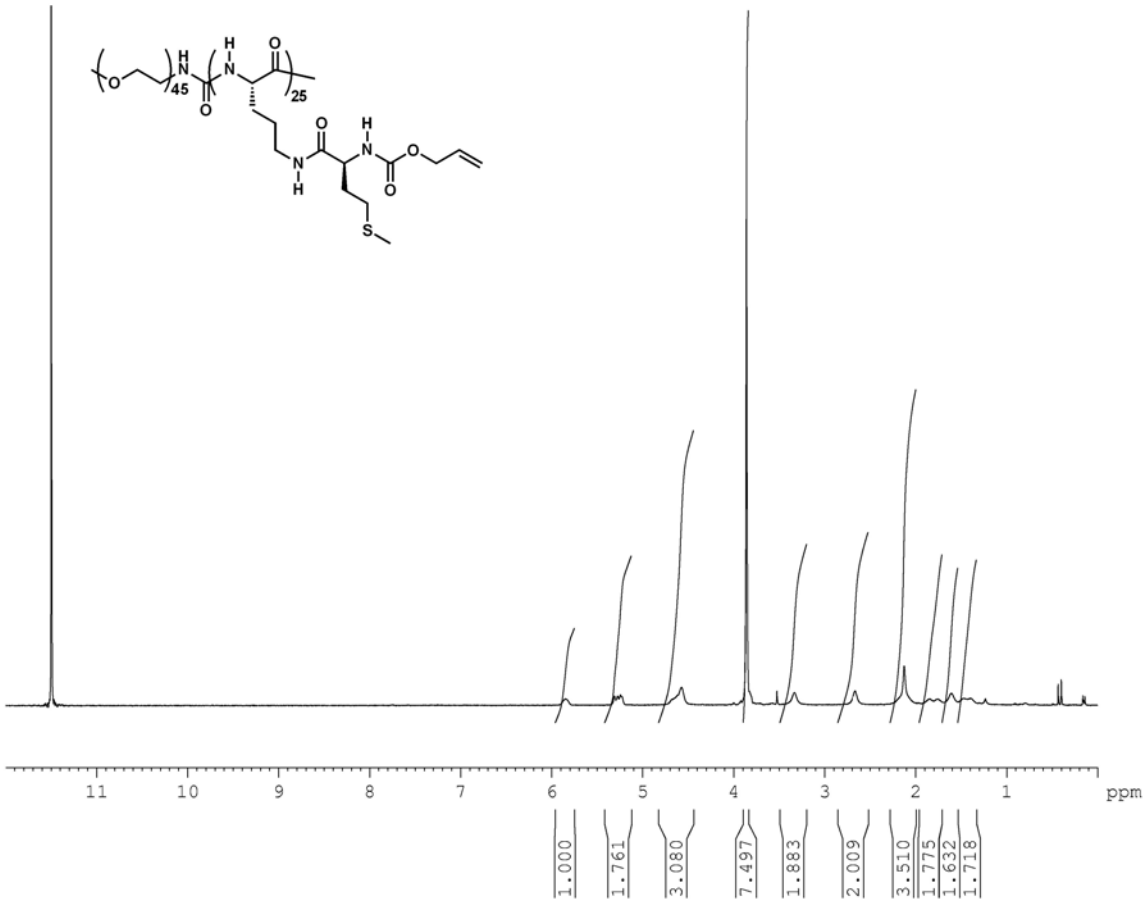
11
10
9
8
7
6
5
4
3
2
1
ppm
1.000
1.761
3.080
7.497
1.883
2.009
3.510
1.775
1.632
1.718

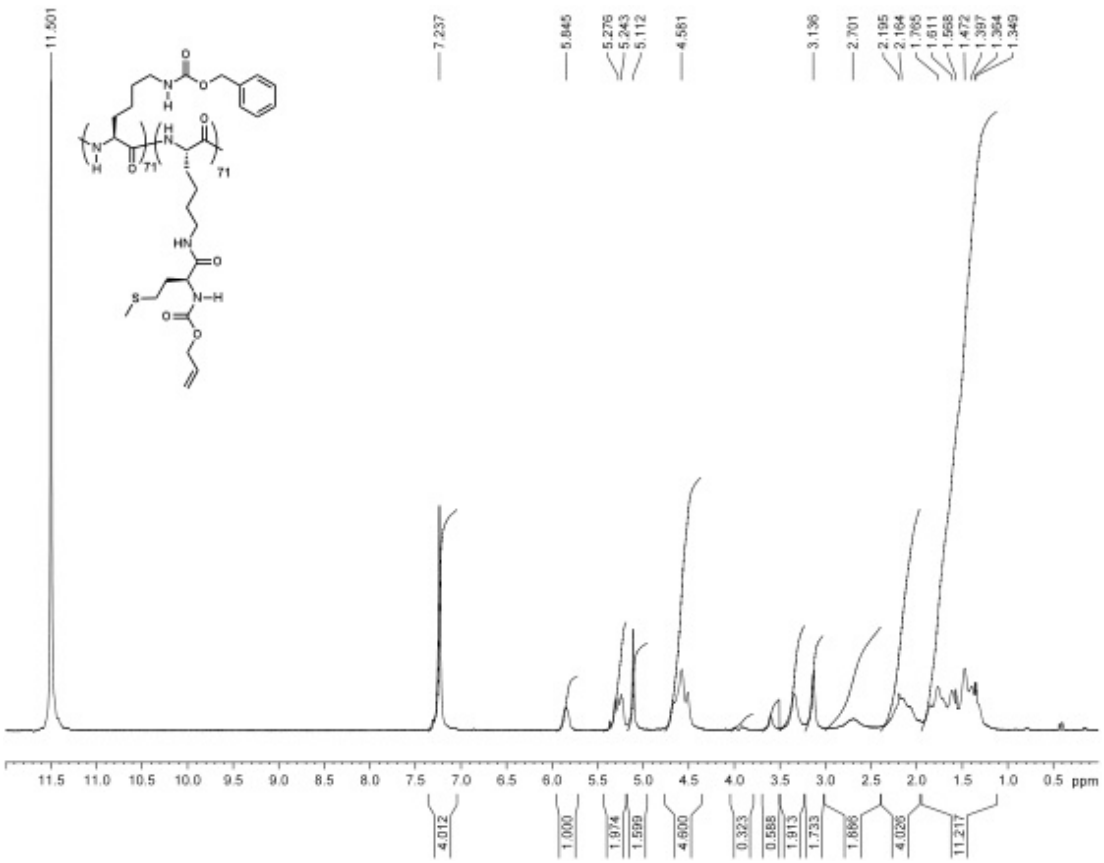
11.501
7.237
5.845
5.276
5.243
5.112
4.561
3.136
2.701
2.195
2.164
1.765
1.611
1.568
1.472
1.397
1.364
1.349
11.5 11.0 10.5 10.0 9.5 9.0 8.5 8.0 7.5 7.0 6.5 6.0 5.5 5.0 4.5 4.0 3.5 3.0 2.5 2.0 1.5 1.0 0.5 ppm
4.012
1.000
1.974
1.599
4.600
0.323
0.588
1.913
1.733
1.886
4.026
11.217

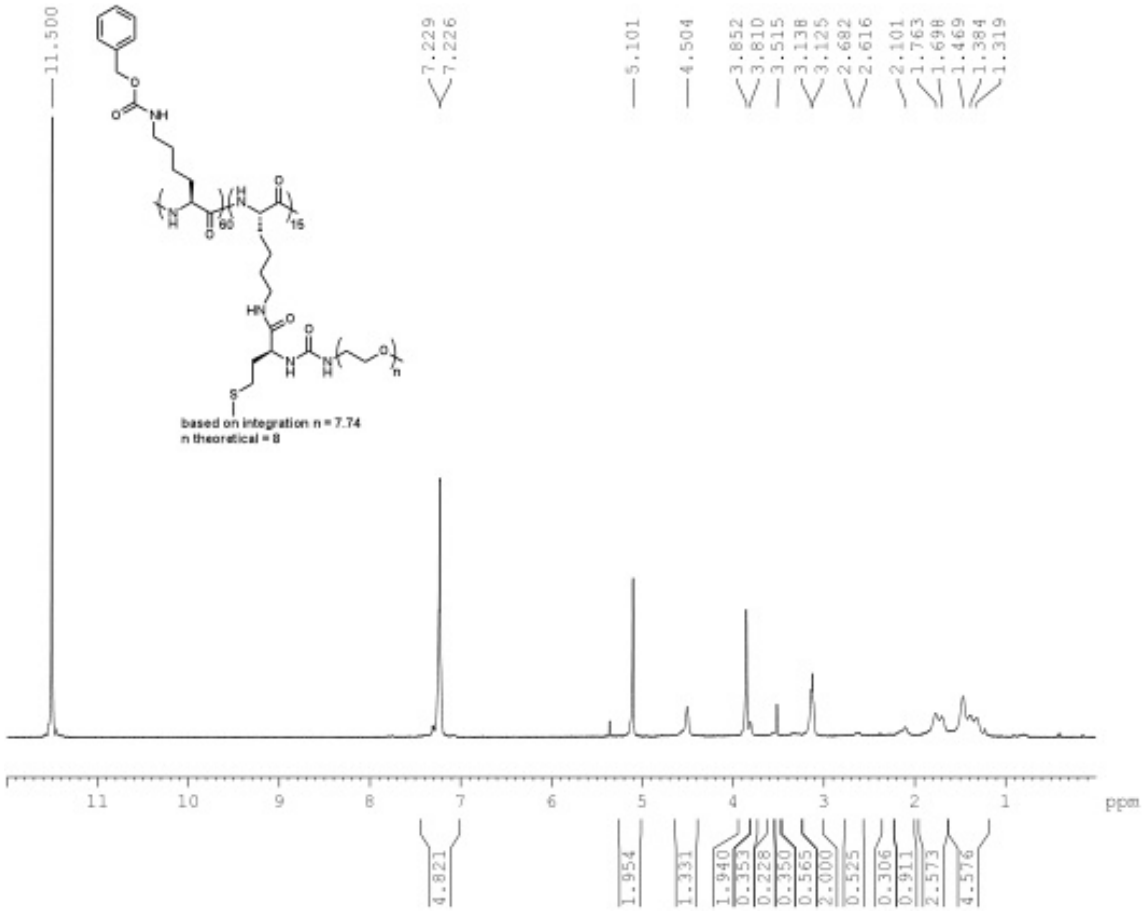
11.500
7.229
7.226
5.101
4.504
3.852
3.810
3.515
3.138
3.125
2.682
2.616
2.101
1.763
1.698
1.469
1.384
1.319
based on integration n = 7.74
n theoretical = 8
11
10
9
8
7
6
5
4
3
2
1
ppm
4.821
1.954
1.331
1.940
0.353
0.228
0.350
0.565
2.000
0.525
0.306
0.911
2.573
4.576

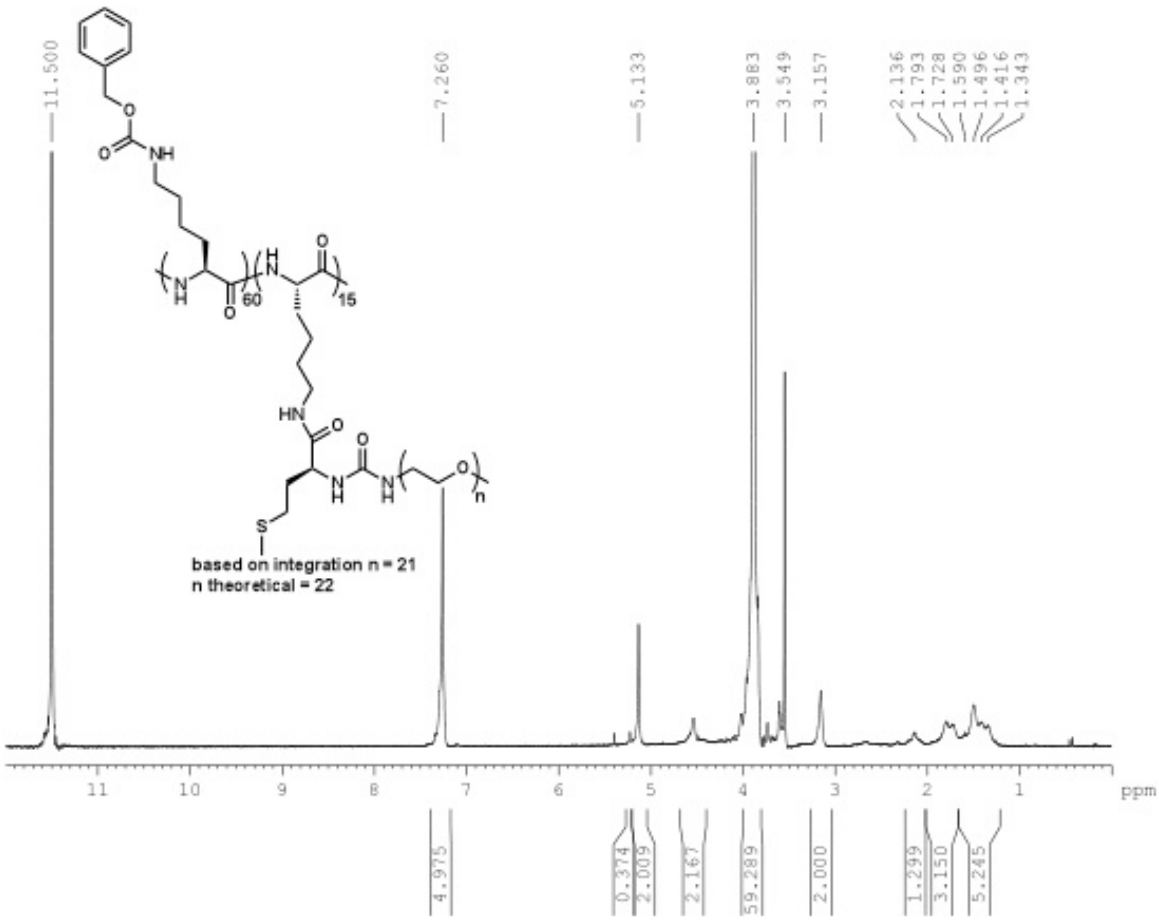
11.500
7.260
5.133
3.883
3.549
3.157
2.136
1.793
1.728
1.590
1.496
1.416
1.343
based on integration n = 21
n theoretical = 22
ppm
4.975
0.374
2.009
2.167
59.289
2.000
1.299
3.150
5.245

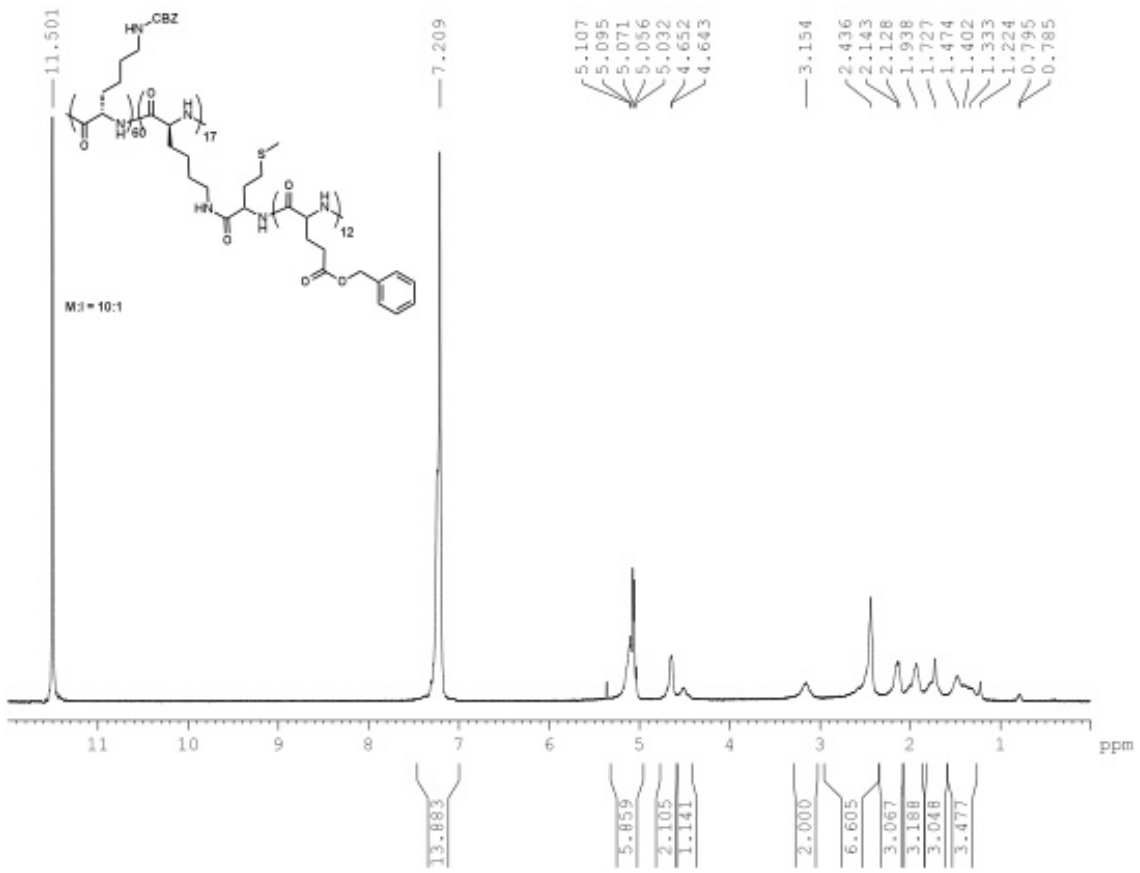
11.501
7.209
5.107
5.095
5.071
5.056
5.032
4.652
4.643
3.154
2.436
2.143
2.128
1.938
1.727
1.474
1.402
1.333
1.224
0.795
0.785
CBZ
M:I = 10:1
ppm
13.883
5.859
2.105
1.141
2.000
6.605
3.067
3.188
3.048
3.477

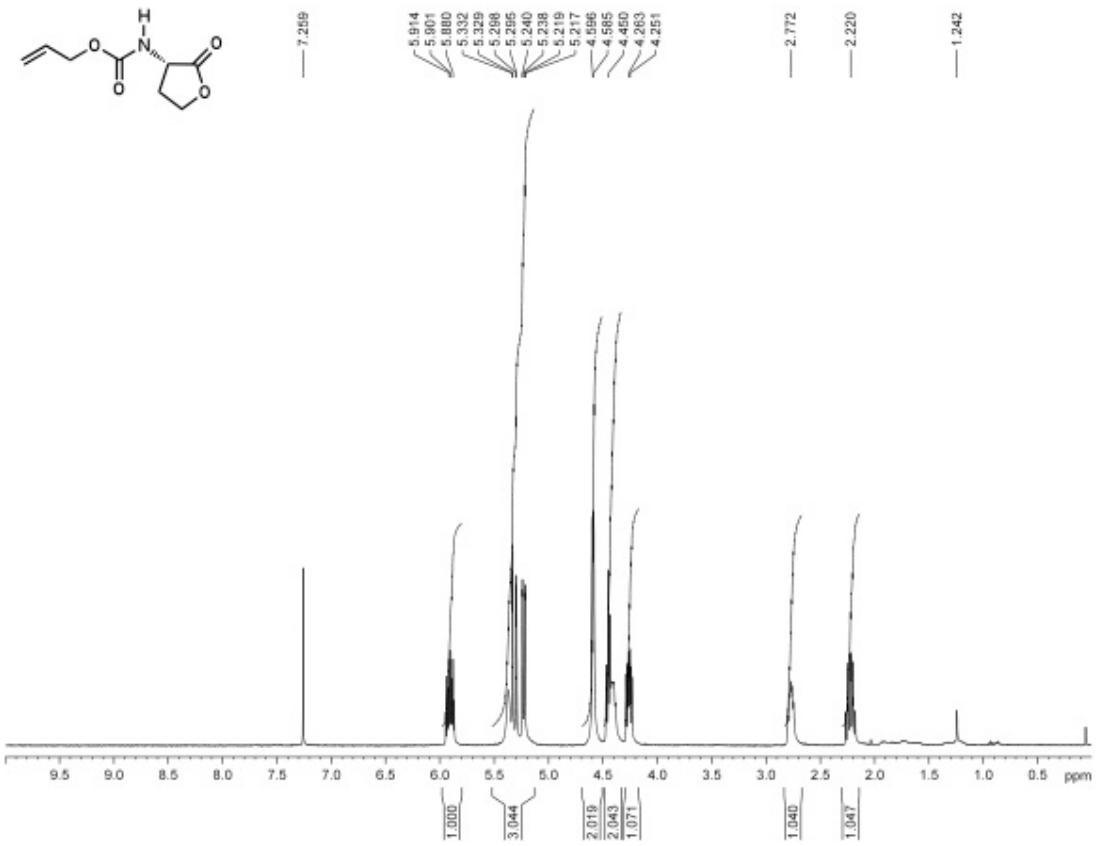
7.259
5.914
5.901
5.880
5.332
5.329
5.298
5.295
5.240
5.238
5.219
5.217
4.596
4.585
4.450
4.263
4.251
2.772
2.220
1.242
9.5
9.0
8.5
8.0
7.5
7.0
6.5
6.0
5.5
5.0
4.5
4.0
3.5
3.0
2.5
2.0
1.5
1.0
0.5
ppm
1.000
3.044
2.019
2.043
1.071
1.040
1.047

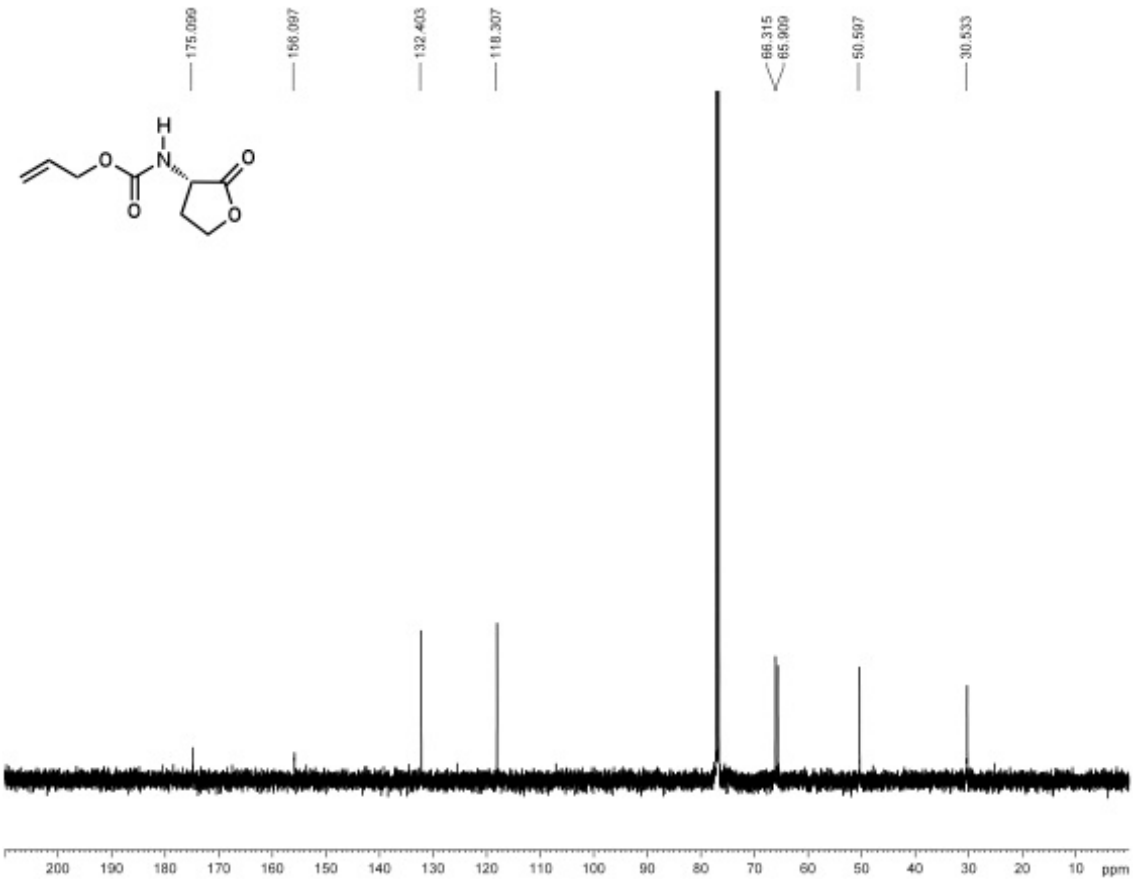
175.099
158.097
132.403
118.307
66.315
65.909
50.597
30.533
200
190
180
170
160
150
140
130
120
110
100
90
80
70
60
50
40
30
20
10
ppm

Chapter 3

Soluble, Clickable Polypeptides Using Azido NCAs

3.1 Introduction

Since its introduction in 2001 by Sharpless, click chemistry has gained popularity in polymer science for its selectivity, efficiency and minimal need for purification.[99,100] In particular the copper-assisted azide alkyne coupling (CuAAC) has been the archetypal click reaction due to its single reaction trajectory, modularity, chemoselectivity and wide scope.[101,102] Hawker, Sharpless, Fretchet and coworkers first demonstrated the importance of click chemistry in polymer science with their convergent approach towards triazole G-4 dendrimers.[103-106]

As a non-natural functional group, azides have been incorporated into biological systems and undergo strain-promoted azide alkyne click chemistry (SPAAC)[107] and the Staudinger ligation.[108] Therefore, it is no surprise azides have been incorporated into proteins and peptides for applications in drug delivery, tissue scaffolding and bioimaging. In 2009, Hammond and coworkers prepared cylindrical brushes with high grafting efficiencies utilizing CuAAC of azido-PEG secondary chains coupled to poly(propargyl glutamate) primary chains.[71] Lecommandoux and coworkers also used CuAAC in the preparation of ‘tree-like’ amphiphilic glycopolypeptides.[109] More recently Van Hest and coworkers utilized imidazole-1-sulfonyl azide for diazotransfer on a solid support to prepare azidopeptides.[110-112]

To the best of our knowledge there have been no examples in the literature of azidopolypeptides prepared from azido functional α-amino-N-carboxyanhydride monomers. This method allows for facile preparation and purification of

azidopolypeptides, ensuring 100% azide functionalization of amino groups prior to polymerization.

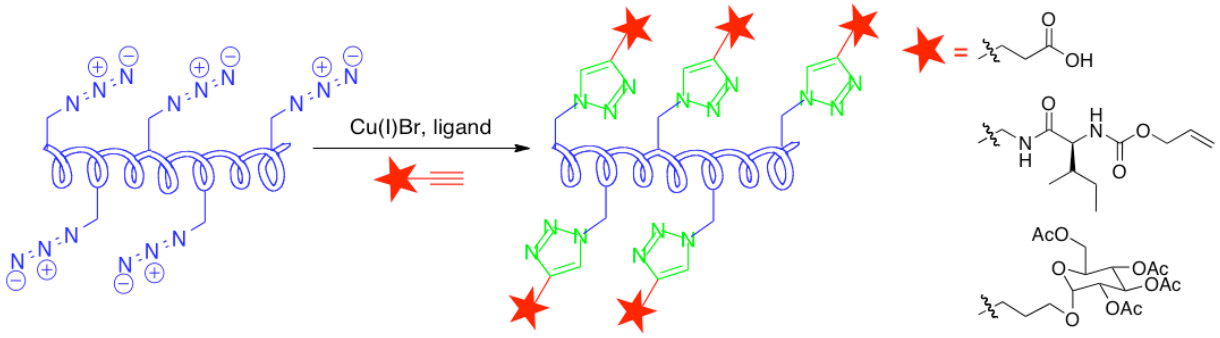

Figure 3-1. Schematic diagram showing the preparation of azidopolypeptides. Azidopolypeptides readily undergo CuAAC using Cu(I)Br, N,N,N',N',N'-pentamethyldiethylenetriamine (PMDETA) and functional alkynes.

3.2 Synthesis of Azido Functionalized NCA Monomers

For the synthesis of azido functionalized NCAs, we chose to use amino acids L-lysine and L-ornithine as starting materials since the side-chain groups can be readily converted to azido groups. Azido functionalized amino acids were prepared from the carboxybenzyl (CBZ) protected amino acids using imidazole-1-sulfonyl-azide HCl as reported by Stick and coworkers (Figure 3-2).[113,114] The azido functionalized lysine and ornithine NCA monomers were subsequently prepared using standard methods,[60,115] and were obtained in reasonable yields after purification (67% yield) using flash column chromatography (Figure 3-2).[116]

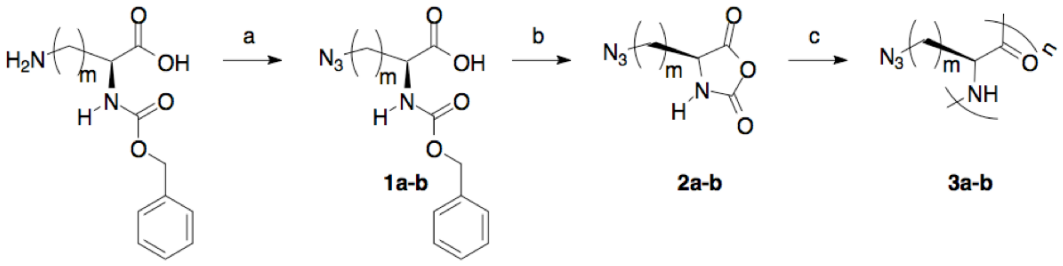

Figure 3-2. Three-step synthesis of azidopolypeptides from N_a-carboxybenzyl amino acids. (a) imidazole-1-sulfonyl-azide·HCl, $CuSO_4 \cdot 5H_2O$, K_2CO_3, 1:1 THF:H_2O, 16 h (88% yield, **1b**); (b) Ghosez's Reagent, THF, 21 ^oC, 48 h (67 % yield, **2b**). (c) $(PMe_3)_4Co$, THF, 21 ^oC, 1 h (96% yield, **3b**). **2a** = L-azidonorvaline-N-carboxyanhydride (m = 3, Anv NCA), **2b** = L-azidonorleucine-N-carboxyanhydride (m = 4, Anl NCA), **3a** = poly (L-azidonorvaline), poly(Anv), **3b** = poly(L- azidonorleucine), poly(Anl).

3.3 Polymerization of Azido Functionalized NCAs

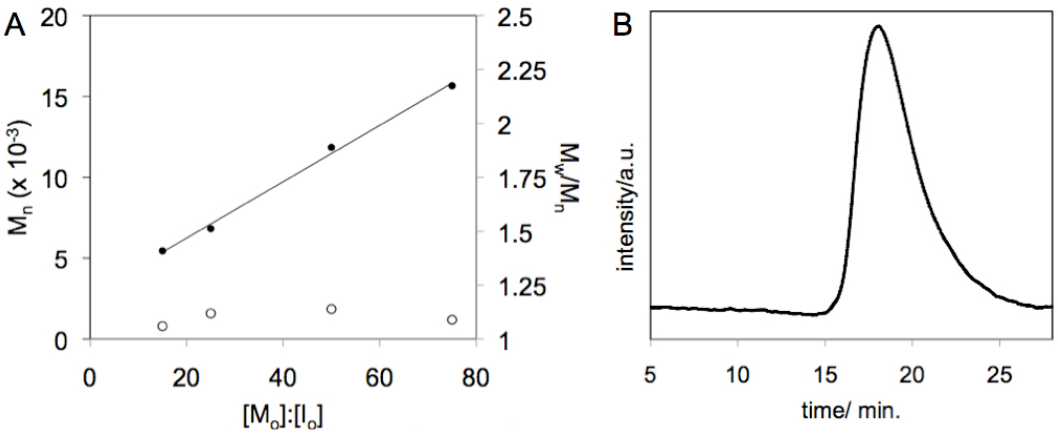

Figure 3-3. (a) Molecular weight (M_n, filled circles) and PDI of poly(Anl) as a function of monomer to initiator ratio ([M]:[I]) after 100% monomer conversion. M_n and M_w/M_n were determined by ^1H NMR and gel permeation chromatography (GPC/LS). (b) GPC chromatogram (normalized DRI intensity in arbitrary units (a.u.) versus elution time) of a poly(Anl) sample (Table 1, entry 3).

Polymerization of Anl NCA using $(PMe_3)_4Co$ in THF proceeded readily at ambient temperature to give poly(N_e-(hydrazidyl)-L-lysine), poly(Anl), with complete monomer conversion and no reaction at the side-chain azido groups (as determined by FT-IR). To determine chain lengths, Anl NCA was polymerized at different monomer to initiator ratios, and after complete monomer consumption, active chains were end-capped with isocyanate terminated PEG (M_n = 2000 Da). Compositional analysis of purified, end-capped polymers by ^1H NMR gave number average poly(Anl) chain lengths that increased linearly with stoichiometry (Figure 3-3A).

entry	M:I	M^n (x 10^{-3})	DP	PDI	% yield
1	15	5.472	36	1.06	96
2	25	6.84	45	1.12	97
3	50	11.856	78	1.14	98
4	75	15.656	103	1.09	97

Table 3-1. Molecular weight (M_n) of poly(Anl) as a function of monomer to initiator ratio using $(PMe_3)_4Co$ in THF at 20 °C.

Chain length distributions of these poly(Anl) samples were obtained by GPC/LS analysis and were found to possess low polydispersity indices (M_w/M_n) between 1.06 and 1.12, indicating the formation of well-defined polypeptides (Figure 3-3B). Poly(Anl) was prepared in high yield with precisely controlled chain lengths up to 103 residues long, and could also be prepared as diblock copolymers with other amino acids (Table 1). Overall, these data show that Anl NCA, similar to other NCAs, is able to undergo living polymerization when initiated with $(PMe_3)_4Co$. Circular dichroism spectroscopy of poly(Anl) in THF revealed this polymer, is predominantly α-helical (Figure 3-6), which imparts poly(Anl) with good solubility in organic solvents as well as provides an exposed

presentation of the side-chain azido groups.[88] Poly(Anl) began to aggregate at M:I ratios greater or equal to 50:1 and this is likely due to increased hydrophobicity of the side chains.

		First segment[b]			Diblock copolymer[c]			
1st monomer[a]	2nd monomer[a]	M_n	M_w/M_n	DP	M_n	M_w/M_n	DP	Yield (%)[d]
15 K NCA	7.5 Anl NCA	14 400	1.17	55	18 700	1.09	83	99
15 K NCA	15 Anl NCA	14 400	1.17	55	22 900	1.17	110	99
15 Anl NCA	7.5 K NCA	5 500	1.19	39	13 600	1.12	61	97
15 Anl NCA	15 K NCA	5 500	1.19	39	16 200	1.1	78	98

Table 3-2. Synthesis of diblock copolypeptides using $(PMe_3)_4Co$ in THF at 21 ^oC. [a] First and second monomers added stepwise to the initiator; number indicates equivalents of monomer per $(PMe_3)_4Co$. K NCA = N_ε-Cbz-L-lysine-N-carboxyanhydride. Anl NCA = L-azidonorleucine-*N*-carboxyanhydride. [b] Molecular weight and polydispersity index after polymerization of the first monomer (determined by GPC/LS for poly(K); determined by GPC/LS and ^1H NMR for poly(Anl). [c]Molecular weight and polydispersity index after polymerization of the second monomer (as determined by GPC/LS and ^1H NMR). [d]Total isolated yield of diblock copolypeptide. DP = degree of polymerization.

Anv NCA could also be polymerized using $(PMe_3)_4Co$ in THF and proceeded readily at ambient temperature to give poly(Anv) with complete monomer conversion (Figure 3-4). Polymerization reactions of Anv NCA became highly viscous during the reaction and viscosity increased as a function of increasing M:I ratio, most likely due to increased polypeptide aggegration as compared to poly(Anl). Polydispersity indices could not be obtained for homopolymers of poly(Anv) due to their aggregation in GPC solvents. Diblock copolypeptides were readily prepared from poly(Anv) and poly(K) and

M_w/M_n of these coupld be determined when poly(K) served as the first segment, which helped solublize the diblock in THF and DMF (Table 3-2). Although both monomers (Anl and Anv NCA) were found to be efficiently polymerized using $(PMe_3)_4Co$, we have focused our studies on the Anl based monomer, to take advantage of polymer solubility in organic solvents for GPC analysis.

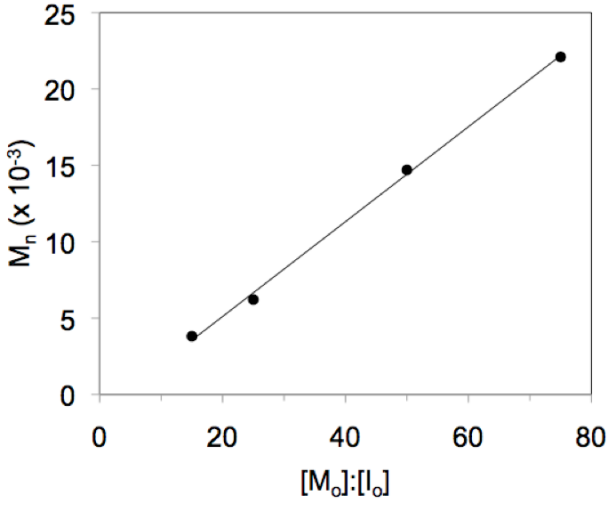

Figure 3-4. (a) Molecular weight (M_n, filled circles) of poly(Anv) as a function of monomer to initiator ratio ([M]:[I]) after 100% monomer conversion. M_n were determined by ^{1}H NMR end-capping experiments (Table 3-3).

entry	M:I	M_n (x 10^{-3})	DP	PDI	% yield
1	15	3.81	27	N/A	99
2	25	6.21	45	N/A	98
3	50	14.7	107	N/A	100
4	75	22.1	160	N/A	99

Table 3-3. Molecular weight (M_n) of poly(Anv) as a function of monomer to initiator ratio using $(PMe_3)_4Co$ in THF at 20 °C.

		First segment[b]			Diblock copolymer[c]			
1st monomer[a]	2nd monomer[a]	M_n	M_w/M_n	DP	M_n	M_w/M_n	DP	Yield (%)[d]
15 K NCA	15 Anv NCA	19 100	1.08	73	29 000	1.08	144	99
15 K NCA	7.5 Anv NCA	19 100	1.08	73	24 300	1.19	111	97
15 Anv NCA	15 K NCA	3 800	N/A	27	10 900	N/A	54	97
15 Anv NCA	7.5 K NCA	3 800	N/A	27	8 800	N/A	46	97

Table 3-4. Synthesis of diblock copolypeptides using $(PMe_3)_4Co$ in THF at 21 ^oC. [a] First and second monomers added stepwise to the initiator; number indicates equivalents of monomer per $(PMe_3)_4Co$. [b]Molecular weight and polydispersity index after polymerization of the first monomer (determined by GPC/LS for poly(K); determined by GPC/LS and ^1H NMR for poly(K^{AM})). [c]Molecular weight and polydispersity index after polymerization of the second monomer (as determined by GPC/LS and ^1H NMR). [d]Total isolated yield of diblock copolypeptide. DP = degree of polymerization.

3.4 Modification of poly(Anl)

After developing the preparation of Anl NCA in high yield and purity, showing the ability to control chain lengths and obtain narrow chain length distributions using $Co(PMe_3)_4$, we explored the modification of poly(Anl) with functional alkynes. A poly(K)-*b*-poly(Anl) diblock copolypeptide was used for these studies to minimize polymer aggregation and to provide a repeat segment in ^1H NMR analysis. To demonstrate versatility, carboxylic acid (4), amino acid (5) and glycoside (6) functionalities were separately added to poly$(K)_{60}$–*b*-poly$(Anl)_{54}$ via CuAAC using Cu(I)Br, PMDETA in

DMSO (Figure 3-5). The modified polymers were obtained in yields of 97.3 % or greater and NMR analysis showed complete conversion to the corresponding triazole derivatized polypeptides. These reactions were also shown to be regioselective resulting in a single proton peak at 8.15 ppm depicting the expected trans product in each case (SI).

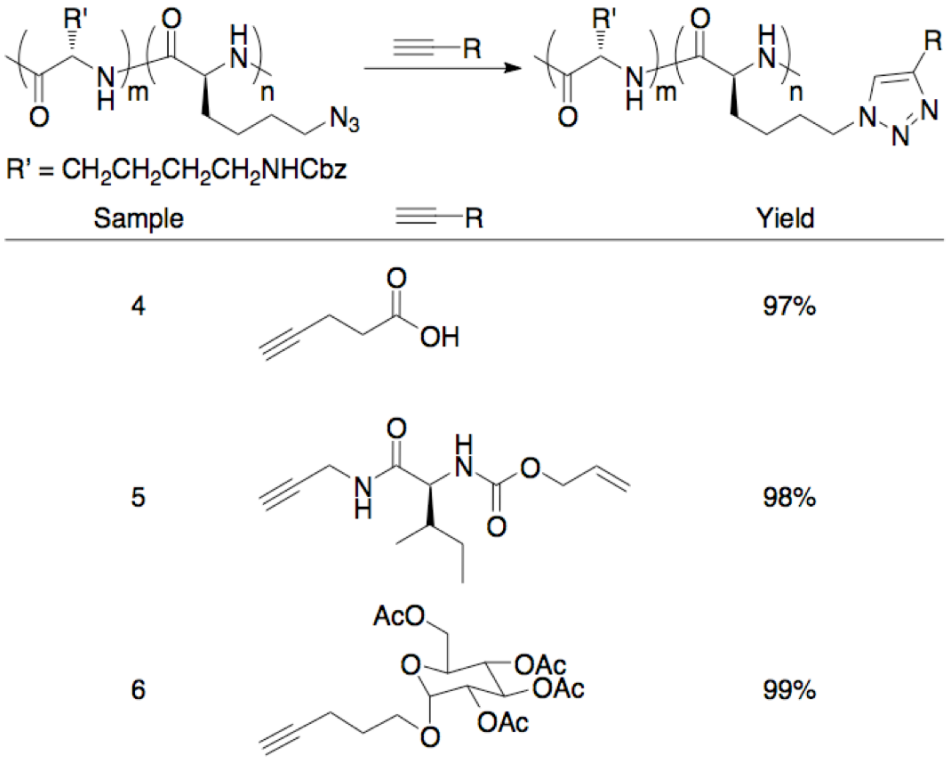

Figure 3-5. Reaction of poly(K)$_m$–*b*-poly(Anl)$_n$ (m = 60, n = 54) with model functional alkynes using CuAAC. Reagents and conditions: 1.8 eq. alkyne per azide group, Cu(I)Br, PMDETA, DMSO, 21 ^{o}C, 48 h. Yield is total isolated yield of completely functionalized copolypeptide.

Poly(Anl) adopts an α-helical conformation in THF but is insoluble in water due to its hydrophobic side chains (Figure 3-6A). Functionalization of poly(Anl)$_{52}$ with glycoside (6) followed by hydrazine deprotection of the acetyl groups (SI) gave a water soluble glycopolypeptide derivative. This glycopolypeptide was also found to be α-helical

showing the poly(Anl) backbone is useful for preparation of helical polypeptide derivatives (Figure 3-6B).

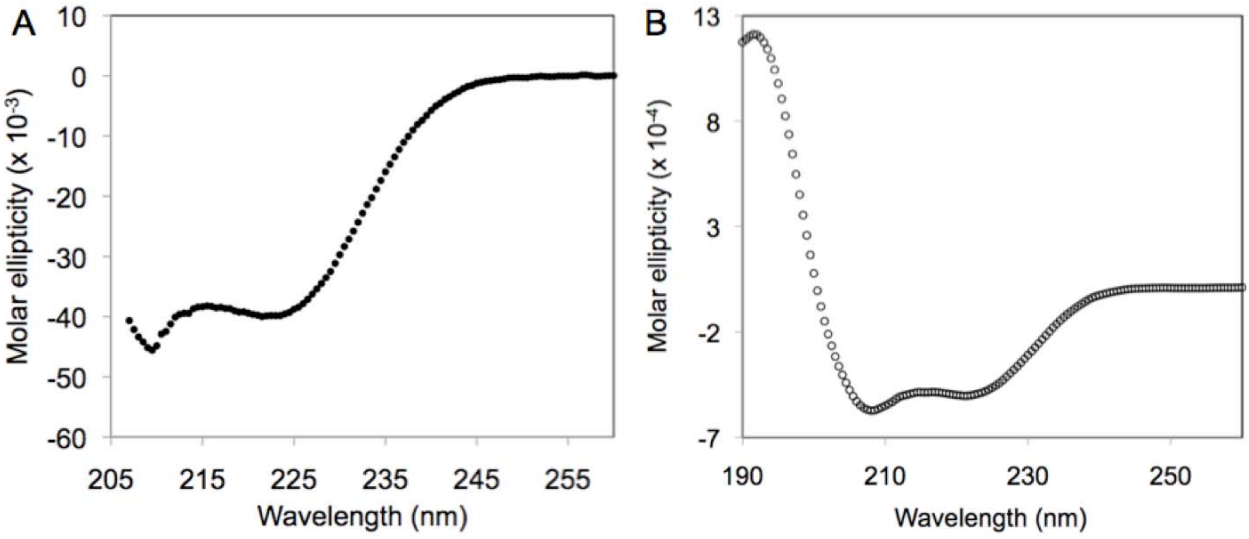

Figure 3-6. Circular dichroism spectra of poly(Anl) and its glycosylated derivative. (a) poly(Anl)$_{52}$ in THF (50 µg/mL); spectrum was cut-off at 205 nm due to solvent absorbance below this wavelength. (b) poly(Anl)$_{52}$ after CuAAC with **6** and removal of acetate groups; in H_2O, pH = 7.0 (5 µg/mL).

3.5 Conclusion

In summary, we prepared new azido functionalized NCAs that undergo living polymerization to give well-defined, high molecular weight homopolypeptides and block copolypeptides. This is an attractive method for preparation of functionalized and side-chain reactive polypeptides with facile, chemoselective incorporation of alkyne reagents. Aside from the examples that have been given here, these methods should also be applicable to a variety of other alkyne reagents developed for CuAAC. These azidopolypeptides are attractive for incorporating functionality in copolypeptide

materials, such as hydrogels for tissue engineering and vesicles for drug delivery.

3.6 Experimental Procedures

A. Synthesis and polymerization of NCA monomers

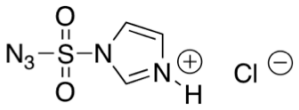

Imidazole-1-sulfonyl Azide Hydrochloride. Prepared according to literature procedures.[113,114]

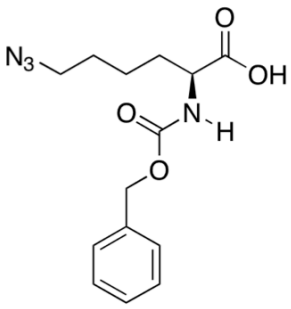

Representative procedure for synthesis of N_{ε}-carboxybenzyl-L-azidobutylglycine K_2CO_3 (2.66 g, 19.28 mmol) was dissolved in 1:1 THF: H_2O (80 mL total volume). $CuSO_4{\cdot}5H_2O$ (18 mg, 0.072 mmol) was added to the stirring solution followed by the addition of N_{α}-carboxybenzyl-L-Lysine (6.48 g, 24.2 mmol). Imidazole-1-sulfonyl-azide (1.78 g, 8.57 mmol) was added and the reaction stirred at room temperature to completion (12 h). THF was removed under reduced pressure and the reaction mixture was neutralized with 10% HCl to a pH of 5. The aqueous layer was extracted with EtOAc (3 x 50 mL), organic layers combined, dried with $MgSO_4$, filtered, and

concentrated. The product was isolated as a clear oil (1.84 g, 84%). No further purification was required. ^{1}H NMR (500 MHz, $CDCl_3$): δ 7.41-7.37 (m. 5 H), 5.37 (s, 1 H), 5.13 (m, 2 H), 4.44 (m, 2 H), 3.29-3.27 (m, 2 H), 1.91-1.76 (m, 2 H), 1.76-1.65 (m, 2 H), 1.63-1.61 (m, 2 H). ^{13}C NMR (125 MHz, $CDCl_3$): δ 176.52, 156.02, 135.78, 128.52, 128.24, 128.08, 67.17, 53.48, 51.01, 31.86, 28.30, 22.35. FT-IR (THF): 2967, 2858, 2100, 1725 cm^{-1}. HRMS-ESI (*m/z*) $[M - N_2 + H]^+$ Calcd for $C_{14}H_{19}N_2O_4$: 279.13; found: 279.13.

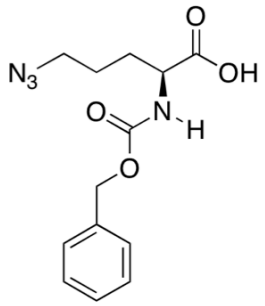

N$_\varepsilon$-carboxybenzyl-L-azidopropylglycine. ^{1}H NMR (500 MHz, $CDCl_3$): δ 7.37-7.28 (m, 5 H), 5.37 (m, 1 H), 5.16-5.13 (s, 2 H), 4.45-4.21 (m, 1 H), 2.02-1.89 (1 H), 1.81-1.76 (m, 1 H), 1.75-1.69 (m, 2 H). ^{13}C NMR (125 MHz, $CDCl_3$): δ 178.1, 136.07, 128.72, 128.46, 128.79, 67.44, 50.89, 29.79, 24.92. FT-IR (THF): 2965, 2860, 2101, 1725 cm^{-1}. HRMS-ESI (*m/z*) $[M - N_2 + H]^+$ Calcd for $C_{13}H_{17}N_2O_4$: 265.11; found: 265.12.

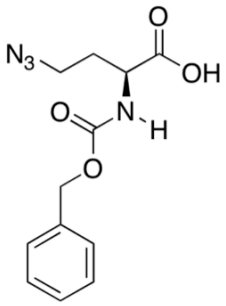

N$_\varepsilon$-carboxybenzyl-L-azidoethylglycine. ^{1}H NMR (500 MHz, $CDCl_3$): δ 7.36-7.28 (m, 5 H), 5.48 (s, 1 H), 5.14 (s, 2 H), 4.53-4.43 (m, 1 H), 3.48-3.45 (m, 2 H), 2.21 (m, 1 H), 2.04-1.99 (m, 1 H). ^{13}C NMR (125 MHz, $CDCl_3$): δ 156.32, 136.02, 128.73, 128.49, 128.23, 68.11, 67.54, 47.79, 31.44. FT-IR (THF): 2967, 2858, 2100, 1725 cm^{-1}. HRMS-ESI (*m/z*) $[M - N_2 + H]^+$ Calcd for $C_{12}H_{15}N_2O_4$: 251.10; found: 251.10.

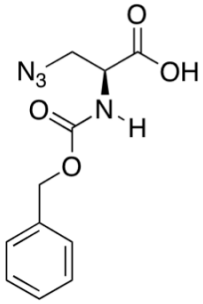

N$_\varepsilon$-carboxybenzyl-L-azidomethylglycine. ^{1}H NMR (500 MHz, $CDCl_3$): 7.37-7.31 (m, 5 H), 5.62-5.61(m, 1 H), 5.16 (s, 2 H), 4.61-4.4.9 (m, 2H), 3.84-3.82 (m, 2 H). δ ^{13}C NMR (125 MHz, $CDCl_3$): δ 173.42, 156.18, 135.85, 128.71, 128.49, 128.23, 57.02, 53.77, 52.37 FT-IR (THF): 2966, 2855, 2101, 1727 cm^{-1}. HRMS-ESI (*m/z*) $[M - N_2 + H]^+$ Calcd for $C_{11}H_{13}N_2O_4$: 237.08; found: 237.09.

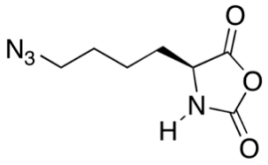

Representative procedure for the synthesis of azide containing NCAs: Anl NCA. N$_\alpha$-carboxybenzyl-L-azidonorleucine (650 mg, 2.12 mmol) was added to a 125 mL Schlenk flask equipped with a Teflon stir bar and then dissolved in 50 mL THF.

Ghosez's reagent (439 µL, 3.32 mmoL) was added via syringe to the stirring solution under N_2. The reaction was stirred at 21 ^oC until completion (48 h). The solution was evaporated to dryness under reduced pressure and dissolved in 10 mL cold EtOAc and extracted with cold 5% sodium bicarbonate solution (3 x 10 mL). The organic layer was separated, diluted in cold EtOAc (10 mL) and dried over $MgSO_4$. The solution was evaporated to dryness under reduced pressure and transferred to a glovebox (N_2 atmosphere) for further purification. The residue was purified by flash chromatography (10% to 75% THF in hexanes) and collected in 10 x 10 mL fractions. 280 mg of NCA was isolated as a clear oil after evaporation of the THF and hexanes from the combined fractions (67% yield). ^1H NMR (500 MHz, $CDCl_3$): δ 6.40 (s, 1 H), 4.37-4.34 (t, J = 5.5, 1 H), 3.40-3.33 (t, J = 2.0, 2 H), 1.99-1.81 (m, 2 H), 1.67-1.58 (m, 2H), 1.55-1.49 (m, 1 H). ^{13}C NMR (125 MHz, $CDCl_3$): δ 169.38, 152.72, 57.57, 51.00, 31.41, 28.35, 22.14. FT-IR (THF): 2210, 2100, 1856, 1791, 1629 cm^{-1}. HRMS-ESI (*m/z*) $[M - H]^+$ Calcd for $C_7H_9N_4O_3$: 197.08; found: 197.07.

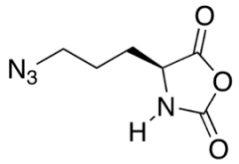

Anv NCA. ^1H NMR (500 MHz, $CDCl_3$): 5.99 (s, 1 H), 4.39-4.37 (t, J = 6.0, 1 H), 3.42 (t, J = 2.0, 2 H), 2.12- 2.01 (m, 1 H) 1.93-1.83 (m, 2 H), 1.79-1.68 (m, 1 H). ^{13}C NMR (125 MHz, $CDCl_3$): δ 169.52, 152.89, 57.27, 50.62, 29.17, 24.31. FT-IR (THF): 2098, 1857, 1789 cm^{-1}. HRMS-ESI (*m/z*) $[M + H]^+$ Calcd for $C_6H_7N_4O_3$: 183.05; found: 183.05.

General procedure for the polymerization of Anl NCA. All polymerization reactions were performed in a dinitrogen filled glove box. To a solution of Anl NCA (20 mg, 0.10 mmol) in dry THF (500 μL) was rapidly added, via syringe, a solution of $(PMe_3)_4Co$ in dry THF (120 μL, 6.8 mmol). The reaction was stirred at room temperature and polymerization progress was monitored by removing small aliquots for analysis by FTIR. Polymerization reactions were generally complete within 1 hour. Reactions were removed from the drybox, all THF was removed, and the polypeptide was washed with 100 mM HCl (2 x 15 mL), centrifuged for 5 minutes at 3000 rpm and the supernatent was removed. The white solid polypeptide was washed with 10 mL water and then lyophilized to yield poly(Anl) as a white solid (14.5 mg, 96% yield). ^{1}H NMR (500 MHz, TFA-*d*): δ 5.87 (s, 1 H), 5.27 (s, 2H), 4.60 (s, 3 H),3.36 (s, 2 H), 2.70 (s, 2 H), 2.16 (s, 3 H), 1.87-1.63 (s, 2 H), 1.62- 1.48 (s, 3 H). FT-IR (THF): 3095, 2922 , 1650, 1622, 1541, 1528 cm^{-1}.

General procedure for endcapping of poly(Anl) with poly(ethylene glycol) and chain length determination by end group analysis. The general procedure for polymerization of Anl NCA was followed. Upon completion of the reaction, as confirmed by FTIR, a solution of a-methoxy-w-isocyanoethyl-poly(ethylene glycol), PEG-NCO (MW = 2000 Da, 5 equiv per $(PMe_3)_4Co$) in THF, was added to the polymerization reaction in a dinitrogen filled glove box. The reaction was stirred overnight at room temperature and then removed from the drybox, all THF was removed, and the polypeptide was washed with 100 mM HCl (2 x 10 mL) to remove unconjugated PEG, centrifuged for 5 minutes at 3000 rpm and the supernatent was removed. The white polypeptide was washed with 10 mL water and then lyophilized to yield PEG-endcapped poly(Anl) as a

white solid. To determine poly(Anl) molecular weights (M_n), ^{1}H NMR spectra were obtained in deuterated trifluoroacetic acid (TFA-*d*). Since it has been shown that end-capping is quantitative for $(PMe_3)_4Co$ initiated NCA polymerizations when excess isocyanate is used,[4] integrations of the methylene group resonance versus the polyethylene glycol resonance at δ 3.64 could be used to obtain poly(Anl) lengths (see example in spectral data section).

B. Sample diblock copolypeptide syntheses

Poly(N_e-carboxybenzyl-L-Lysine)-*block*-poly(L-azidonorleucine), poly(K)-*b*-poly(Anl). A solution of $(PMe_3)_4Co$ in THF (61 µL, 3.33 mmol) was added to a solution of *N*$_e$-carboxybenzyl-L-Lysine NCA (K NCA) (15 mg, 0.05 mmol) in THF (375 µL). After 1 h, the polymerization reaction was complete as determined by FTIR. An aliquot (50 mL) of poly(Z-L-lysine) was removed and analyzed by GPC/LS (M_n = 15700, M_w/M_n = 1.12, DP = 60). Anl NCA (10 mg, 0.05 mmol in 250 µL THF) was then added to the stirring solution of poly(K). The reaction was stirred for an additional 1 h after which all NCA was consumed. An aliquot of poly(K)-*b*-poly(Anl) was removed from the reaction and analyzed by GPC/LS (M_w/M_n = 1.18). The remainder of the reaction mixture was concentrated to dryness. The sample was then dissolved in minimal THF (1 mL), and precipitated by the slow addition of 100 mM aqueous HCl (3 x 10 mL) followed by centrifugation (3000 rpm) for 5 minutes. The supernatants were discarded and the residue was lyophilized to remove remaining water, giving the product as a white solid (19 mg, 92% yield). The sample was analyzed by ^{1}H NMR to give a DP = 114. ^{1}H NMR

(500 MHz, TFA-*d*): δ 7.28 (bs), 5.16 (bs), 4.63 (bs), 4.55 (bs), 3.39 (bs), 3.18 (bs), 1.91-1.37 (m). FT-IR (THF): 3095, 2922, 2101, 1741, 1651, 1540 cm^{-1}.

Poly(N_e-carboxybenzyl-L-Lysine)-*block*-poly(L-azidonorvaline), Poly(K)-*b*-poly(Anv). A solution of $(PMe_3)_4Co$ in THF (60 µL, 4.4 mmol) was added to a solution of *N*$_e$-carboxybenzyl-L-Lysine NCA (K NCA) (20 mg, 0.065 mmol) in THF (500 mL). After 1 h, the polymerization reaction was complete as determined by FTIR. An aliquot (50 mL) of poly(Z-L-lysine) was removed and analyzed by GPC/LS (M_n = 19100, M_w/M_n = 1.08, DP = 73). Anv NCA (11 mg, 58.7 mmol in 220 mL THF) was then added to the stirring solution of poly(K). The reaction was stirred for an additional 1 h after which all NCA was consumed. An aliquot of poly(K)-*b*-poly(Anv) was removed from the reaction and analyzed by GPC/LS (M_w/M_n = 1.19). The reaction mixture was concentrated to dryness and the copolypeptide was removed from the glovebox. The copolypeptide was dissolved in minimal THF (250 µL), and precipitated by the slow addition of 100 mM aqueous HCl (3 x 15 mL) followed by centrifugation (3000 rpm) for 5 minutes. The supernatants were discarded and the residue was lyophilized to remove remaining water, giving the product as a white solid. (25 mg, 99 % yield). The sample was analyzed by ^{1}H NMR to give a DP = 144. ^{1}H NMR (500 MHz, TFA-*d*): δ 7.35 (bs), 5.28 (bs), 4.62 (bs), 4.16 (bs), 3.33 (m), 2.12 (bs), 2.03-1.45 (m). FT-IR (THF): 3095, 2922, 2101, 1741, 1651, 1540 cm^{-1}.

Poly(L-azidonorvaline)-block-poly((N_e-carboxybenzyl-L-Lysine), Poly(Anv)-*b*-poly(K). A solution of $(PMe_3)_4Co$ in THF (65 µL, 3.5 mmol) was added to a solution of

Anv NCA (10 mg, 0.054 mmol) in THF (250 µL). After 1 h, the polymerization reaction was complete as determined by FTIR. K NCA (17 mg, 0.054 mmol) was then added to a stirring solution of poly(Anv) (0.054 mmol). The reaction was stirred overnight, after which all NCA was consumed and was then analyzed by ^{1}H NMR (M_n = 10900, DP = 54). The reaction mixture was concentrated to dryness and the copolypeptide was removed from the glovebox. The copolymer was then dissolved in minimal THF (250 µL), and precipitated by the slow addition of 100 mM aqueous HCl (3 x 15 mL) followed by centrifugation (3000 rpm) for 5 minutes. The supernatants were discarded and the residue was lyophilized to remove remaining water, giving the product as a white fluffy solid. (20 mg, 97 % yield). δ ^{1}H NMR (500 MHz, TFA-*d*): δ 7.34 (m), 5.24 (bs), 4.61 (bs), 3.51-3.48 (bs), 3.27-3.26 (bs), 2.07-1.87 (m), 1.58-1.29 (m) FT-IR (THF): 3095, 2922, 2101, 1741, 1651, 1540 cm^{-1}. FT-IR (THF): 3095, 2922, 2101, 1741, 1651, 1540 cm^{-1}.

C. CuACC of Azidopolypeptides

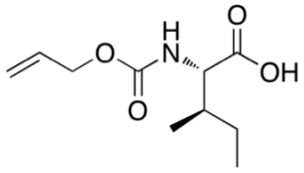

Allyloxycarbonyl-L-isoleucine. Prepared according to the literature**.** [3]

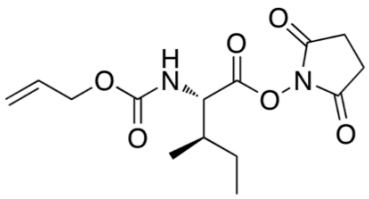

Allyloxycarbonyl-L-isoleucine-*N*-hydroxysuccinimide ester. Prepared according to the literature.[115]

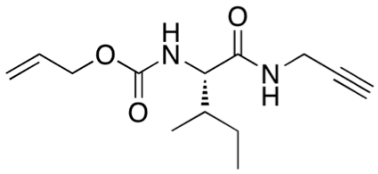

Compound 5. Under an atmosphere of N_2, allyloxycarbonyl-L-isoleucine-*N*-hydroxysuccinimide ester (5.0 g, 16.0 mmol) was dissolved in THF. The reaction vessel was cooled to 0 ^{o}C and propargyl amine (1.13 mL, 17.6 mmol) was added dropwise followed by the dropwise addition of triethylamine (2.46 mL, 17.6 mmol). The ice bath was removed and the reaction was allowed to warm to room temperature and stir for 1 h. The reaction was concentrated and acidified with 10% HCl (2 x 100 mL). Compound **5** was extracted with EtOAc (3 x 30 mL) and this orgranic layer was separated and dried over $MgSO_4$. The organic layer was filtered and concentrating giving compound **5** (3.75 g, 94% yield). No further purification was necessary. ^{1}H NMR (500 MHz, $CDCl_3$): δ 6.36 (bs, 1 H), 5.92-5.88 (m, 1 H), 5.40 (s, 1 H), 5.26-5.24 (d, J= 8, 1 H), 5.24-5.22 (d, J= 8 Hz, 1 H), 4.58 (m, 2 H), 4.09-4.00 (m, 3 H), 2.24 (s, 1 H), 1.91-1.70 (bs, 1 H), 1.53 (bs, 1 H), 1.16-1.11 (m, 1 H), 0.96-0.92 (m, 6 H). ^{13}C NMR (125 MHz, $CDCl_3$): δ 171.26, 156.52, 132.62, 118.13, 79.23, 71.93, 66.16, 59.74, 37.48, 29.29, 24.90, 15.64, 11.43. FT-IR (THF): 210, 2100, 1722, 1691, 1642, 1533 cm^{-1}. HRMS-ESI (*m/z*) $[M + H]^+$ Calcd for $C_{13}H_{21}N_2O_3$: 253.15; found: 253.16.

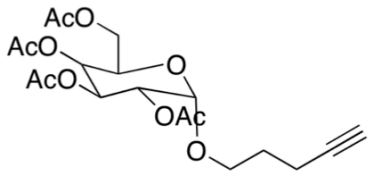

Prepared according to literature procedure.[117,118]

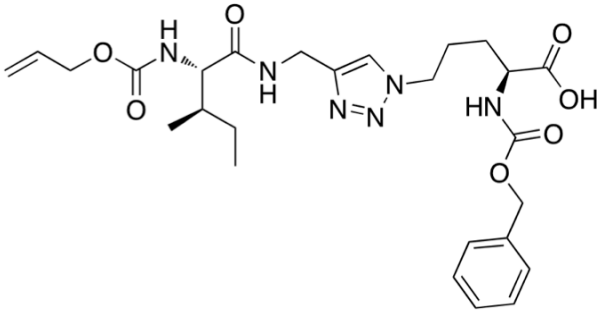

Small-molecule CuAAC Reaction.

Under an atmosphere of N_2, Z-orn-azide (116 mg, 0.397 mmol) was dissolved in 10 mL DMF followed by the addition of alloc-isoleucine-propargyl amide (**5**) (100 mg, 0.397 mmol). 794 uL PMDETA (0.0397 mmol, 50 mM) was added to the stirring solution followed by 794 uL Cu(I)Br (0.0397 mmol in a 50 mM DMF solution). The reaction mixture was stirred overnight at room temperature. The reaction was concentrated and acidified with 10% HCl (50 mL) and extracted with EtOAc (3 x 10 mL). The organic layer was separated, dried over $MgSO_4$ and concentrated. The crude product was a white solid and required no further purification (211 mg isolated, 98% yield). ^{1}H NMR (500 MHz, $CDCl_3$): δ 7.58 (s, 1 H), 7.47 (s, 1 H), 7.46-7.36 (m, 5 H), 5.85-5.77 (m, 1 H), 5.76-5.69 (s, 1 H), 5.74-5.66 (s, 1 H), 5.30-5.29 (d, J= 10 Hz, 1 H), 5.19-5.17 (d, J= 8 Hz, 1 H), 5.11 (s, 2 H), 4.53-4.36 (m, 6 H), 4.08-3.91 (m, 1 H), 2.01-1.71 (m, 4 H), 1.70-

1.65 (m, 1 H), 1.43 (m, 1 H), 1.09 (m, 1 H), 0.86 (m, 6 H). HRMS-ESI (*m/z*) $[M + H]^+$ Calcd for $C_{26}H_{37}N_6O_7$: 545.26; found: 545.27.

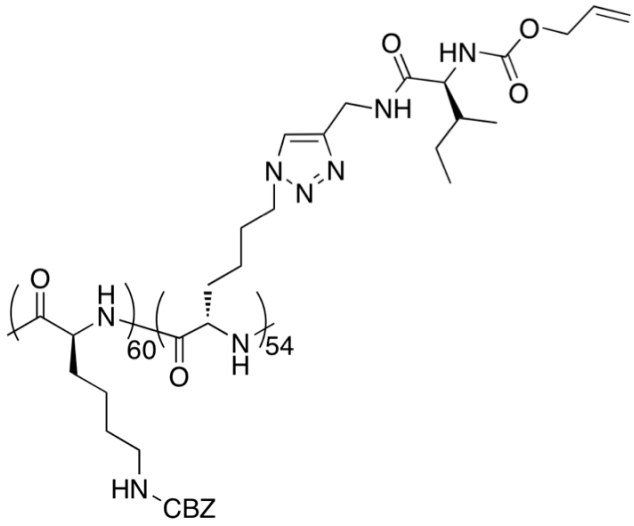

Representative Procedure for CuAAC reaction of small molecules with poly(γ-carboxybenzyl-L-Lysine)-*block*-poly(L-azidobutylglycine)

0.0244 mmol of poly(γ-carboxybenzyl-L-Lysine)$_{60}$-*block*-poly(azido lysine)$_{54}$ in THF (0.033 M) was directly transferred from the glovebox to a 20 mL scintillation vial equipped Teflon stir bar and Teflon cap with septum. Allyloxycarbonyl-L-isoleucine-propargyl amide (**5**) (12.3 mg, 0.045 mmol) was added to the stirring solution followed by the addition of PMDETA (0.01610 mmol, 50 mM in DMSO). A 50 mM solution of Cu(I)Br in DMSO was freshly prepared and used immediately (0.00805 mmol, 161 µL). The reaction was stirred under a dinitrogen atmosphere at room temperature for 48 h. The polymer was precipitated from the solution using 10 mL Millipore water. The sample

was centrifuged for 3 minutes (3000 rpm) and water/DMSO mixture was removed. The polymer was washed 2 more times to ensure the complete removal of DMSO. The polymer was then dissolved in minimal THF and precipitated with hexanes. THF/hexanes was removed and the polymer was washed again with water and lyophilized. ^{1}H NMR (500 MHz, TFA_d): δ 8.37,(bs), 7.34-7.27 (m), 5.83 (bs), 5.40-5.24 (m), 4.78 (bs), 4.61 (bs), 4.21 (bs), 3.18-2.93 (bs), 2.09-1.27 (m), 0.97-0.92 (m) .

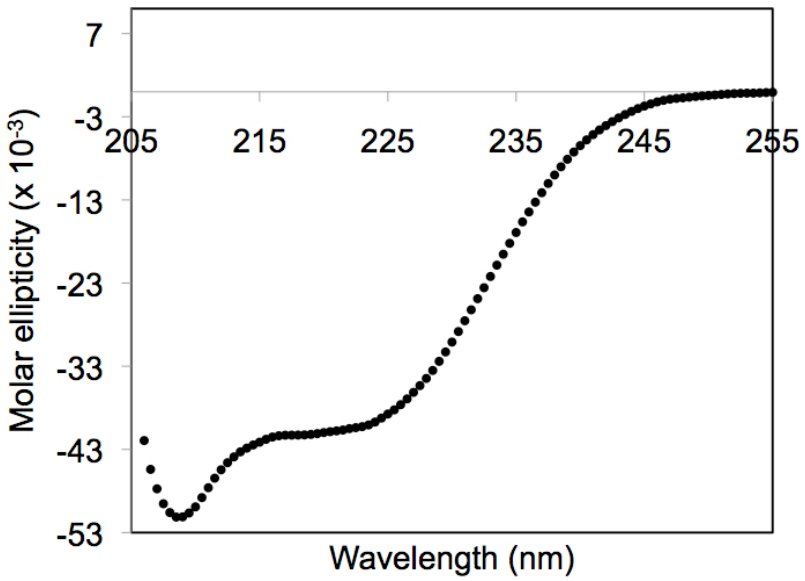

Figure 3-7. Circular dichroism of poly(Anl)$_{52}$ in THF (filled circles) at concentration of 50 µg/mL.

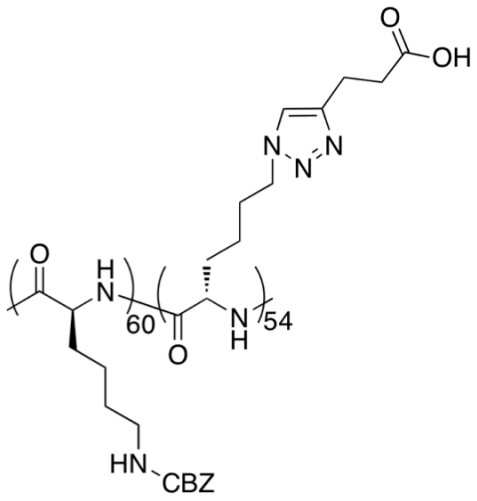

^{1}H NMR (500 MHz, TFA_d): δ 8.41-8.25 (bs), 7.43-7.06 (m), 5.14 (s), 4.59-4.35 (m), 3.29 (s), 3.18 (s), 1.80-1.26 (m).

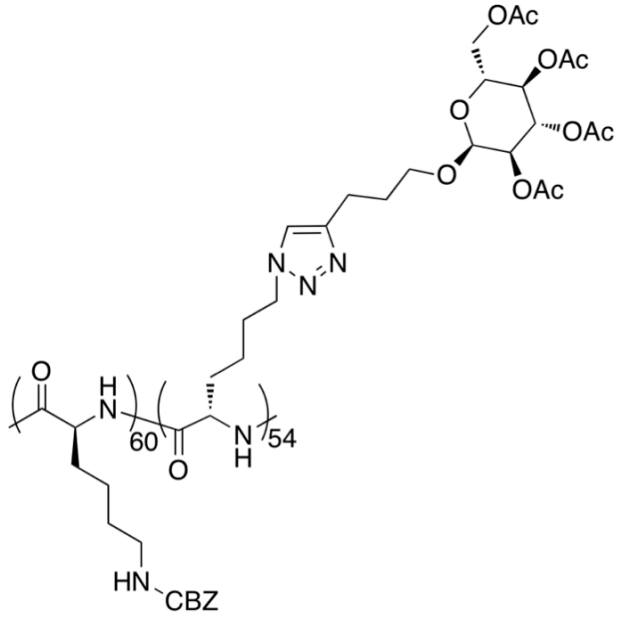

^{1}H NMR (500 MHz, TFA_d): δ 8.17 (s), 7.36 (s), 7.29 (s), 5.54 (s), 5.16-5.5.07 (bs), 4.78-4.58)bs), 3.96 (bs), 3.19-2.94 (bs), 2.21-2.01 (m), 1.81-1.72 (bs), 1.53-1.40 (bs).

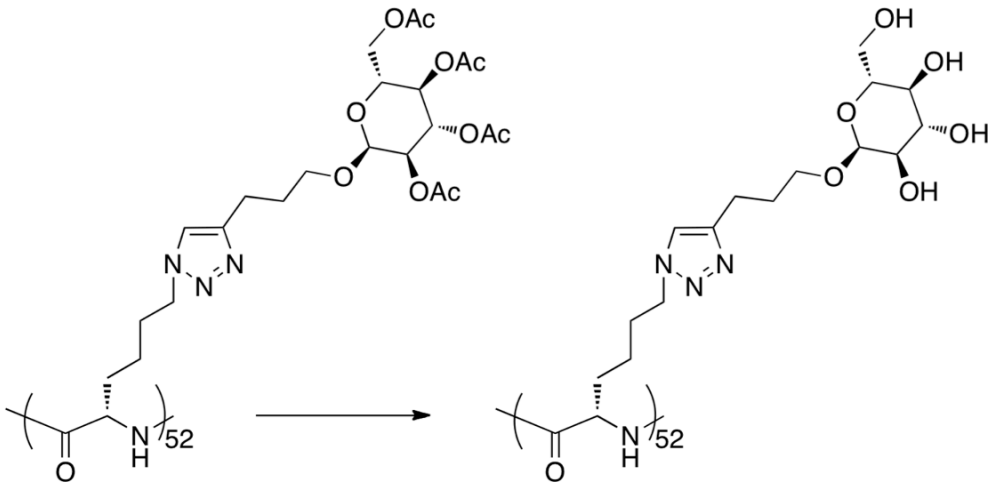

Glycopolymer deprotection.

The polymer (50 mg) was dissolved in methanol (5 mL). Hydrazine monohydrate (290 μL, 4.05 mmol) was added and the reaction was stirred at 21 ^{o}C for 24 h. Reaction was quenched by dropwise addition of acetone. and concentrated to half its volume under reduced pressure. The mixture was diluted in 10 mL H_2O, dialyzed and concentrated.^{1}H NMR (500 MHz, D_2O): δ 7.67 (s), 4.79 (bs), 4.38 (bs), 3.87-3.99 (m), 3.70-3.59 (m), 3.54-3.27 (m), 2.73-2.66 (bs), 2.02-1.89 (bs).

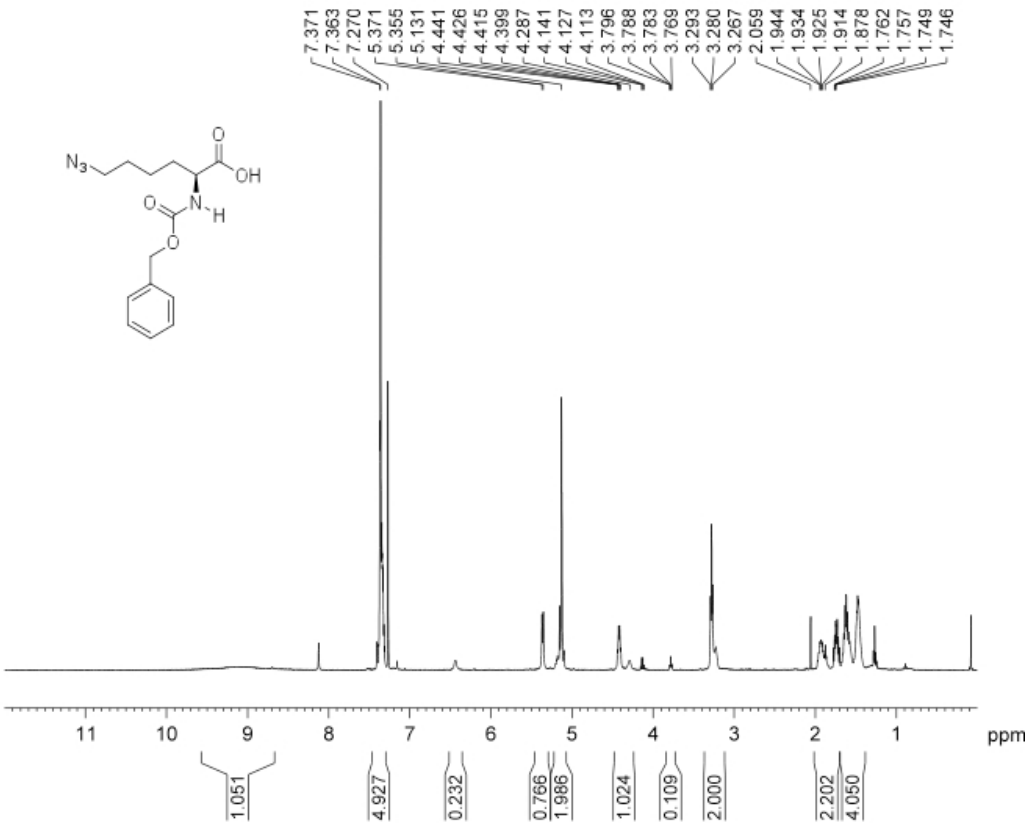
7.371
7.363
7.270
5.371
5.355
5.131
4.441
4.426
4.415
4.399
4.287
4.141
4.127
4.113
3.796
3.788
3.783
3.769
3.293
3.280
3.267
2.059
1.944
1.934
1.925
1.914
1.878
1.762
1.757
1.749
1.746
N3
O
OH
O
N
H
O
O
11
10
9
8
7
6
5
4
3
2
1
ppm
1.051
4.927
0.232
0.766
1.986
1.024
0.109
2.000
2.202
4.050

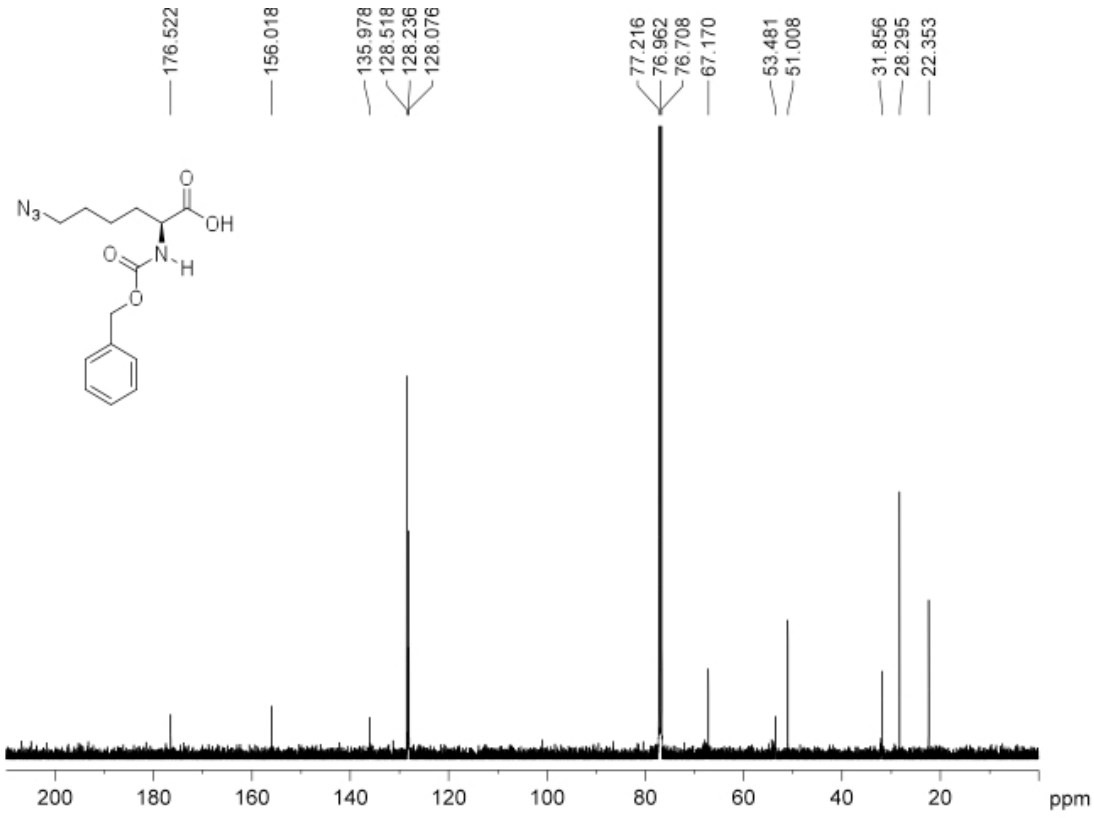
176.522
156.018
135.978
128.518
128.236
128.076
77.216
76.962
76.708
67.170
53.481
51.008
31.856
28.295
22.353
N3
OH
O
N
H
200
180
160
140
120
100
80
60
40
20
ppm

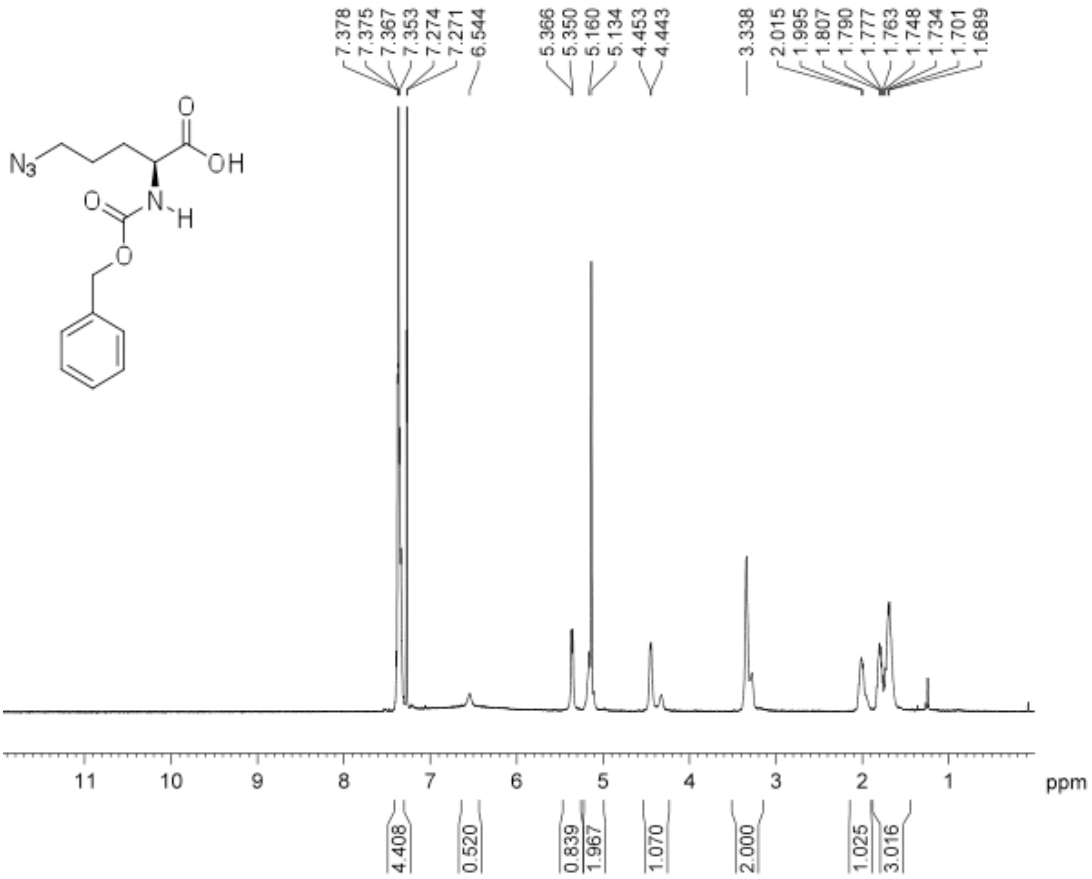
7.378
7.375
7.367
7.353
7.274
7.271
6.544
5.366
5.350
5.160
5.134
4.453
4.443
3.338
2.015
1.995
1.807
1.790
1.777
1.763
1.748
1.734
1.701
1.689
N3
OH
O
N
H
11
10
9
8
7
6
5
4
3
2
1
ppm
4.408
0.520
0.839
1.967
1.070
2.000
1.025
3.016

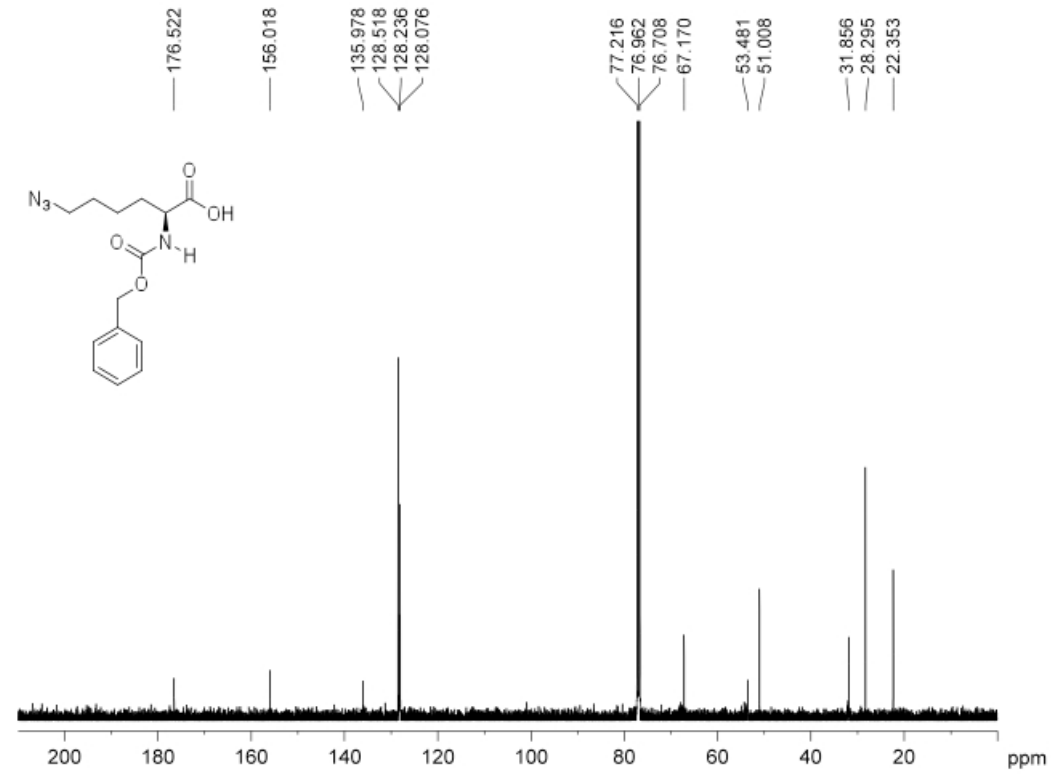
176.522
156.018
135.978
128.518
128.236
128.076
77.216
76.962
76.708
67.170
53.481
51.008
31.856
28.295
22.353
N3
OH
O
N
H
200
180
160
140
120
100
80
60
40
20
ppm

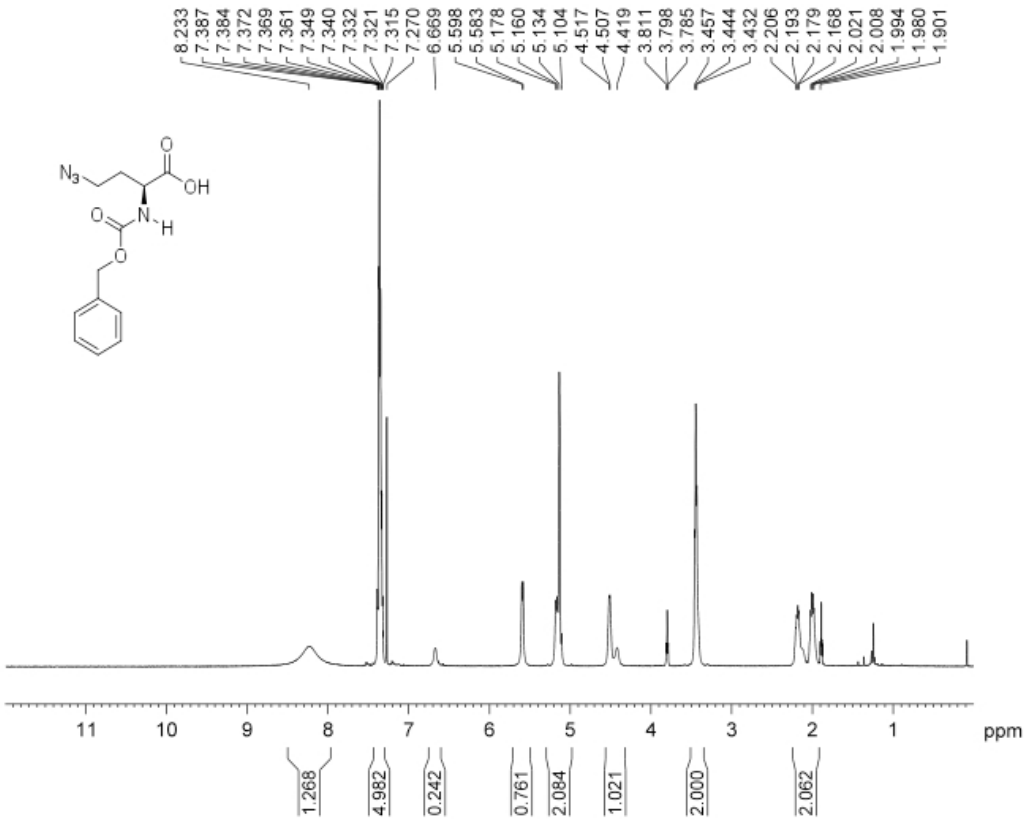
8.233
7.387
7.384
7.372
7.369
7.361
7.349
7.340
7.332
7.321
7.315
7.270
6.669
5.598
5.583
5.178
5.160
5.134
5.104
4.517
4.507
4.419
3.811
3.798
3.785
3.457
3.444
3.432
2.206
2.193
2.179
2.168
2.021
2.008
1.994
1.980
1.901
N3
O
OH
O
N
H
O
O
11
10
9
8
7
6
5
4
3
2
1
ppm
1.268
4.982
0.242
0.761
2.084
1.021
2.000
2.062

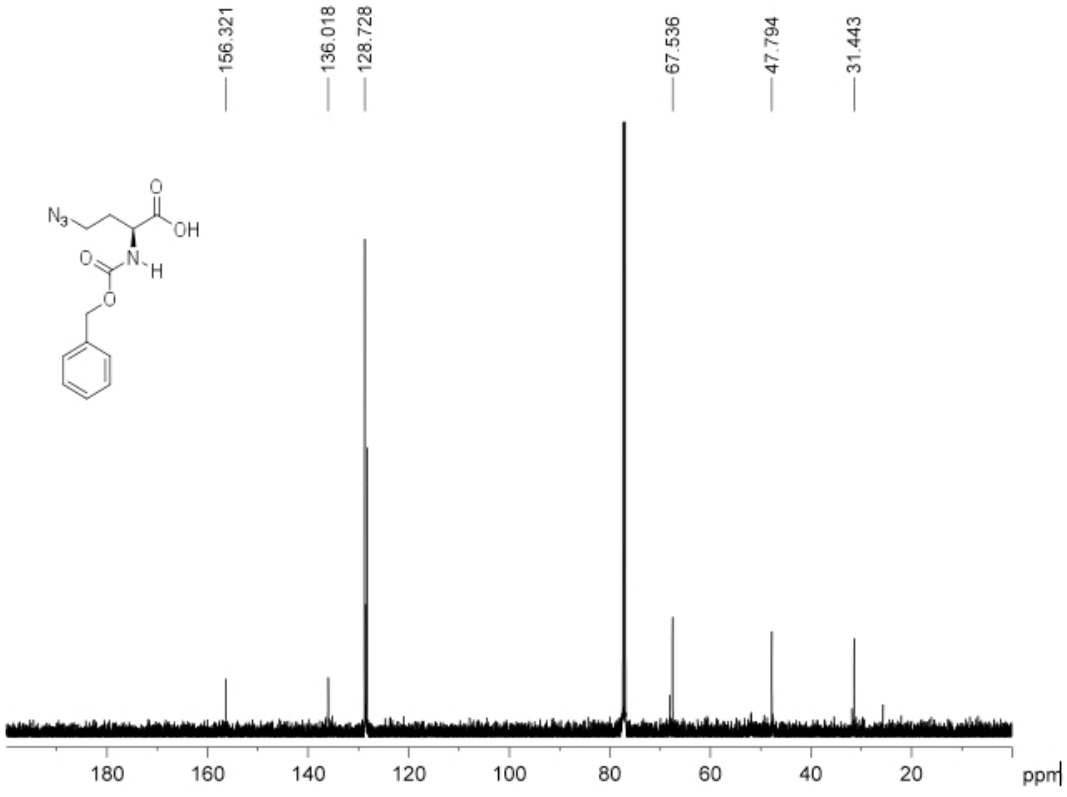
156.321
136.018
128.728
67.536
47.794
31.443
N3
O
OH
N
H
O
O
180
160
140
120
100
80
60
40
20
ppm

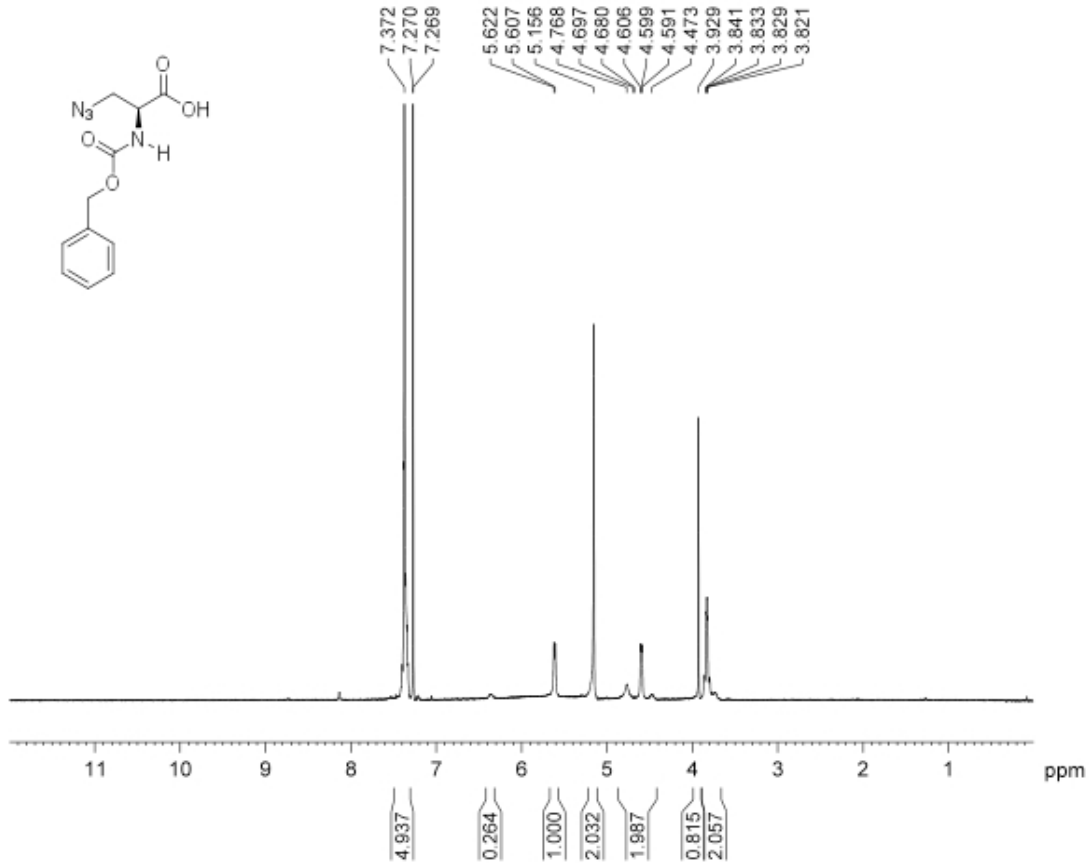
7.372
7.270
7.269
5.622
5.607
5.156
4.768
4.697
4.680
4.606
4.599
4.591
4.473
3.929
3.841
3.833
3.829
3.821
N3
OH
O
N
H
O
O
11
10
9
8
7
6
5
4
3
2
1
ppm
4.937
0.264
1.000
2.032
1.987
0.815
2.057

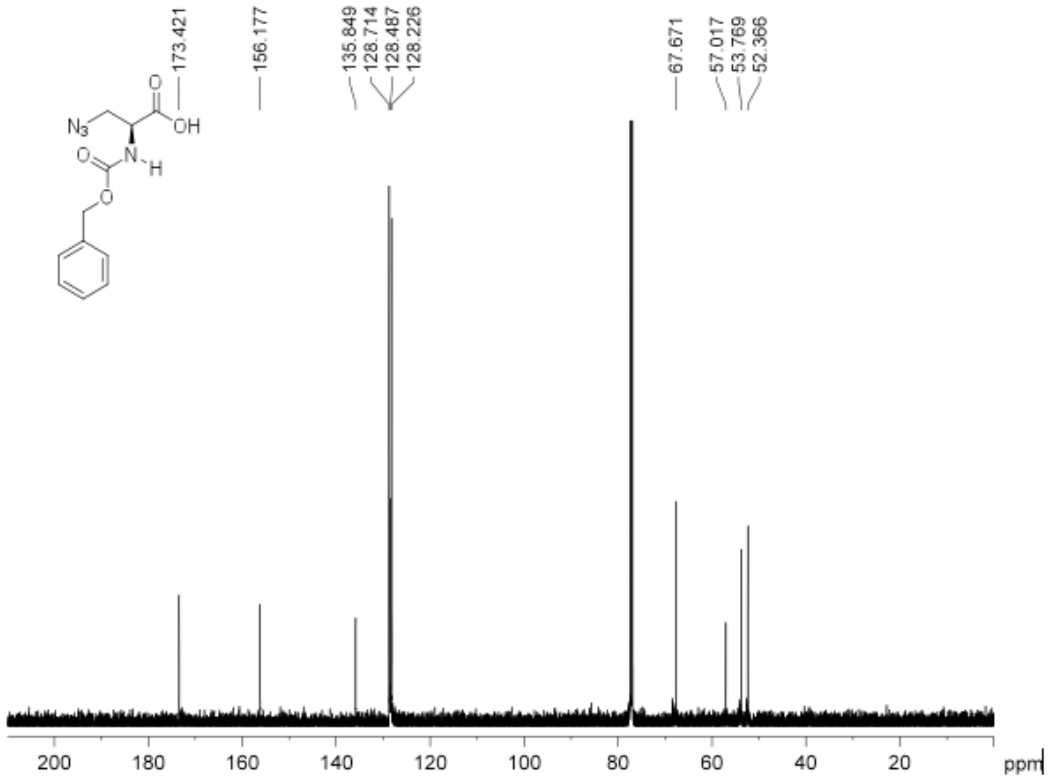
173.421
156.177
135.849
128.714
128.487
128.226
67.671
57.017
53.769
52.366
N3
OH
O
N
H
O
O
200
180
160
140
120
100
80
60
40
20
ppm

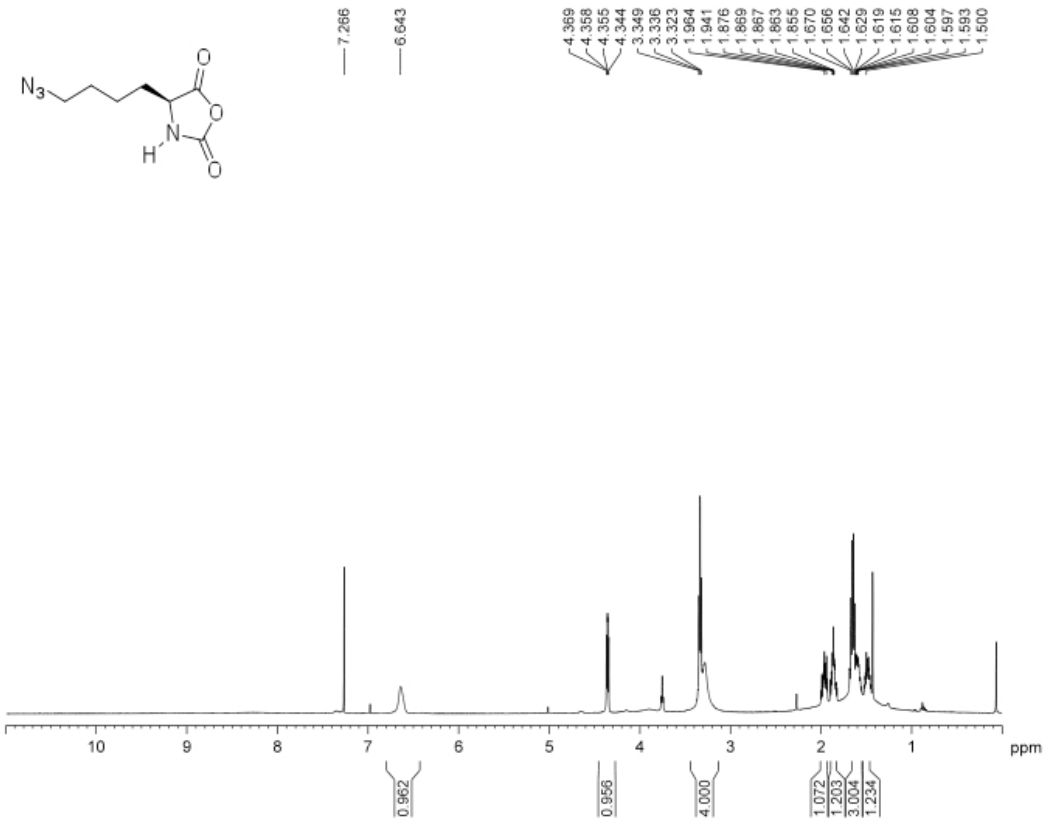
7.266
6.643
4.369
4.358
4.355
4.344
3.349
3.336
3.323
1.964
1.941
1.876
1.869
1.867
1.863
1.855
1.670
1.656
1.642
1.629
1.619
1.615
1.608
1.604
1.597
1.593
1.500
N3
O
O
N
H
O
10
9
8
7
6
5
4
3
2
1
ppm
0.962
0.956
4.000
1.072
1.203
3.004
1.234

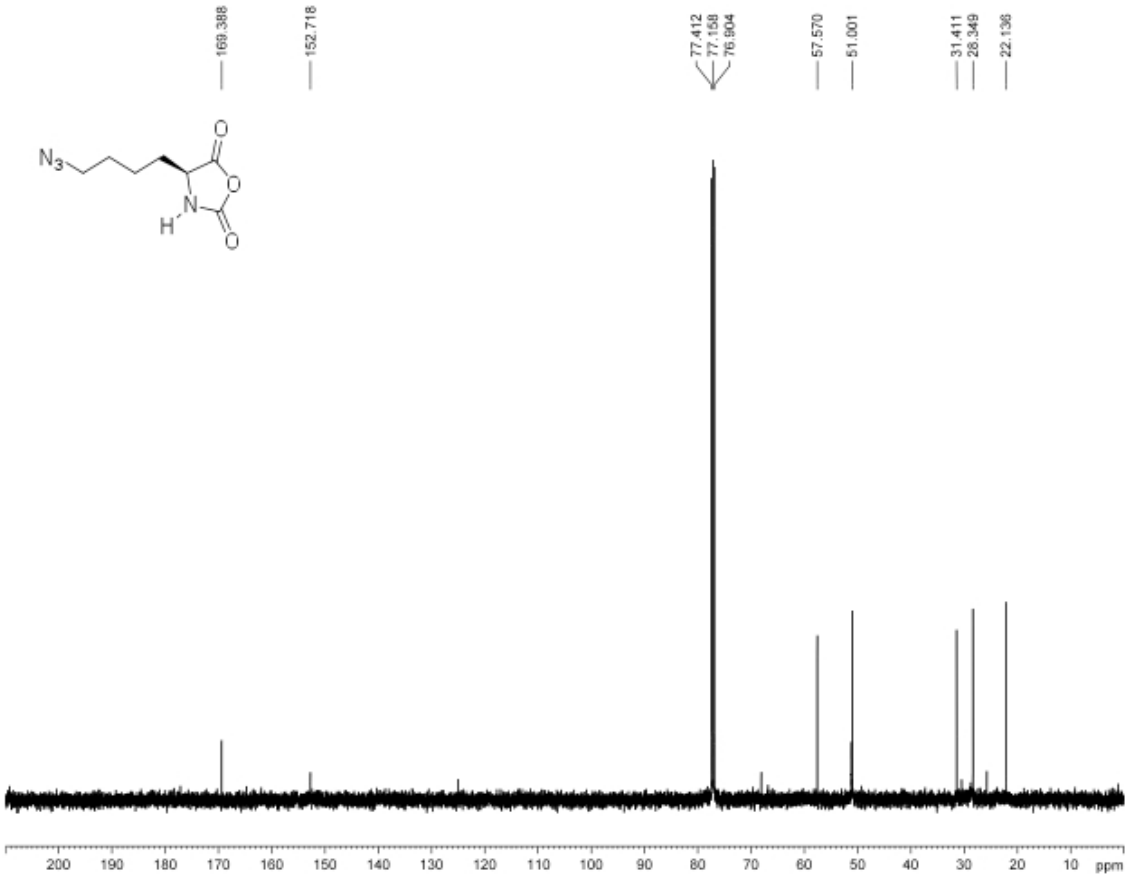
169.388
152.718
77.412
77.158
76.904
57.570
51.001
31.411
28.349
22.136
N3
O
O
N
H
O
200 190 180 170 160 150 140 130 120 110 100 90 80 70 60 50 40 30 20 10 ppm

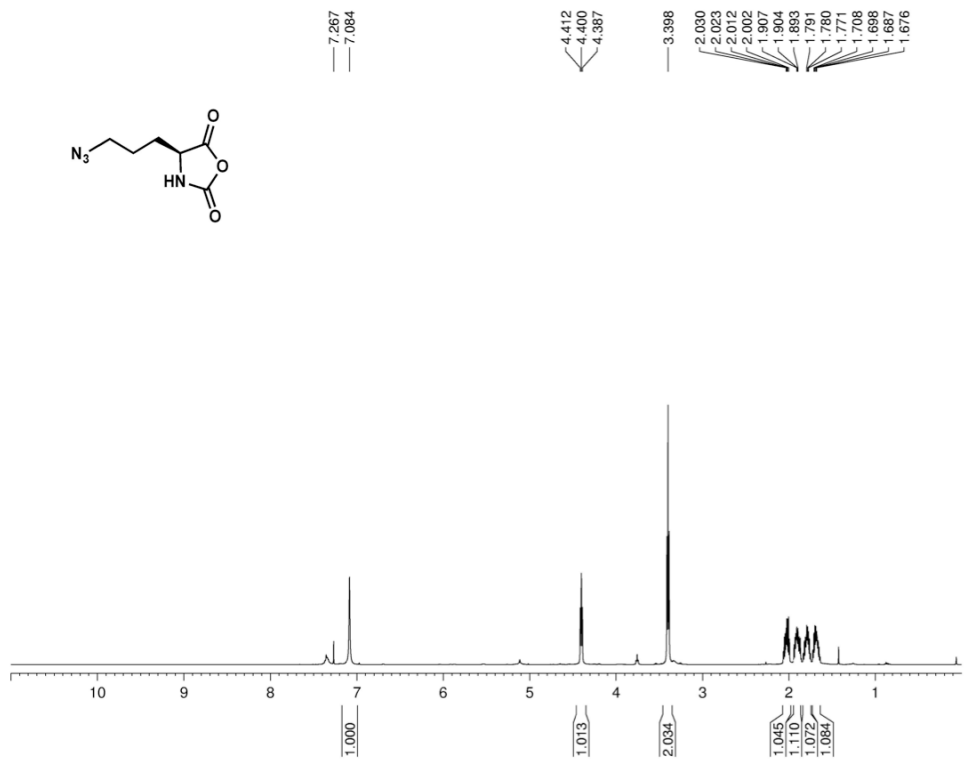
7.267
7.084
4.412
4.400
4.387
3.398
2.030
2.023
2.012
2.002
1.907
1.904
1.893
1.791
1.780
1.771
1.708
1.698
1.687
1.676
N3
HN
O
O
O
10 9 8 7 6 5 4 3 2 1
1.000
1.013
2.034
1.045
1.110
1.072
1.084

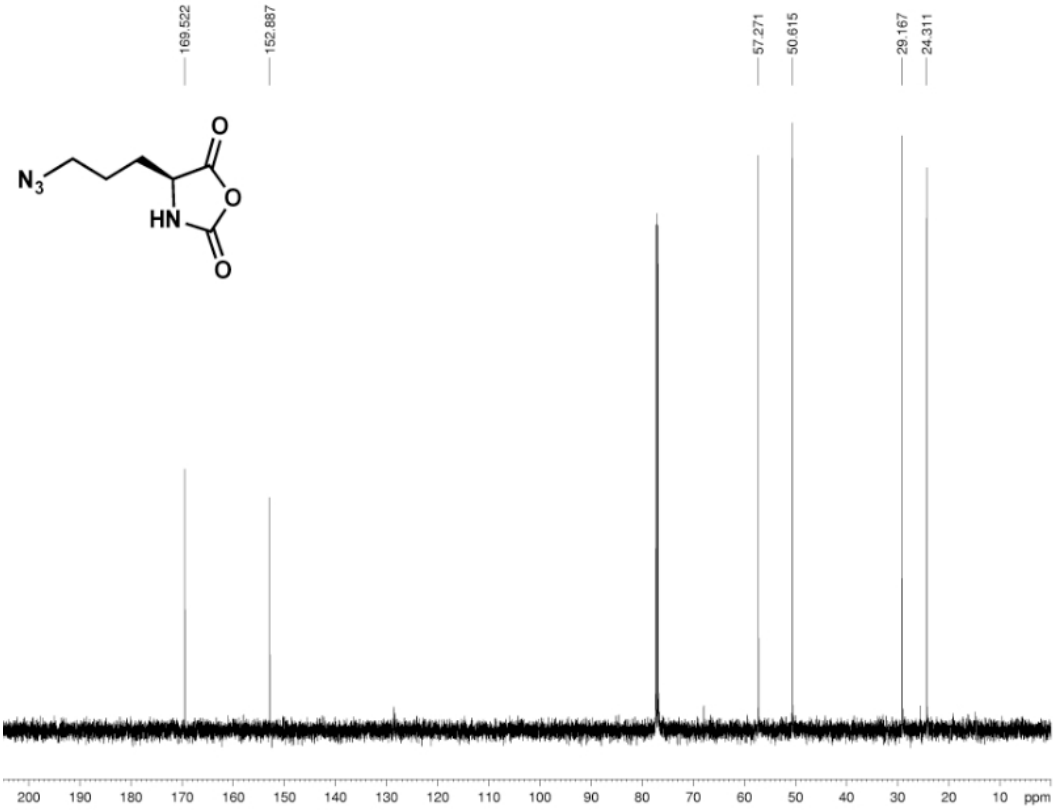
169.522
152.887
57.271
50.615
29.167
24.311
N3
HN
O
O
O
200 190 180 170 160 150 140 130 120 110 100 90 80 70 60 50 40 30 20 10 ppm

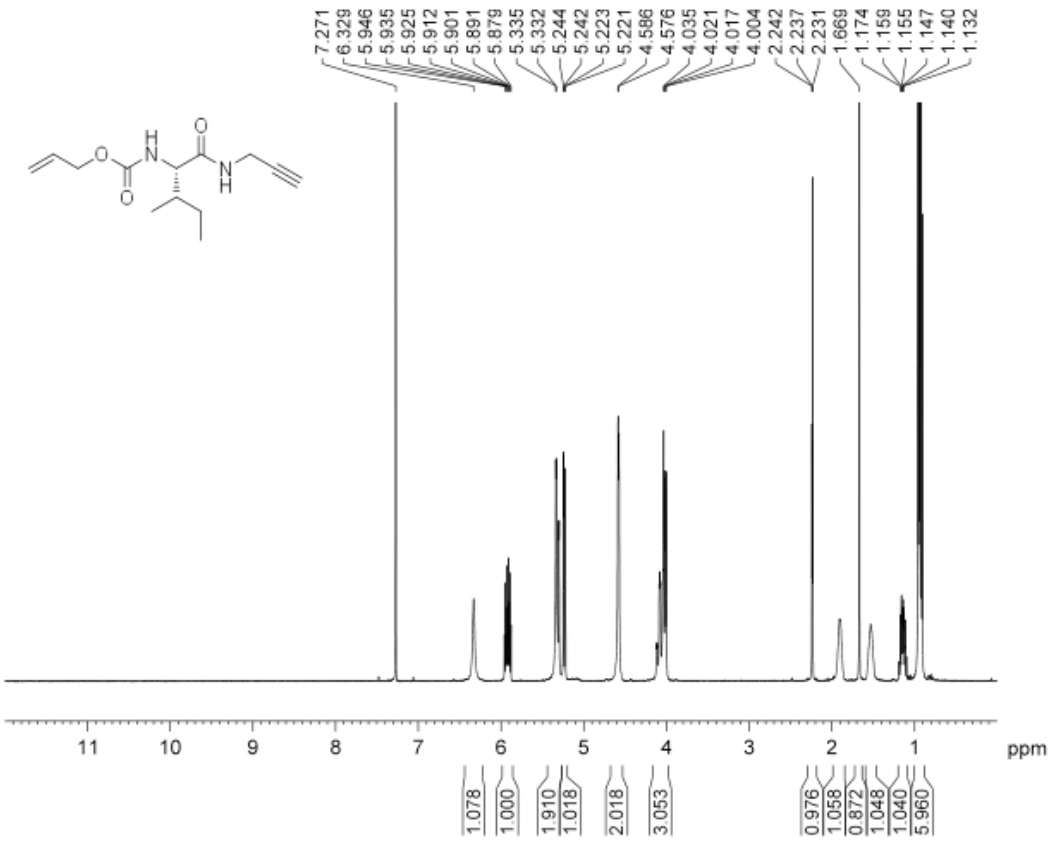
7.271
6.329
5.946
5.935
5.925
5.912
5.901
5.891
5.879
5.335
5.332
5.244
5.242
5.223
5.221
4.586
4.576
4.035
4.021
4.017
4.004
2.242
2.237
2.231
1.669
1.174
1.159
1.155
1.147
1.140
1.132
11 10 9 8 7 6 5 4 3 2 1 ppm
1.078
1.000
1.910
1.018
2.018
3.053
0.976
1.058
0.872
1.048
1.040
5.960

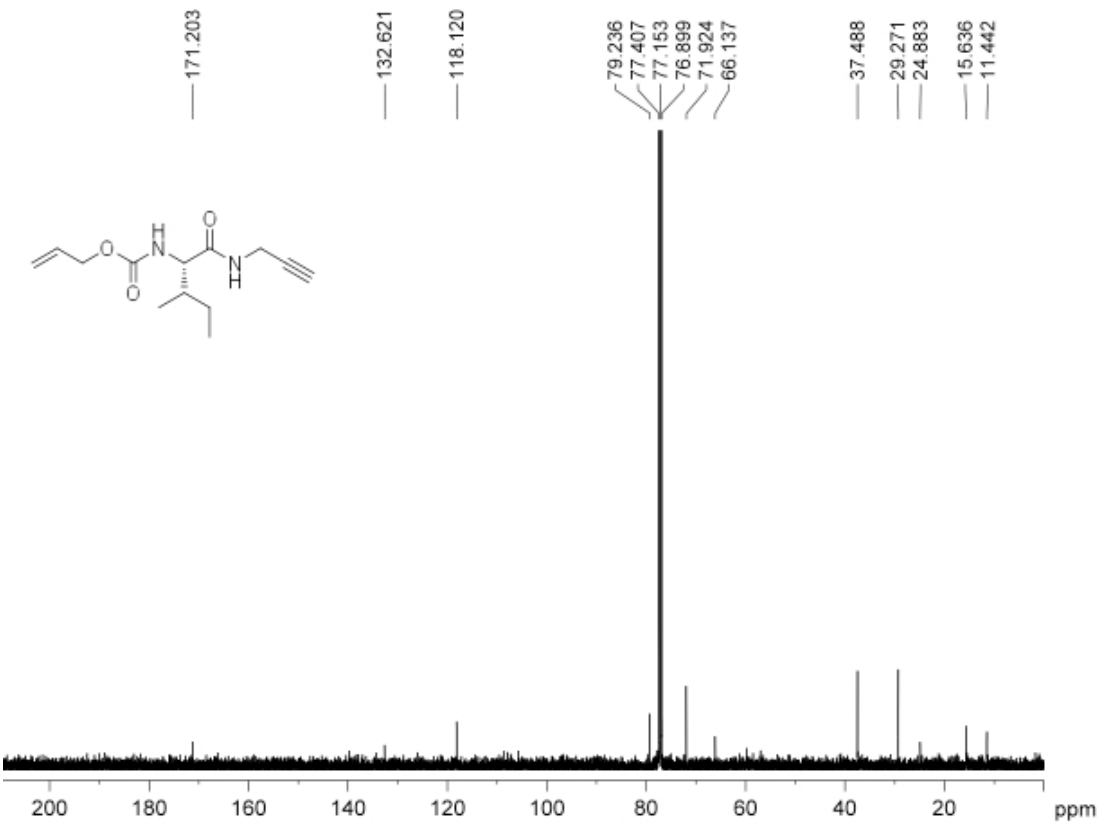
171.203
132.621
118.120
79.236
77.407
77.153
76.899
71.924
66.137
37.488
29.271
24.883
15.636
11.442
200
180
160
140
120
100
80
60
40
20
ppm

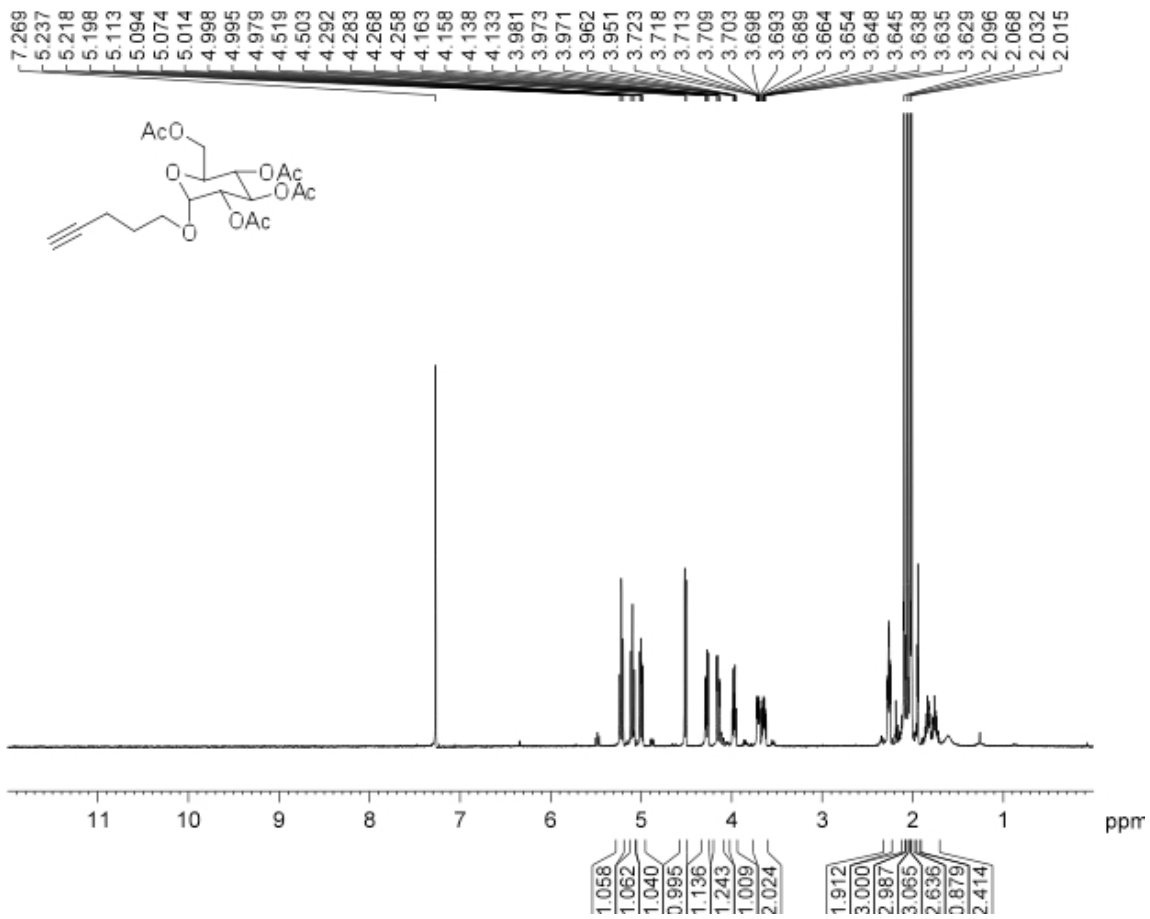
7.269
5.237
5.218
5.198
5.113
5.094
5.074
5.014
4.998
4.995
4.979
4.519
4.503
4.292
4.283
4.268
4.258
4.163
4.158
4.138
4.133
3.981
3.973
3.971
3.962
3.951
3.723
3.718
3.713
3.709
3.703
3.698
3.693
3.689
3.664
3.654
3.648
3.645
3.638
3.635
3.629
2.096
2.068
2.032
2.015
AcO
OAc
OAc
OAc
O
O
11
10
9
8
7
6
5
4
3
2
1
ppm
1.058
1.062
1.040
0.995
1.136
1.243
1.009
2.024
1.912
3.000
2.987
3.065
2.636
0.879
2.414

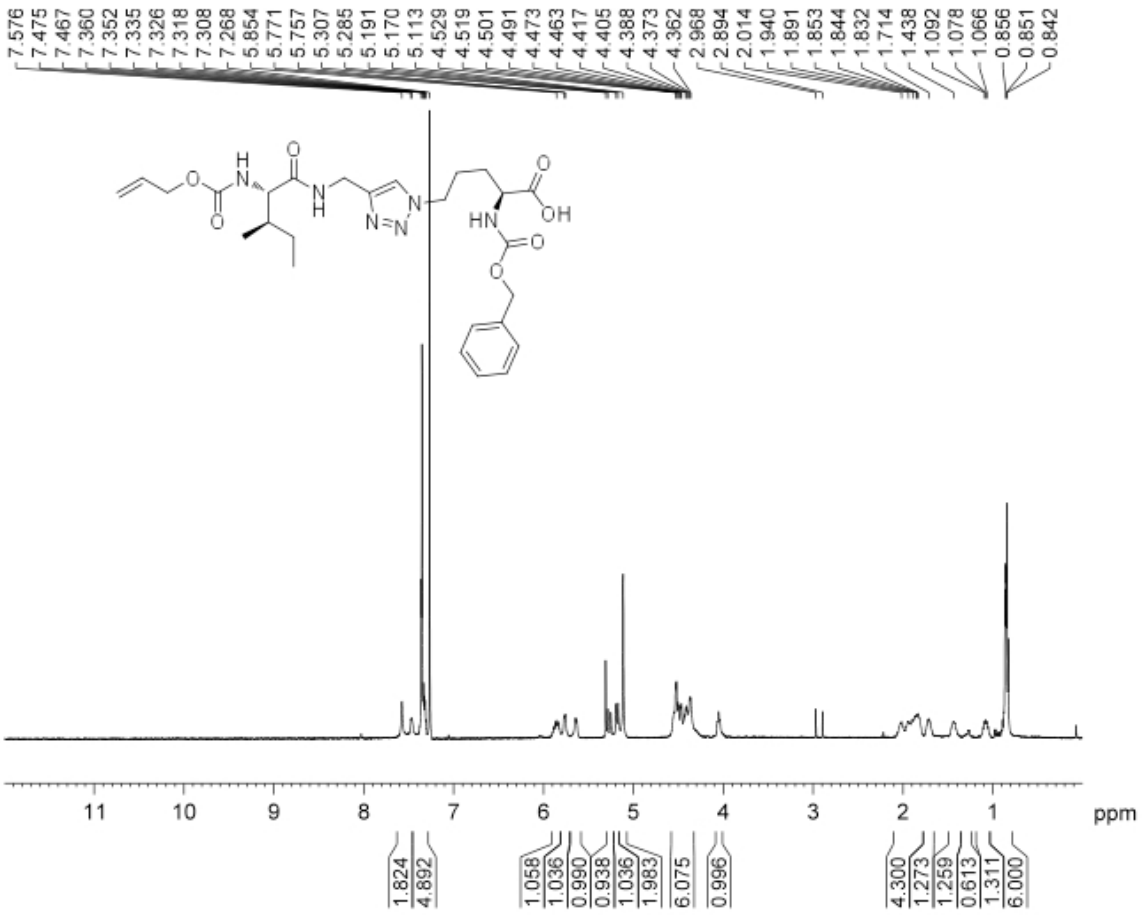
7.576
7.475
7.467
7.360
7.352
7.335
7.326
7.318
7.308
7.268
5.854
5.771
5.757
5.307
5.285
5.191
5.170
5.113
4.529
4.519
4.501
4.491
4.473
4.463
4.417
4.405
4.388
4.373
4.362
2.968
2.894
2.014
1.940
1.891
1.853
1.844
1.832
1.714
1.438
1.092
1.078
1.066
0.856
0.851
0.842
11
10
9
8
7
6
5
4
3
2
1
ppm
1.824
4.892
1.058
1.036
0.990
0.938
1.036
1.983
6.075
0.996
4.300
1.273
1.259
0.613
1.311
6.000

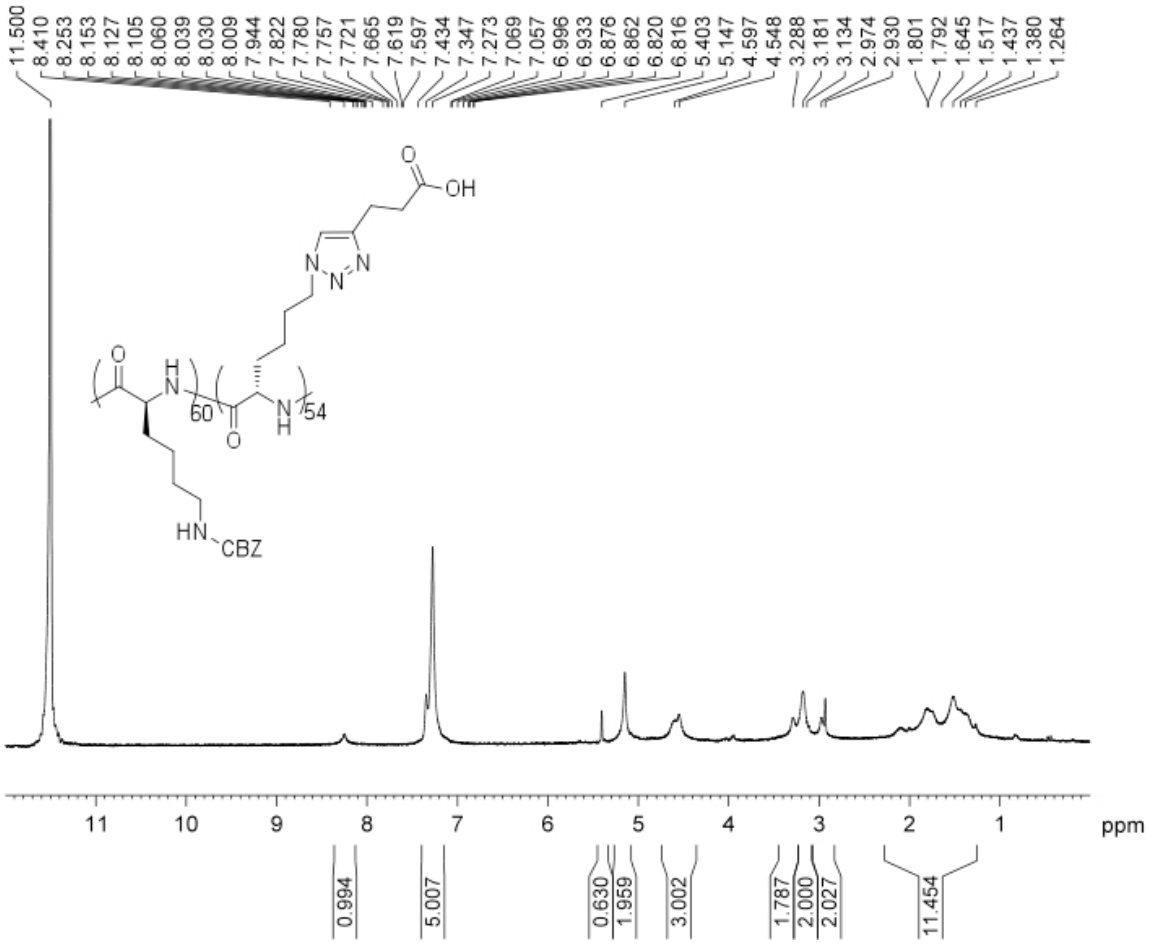
11.500
8.410
8.253
8.153
8.127
8.105
8.060
8.039
8.030
8.009
7.944
7.822
7.780
7.757
7.721
7.665
7.619
7.597
7.434
7.347
7.273
7.069
7.057
6.996
6.933
6.876
6.862
6.820
6.816
5.403
5.147
4.597
4.548
3.288
3.181
3.134
2.974
2.930
1.801
1.792
1.645
1.517
1.437
1.380
1.264
O
OH
N
N
N
O
H
N
60
O
N
H
54
HN
CBZ
11
10
9
8
7
6
5
4
3
2
1
ppm
0.994
5.007
0.630
1.959
3.002
1.787
2.000
2.027
11.454

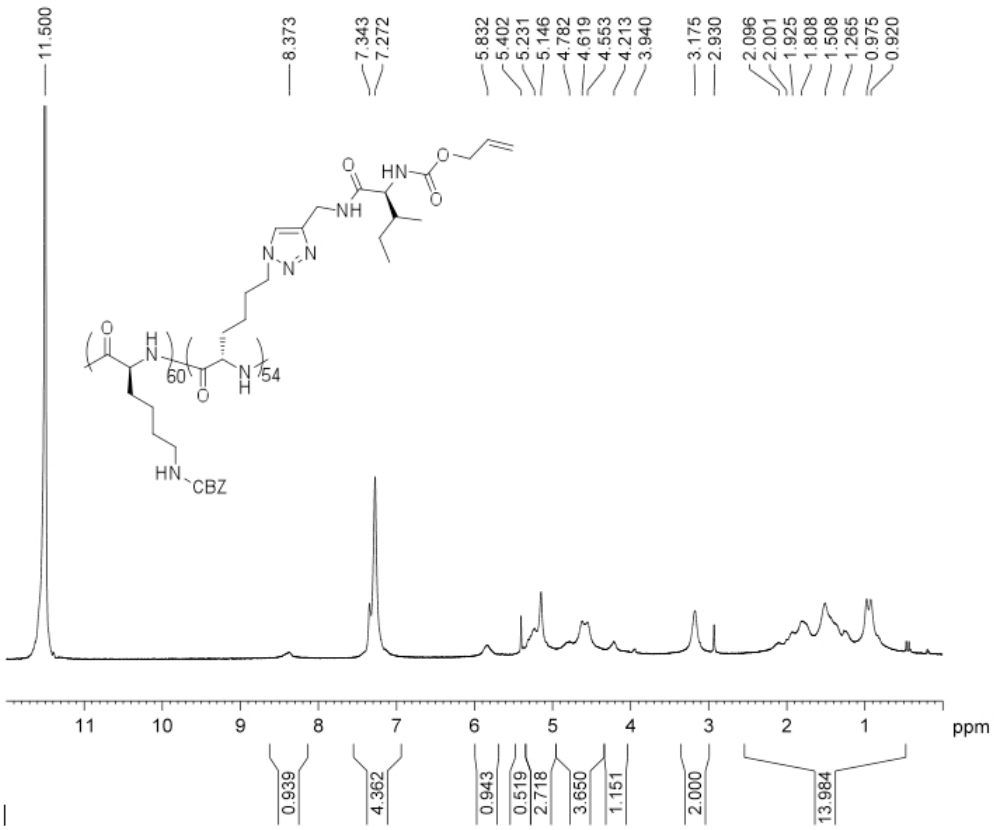
11.500
8.373
7.343
7.272
5.832
5.402
5.231
5.146
4.782
4.619
4.553
4.213
3.940
3.175
2.930
2.096
2.001
1.925
1.808
1.508
1.265
0.975
0.920
HN
O
NH
N
N
N
O
O
H
N
60
O
N
H
54
HN
CBZ
11 10 9 8 7 6 5 4 3 2 1 ppm
0.939
4.362
0.943
0.519
2.718
3.650
1.151
2.000
13.984

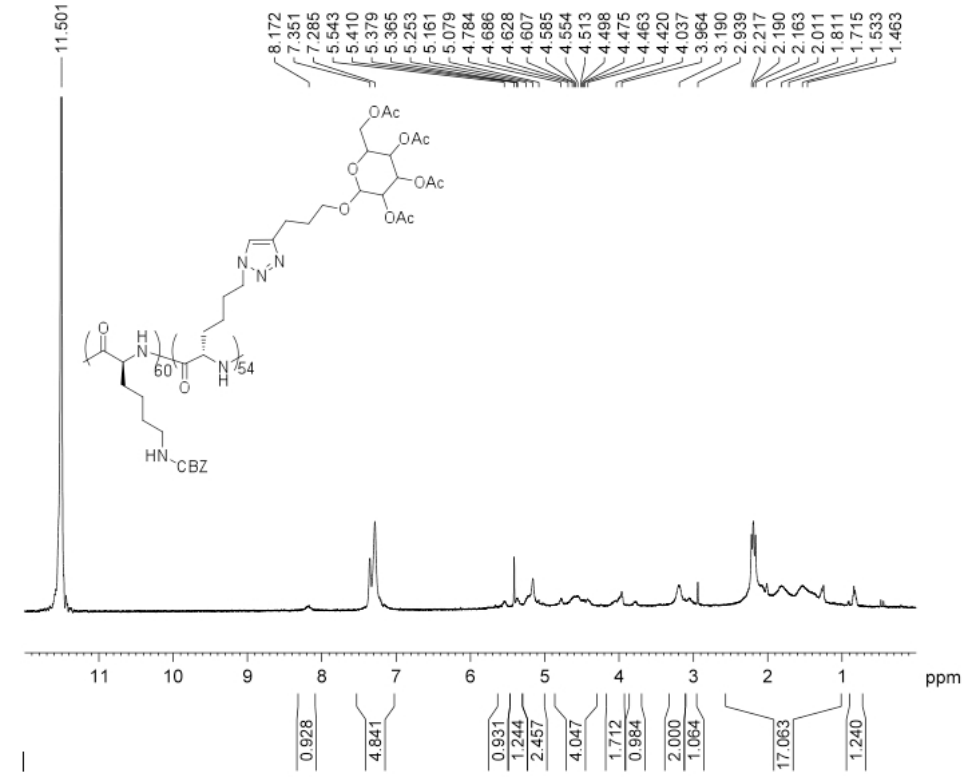
11.501
8.172
7.351
7.285
5.543
5.410
5.379
5.365
5.253
5.161
5.079
4.784
4.686
4.628
4.607
4.585
4.554
4.513
4.498
4.475
4.463
4.420
4.037
3.964
3.190
2.939
2.217
2.190
2.163
2.011
1.811
1.715
1.533
1.463
OAc
OAc
OAc
OAc
O
O
N
N
N
O
O
H
N
60
O
N
H
54
HN
CBZ
11 10 9 8 7 6 5 4 3 2 1 ppm
0.928
4.841
0.931
1.244
2.457
4.047
1.712
0.984
2.000
1.064
17.063
1.240

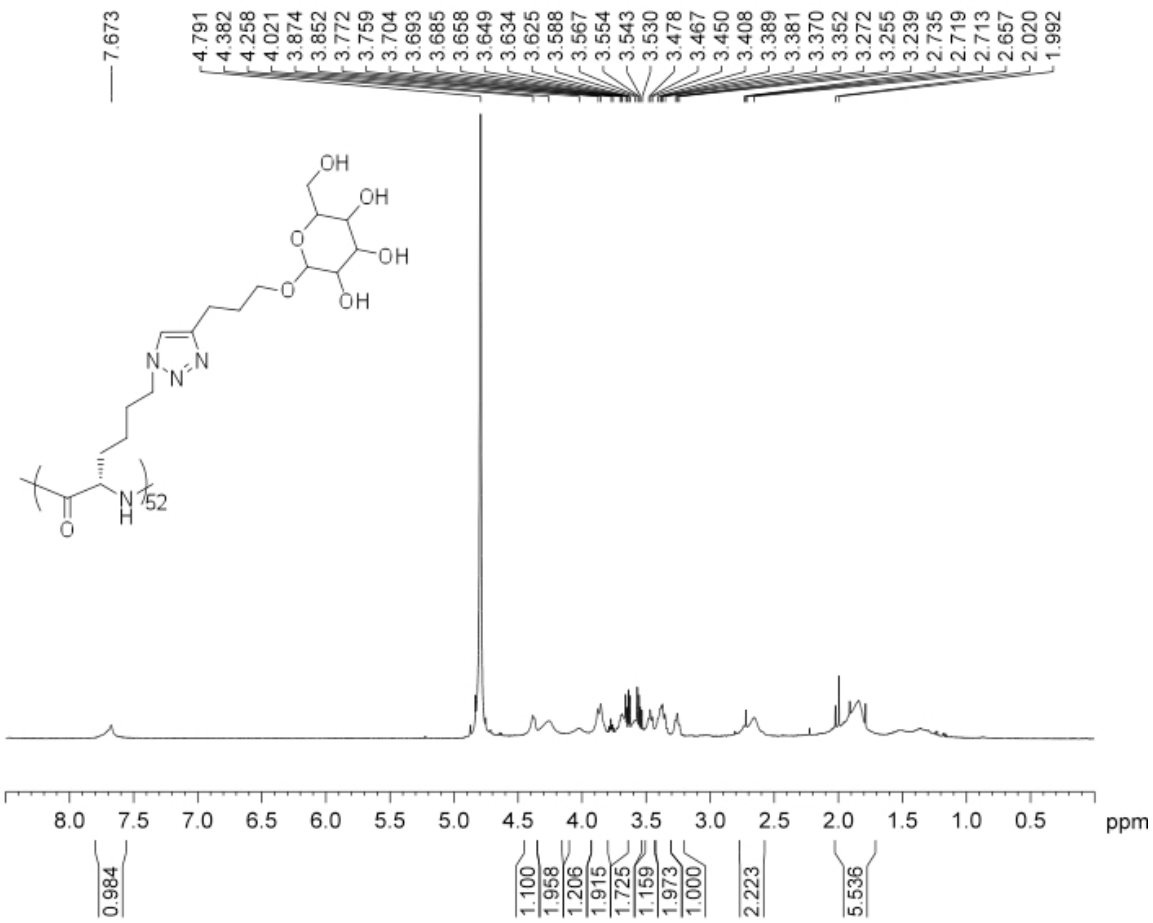
7.673
4.791
4.382
4.258
4.021
3.874
3.852
3.772
3.759
3.704
3.693
3.685
3.658
3.649
3.634
3.625
3.588
3.567
3.554
3.543
3.530
3.478
3.467
3.450
3.408
3.389
3.381
3.370
3.352
3.272
3.255
3.239
2.735
2.719
2.713
2.657
2.020
1.992
OH
OH
OH
OH
O
O
N
N
N
N
H
O
52
8.0
7.5
7.0
6.5
6.0
5.5
5.0
4.5
4.0
3.5
3.0
2.5
2.0
1.5
1.0
0.5
ppm
0.984
1.100
1.958
1.206
1.915
1.725
1.159
1.973
1.000
2.223
5.536

Chapter 4

Synthesis and polymerization of NTA monomers

4.1 NTA Introduction

α-amino-*N*-thiocarboxyanhydrides (NTAs), a thio-analogue of NCAs, exhibit greater stability in water (stable at pH lower than 11.0), making them attractive candidates for polymerization under less stringent (i.e. water-free) conditions (Figure 4-1). The research involving the preparation of NTAs has been limited.[119-121] There is no precedent for the preparation and polymerization of NTAs containing polar side chains such as L-lysine and L-glutamic acid amino acids. Although the literature available on the polymerization of NTAs is limited, NTAs are well-established monomers that react with various organoinitiators.[120,122,123] If a viable initiator and polymerization process can be developed, NTAs could be used as monomers in polypeptide preparation.

The reactivity difference between NTAs and NCAs may also be exploited to prepare hyperbranched polypeptides with defined branching. This would be significant since no methods are available for the controlled synthesis of hyperbranched polymers, let alone biologically relevant hyperbranched polypeptides. In addition, the stability of the NTA monomer could lead to well-defined polypeptide preparation on the bench top if the appropriate initiator is found. Bench top preparation would revolutionize the field of polypeptide chemistry, leading to cost effective, well-defined polypeptide materials through a facile methodology. This would allow for industrial scale up and the preparation of pharmaceutical drug carriers, household products as well other applications.

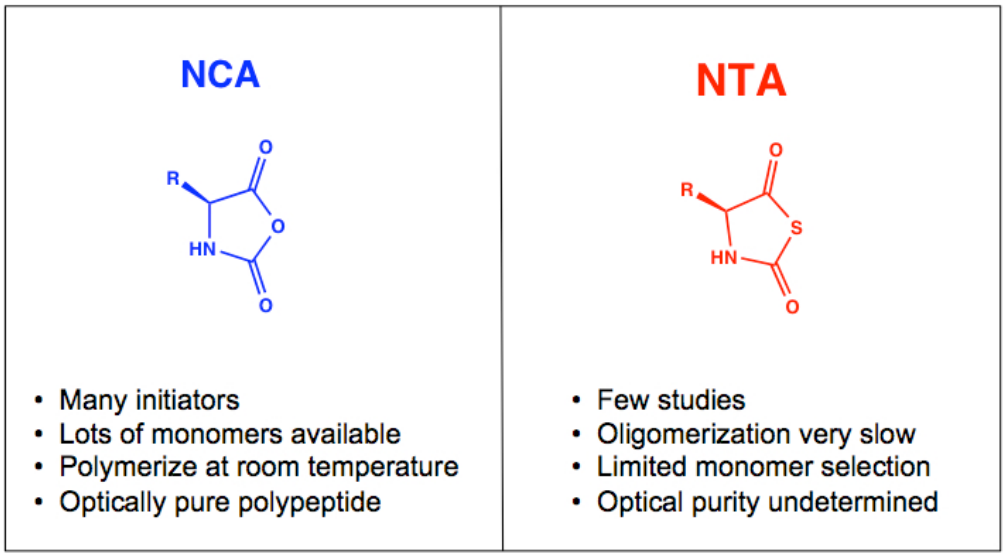

Figure 4-1. NCA/NTA structure and reactivity

4.2 Synthesis of NCAs and NTAs

NCAs are prepared using two methods: the Leuchs method (Figure 4-2, 1→2→3) and the Fuchs-Farthing method (Figure 4-2, 4→5→6).[9,124] Leuchs method utilizes a carbamate protected amino acid (1) starting material and chlorinating reagent, forming an acid chloride intermediate (2). NCA and the corresponding alkylchloride byproduct form when heat is applied. The Fuchs-Farthing method utilizes an unprotected amino acid (4) and phosgene forming an acid chloride intermediate (5). The acid chloride undergoes an intramolecular reaction with loss of HCl. The NCA product is purified by either crystallization from THF/hexanes or flash column chromatography depending on side chain functionality/polarity.

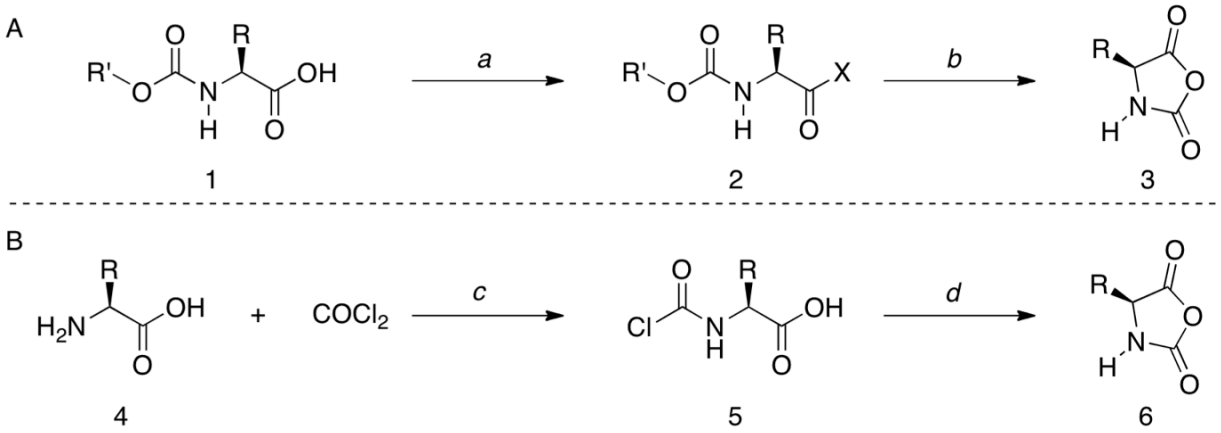

Figure 4-2. Synthesis of NCA monomers. A. Leuchs Method; a.) $SOCl_2$, PBr_3, or PCl_3, b.) heat. B. Fuchs-Farthing Method; c.) and d.) loss of HCl.

NTAs are traditionally prepared by a modified Leuchs method where the amino acid is protected with a thiocarbonyl (Figure 4-3). Aqueous (1)[123,125-127] and non-aqueous conditions (2)[128,129] are used for the protection of these amino acids. Facile aqueous conditions are compatible with R groups that tolerate strong base. The non-aqueous reaction conditions were developed for base labile R groups and are a bit more time consuming with DMF as the solvent. Once the thiocarbonyl-protected amino acid is formed and purified, it reacts with a chlorinating reagent (3), forming the NTA product. The NTA is then purified by crystallization from THF/hexanes since the recovery of NTA from column chromatography[116] is challenging.

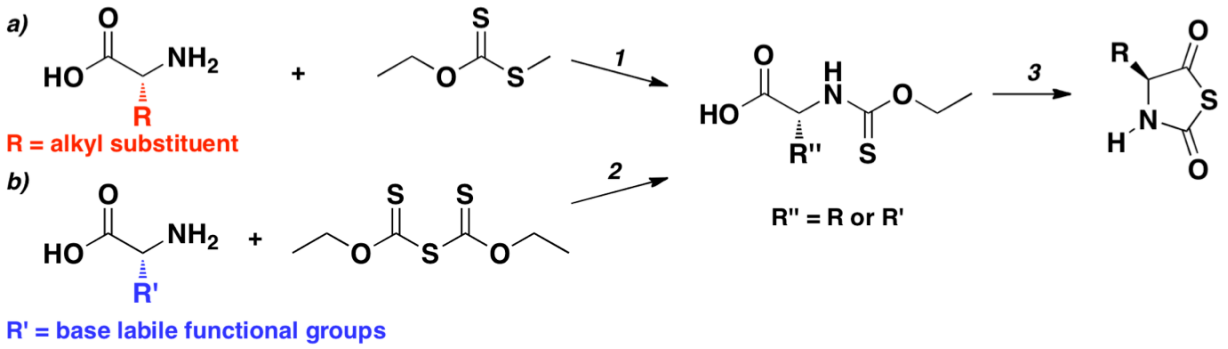

Figure. 4-3 a.) Literature procedure for thiocarbonyl protection of amino acids[1]; *1).* 50% aqueous NaOH, methanol, 45 ^{o}C, 2 h and *b.)* Non-aqueous procedure for base labile amino acid derivatives. Stereochemistry of amino acid is maintained. *2)* Triethylamine, DMF, 21 ^{o}C, overnight. 3.) Phosphorus tribromide, imidazole, THF, 0 ^{o}C → 21 ^{o}C, 10 min.

A wide array of NTAs were prepared utilizing both the traditional aqueous conditions as well as the modified non-aqueous procedures (Figure 4-4, 1-4). Benzyl glutamate (5), Benzyl aspartate (6), phalimidyl Lysine (7), and β-alanine NTA (8) have all been prepared using xanthic anhydride[129,130] in DMF in the presence of triethylamine (Figure 4-4). The structure and purity of these NTAs have been confirmed by NMR, mass spectrometry, and X-Ray crystallography (confirmation of optical activity; E NTA only). These monomers were very stable and not air sensitive. Purification was straightforward and conducted in air, unlike traditional NCA purification methods.

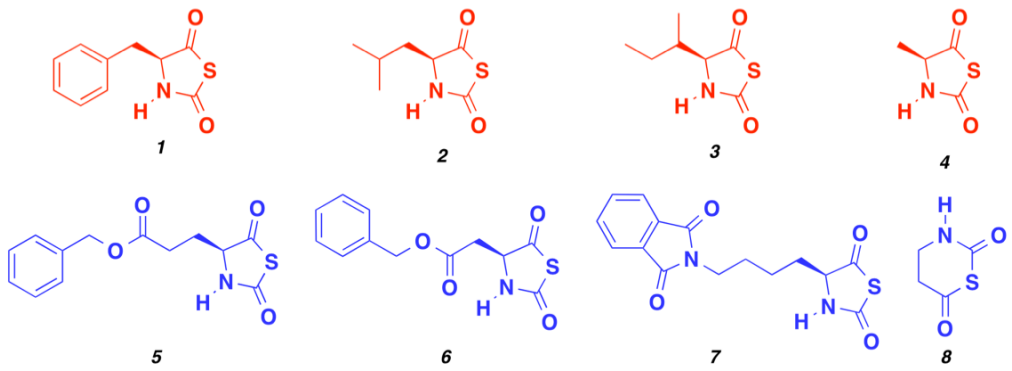

Figure 4-4. α-amino-*N*-thiocarboxyanhydrides (NTAs) *1-4* prepared by literature methods; *5-8* prepared using non-aqueous protection method.

Preparation of a protected K NTA (γ-protected lysine, unknown in the literature) was the first goal of this research project since the polar side chain would allow for facile characterization of polymer size and distribution by GPC. In addition, poly(K) prepared from K NCA is well established and would allow for direct comparison of the polymers prepared using the NTA. H-Lysine-CBZ was reacted with *O*-dimethylxanthate according to Leuchs' method, resulting in multiple side reactions with no K NTA product recovery. This result was surprising since L-, A- and P-NTA were all easily synthesized using the same procedure. Different amino protected amino acids (namely *O*-benzylmethyl xanthate, *O*-ethylmethyl xanthate, and *O*-dimethyl xanthate) were synthesized for use in this reaction but again did not render the desired product. Electronic issues at the γ-amine of lysine could inhibit NTA formation, therefore the protecting group was modified at this position. In an effort to synthesize K NTA, a wide array of γ-amine protecting group chemistry was used including: dithiocarbonyl, tosyl, alloc, TFA, Fmoc and more. The phthalimidyl amino protecting group is very stable and an ideal candidate as it

blocks both N-H protons of the amino group. Phthalimidyl Lysine NTA was prepared using a 4-step synthesis (Figure 4-5).

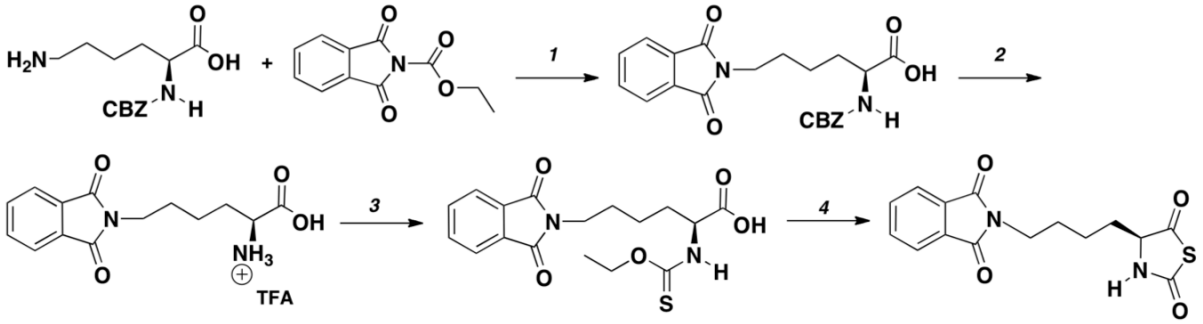

Figure 4-5. Preparation of phthalimidyl lysine NTA. *1.)* Na_2CO_3, 1:1 THF: H_2O, 77% yield; *2.)* 33% HBr in AcOH, TFA, 71% yield; *3.)* Bis(ethoxythiocarbonyl) Sulfide (Ethylxanthic Anhydride)**,** triethylamine, DMF, overnight, 69% yield. *4.)* phosphorus tribromide, imidazole, THF, 0 ^{o}C → 21 ^{o}C, 10 min, 75% yield.

After these measures to optimize the γ-amine protecting group and reaction conditions (i.e. solvent, temperature, time, and reagents), the synthesis of other polar side chain amino acids was pursued. The modification of the γ-amine protecting group resulted in numerous side reactions. In literature, ten thiocarbonyls of α-amino acids have been synthesized while only three of those possess polar side chains. Therefore it is no surprise that difficulties were encountered with the synthesis of the thiocarbonyl of various derivatives of lysine, which also contains a polar side chain. To circumvent this problem, the synthesis of thiocarbonyl derivatives of L-arginine, L-histidine and L-aspartic acid was attempted. L-arginine and L-histidine protected amino acids could not be obtained as the free base according to literature protocol (most likely due to side

reactions). A protection sequence would most likely be required to obtain the desired thiocarbonyl due to the harsh, basic reaction conditions (refer to experimental section).

4.3 Polymerization of NTAs

Several factors determine the success of NCA polymerization: solvent and monomer purity, reaction kinetics and side reactions. Woodward and Schramm reported the first copolymerization of phenylalanine and leucine NCAs in 1947 spurring intensive research in NCA polymerization.[131] However, research activity dwindled by the mid 1980s since NCA polymerization was uncontrollable using traditional initiators such as water and alkyl amines.

In 1976, Kricheldorf showed that tertiary amines could initiate polymerization of sarcosine NCA and NTA.[123] The NTA derived polysarcosine exhibited a lower molecular weight (M_w) than the polypeptide derived from sarcosine NCA.[123] In 2008 Kricheldorf reported the primary amine initiation of F-NTA, L-NTA, and -NTA resulted in low molecular weight polypeptides (by MALDI-TOF MS).[120] The author reported no side reactions occurred in these oligomerizations but he reasoned that hydrogen bonding induced steric hinderance during propagation explaining the low molecular weights. Low molecular weight is a sign of incomplete polymerizations and reactions such as chain termination. Since zerovalent cobalt and nickel initiators are highly reactive toward NCAs they were also expected to polymerize the less reactive thio-analogs of NCAs (NTAs), albeit more slowly.

With the discovery and implementation of zerovalent cobalt and nickel initiators for the efficient polymerization of NCAs,[36,40] it was reasonable to try the same initiators for NTA polymerization. Typical NCA polymerizations are conducted in a dinitrogen

filled atmosphere and air-free environment/glovebox. After about an hour, an aliquot is removed from the reaction vessel and its progress monitored by FT-IR. The polymerization is observed while strong amide I and II bands are observed at approximately 1650 and 1540 cm^{-1}. The NTA carbonyl peak has a strong, sharp absorbance at approximately 1719 cm^{-1}. When NTA was reacted with cobalt and dmpeNi(COD) initiators, no polypeptide was formed; this was surprising due to the reactivity of these initiators. NTA monomer type, reaction time, solvent and temperature were systematically varied with only minor improvement in polypeptide yields.

Interestingly, when NTA monomer was reacted with a 'pre-initiated' form of the Ni initiator (Figure 4-6), poly(L) was readily prepared (albeit it in low M_w due to its solubility in THF) at 80 ^oC. Higher M:I ratios were possible but the polymer crashed out of solution which limited further characterization of these samples. Since poly(L) is insoluble in 0.1 M LiBr DMF, polydispersity and molecular weights of the sample could not be obtained by size exclusion chromatography (SEC). However, once all monomer was consumed the samples were end-capped with PEG-NCO and analyzed by ^1H NMR for molecular weight determination.

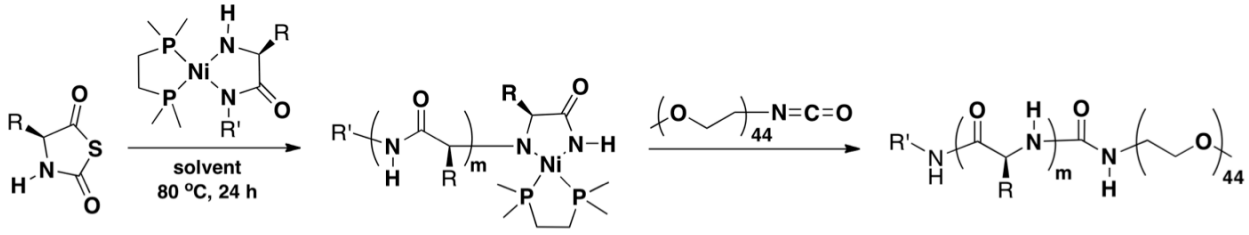

Figure 4-6. Reaction of L NTA with 'pre-initiated' nickel amidoamidate

The polymerization of L NTA was found to give molecular weight control with a directly proportional relationship between M:I and molecular weight (Figure 4-7, Table 4-1). The

chain-ends remained active after the consumption of all monomer as displayed by PEG-NCO end-capping experiments.

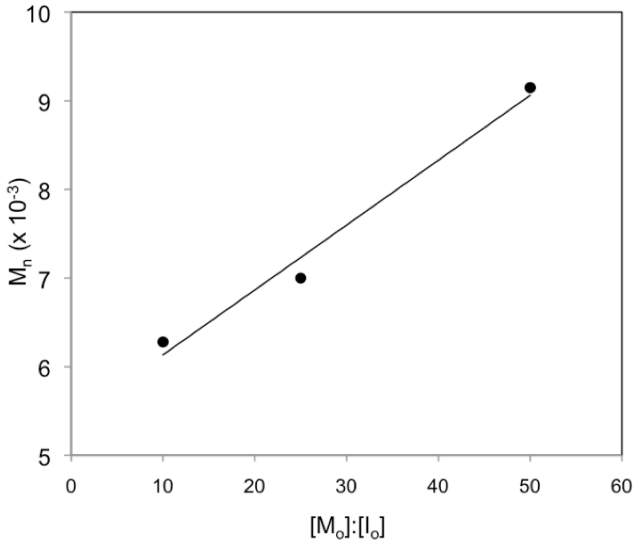

Figure 4-7. Molecular weight (M_n, filled circles) of poly(L) as a function of monomer to initiator ratio ([M]:[I]) after 100% monomer conversion at 80 ^{o}C in DMF using nickel amido amidate initiator. M_n was determined by ^{1}H NMR of PEGylated poly(L).

entry[a]	M:I	M_n (x 10^{-3})	DP	% yield
1	10	33.11	293	99
2	25	24.86	220	99
3	50	41.47	367	95
4	10	6.28	56	96
5	25	7	62	98
6	50	9.15	81	99

Table 4-1. Molecular weights of poly (L) as a function of monomer to initiator ratio after 100% conversion. a. Entries 1-3 reaction solvent = THF, entries 4-6 reaction solvent = DMF. Entries 1-3 monitored by IR for 24 h.

Diblocks of poly(K)-*b*-poly(L) could also be prepared from K NCA and L NTA with 100% conversion of both NCA and NTA to polypeptide (Figure 4-8, Table 4-2). For NTA polymerization to occur, the formation of a preinitiated species in the form of small molecule nickel amido amidate or active chain end polypeptides was required.

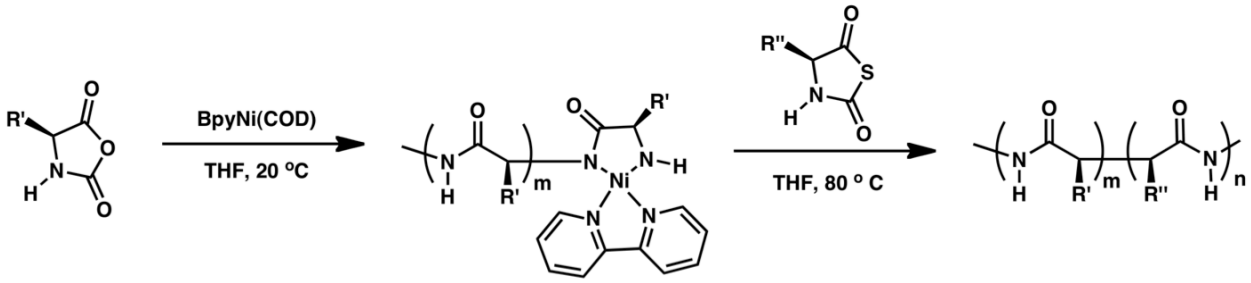

Figure 4-8. Diblock prepared from K NCA and L NTA

	Lys Block			Leu Block		
entry	M:I[a]	DP[b]	PDI[b]	DP[c]	% Conv.[d]	% Yield[e]
1	51	229	1.05	25	100	95
2	40	191	1.05	21	100	96
3	38	212	1.05	27	100	92
4	27	186	1.04	22	100	90

Table 4-2. Preparation of poly(carboxybenzyl-L-lysine)-*b*-poly(L-leucine) from Leu NTA. R' = -$CH_2CH_2CH_2CH_2NH(CO)$-$OCH_2C_6H_5$, R'' = -$CH_2CH(CH_3)_2$ [a] Monomer-to-initiator ration; [b] Degree of polymerization (DP) and Polydispersity index (PDI) of first block determined by Gel permeation chromatography (GPC), [c]DP for second block determined by ^{1}H NMR, [d] Percent conversion determined by infrared spectroscopy (IR); [e]Isolated yield.

Benzyl-Glutamate (E) NTA was found to differ greatly in reactivity from other NTAs in that almost no polypeptide formation was observed given the same reaction conditions as L NTA. One explanation for this is that the purity of NTAs varied from monomer to

monomer, despite each being crystalline. This is unlikely as the NTAs were purified both by aqueous work-up (due to stability) and three recrystallizations in the glovebox. Another reason may be due to the side chain ester linkage where the E NTA can undergo an intramolecular nucleophilic addition with the activated nickelocycle. The ester linkage could be cleaved forming a side product that could react with another monomer unit or the initiator (eventually terminating the reaction). L NTA was the best performing NTA of all the monomers studied (F NTA, V NTA, K NTA, E NTA).

4.4 Mechanistic Studies

Mechanistic studies on NCA polymerizations were conducted using bis(triphenylphosphine)nickel(cyclooctadiene) as the initiating species. The electron poor donation of the triphenylphosphine ligands inhibit more than two NCA unit additions.[42] After the first addition carbon monoxide is given off, followed by the second addition and loss of CO_2 resulting in the active intermediate. Loss of triphenylphosphine ligands from the complex leads to aggregation of metal complexes and loss of activity. Upon addition of a different ligand, ligand exchange occurs and the intermediate can further polymerize NCA or can be quenched with acid. When conducting the same study with NTA monomer (V NTA), carbon monoxide peaks, 2000 and 1942 cm^{-1}, were also observed and confirmed by IR (red structure, Figure 4-9). However, the loss of COS was not confirmed by IR nor the formation of amidate **1** (Figure 4-9).

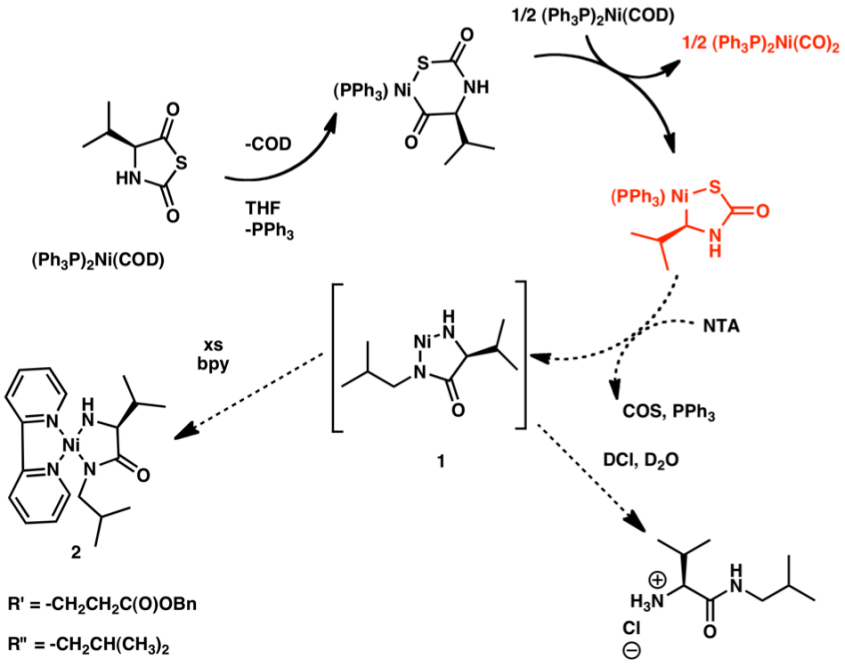

Figure 4-9. Proposed initiation mechanism. Formation of $(Ph_3P)_2Ni(CO)_2$ readily occurs (IR in THF, ν(CO) = 2000 and 1942 cm^{-1}; no 1577 cm^{-1} was observed (amidate 1).

When the acid quenching experiment was conducted to determine the active species, the expected amino acid derivative was not obtained, indicating the propagating species (1) is not formed (Figure 4-9). It appears that COS is not eliminated but remains bound to nickel and thus prevents formation of the active species. This is a valid hypothesis since, according to the literature, sulfur has a high affinity for nickel.

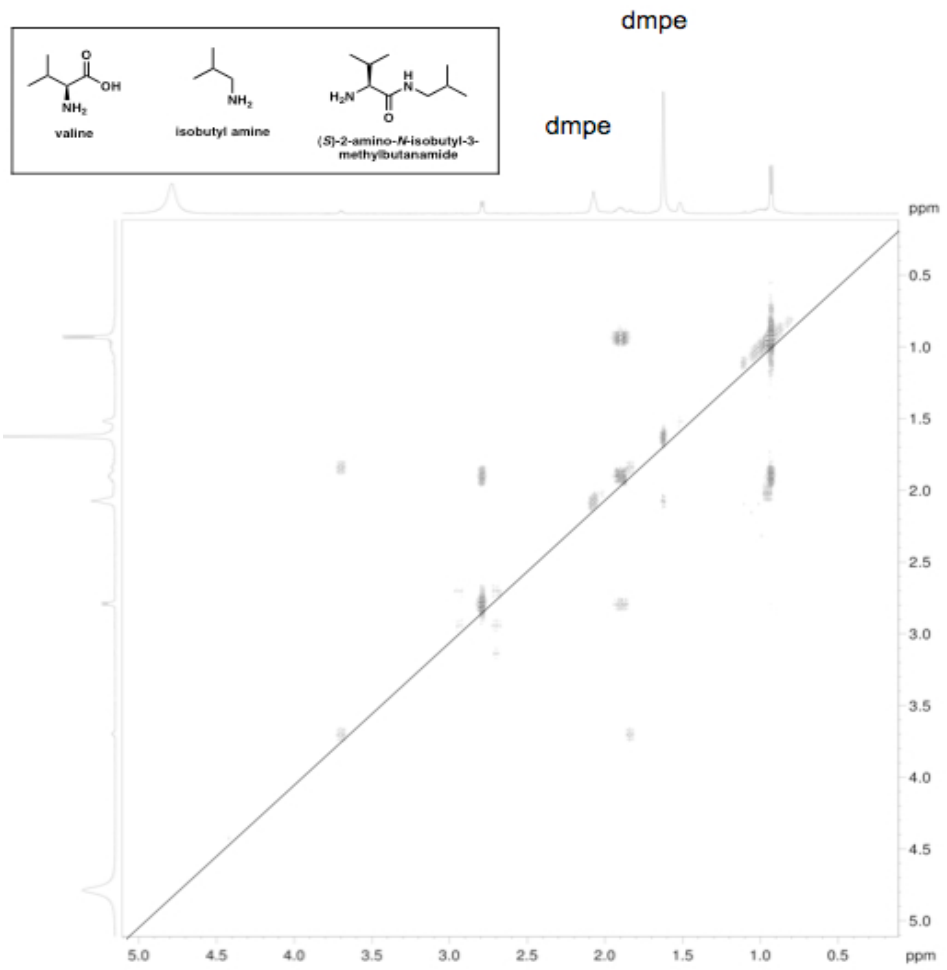

Figure 4-10. ^{1}H COSY NMR of active species acidolysis product in $CDCl_3$

If oxidative addition does not occur then the NTA would be hydrolyzed to L-valine. If the NTA undergoes oxidative addition and the loss of CO, but does not lose COS, then isobutylamine will be the product. If the reaction goes to completion with the loss of COS, and 2nd NTA addition then hydrolysis of the active species would result in the amino acid derivative (S)-valine isobutylamide. In order to analyze the products of the acid hydrolysis, a COSY NMR experiment was conducted. Since oxidative addition and

loss of CO was observed by infrared spectroscopy, the product should not be L-valine. When comparing the sample to an authentic sample of isobutylamine, the samples were exactly the same by comparison of the COSY spectra. Therefore the loss of COS likely did not occur and is problematic step in these initiation reactions.

4.5 Alternative Initiators

Nickel compounds have a high affinity for sulfur, which could inhibit polymerization. To test this theory, alternative initiators were tested for activity with various NTA monomer units (i.e. E NTA, F NTA, V NTA, K NTA). Some of the initiators tested included: hexylamine,[120,132] hexamethyldisilizane (HMDS),[133] $Fe(acac)_3$, a ruthenium amidosulfonamide initiator[134] and $Ti[N(CH_3)_2]_4$. In each of these cases, the initiator was tested for activity and COS scavenger ability (refer to section below). Also, control experiments were conducted with corresponding NCAs for comparison. Unfortunately all initiators failed to fully polymerize the NTAs (as observed by FT-IR) or act as cocatalysts in scavenging COS.

4.6 COS Scavenger

NTA polymerization should proceed through a similar mechanistic pathway as NCA polymerization however metallacycle formation of the active species with NTAs is inhibited by COS release. Elimination of COS is the rate-limiting step and requires assistance to overcome the energy barrier allowing the reaction to proceed. The most

promising strategy involves the capture of COS by a thiophilic reagent that is stable towards monomer and initiator. If the thiophilic reagent selectively reacts with COS then the reaction will proceed quickly with fewer side reactions and complete consumption of monomer.

4.6.1 Transition Metal Capture of COS

Unlike extensively studied heterocumulenes CS_2 and CO_2 and their reaction with transition metals, COS has received little attention.[135,136] Carbonyl sulfide reacts with transition metals through: end-on coordination (M-η^1-OCS), two forms of side-on coordination (M-η^2-COS) and bridging carbonyl sulfide complexes (Figure 4-11).[136]

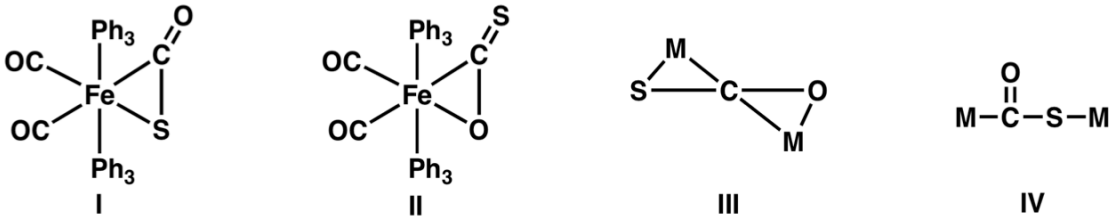

Figure 4-11. Side-on coordination of COS, I and II; Bridging complexes, III and IV.

Iron and ruthenium complexes are known to readily react with COS in toluene forming an unstable M-COS intermediate that decomposes forming a stable metal complex and triphenylphosphine sulfide in the presence of excess ligand (Figure 4-12).[135] The reaction requires stoichiometric amounts of ligand since every equivalent of COS bound reacts with one ligand molecule producing triphenylphosphine sulfide. The source of COS production in our experiment are NTA monomer molecules meaning the number of monomer equivalents should equal the number of ligand equivalents. $Fe(CO)_3(PPh_3)_2$

was chosen as an appropriate iron complex to promote COS capture in NTA nickel-initiated polymerization. Other transition metal complexes were also screened for ability to facilitate NTA polymerization.

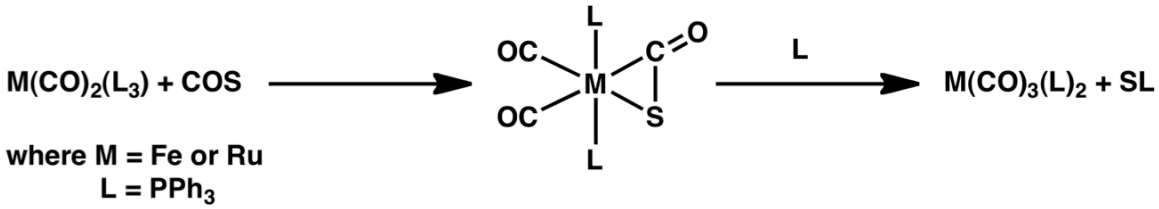

Figure 4-12. Synthesis and reactions of M(COS) complexes

To test transition metal scavengers, the transition metal (i.e. $Fe(CO)_3(PPh_3)_2$, $Ti(NCH_3)_2$ of interest was reacted with monomer at 80 ^oC and was observed over 24 h, Cp_2ZrCl_2 and $Fe(acac)_3$). If no polymer had formed then the pre-initiated nickelacycle complex was added to the solution and the reaction was again monitored over a 24 h period at 80 ^oC. Due to polymer formation, 10 mol % $Fe(acac)_3$ and $Ti(NCH_3)_2$ in the presence of Leu NTA were not used in further studies. Cp_2ZrCl_2 and $Fe(CO)_3(PPh_3)_2$ were unreactive towards Leu NTA at 80 ^oC and nickel initiator was added.

The reactions were monitored for 24 h and it was determined that $Fe(CO)_3(PPh_3)_2$ yielded better NTA conversion compared to Cp_2ZrCl_2. In the presence of the iron carbonyl complex polymer clearly formed after 6 h in the presence of initiator while no polymer formed after 6 h in presence of Cp_2ZrCl_2. After 24 h almost all monomer was consumed in the iron reaction while monomer was still present in the Cp_2ZrCl_2 reaction. Preliminary results show that 10 mol % $Fe(CO)_2PPh_3$ with excess PPh_3 increased the rate of monomer consumption after 6 h compared to 25:1 Leu NTA:

intiator reaction where no scavenger is present. After 24 h the reactions appear to have similar monomer to polymer ratio by IR.

Figure 4-13. Infrared spectroscopy (IR) of 25:1 Leu NTA: nickel initiator at 80 ^{o}C in the absence (dark purple line) and presence (light purple line) of 10 mol % $Fe(CO)_3(PPh_3)_2$

4.6.2 SELEXSORB© Capture of COS

COS is a common contaminant in liquid propane and dangerous when hydrolyzed by water forming H_2S and CO_2 gases. Sorbent technologies and amines are typically used to reduce COS contaminants in propane. SELEXSORB© COS selectively removes CO_2, COS, H_2S and CS_2 contaminants by chemisorption and can be regenerated upon heating. SELEXSORB© COS is an alumina-based proprietary material that was generously provided by BASF. The setup for the COS scavenger experiments begins with dissolving E NTA in 500 μL DMF (or THF) and the addition of nickel preinitiator **1** (Figure 4-14). All reactions were conducted in bomb tubes (pressure bottles) with control experiment (samples 1 and 4) containing no COS

scavenger and samples 2 and 5 containing SELEXSORB and tetraethylene pentamine (TEPA), respectively, in the presence of solvent and NTA (E NTA or L NTA, no initiator). Experiments 3 and 6 contained scavenger in the bomb tube within a secondary container (a 2 mL vial uncapped).

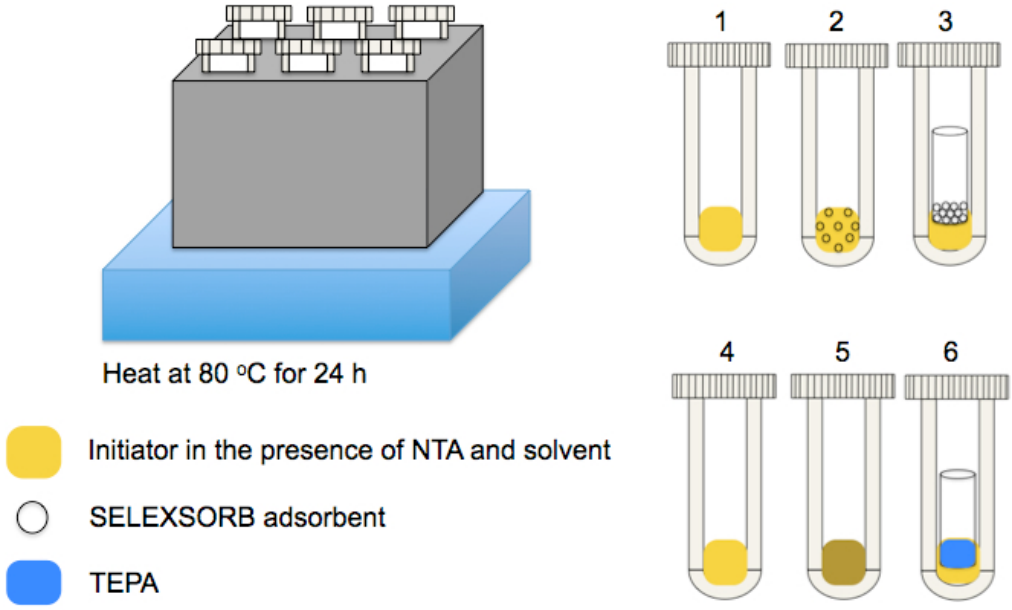

Figure 4-14. COS scavenger experimental setup

The effect of SELEXSORB on L NTA preinitiator reaction was monitored over the course of 24 h. It was determined that SELEXSORB in a secondary container had little effect on the rate of L NTA polymerization (and no effect on E NTA polymerization reactions). When L NTA was heated in solvent with SELEXSORB in solution, the monomer was consumed but no polymer was formed (by IR spectroscopy). TEPA had no effect on the polymerization of either L or E NTA.

4.7 Experimental Procedures

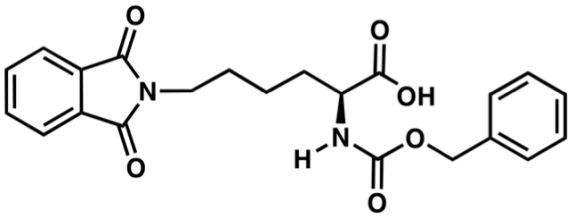

***N*$_\alpha$-benzoyloxycarbonyl-*N*$_\varepsilon$-phthalimidyl-L-Lysine (Cbz-Lys-Phth-OH).** Sodium carbonate (Na_2CO_3) (4.10 g, 18.0 mmol) was added to a vigorously stirring solution of α-benzoyloxycarbonyl-Lysine (5.0 g, 17.8 mmol) in 1:1 H_2O and THF (54 mL total). *N*-ethoxyphthalimide (4.10 g, 18.7 mmol) was added to the stirring solution at room temperature. The reaction mixture was concentrated to remove all THF and was then acidified with 5.0 M HCl (7.5 mL). The aqueous layer was extracted with DCM (3 x 10 mL) dried over $MgSO_4$ and concentrated. 5.8 g of Cbz-Lys-Phth-OH was isolated (77% yield). ^{1}H NMR ($CDCl_3$): δ 7.81 (m, 2H), 7.70 (m, 2H), 5.47 (s, 1H), 5.09 (s, 2H), 4.40 (m, 1H), 3.71 (t, 2H), 1.96-1.71 (m, 2H), 1.69 (m, 2H), 1.29 (m, 2H); ^{13}C NMR (125 MHz, $CDCl_3$): 171.52, 134.85, 130.25, 123.50, 53.40, 36.81, 28.51, 26.74, 26.74, 21.30 δ; IR (film in THF): 2974, 2860, 1773, 1717, 1533 cm^{-1}, HRMS-ESI (*m/z*) $[M + Na_2]^+$ Calcd for $C_{22}H_{22}N_2O_6Na$ 433.14; found 433.14.

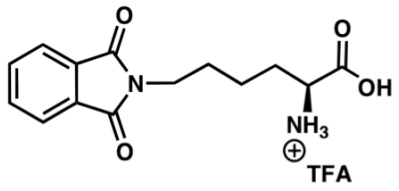

***N*$_\varepsilon$-phthalimidyl-L-Lysine (H-Lys-Phth-OH).** Cbz-Lys-Phth-OH (5.33 g, 12.5 mmol) was dissolved in trifluoroacetic acid (TFA) (20 mL) followed by the addition of 2.5 equivalents 33%

HBr in acetic acid. The reaction was allowed to stir at room temperature for 1 h. The reaction mixture was washed with diethyl ether (4 X 20 mL). The reaction mixture was concentrated and H-Lys-Phth-OH was isolated (3.45 g, 71% yield). ^{1}H NMR (D_2O): δ 7.75 (s, 4H), 4.01 (t, 1H), 3.62 (t, 2H), 1.98 (m, 2H), 1.69 (m, 2H), 1.50 (m, 2H); ^{13}C NMR (125 MHz, TFA_d): 171.52, 134.85, 130.25, 123.50, 33.45, 36.81, 28.54, 26.74, 21.30 δ; IR (film): 2976, 2856, 1713 cm^{-1}, HRMS-ESI (*m/z*) $[M]^+$ Calcd for $C_{14}H_{17}N_2O_4$, 277.12; found 277.12.

A. Synthesis α-amino acid-*N*-thiocarboxyanhydrides (NTAs)

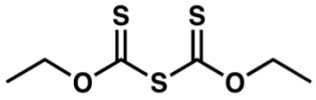

Bis(ethoxythiocarbonyl) Sulfide (Ethylxanthic Anhydride). (yield: 13.29 g; percent yield: 65 %). Isolated as yellow, needle-like crystals after recrystalization. Prepared according to the literature procedure.[1]

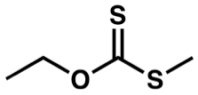

***O*-ethylmethylxanthate.** (yield: 11.03 g; percent yield: 94 %). Prepared according to the literature procedure.[2] ^{1}H NMR (500 MHz, $CDCl_3$) δ 4.65-4.70 (q, 2H), 2.54 (s, 3H), 1.39-1.42 (t, 2H).

NTA Precursors

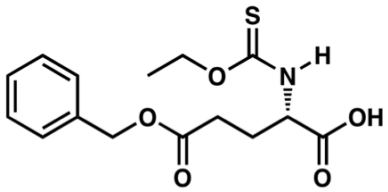

Sample procedure for non-aqueous preparation of *N*-thiocarbomoyl amino acids (*N*-thiocarbomoyl-L-glutamic acid-γ-benzyl ester shown. L-glutamic acid γ-benzyl ester (6.0 g, 25.4 mmol) was partially dissolved in DMF (152 mL). Triethylamine (15.2 mL) was added to the stirring solution followed by the addition of bis(ethoxythiocarbonyl)sulfide (8.0 g, 38.0 mmol). The solution quickly turned yellow and was then stirred at room temperature overnight. After 20 h stirring the reaction was concentrated and residue acidified with dilute HCl (pH=2) and extracted with dichloromethane (DCM), (3 X 45 mL). yellow oil, Isolated yield: 7.36 g, 89 % yield. No further purification required.^{1}H NMR (500 MHz, $CDCl_3$) 7.27-7.36 (m, 5 H), 6.94 (s, 1 H), 5.03-5.13 (m, 2 H), 4.46-4.57 (m, 1 H), 2.51-2.59 (m, 3 H), 2.11-2.28 (m, 3 H), 1.27-1.34 (t, 3 H) δ; ^{13}C NMR (125 MHz, $CDCl_3$): 191.03, 189.87, 176.10, 173.13, 172.52, 135.57, 128.75, 128.55, 128.50, 68.44, 67.16, 56.82, 30.43, 27.08, 14.27.

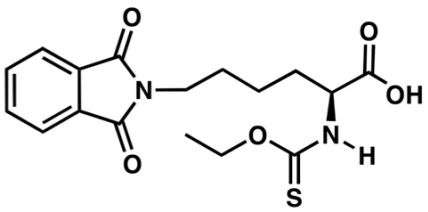

ε-phthalyl-*O*-ethoxythiocarbonyl-L-Lysine.[137] (yield: 0.280 g; percent yield: 63%). ^{1}H NMR (500 MHz, $CDCl_3$, 25 ^{o}C): δ 9.20-8.80 (s, 1H), 7.95-7.80 (m, 2H), 7.60-7.78 (m, 2H), 6.88-6.78 (s, N-H, 1H), 5.90 (m, 1H), 4.62-4.43 (m, 2H), 3.72 (t, 2H), 2.11 (m, 2H), 1.96 (m, 2H), 1.73 (m, 2H), 1.46 (m, 2H), 1.32 (t, 3H); ^{13}C NMR (125 MHz, $CDCl_3$): δ190.83, 173.80, 134.18, 132.08, 132.04, 123.50, 123.44, 66.98, 37.36, 31.39, 31.00, 28.13, 28.07, 22.62, 22.42, 14.25, 14.18; HRMS-ESI (*m/z*) $[M + H]^+$ Calcd for $C_{18}H_{20}N_2O_5S_1$, 365.12; found 365.12.

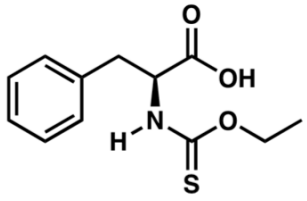

Sample procedure for aqueous preparation of *N*-thiocarbomoyl amino acids (*N*-thiocarbomoy-L-phenyl alanine shown). L-phenylalanine (2.0 g, 12.1 mmol) was added to a 100 mL round-bottom-flask and dissolved in a solution of potassium hydroxide in water (2.0 g in 10 mL). *O*-ethylmethyl-xanthate (12.1 mmol) in methanol was added to the solution and heated to 45^{o}C. The solution was stirred for 2 h concentrated under reduced pressure. The reaction mixture was diluted in 10 mL ether. The solution was acidified with 3 x 10 mL 10% HCl. The ether layer was removed and set aside. The aqueous layer was extracted with 3 x 10 mL EtOAc. The organic layer was dried over $MgSO_4$, filtered and concentrated. ^{1}H NMR (300 MHz, $CDCl_3$) δ 7.17-7.29 (m, 3H), 7.13-7.30 (m, 2H), 5.22-5.28 (dd, 1H), 3.99 (s, 3H), 3.17-3.22 (m, 1H), 3.34-3.36 (m, 1H). Additional data available in literature.[3]

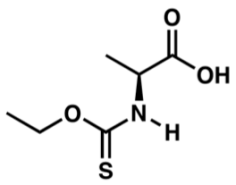

***O*-ethylthiocarbonyl-L-alanine.** Prepared according to the literature procedure.[3]

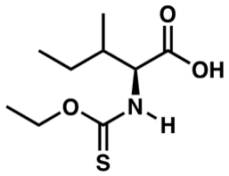

***O*-ethylthiocarbonyl-L-isoleucine.** Prepared according to the literature procedure.[3]

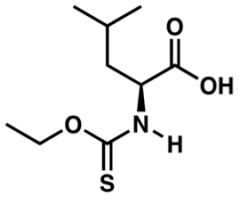

***O*-ethylthiocarbonyl-L-leucine.** Prepared according to the literature procedure.[1]

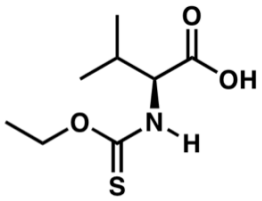

***O*-ethylthiocarbonyl-L-valine.** Prepared according to the literature procedure.[1]

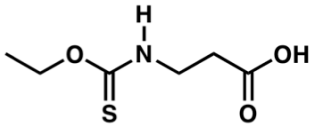

***O*-ethylthiocarbonyl-β alanine.** Product has two distinct conformations by ^{1}H NMR and ^{13}C NMR. ^{1}H NMR (500 MHz, $CDCl_3$): 7.77 (bs, 1 H), 6.78 (bs, 1 H), 4.48 (q, 1), 4.45 (q, 2 H), 3.56-3.58 (q, 1 H), 2.60 (t, 2 H), 2.60 (t, 1 H), 1.31 (q, 2 H), 1.25 (q, 3 H) δ; ^{13}C NMR (125 MHz, $CDCl_3$): 190.68, 189.69, 68.04, 66.56, 40.00, 38.12, 33.42, 32.79, 14.26 δ;

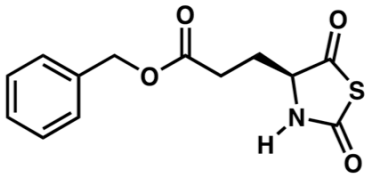

Sample procedure for γ-benzyl-L-glutamate, L-aspartatic acid acid β-benzyl ester, and ε-phthalyl-L-Lysine NTAs. *N*-thiocarbomoyl-L-glutamic acid-γ-benzyl ester (7.0 g, 21.5 mmol) was dissolved in THF (125 mL) and imidazole (1.46 g, 21.5 mmol) was added to the stirring solution. The reaction vessel was cooled to 0 ^{o}C and phosphorus tribromide (PBr_3) (6.90 mL, 25.55 mmol) was added dropwise. After 10 min. at 0 ^{o}C the reaction mixture was poured into a 1:1 sodium bicarbonate ($NaHCO_3$) saturated solution: EtOAc mixture (100 mL total). The organic layer was separated and washed with $NaHCO_3$ saturated solution (3 x 10 mL) and of sodium chloride (NaCl) saturated solution (3 x 5 mL). The organic layer was dried over $MgSO_4$, filtered and concentrated**.** The white solid was recrystallized from 3:1 Hex: EtOAc using the layering method. White crystals, isolated yield: 4.64 g, percent yield: 77 %. ^{1}H NMR (500 MHz, $CDCl_3$, 25 ^{o}C): δ 7.37-7.36 (m, 5H), 7.12 (s, 1H), 5.14 (s, 2H), 4.39 (t, 1 H), 2.30-2.27 (m, 1H),

2.15-2.12 (m, 1H). ^{13}C NMR (500 MHz, $CDCl_3$, 25 ^{o}C): δ 198.36, 172.55, 166.76, 135.42, 128.81, 128.65, 128.48, 67.14, 66.13, 29.66, 27.87; IR (film): 1714, 1737 cm^{-1}.

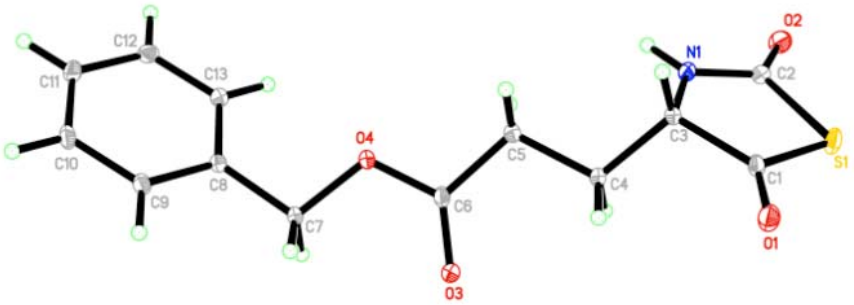

Figure X. X-ray crystal structure of γ-benzyl-L-glutamate-*N*-thiocarboxyanhydride (Bn-Glu NTA)

For comparison, γ-benzyl-L-glutamate NCA prepared through phosgenation of γ-benzyl-L-glutamic acid gave the following NMR chemical shifts. ^{1}H NMR (500 MHz, $CDCl_3$, 25 ^{o}C): δ 7.37-7.36 (m, 5H), 6.63 (s, 1H), 5.15 (s, 1 H), 4.39 (t, 1H), 2.60 (t, 2 H), 2.27-2.26 (m, 1H), 2.15-2.12 (m, 1H). ^{13}C NMR (500 MHz, $CDCl_3$, 25 ^{o}C): δ 172.53, 169.49, 151.99, 135.33, 128.85, 128.68, 128.50, 67.25, 57.07, 29.97, 27.03.

X-ray data for γ-benzyl-L-glutamate NTA.

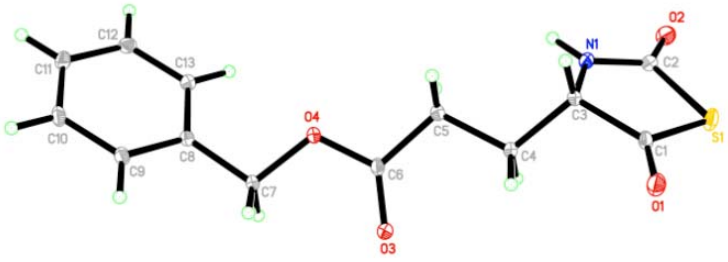

Bn-Glu NTA		**Bn-Glu NCA**		
Bond	**Bond Length (Å)**	**Bond**	**Bond Length (Å)**	**Bond Length Δ**
S(1)-C(1)	1.769	O(2)-C(2)	1.368	0.401
C(1)-C(3)	1.531	C(2)-C(3)	1.512	0.019
C(3)-N(1)	1.449	C(3)-N(1)	1.447	0.002
N(1)-C(2)	1.35	N(1)-C(1)	1.333	0.017
C(2)-S(1)	1.803	C(1)-O(2)	1.404	0.399
C(1)-C(3)	1.531	C(2)-C(3)	1.512	0.019
C(3)-C(4)	1.527	C(3)-C(4)	1.522	0.005
C(4)-C(5)	1.526	C(4)-C(5)	1.528	-0.002
C(5)-C(6)	1.513	C(5)-C(6)	1.495	0.018
C(7)-C(8)	1.506	C(7)-C(8)	1.504	0.002
C(8)-C(9)	1.388	C(8)-C(9)	1.376	0.012
C(9)-C(10)	1.393	C(9)-C(10)	1.383	0.01
C(10)-C(11)	1.389	C(10)-C(11)	1.365	0.024
C(11)-C(12)	1.392	C(11)-C(12)	1.364	0.028
C(12)-C(13)	1.401	C(12)-C(13)	1.396	0.005

C(13)-C(8)	1.398	C(13)-C(8)	1.37	0.028

Bn-Glu NTA		**Bn-Glu NCA**		
Bonds	**Bond Angle**	**Bonds**	**Bond Angle**	**Bond Angle Δ**
S(1)-C(1)-C(3)	110.89	O(2)-C(2)-C(3)	108.9	1.99
C(1)-C(3)-N(1)	**106.72**	**C(2)-C(3)-N(1)**	**100.5**	**6.22**
C(3)-N(1)-C(2)	**119.85**	**C(3)-N(1)-C(1)**	**112.8**	**7.05**
N(1)-C(2)-S(1)	109.82	N(1)-C(1)-O(2)	108.7	1.12
C(2)-S(1)-C(1)	**92.53**	**C(1)-O(2)-C(2)**	**109**	**-16.47**
C(1)-C(3)-C(4)	**114.34**	**C(2)-C(3)-C(4)**	**110.6**	**3.74**
C(3)-C(4)-C(5)	113.47	C(3)-C(4)-C(5)	112.9	0.57
C(4)-C(5)-C(6)	110.38	C(4)-C(5)-C(6)	111.3	-0.92
C(5)-C(6)-O(4)	111.77	C(5)-C(6)-O(4)	111.9	-0.13
C(6)-O(4)-C(7)	115.58	C(6)-O(4)-C(7)	115.1	0.48
O(4)-C(7)-C(8)	107.68	O(4)-C(7)-C(8)	109.6	-1.92
C(7)-C(8)-C(9)	118.54	C(7)-C(8)-C(9)	117.1	1.44
C(8)-C9(9)-C(10)	120.53	C(8)-C9(9)-C(10)	120.8	-0.27

C(9)-C(10)-C(11)	120.32	C(9)-C(10)-C(11)	120.5	-0.18
C(10)-C(11)-C(12)	119.53	C(10)-C(11)-C(12)	119.3	0.23
C(11)-C(12)-C(12)	120.29	C(11)-C(12)-C(12)	120.4	-0.11
C(12)-C(13)-C(8)	119.86	C(12)-C(13)-C(8)	120.5	-0.64

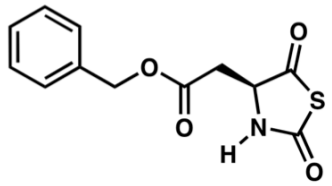

L-Aspartatic acid β-benzyl ester NTA. ^{1}H NMR (500 MHz, $CDCl_3$) 77.28-7.40 (m, 5 H), 6.85 (s, 1 H), 5.20 (s, 1 H), 4.60-4.63 (dd, 1 H), 3.09-3.13 (dd, 1 H), 2.73-2.79 (dd, 1 H) δ; ^{13}C NMR (125 MHz, $CDCl_3$): 198.21, 170.19, 165.88, 134.89, 128.88, 128.61, 167.01, 63.00, 37.22 δ; IR (film): 1741, 1713 cm^{-1}.

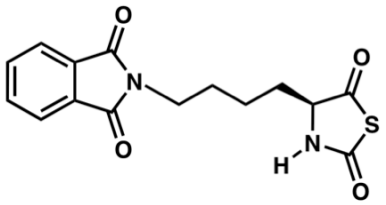

L-Lysine ε-phthalyl α-amino-*N*-thiocarboxyanhydride. ^{1}H NMR ($CDCl_3$): δ 7.85 (m, 2H), 7.74 (m, 2H), 6.774(s, 1H), 4.33 (dd, 1H), 3.73 (t, 2H), 2.00-1.88 (m, 2H), 1.76 (m, 2H), 1.26 (m, 2H). ^{13}C NMR ($CDCl_3$): δ 198.51 (C=O), 168.69 (C=O), 166.92 (C=O), 134.24 (C=C), 132.10 (C=C), 123.49 (C=C), 66.72 (C-H), 37.13 (CH_2), 32.00 (CH_2),

28.02 (CH_2), 21.65 (CH_2); δ IR (film): 1734, 1714 cm^{-1}, HRMS-ESI (*m/z*) $[M + H]^+$ Calcd for $C_{15}H_{15}N_2O_4S$, 319.075; found 319.075.

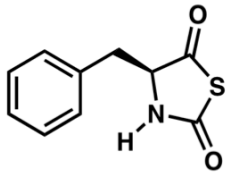

L-Phenyl Alanine NTA. (0.250 g obtained: 65% yield). ^1H NMR (500 MHz, $CDCl_3$, 25 ^oC): 7.189-7.365 (m, 5H), 6.294 (s, 1 H), 4.509 (dd, 1H), 3.328 (dd, 1H), 2.950 (dd, 1H). Prepared according to literature procedure.[3]

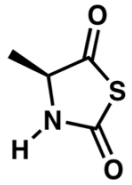

L-Alanine NTA. Prepared according to literature procedure.[3]

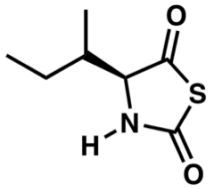

L-Isoleucine NTA. Prepared according to literature procedure.[3] ^1H NMR (300 MHz, $CDCl_3$) δ 7.886 (s, 1H), 4.355 (d, 1H), 2.029-2.052 (m, 1H), 1.470-1.522 (m, 1H), 1.344-1.495 (m, 1H), 1.023 (d, 3H), 0.836 (m, 3H).

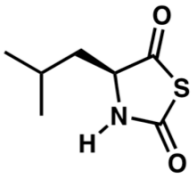

L-Leucine NTA. Prepared according to literature procedure.[5] ^{1}H NMR (300 MHz, $CDCl_3$) δ 7.018 (s, 1H), 4.317-4.361 (dd, 1H), 1.685-1.811 (m, 3H), 1.003 (d, 6H). Prepared according to literature procedure.[3]

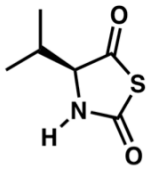

L-Valine NTA. Prepared according to literature procedure.[3]Recrystallized from 1: 38 THF: hexanes. ^{1}H NMR (300 MHz, $CDCl_3$) δ 7.260 (s, 1H), 4.230 (dd, 1H), 2.305-2.352 (m, 1H), 1.104 (d, 3H), 1.012 (d, 3H).

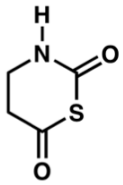

ß-alanine NTA. (yield: 0.130 g; percent yield: 63%)^{1}H NMR (500 MHz, $CDCl_3$, 25 ^{o}C): 6.51-6.40 (s, 1 H), 3.63-3.60 (m, 2 H), 2.88-2.85 (m, 2 H) δ ;^{13}C NMR (125 MHz, $CDCl_3$): 196.72, 166.96, 41.03, 38.54.

B. Initiator Synthesis

Preparation of 'prinitiated' nickel amidoamidate.

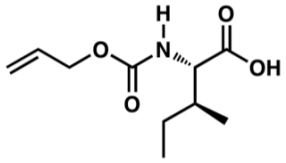

Carbamate X. (77% yield). ^{1}H NMR (500 MHz, $CDCl_3$): δ 9.73 (b, 1H), 5.91-5.89 (J = 5.1, 1 H), 5.34-5.31 (d, J = 18, 1 H), 5.24-5.21 (d, J = 9, 1 H), 4.59 (m, 2 H), 4.38 (m, 1 H), 1.96 (m, 1 H),

1.48 (m, 1 H), 1.21 (m, 1 H), 0.99-0.94 (m, 6 H) ^{13}C NMR (125 MHz, $CDCl_3$): δ 177.13, 156.28, 132.65, 118.14, 66.15, 58.36, 37.88, 24.95, 15.63, 11.73. Additional characterization data available in the literature.[5]

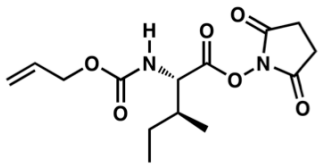

Alloc-isoleucine-NHS ester. (94% yield). ^{1}H NMR (500 MHz, $CDCl_3$): δ 5.91-5.89 (m, 1 H), 5.34-5.31 (d, J = X, 1 H), 5.24-5.21 (d, J = X, 1 H), 4.70 (m, 1 H), 4.59 (m, 2 H), 2.84 (s, 4 H), 1.96 (m, 1 H), 1.61-1.58 (m, 1 H), 1.29-1.25 (m, 1 H), 1.06-0.98 (d, J = X, 3 H), 0.98-0.97 (t, J = X, 3 H). ^{13}C NMR (125 MHz, $CDCl_3$): δ 169.68, 168.84, 156.66, 133.54, 119.32, 67.34, 58.00, 39.45, 26.73, 25.84, 16.25, 12.65.

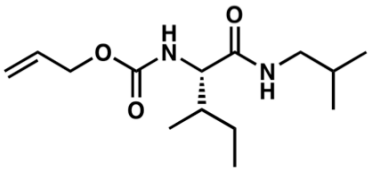

Alloc-isoleucine-isobutyl amide ligand. (80% yield) ^{1}H NMR (500 MHz, $CDCl_3$): δ 6.10 (s, 1H), 5.93-5.88 (m, J = 10, 1H), 5.32 (d, J = 1, 1H), 5.23-5.21 (d, J = 10, 1H), 5.10 (s, 1H), 4.58 (d, J = 5, 2H), 4.14-4.13 (m, 1H), 3.10-3.07 (m, 2H), 1.79 (m, 1 H), 1.75 (m, 2H), 1.52 (m, 1H), 0.91 (m, 12H); ^{13}C NMR (125 MHz, $CDCl_3$): δ 172.18,

156.09, 132.45, 117.69, 65.70, 53.51, 46.69, 41.35, 28.32, 24.60, 22.75, 21.98, 19.92; HRMS-ESI (*m/z*) $[M + Na]^+$ Calcd for $C_{14}H_{27}N_2O_3$, 271.20; found 271.20.

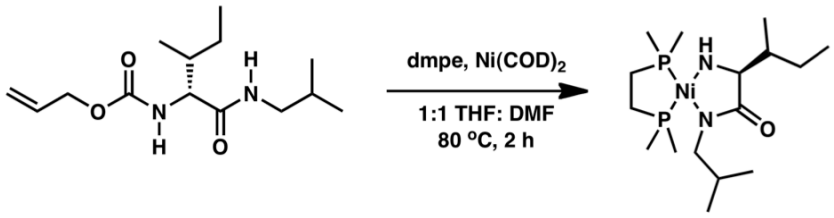

Amido-amidate initiator. Prepared according to literature procedure[6]

C. Polymerization of NTAs

Homopolymerization of L NTA monomer. In the glovebox 10 mg (0.0579 mmol) Leu NTA was dissolved in 1.0 mL THF in a 15 mL bomb tube. 64 μL pre-initiated nickel initiator was added to the solution. The reaction vessel was sealed, removed from the glovebox and heated to 80 °C until NTA monomer was consumed.

E. K_xL_y Diblock Copolypeptides using L NTA

K_xL_y Diblock Copolypeptides from Cbz-Lys NCA and L NTA. In the glovebox 100 mg of Cbz-Lys NCA was dissolved in 2.0 mL THF in a bomb tube equipped with a Teflon spin bar. 66.7 μL of bpyNi(COD) initiator (50 mg/mL stock solution) was added to the stirring solution of NCA and the reaction was allowed to stir at room temperature for 1 h. The reaction was monitored by IR after which GPC analysis was conducted. Once the M_n of the lysine block was determined (K_{229} in this case) 6.0 mg (0.035 mmol) L NTA was added to the stirring solution. The bomb tube was sealed and removed from the glovebox. The reaction vessel was heated to 80 °C for 24 h and checked

periodically by IR for consumption of monomer. Deprotection and subsequent dialysis were the same as diblocks prepared from NCAs.

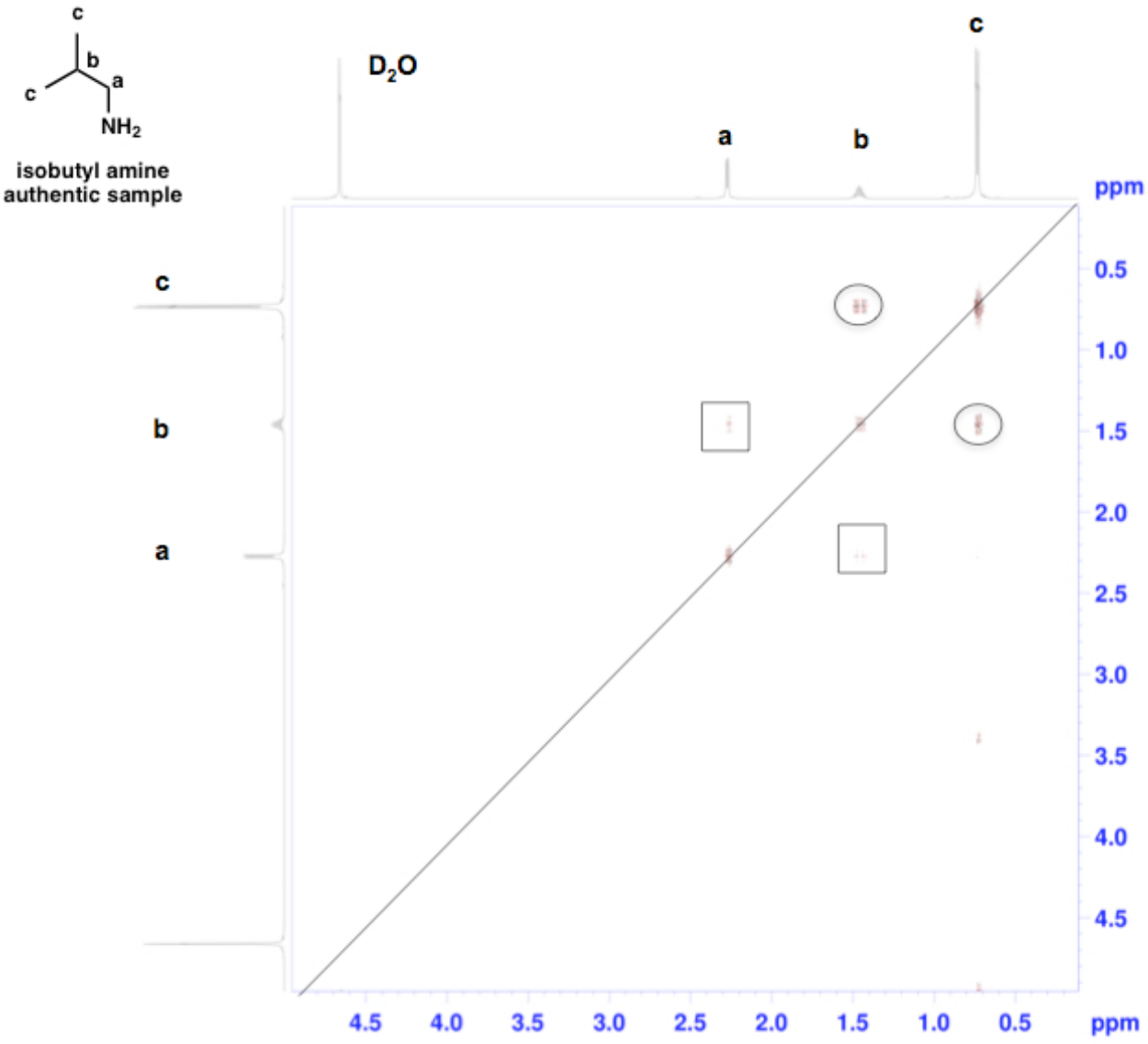

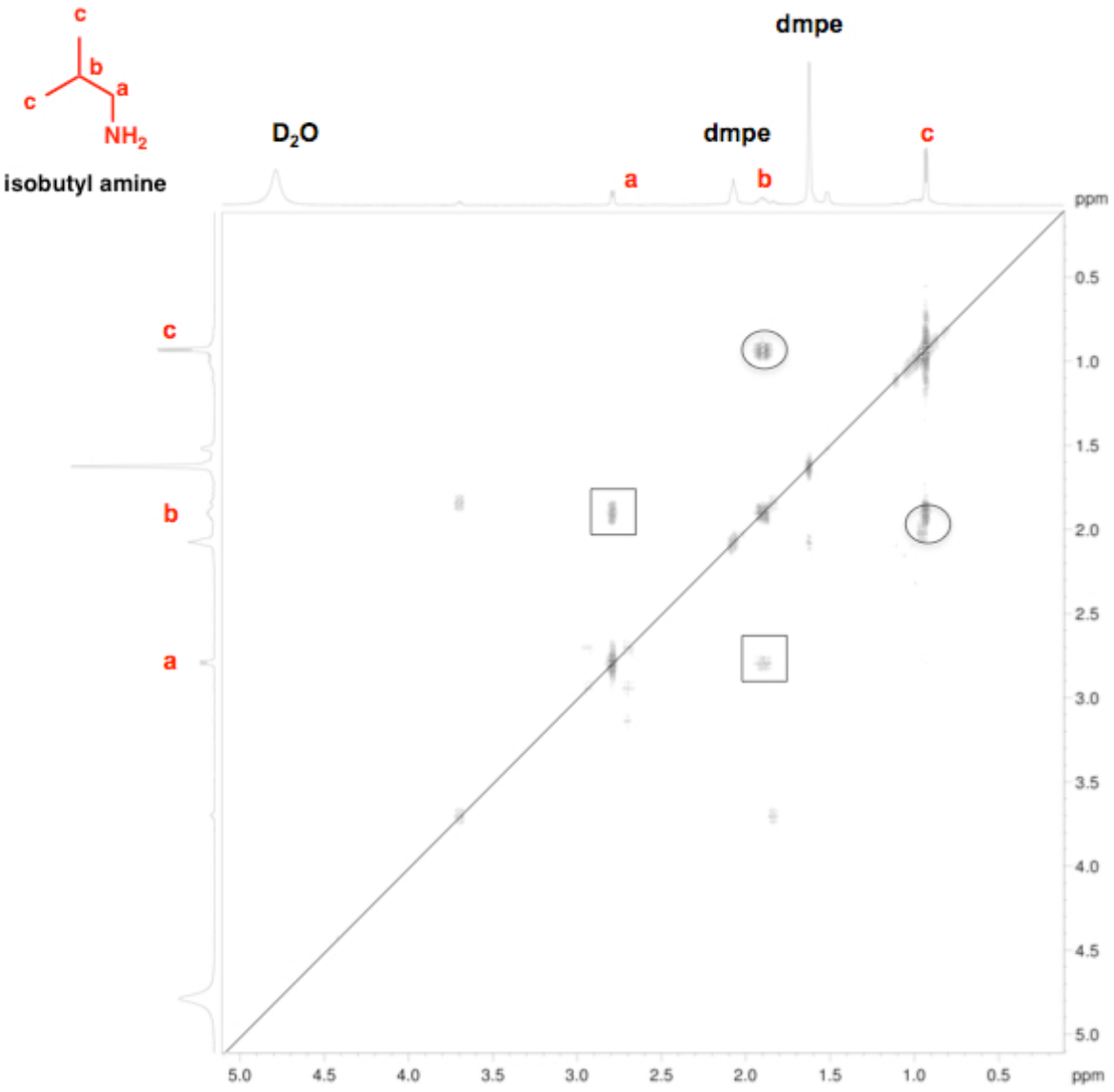
c
b
a
c
NH2
isobutyl amine
D2O
dmpe
a
dmpe
b
c
ppm
0.5
1.0
1.5
2.0
2.5
3.0
3.5
4.0
4.5
5.0
c
b
a
5.0
4.5
4.0
3.5
3.0
2.5
2.0
1.5
1.0
0.5
ppm

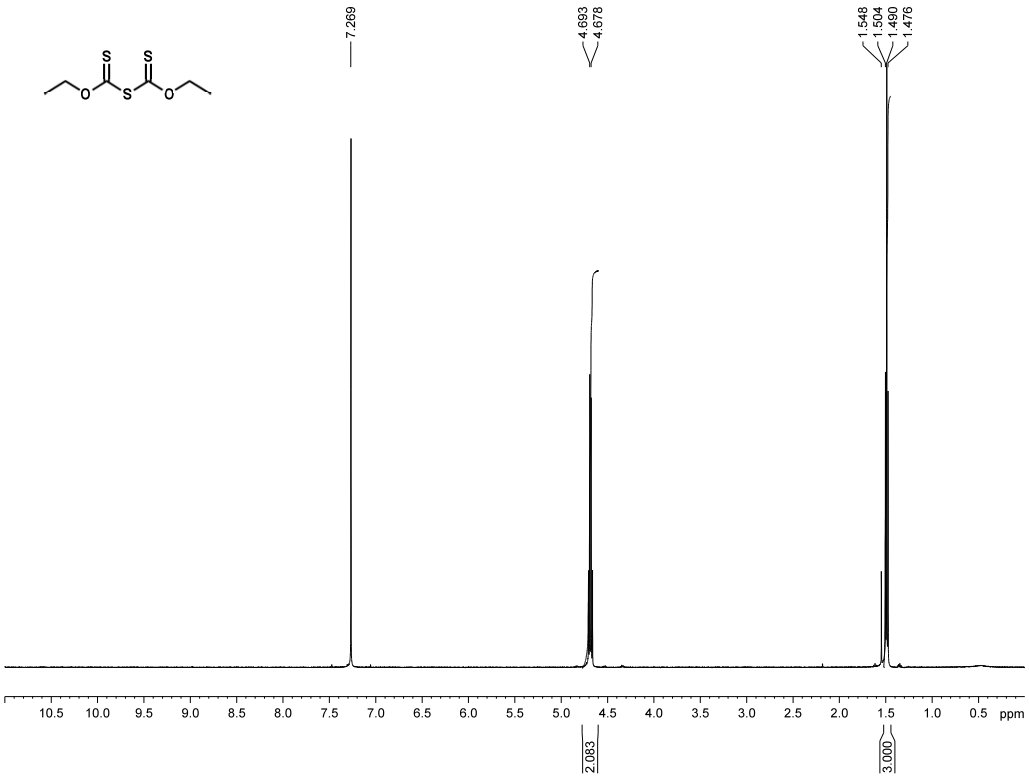
7.269
4.693
4.678
1.548
1.504
1.490
1.476
10.5 10.0 9.5 9.0 8.5 8.0 7.5 7.0 6.5 6.0 5.5 5.0 4.5 4.0 3.5 3.0 2.5 2.0 1.5 1.0 0.5 ppm
2.083
3.000

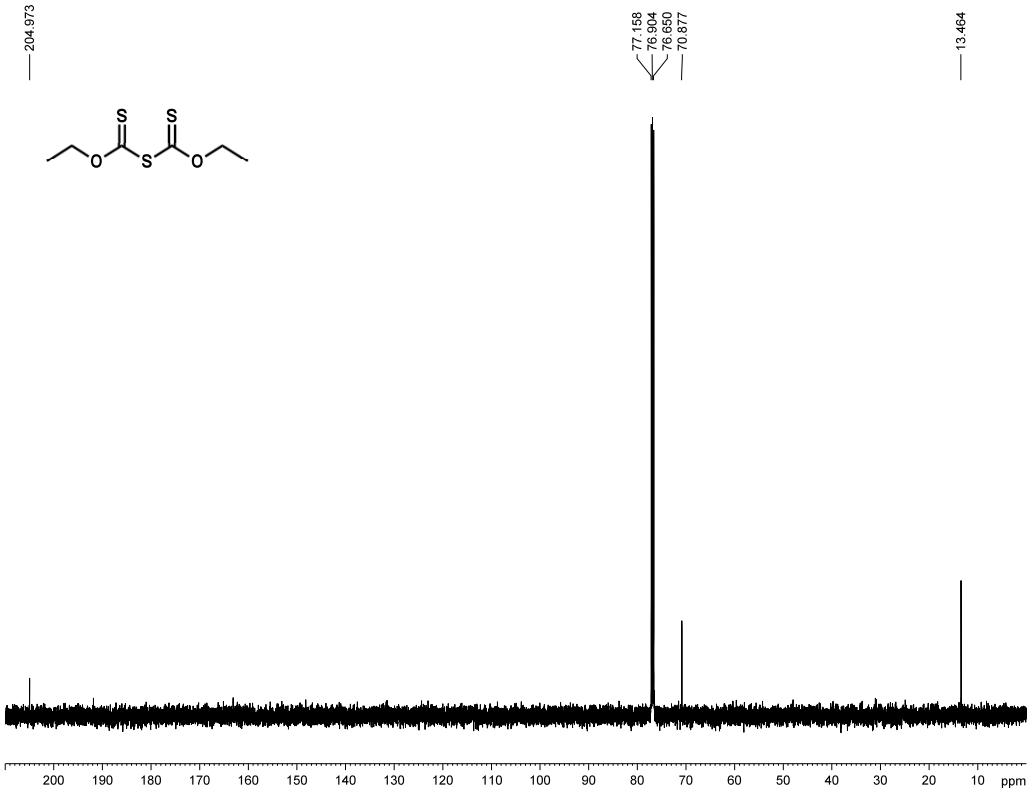
204.973
77.158
76.904
76.650
70.877
13.464
S
S
O
S
O
200
190
180
170
160
150
140
130
120
110
100
90
80
70
60
50
40
30
20
10
ppm

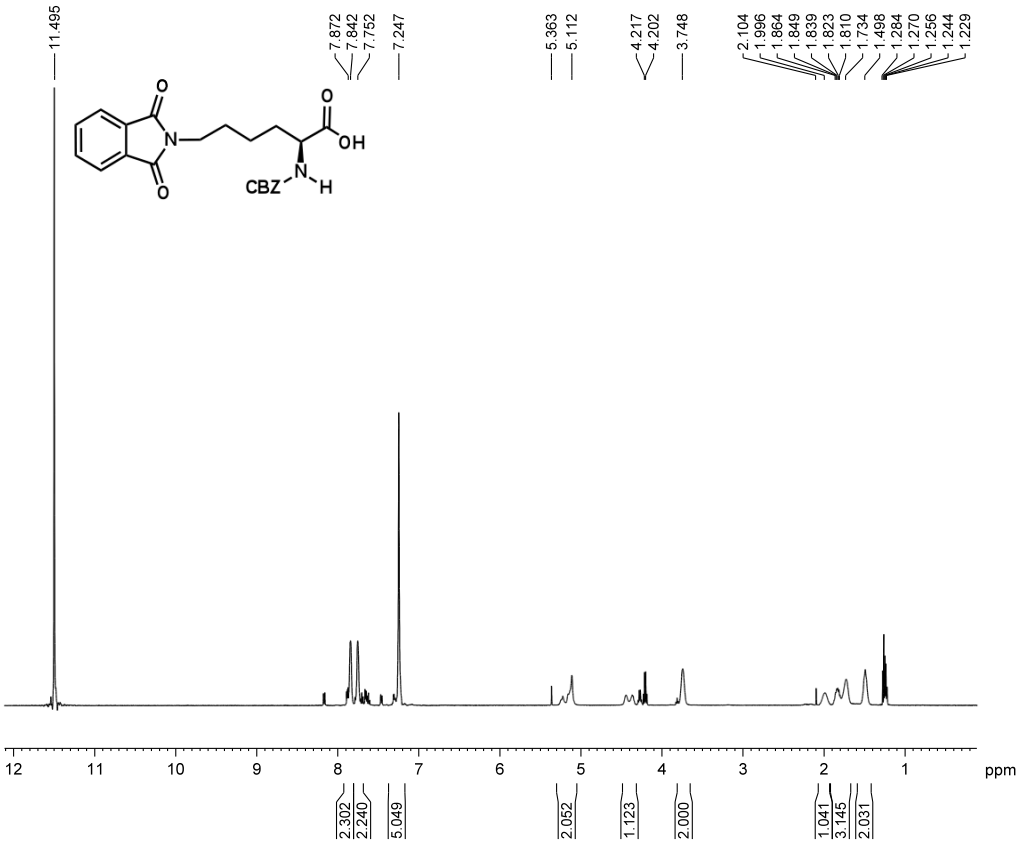
11.495
7.872
7.842
7.752
7.247
5.363
5.112
4.217
4.202
3.748
2.104
1.996
1.864
1.849
1.839
1.823
1.810
1.734
1.498
1.284
1.270
1.256
1.244
1.229
O
O
N
O
OH
CBZ
N
H
12
11
10
9
8
7
6
5
4
3
2
1
ppm
2.302
2.240
5.049
2.052
1.123
2.000
1.041
3.145
2.031

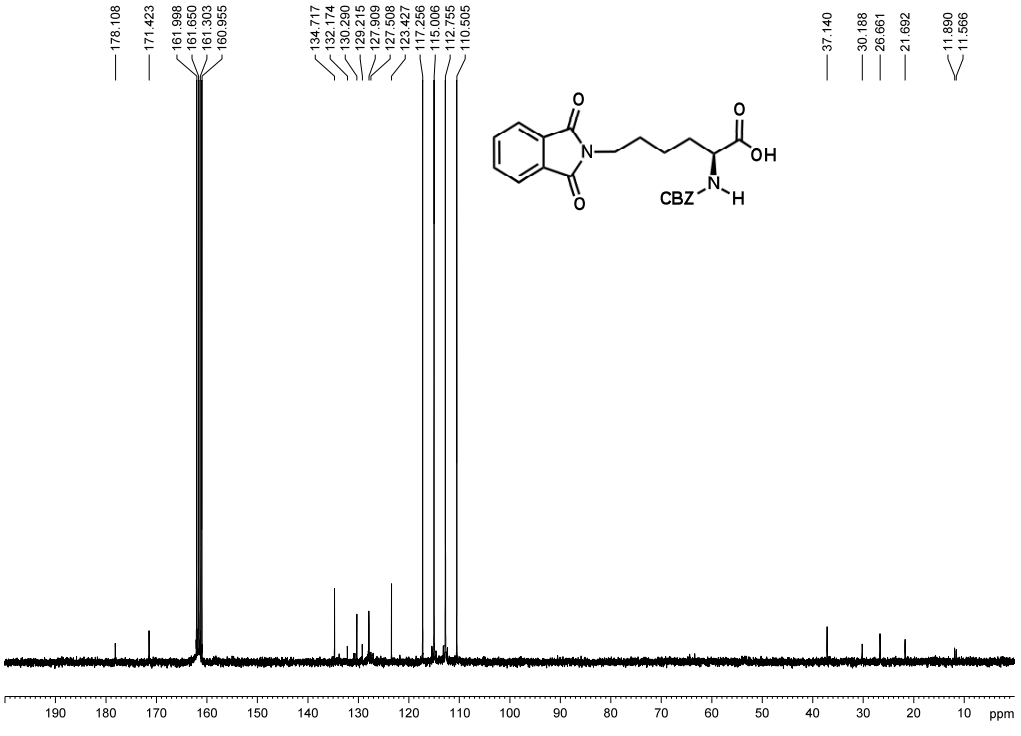
178.108
171.423
161.998
161.650
161.303
160.955
134.717
132.174
130.290
129.215
127.909
127.508
123.427
117.256
115.006
112.755
110.505
37.140
30.188
26.661
21.692
11.890
11.566
O
O
N
O
OH
CBZ
N
H
190
180
170
160
150
140
130
120
110
100
90
80
70
60
50
40
30
20
10
ppm

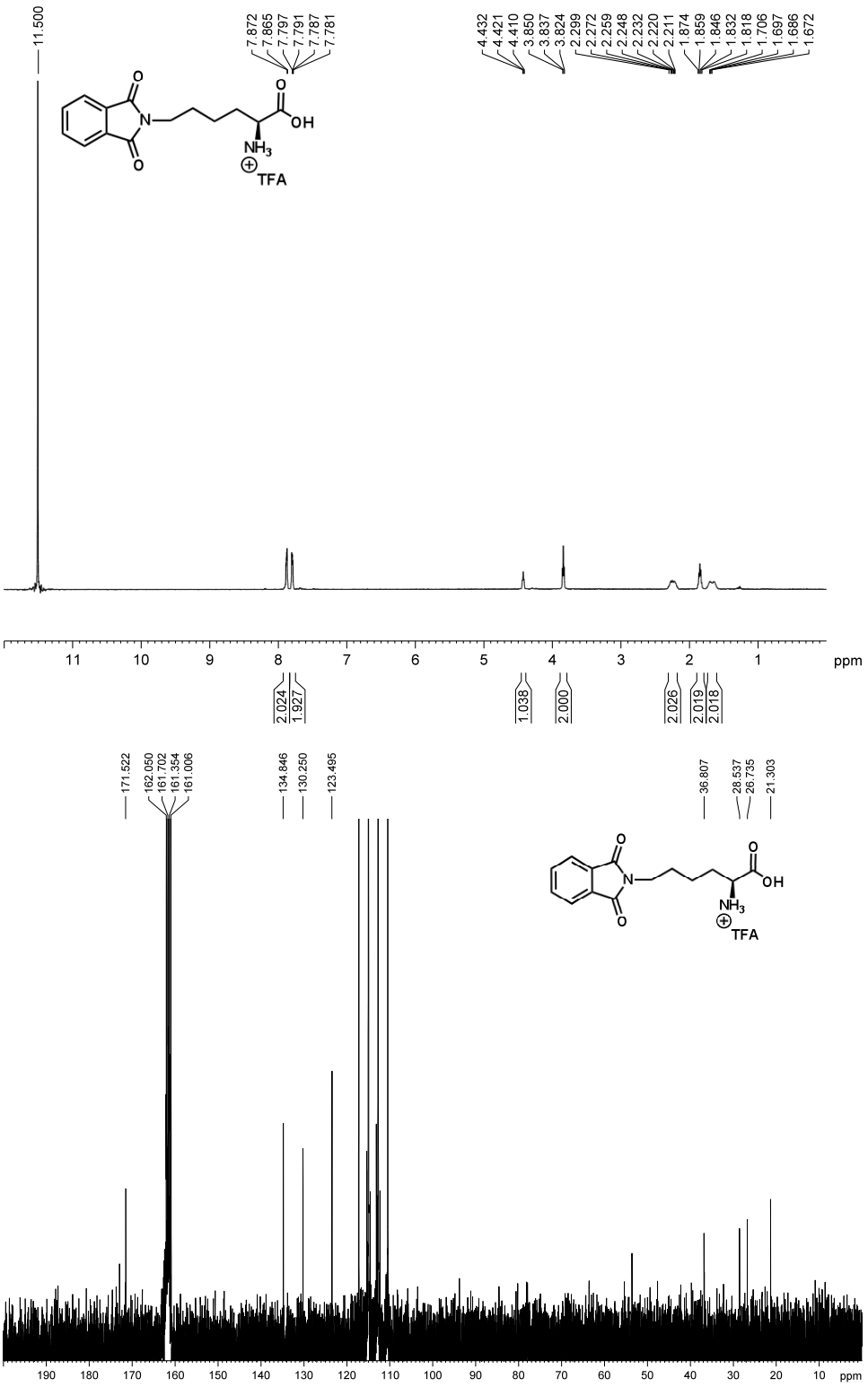
11.500
7.872
7.865
7.797
7.791
7.787
7.781
4.432
4.421
4.410
3.850
3.837
3.824
2.299
2.272
2.259
2.248
2.232
2.220
2.211
1.874
1.859
1.846
1.832
1.818
1.706
1.697
1.686
1.672
O
N
O
O
OH
NH3
TFA
11
10
9
8
7
6
5
4
3
2
1
ppm
2.024
1.927
1.038
2.000
2.026
2.019
2.018
171.522
162.050
161.702
161.354
161.006
134.846
130.250
123.495
36.807
28.537
26.735
21.303
190
180
170
160
150
140
130
120
110
100
90
80
70
60
50
40
30
20
10
ppm

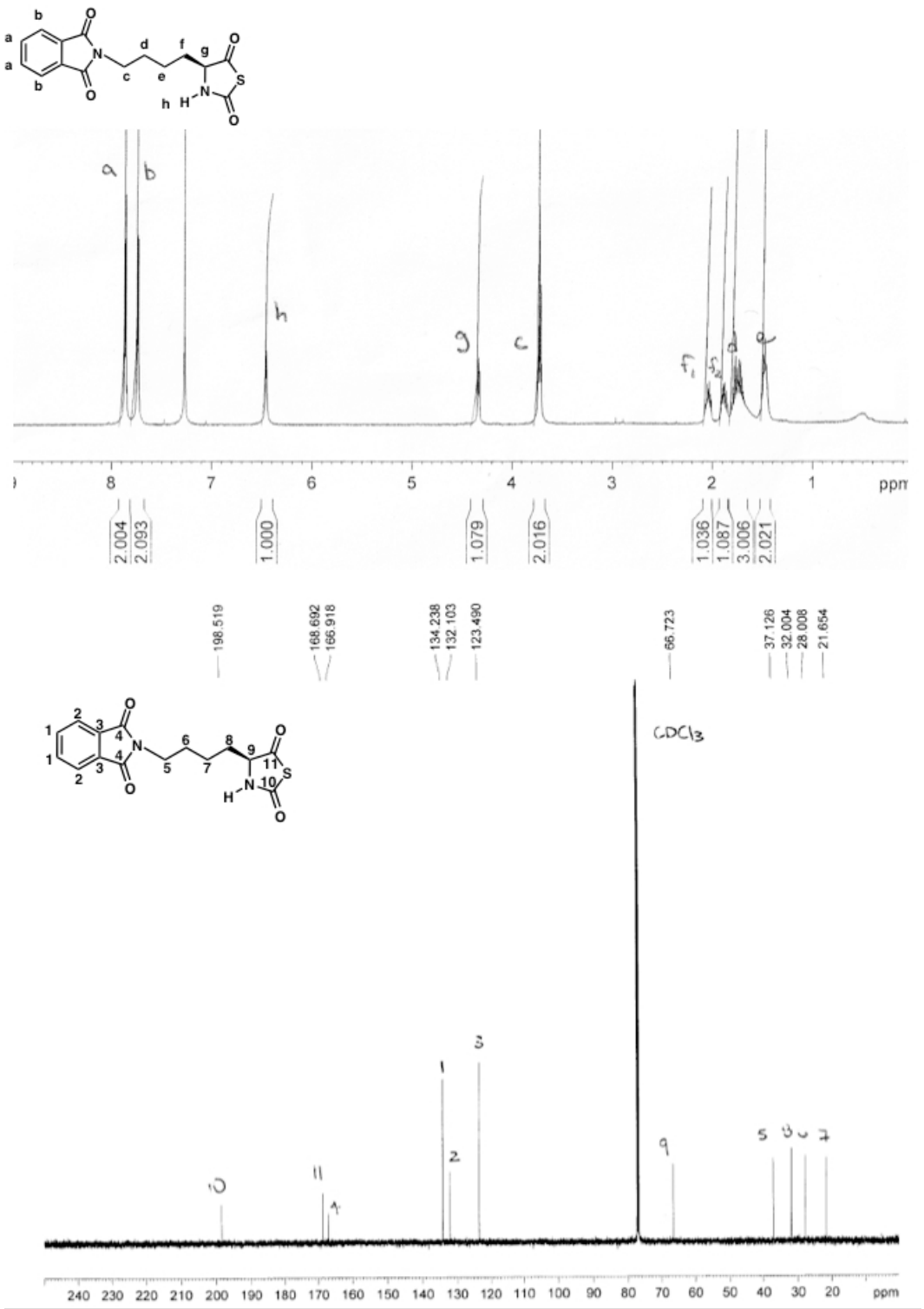
a
a
b
b
c
d
e
f
g
h
O
N
S
H
ppm
2.004
2.093
1.000
1.079
2.016
1.036
1.087
3.006
2.021
198.519
168.692
166.918
134.238
132.103
123.490
66.723
37.126
32.004
28.008
21.654
CDCl3
240 230 220 210 200 190 180 170 160 150 140 130 120 110 100 90 80 70 60 50 40 30 20 ppm

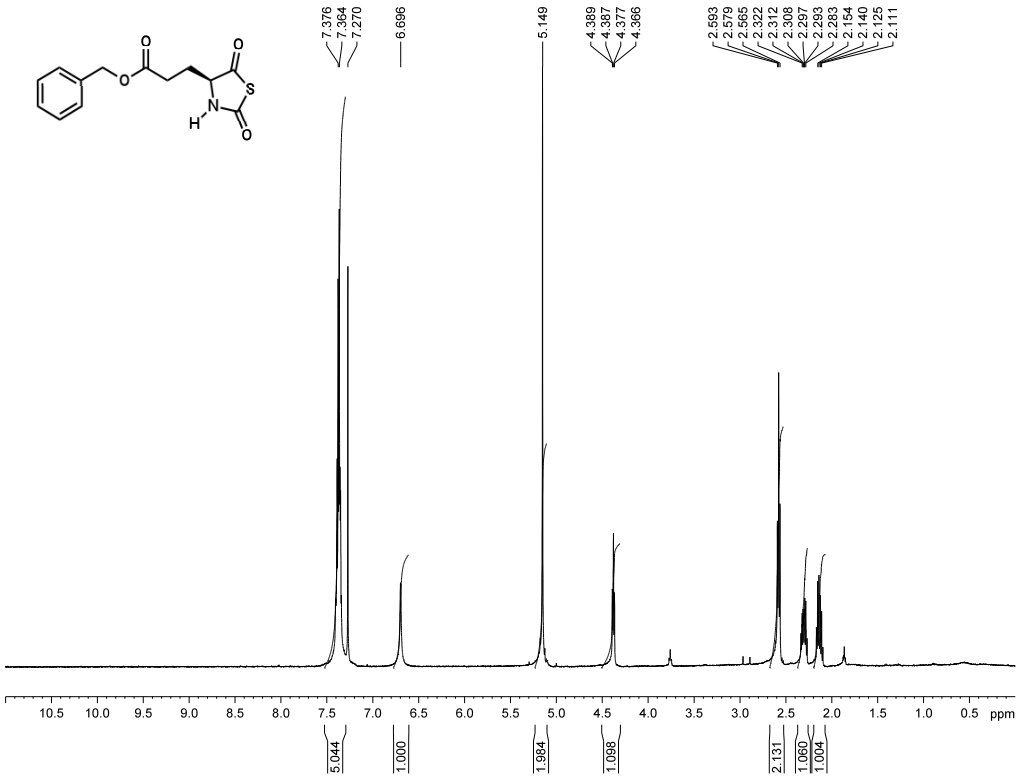
7.376
7.364
7.270
6.696
5.149
4.389
4.387
4.377
4.366
2.593
2.579
2.565
2.322
2.312
2.308
2.297
2.293
2.283
2.154
2.140
2.125
2.111
O
O
O
O
S
N
H
10.5 10.0 9.5 9.0 8.5 8.0 7.5 7.0 6.5 6.0 5.5 5.0 4.5 4.0 3.5 3.0 2.5 2.0 1.5 1.0 0.5 ppm
5.044
1.000
1.984
1.098
2.131
1.060
1.004

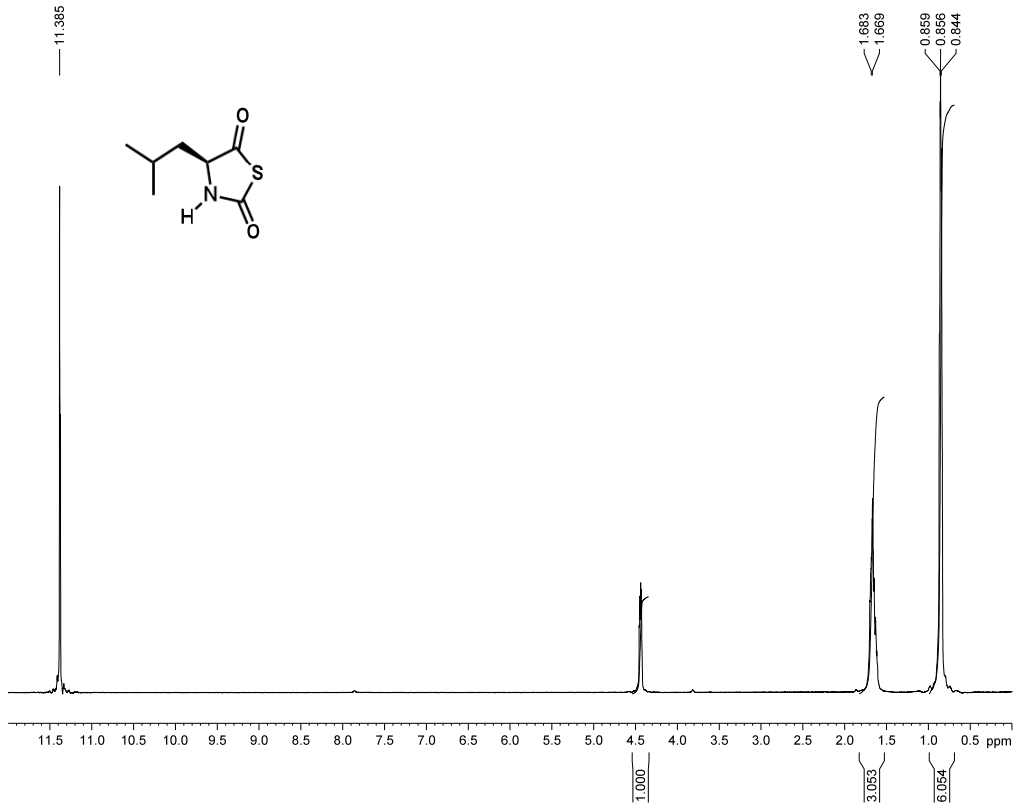
11.385
1.683
1.669
0.859
0.856
0.844
O
O
S
N
H
11.5 11.0 10.5 10.0 9.5 9.0 8.5 8.0 7.5 7.0 6.5 6.0 5.5 5.0 4.5 4.0 3.5 3.0 2.5 2.0 1.5 1.0 0.5 ppm
1.000
3.053
6.054

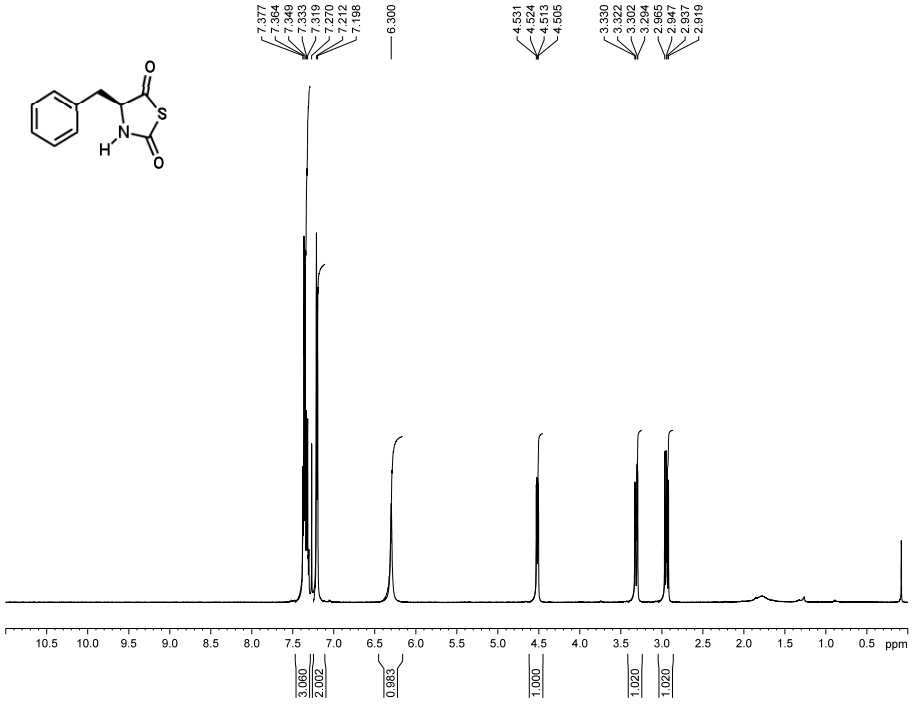
7.377
7.364
7.349
7.333
7.319
7.270
7.212
7.198
6.300
4.531
4.524
4.513
4.505
3.330
3.322
3.302
3.294
2.965
2.947
2.937
2.919
O
S
N
H
O
10.5 10.0 9.5 9.0 8.5 8.0 7.5 7.0 6.5 6.0 5.5 5.0 4.5 4.0 3.5 3.0 2.5 2.0 1.5 1.0 0.5 ppm
3.060
2.002
0.983
1.000
1.020
1.020

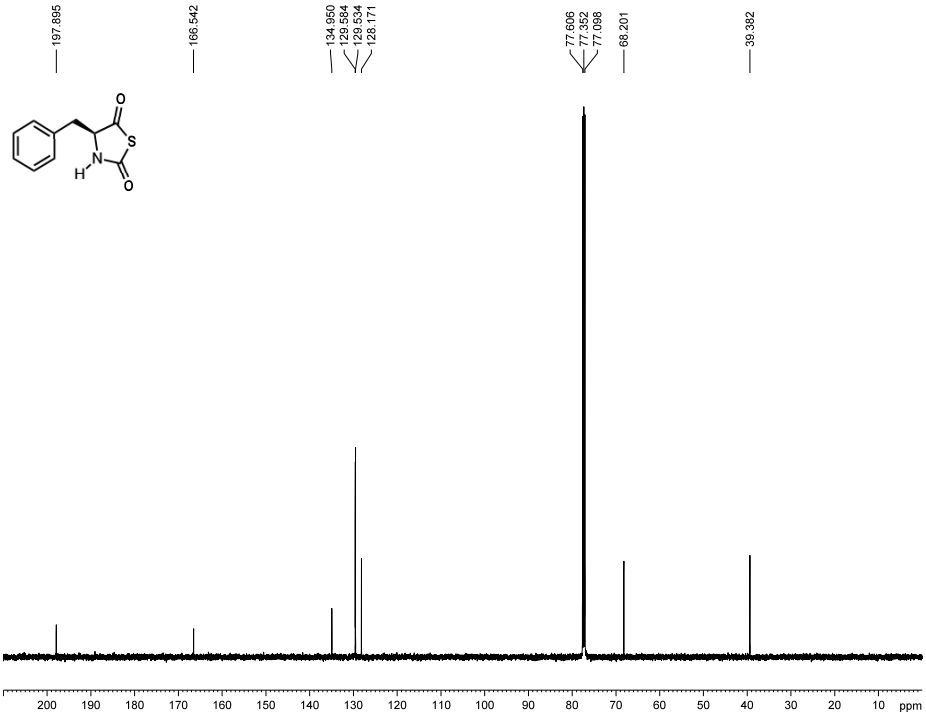
197.895
166.542
134.950
129.584
129.534
128.171
77.606
77.352
77.098
68.201
39.382
O
S
N
H
O
200 190 180 170 160 150 140 130 120 110 100 90 80 70 60 50 40 30 20 10 ppm

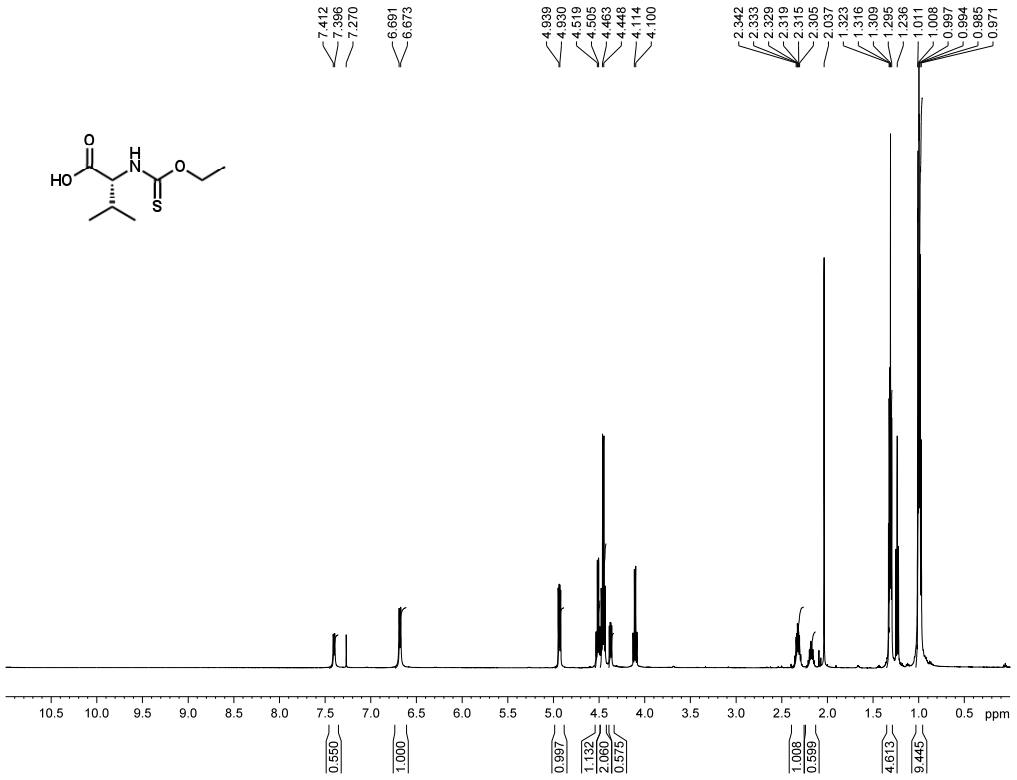
7.412
7.396
7.270
6.691
6.673
4.939
4.930
4.519
4.505
4.463
4.448
4.114
4.100
2.342
2.333
2.329
2.319
2.315
2.305
2.037
1.323
1.316
1.309
1.295
1.236
1.011
1.008
0.997
0.994
0.985
0.971
HO
O
H
N
O
S
10.5 10.0 9.5 9.0 8.5 8.0 7.5 7.0 6.5 6.0 5.5 5.0 4.5 4.0 3.5 3.0 2.5 2.0 1.5 1.0 0.5 ppm
0.550
1.000
0.997
1.132
2.060
0.575
1.008
0.599
4.613
9.445

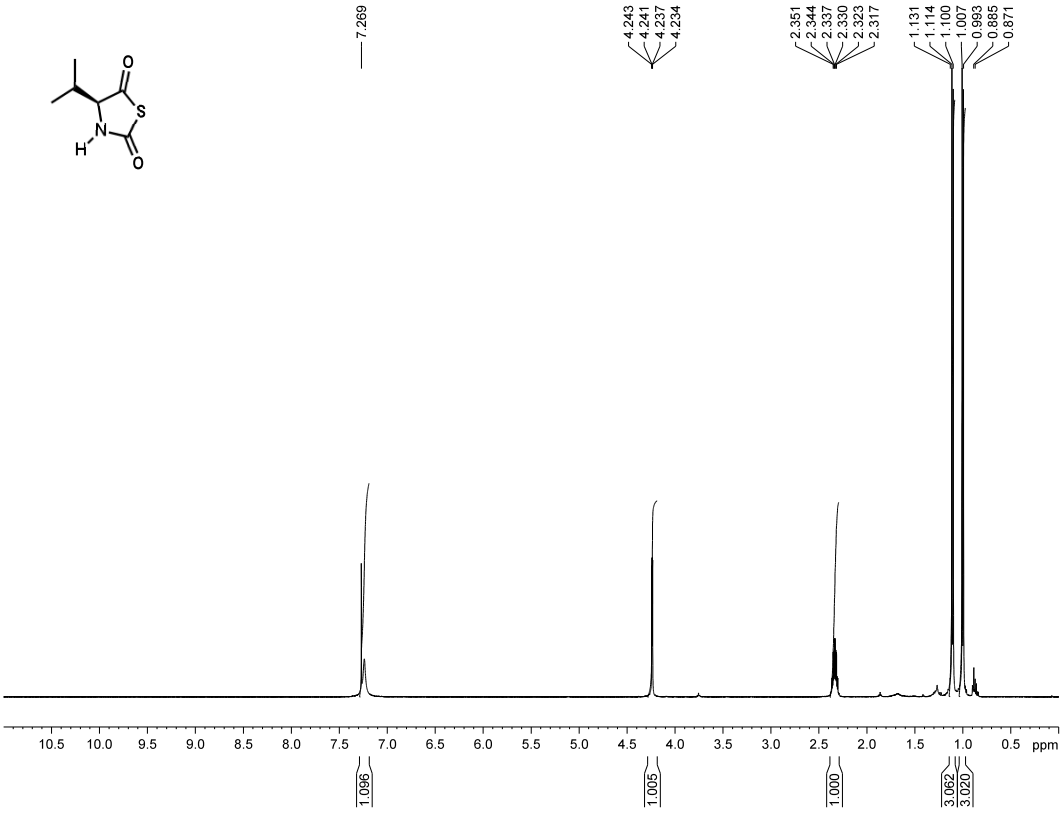
7.269
4.243
4.241
4.237
4.234
2.351
2.344
2.337
2.330
2.323
2.317
1.131
1.114
1.100
1.007
0.993
0.885
0.871
10.5 10.0 9.5 9.0 8.5 8.0 7.5 7.0 6.5 6.0 5.5 5.0 4.5 4.0 3.5 3.0 2.5 2.0 1.5 1.0 0.5 ppm
1.096
1.005
1.000
3.062
3.020

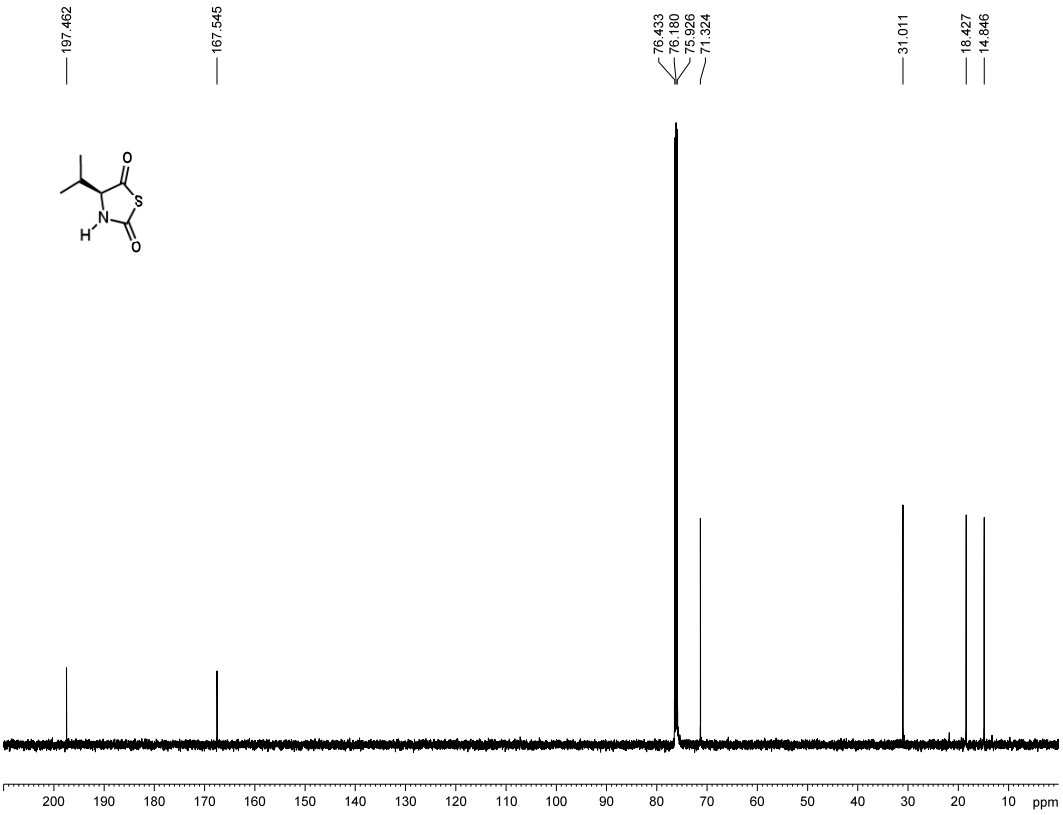
197.462
167.545
76.433
76.180
75.926
71.324
31.011
18.427
14.846
200 190 180 170 160 150 140 130 120 110 100 90 80 70 60 50 40 30 20 10 ppm

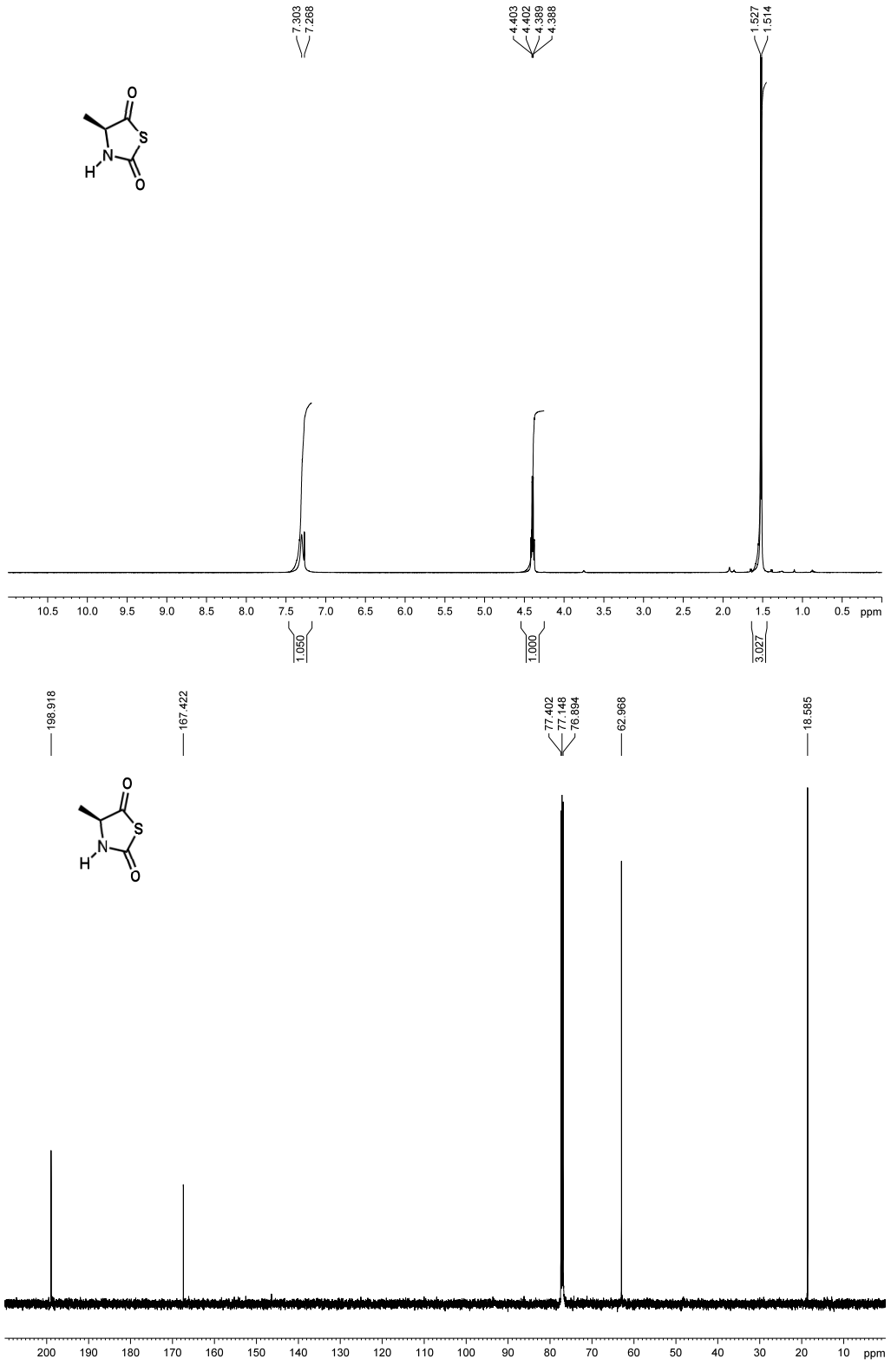
7.303
7.268
4.403
4.402
4.389
4.388
1.527
1.514
O
S
N
H
O
10.5 10.0 9.5 9.0 8.5 8.0 7.5 7.0 6.5 6.0 5.5 5.0 4.5 4.0 3.5 3.0 2.5 2.0 1.5 1.0 0.5 ppm
1.050
1.000
3.027
198.918
167.422
77.402
77.148
76.894
62.968
18.585
200 190 180 170 160 150 140 130 120 110 100 90 80 70 60 50 40 30 20 10 ppm

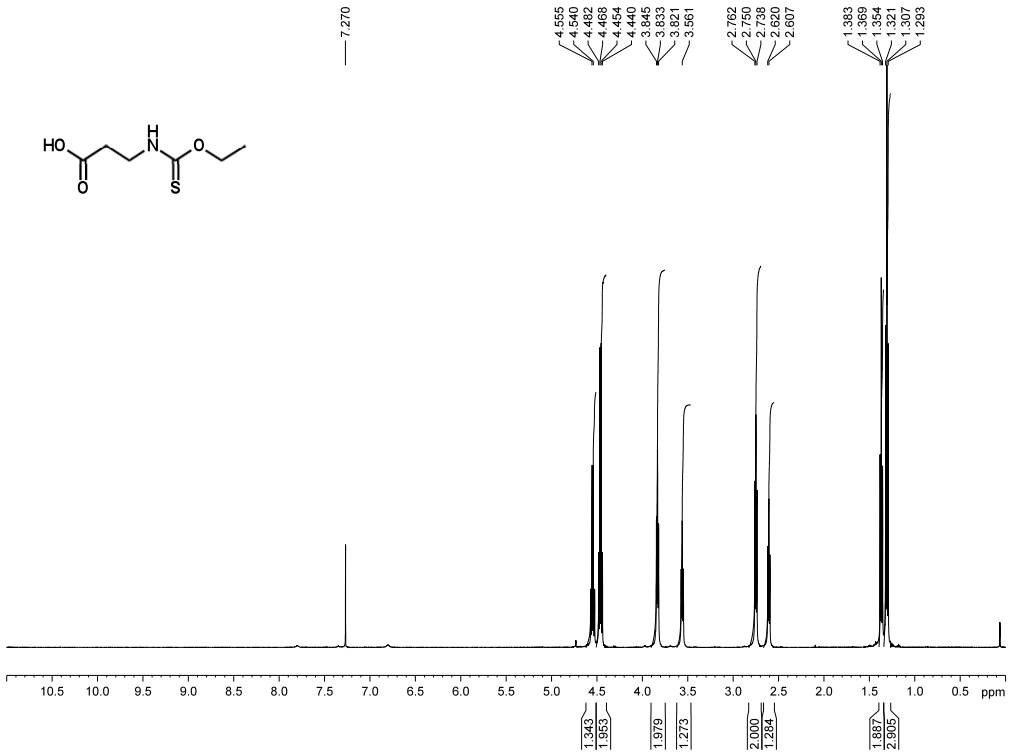
7.270
4.555
4.540
4.482
4.468
4.454
4.440
3.845
3.833
3.821
3.561
2.762
2.750
2.738
2.620
2.607
1.383
1.369
1.354
1.321
1.307
1.293
HO
O
H
N
O
S
10.5 10.0 9.5 9.0 8.5 8.0 7.5 7.0 6.5 6.0 5.5 5.0 4.5 4.0 3.5 3.0 2.5 2.0 1.5 1.0 0.5 ppm
1.343
1.953
1.979
1.273
2.000
1.284
1.887
2.905

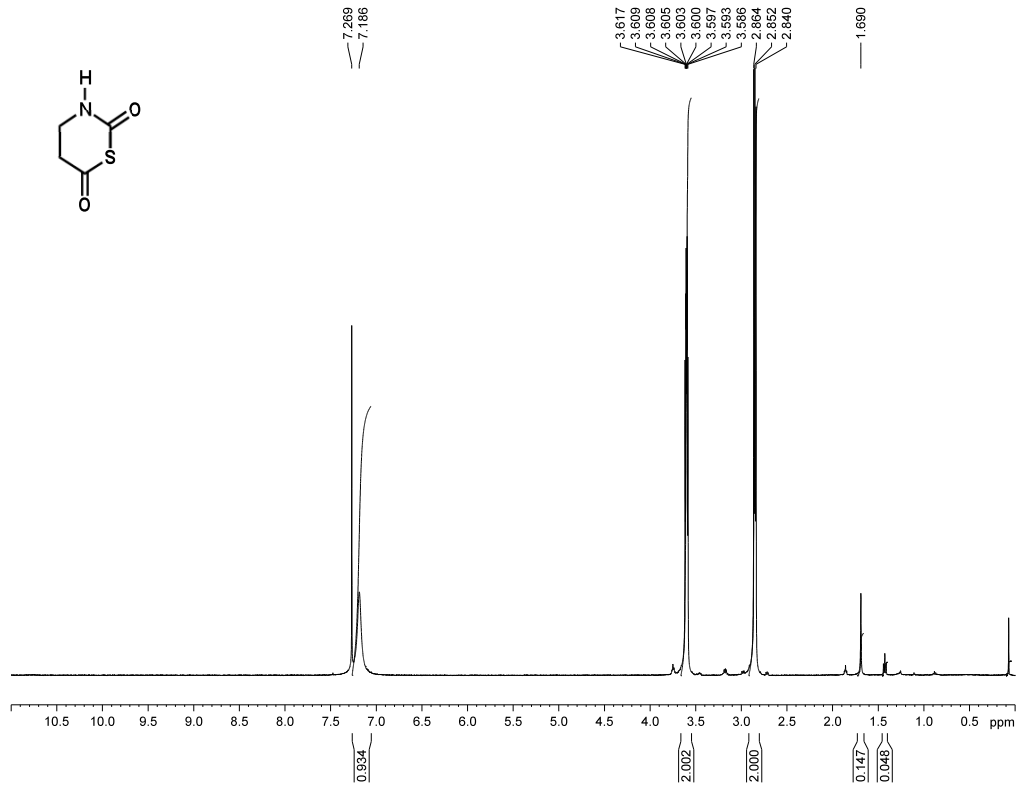
7.269
7.186
3.617
3.609
3.608
3.605
3.603
3.600
3.597
3.593
3.586
2.864
2.852
2.840
1.690
10.5 10.0 9.5 9.0 8.5 8.0 7.5 7.0 6.5 6.0 5.5 5.0 4.5 4.0 3.5 3.0 2.5 2.0 1.5 1.0 0.5 ppm
0.934
2.002
2.000
0.147
0.048

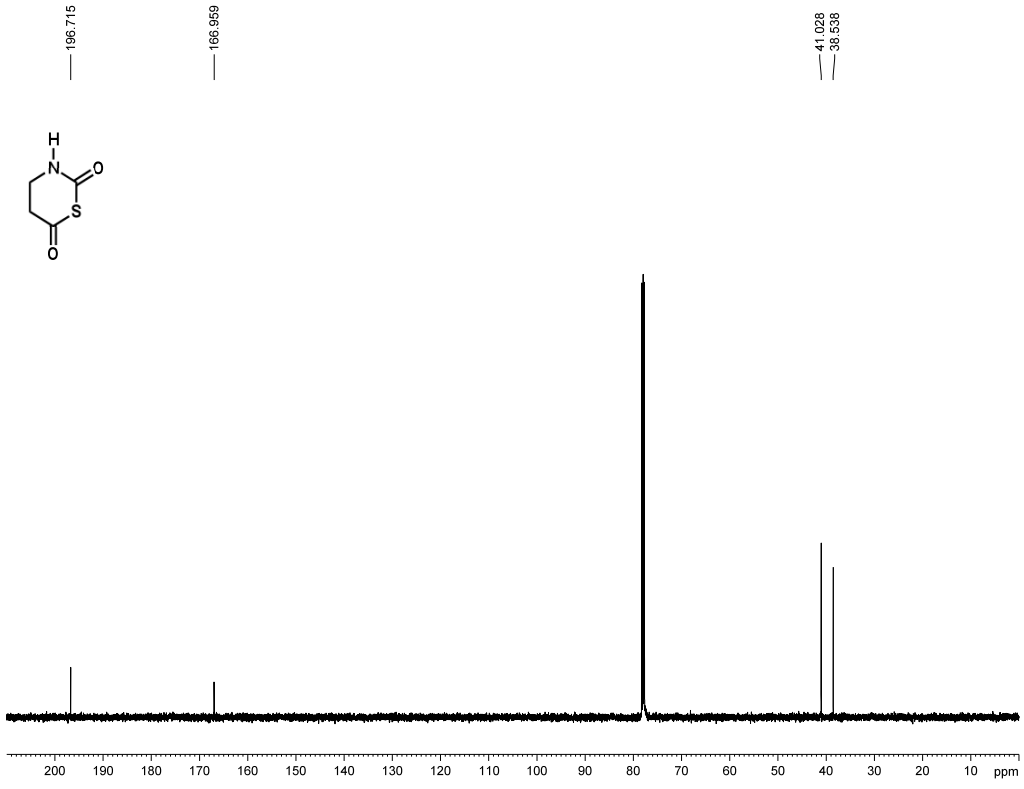
196.715
166.959
41.028
38.538
200 190 180 170 160 150 140 130 120 110 100 90 80 70 60 50 40 30 20 10 ppm

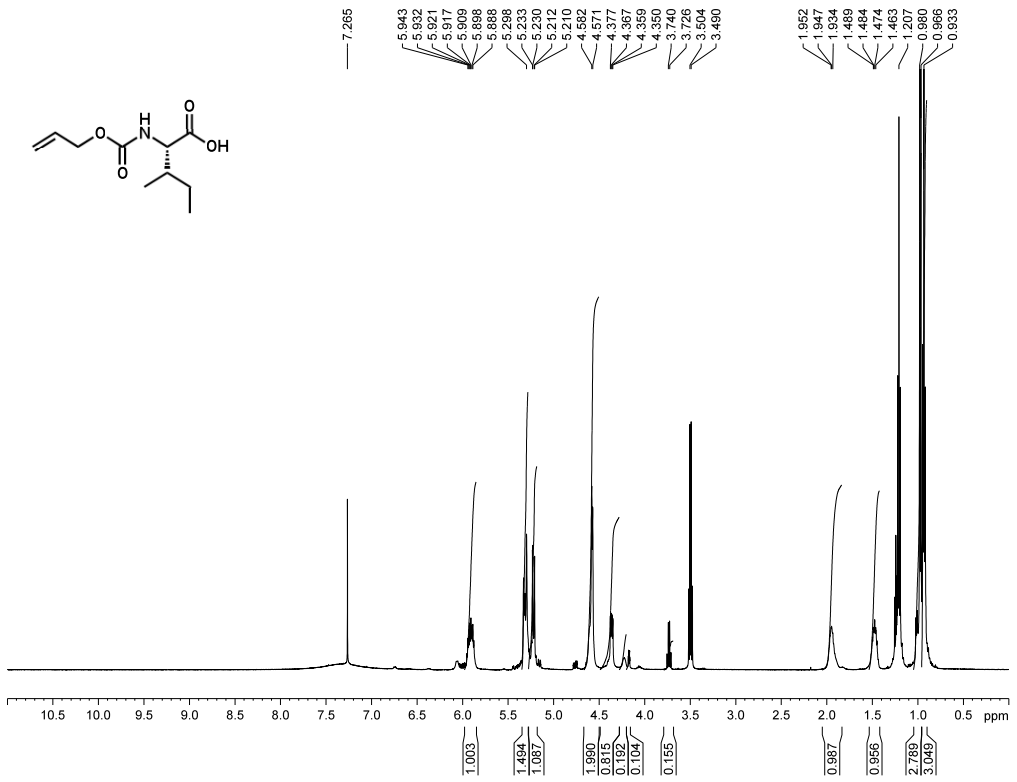
7.265
5.943
5.932
5.921
5.917
5.909
5.898
5.888
5.298
5.233
5.230
5.212
5.210
4.582
4.571
4.377
4.367
4.359
4.350
3.740
3.726
3.504
3.490
1.952
1.947
1.934
1.489
1.484
1.474
1.463
1.207
0.980
0.966
0.933
O
H
N
O
O
O
OH
10.5 10.0 9.5 9.0 8.5 8.0 7.5 7.0 6.5 6.0 5.5 5.0 4.5 4.0 3.5 3.0 2.5 2.0 1.5 1.0 0.5 ppm
1.003
1.494
1.087
1.990
0.815
0.192
0.104
0.155
0.987
0.956
2.789
3.049

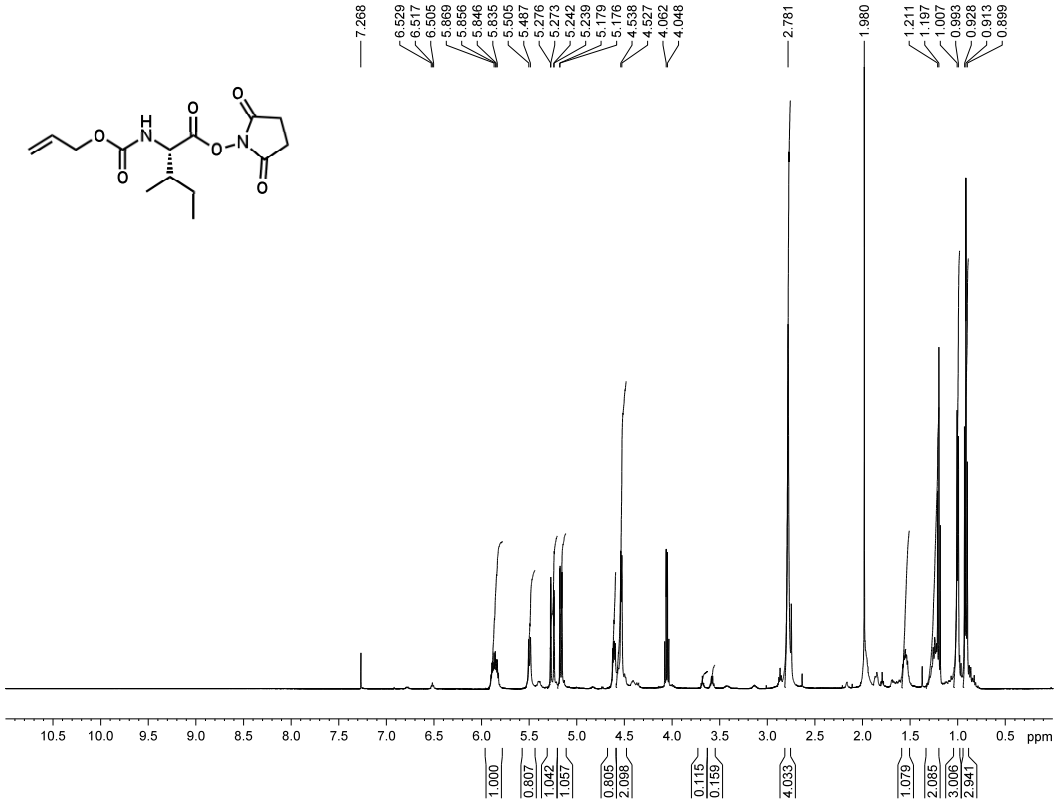
7.268
6.529
6.517
6.505
5.869
5.856
5.846
5.835
5.505
5.487
5.276
5.273
5.242
5.239
5.179
5.176
4.538
4.527
4.062
4.048
2.781
1.980
1.211
1.197
1.007
0.993
0.928
0.913
0.899
10.5 10.0 9.5 9.0 8.5 8.0 7.5 7.0 6.5 6.0 5.5 5.0 4.5 4.0 3.5 3.0 2.5 2.0 1.5 1.0 0.5 ppm
1.000
0.807
1.042
1.057
0.805
2.098
0.115
0.159
4.033
1.079
2.085
3.006
2.941

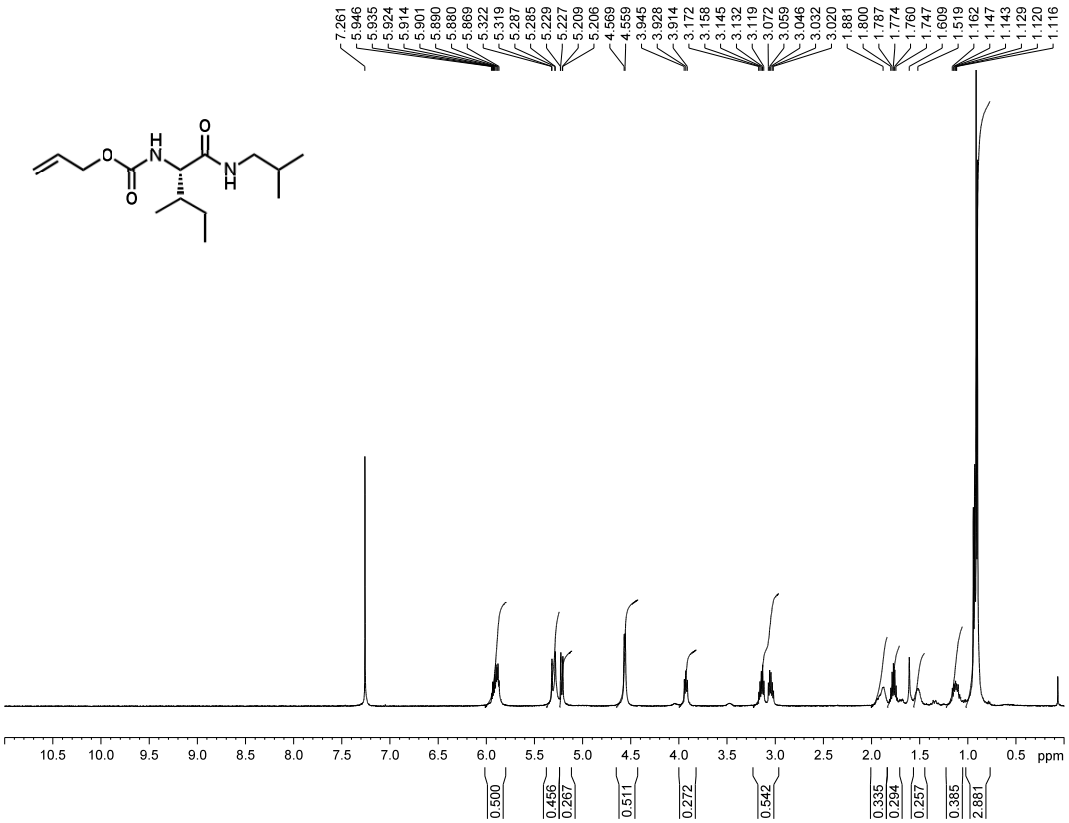
7.261
5.946
5.935
5.924
5.914
5.901
5.890
5.880
5.869
5.322
5.319
5.287
5.285
5.229
5.227
5.209
5.206
4.569
4.559
3.945
3.928
3.914
3.172
3.158
3.145
3.132
3.119
3.072
3.059
3.046
3.032
3.020
1.881
1.800
1.787
1.774
1.760
1.747
1.609
1.519
1.162
1.147
1.143
1.129
1.120
1.116
O
N
H
O
O
N
H
10.5 10.0 9.5 9.0 8.5 8.0 7.5 7.0 6.5 6.0 5.5 5.0 4.5 4.0 3.5 3.0 2.5 2.0 1.5 1.0 0.5 ppm
0.500
0.456
0.267
0.511
0.272
0.542
0.335
0.294
0.257
0.385
2.881

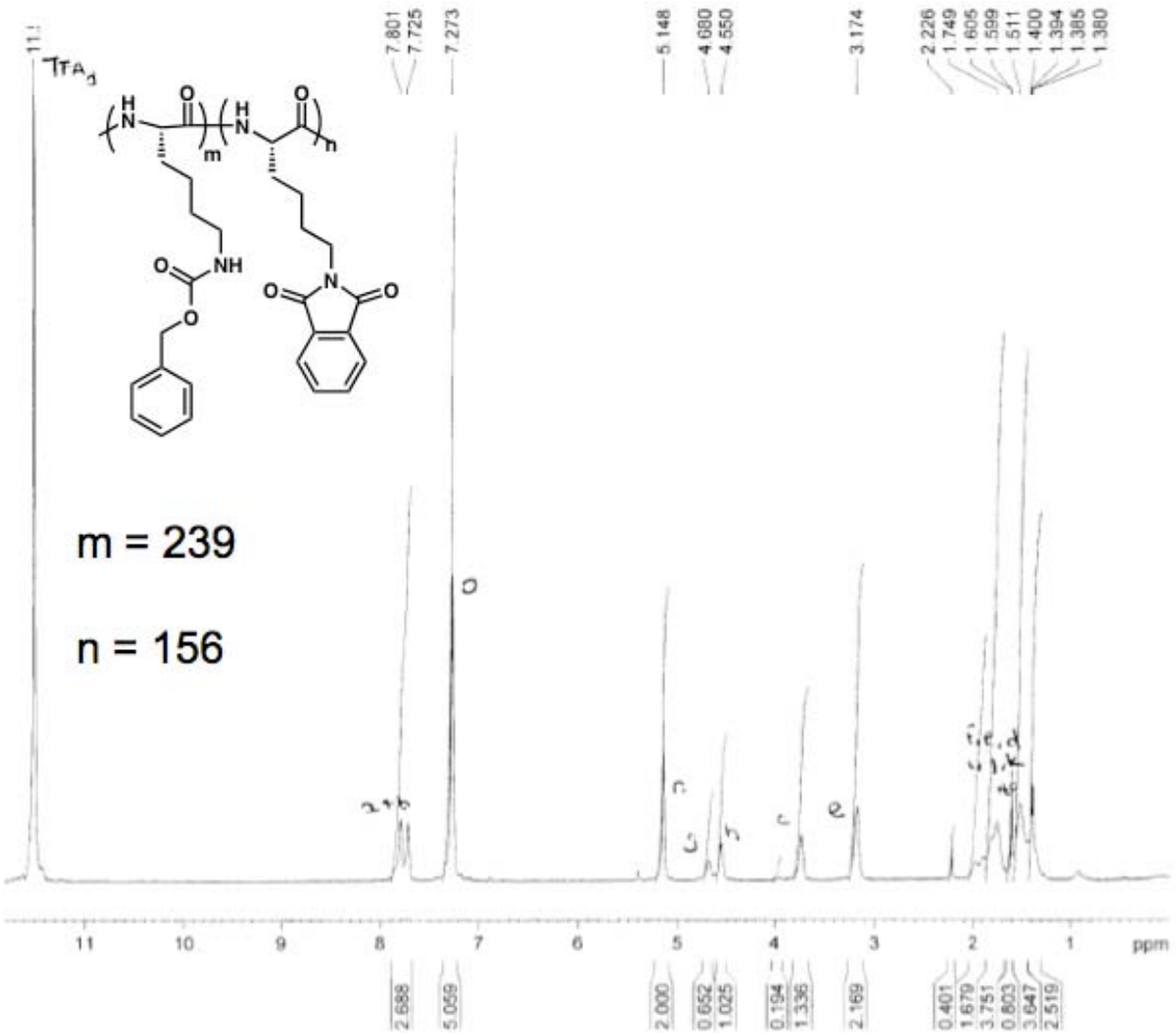
m = 239
n = 156
7.801
7.725
7.273
5.148
4.680
4.550
3.174
2.226
1.749
1.605
1.599
1.511
1.400
1.394
1.385
1.380
ppm
2.688
5.059
2.000
0.652
1.025
0.194
1.336
2.169
0.401
1.679
3.751
0.803
3.647
2.519

References

(1) Bodansky, M. *Peptide Chemistry: A Practical Textbook*, 1993.

(2) Smith, B. L.; Schaffer, T. E.; Viani, M.; Thompson, J. B.; Frederick, N. A.; Kindt, J.; Belcher, A.; Stucky, G. D.; Morse, D. E.; Hansma, P. K. *Nature* **1999**, *399,* 761-763.

(3) Vollrath, F.; Porter, D. *Soft Matter* **2006**, *2,* 377-385.

(4) Daamen, W. F.; Veerkamp, J. H.; van Hest, J. C. M.; van Kuppevelt, T. H. *Biomaterials* **2007**, *28*, 4378-4398.

(5) Merrifield, R. B. *J Am Chem Soc* **1963**, *85*, 2149-2155.

(6) Bayer, E. *Angew. Chem. Int. Ed.* **1991**, *30,* 113-129.

(7) Doel, M. T.; Eaton, M.; Cook, E. A.; Lewis, H.; Patel, T.; Carey, N. H. *Nucleic Acids Research* **1980**, *8*, 4575-4592.

(8) Dawson, P. E.; Muir, T. W.; Clarklewis, I.; Kent, S. B. H. *Science* **1994**, *266*, 776-779.

(9) Kricheldorf, H. R. *Angew. Chem. Int. Ed.* **2006**, *45,* 5752-5784.

(10) Merrifield. R. *Advances in Enzymology and Related Areas of Molecular Biology* **1969**, *32*, 21-29.

(11) Fruchtel, J. S.; Jung, G. *Angew. Chem. Int. Ed.* **1996**, *35*, 17-42.

(12) Lam, K. S.; Lebl, M.; Krchnak, V. *Chem. Rev.* **1997**, *97*, 411-448.

(13) Houghten, R. A.; Pinilla, C.; Blondelle, S. E.; Appel, J. R.; Dooley, C. T.; Cuervo, J. H. *Nature* **1991**, *354*, 84-86.

(14) Guillier, F.; Orain, D.; Bradley, M. *Chem. Rev.* **2000**, *100*, 2091-2157.

(15) Fields, G. B.; Noble, R. L. *International Journal of Peptide and Protein Research* **1990**, *35,* 161-214.

(16) Bayer, E.; Jung, G.; Hagenmai, H. *Tetrahedron* **1968**, *24,* 4853-4858.

(17) Sano, S.; Kurihara, M. *Hoppe-Seylers Zeitschrift Fur Physiologische Chemie* **1969**, *350*,1183-1189.

(18) Sharp, J. J.; Robinson, A. B.; Kamen, M. D. *J Am Chem Soc* **1973**, *95*, 6097-6108.

(19) Dawson, P. E.; Kent, S. B. H. *Annual Review of Biochemistry* **2000**, *69*, 923-960.

(20) Kopecek, J. *European Journal of Pharmaceutical Sciences* **2003**, *20*, 1-16.

(21) Smith, M. *Angew. Chem. Int. Ed.***1994**, *33*, 1214-1221.

(22) Yan, L. Z.; Dawson, P. E. *J Am Chem Soc* **2001**, *123*, 526-533.

(23) Canne, L. E.; Botti, P.; Simon, R. J.; Chen, Y. J.; Dennis, E. A.; Kent, S. B. H. *J Am Chem Soc* **1999**, *121*, 8720-8727.

(24) Dawson, P. E.; Churchill, M. J.; Ghadiri, M. R.; Kent, S. B. H. *J Am Chem Soc* **1997**, *119*, 4325-4329.

(25) Holowka, E. P.; Pochan, D. J.; Deming, T. J. *J Am Chem Soc* **2005**, *127*, 12423-12427.

(26) Hanson, J. A.; Chang, C. B.; Graves, S. M.; Li, Z.; Mason, T. G.; Deming, T. J. *Nature* **2008**, *455*, 85-88.

(27) Nowak, A. P.; Breedveld, V.; Pakstis, L.; Ozbas, B.; Pine, D. J.; Pochan, D.; Deming, T. J. *Nature* **2002**, *417*, 424-428.

(28) Breedveld, V.; Nowak, A. P.; Sato, J.; Deming, T. J.; Pine, D. J. *Macromolecules* **2004**, *37*, 3943-3953.

(29) Pochan, D. J.; Pakstis, L.; Ozbas, B.; Nowak, A. P.; Deming, T. J. *Macromolecules* **2002**, *35*, 5358-5360;.

(30) Deming, T. J. *Journal of Polymer Science Part a-Polymer Chemistry* **2000**, *38*, 3011-3018.

(31) Curtius, T. *Journal Fur Praktische Chemie-Leipzig* **1930**, *125*, 211-218.

(32) Curtius, T.; Sieber, W. *Berichte Der Deutschen Chemischen Gesellschaft* **1921**, *54*, 1430-1437.

(33) Curtius, T.; Sieber, W. *Berichte Der Deutschen Chemischen Gesellschaft* **1922**, *55*, 1543-1558.

(34) Wessely, F.; Riedl, K.; Tuppy, H. *Monatshefte Fur Chemie* **1950**, *81*, 861-872.

(35) Wessely, F.; Swoboda, W. *Monatshefte Fur Chemie* **1951**, *82*, 621-627.

(36) Deming, T. J. *Nature* **1997**, *390*, 386-389.

(37) Deming, T. J. *Prog Polym Sci* **2007**, *32*, 858-875.

(38) Deming, T. J. *Macromolecules* **1999**, *32*, 4500-4502.

(39) Goodwin, A. A.; Bu, X. H.; Deming, T. J. *Journal of Organometallic Chemistry* **1999**, *589*, 111-114.

(40) Deming, T. J.; Curtin, S. A. *J Am Chem Soc* **2000**, *122*, 5710-5717.

(41) Deming, T. J. *Abstr Pap Am Chem.* **2005**, *229*, 972.

(42) Deming, T. J. *J Am Chem Soc* **1998**, *120*, 4240-4241.

(43) Duncan, R. *Nature Reviews Drug Discovery* **2003**, *2*, 347-360.

(44) Duncan, R. *Nature Reviews Cancer* **2006**, *6*, 688-701.

(45) Orive, G.; Pedraz, J.; D., E. *Nature Reviews: Neuroscience* **2009**, *10*, 682-692.

(46) Volt, B. I.; Lederer, A. *Chem. Rev.* **2009**, *109*, 5924-5973.

(47) Sheiko, S. S. *Prog. Polym. Sci.* **2008**, *33*, 759-785.

(48) Fox, M. E.; Szoka, F. C.; Frechet, J. M. J. *Accounts Chem. Res.* **2009**, *42*, 1141-1151.

(49) Frechet, J. M. J.; Dy, E. E.; Szoka, F. C. *Natl. A. Sci. USA* **2006**, *103*, 16649-16654.

(50) Iyer, A. K.; Khaled, G.; Fang, J.; Maeda, H. *Drug Discovery Today* **2006**, *11*, 812-818.

(51) Seymour, L. W. *Critical Reviews in Therapeutic Drug Carrier Systems* **1992**, *9*, 135-187.

(52) Danhier, F.; Feron, O.; Preat, V. *Journal of Controlled Release* **2010**, *148*, 135-146.

(53) Deming, T. J. *Advanced Materials* **1997**, *9*, 299-311.

(54) Rodriguez, A. R.; Choe, U.-J.; Kamei, D. T.; Deming, T. J. *Macromolecular Bioscience* **2012**, *12*, 805-811.

(55) Sun, V. Z.; Li, Z.; Deming, T. J.; Kamei, D. T. *Biomacromolecules* **2011**, *12*, 10-13.

(56) Song, B.; Song, J.; Zhang, S.; Anderson, M. A.; Ao, Y.; Yang, C.-Y.; Deming, T. J.; Sofroniew, M. V. *Biomaterials* **2012**, *33*, 9105-9116.

(57) Yang, C. Y.; Song, B. B.; Ao, Y.; Nowak, A. P.; Abelowitz, R. B.; Korsak, R. A.; Havton, L. A.; Deming, T. J.; Sofroniew, M. V. *Biomaterials* **2009**, *30*, 2881-2898.

(58) Nowak, A. P.; Breedveld, V.; Pine, D. J.; Deming, T. J. *J Am Chem Soc* **2003**, *125*, 15666-15670.

(59) Hanson, J. A.; Deming, T. J. *Polymer Chemistry* **2011**, *2*, 1473-1475.

(60) Kramer, J. R.; Deming, T. J. *J Am Chem Soc* **2010**, *132*, 15068-15071.

(61) Duncan, R.; Izzo, L. *Advanced Drug Delivery Reviews* **2005**, *57,* 2215-2237.

(62) Crespo, L.; Sanclimens, G.; Pons, M.; Giralt, E.; Royo, M.; Albericio, F. *Chem. Rev.* **2005**, *105*, 1663-1681.

(63) Lu, H.; Wang, J.; Lin, Y.; Cheng, J. *J Am Chem Soc* **2009**, *131*, 13582-13586.

(64) Wang, J.; Lu, H.; Kamat, R.; Pingali, S. V.; Urban, V. S.; Cheng, J.; Lin, Y. *J Am Chem Soc* **2011**, *133*, 12906-12909.

(65) Tekade, R. K.; Kumar, P. V.; Jain, N. K. *Chem. Rev.* **2009**, *109*, 49-87.

(66) Lee, C. C.; Gillies, E. R.; Fox, M. E.; Guillaudeu, S. J.; Frechet, J. M. J.; Dy, E. E.; Szoka, F. C. *Proceedings of the National Academy of Sciences of the United States of America* **2006**, *103*, 16649-16654.

(67) Kim, Y.; Zeng, F. W.; Zimmerman, S. C. *Chemistry-a European Journal* **1999**, *5*, 2133-2138.

(68) Ruoslahti, E.; Yamaguchi, Y. *Cell* **1991**, *64*, 867-869.

(69) Bernfield, M.; Gotte, M.; Park, P. W.; Reizes, O.; Fitzgerald, M. L.; Lincecum, J.; Zako, M. *Annual Review of Biochemistry* **1999**, *68*, 729-777.

(70) Mow, V. C.; Ratcliffe, A.; Poole, A. R. *Biomaterials* **1992**, *13*, 67-97.

(71) Engler, A. C.; Lee, H.-i.; Hammond, P. T. *Angew. Chem. Int. Ed.* **2009**, *48*, 9334-9338.

(72) Lu, H.; Cheng, J. J. *J Am Chem Soc* **2008**, *130*, 12562-12564.

(73) Sela, M. *Advance Immunol* **1966**, *5*, 29-129.

(74) Niederhafner, P.; Sebestik, J.; Jezek, J. *Journal of Peptide Science* **2005**, *11*, 757-788.

(75) Lubbert, A.; Nguyen, T. Q.; Sun, F.; Sheiko, S. S.; Klok, H. A. *Macromolecules* **2005**, *38*,2064-2071.

(76) Vlasov, G. P. *Russ. J. Bioorg. Chem.* **2006**, *32*, 227-242.

(77) Hartwig, S.; Nguyen, M. M.; Hecht, S. *Polymer Chemistry* **2010**, *1*, 69-71.

(78) North, M.; Birchall, A. C. *Chem. Comm.* **1998**, 1335-1336.

(79) Klok, H. A.; Rodriguez-Hernandez, J. *Macromolecules* **2002**, *35*, 8718-8723.

(80) Rodriguez-Hernandez, J.; Gatti, M.; Klok, H. A. *Biomacromolecules* **2003**, *4*, 249-258.

(81) Tsogas, I.; Theodossiou, T.; Sideratou, Z.; Paleos, C. M.; Collet, H.; Rossi, J. C.; Romestand, B.; Cornmeyras, A. *Biomacromolecules* **2007**, *8,3263-3270.*

(82) Vlasov, G. P.; Tarasenk, I. I.; Valueva, S. V.; Kipper, A. I.; Tarabukina, E. B.; Filippov, A. P.; Avdeeva, E. V.; Vorob'ev, V. I. *Polym. Sci. Ser. A* **2005**, *475*, 731-739.

(83) Kim, K. T.; Park, C.; Kim, C.; Winnik, M. A.; Manners, I. *Chem. Comm.* **2006**, 1372-1374.

(84) Kim, K. T.; Winnik, M. A.; Manners, I. *Soft Matter* **2006**, *2*, 657-665.

(85) Wang, J.; Lu, H.; Kamat, R.; Pingali, S. V.; Urban, V. S.; Cheng, J. J.; Lin, Y. *J Am Chem Soc* **2011**, *133*, 12906-12909.

(86) Zhang, B.; Fischer, K.; Schmidt, M. *Macromolecular Chemistry and Physics* **2005**, *206*, 157-162.

(87) Breitenkamp, R. B.; Emrick, T. *Biomacromolecules* **2008**, *94*, 2495-2500.

(88) Engler, A. C.; Lee, H.-i.; Hammond, P. T. *Angew. Chem. Int. Ed.* **2009**, *48*, 9334-9338.

(89) Liu, Y.; Chen, P.; Li, Z. *Macromolecular Rapid Communications* **2012**, *33*, 287-295.

(90) Curtin, S. A.; Deming, T. J. *J Am Chem Soc* **1999**, *121*, 7427-7428.

(91) Yu, M.; Nowak, A. P.; Deming, T. J.; Pochan, D. J. *J Am Chem Soc* **1999**, *121*, 12210-12211.

(92) Schaefer, K. E.; Keller, P.; Deming, T. J. *Macromolecules* **2006**, *39*, 19-22.

(93) Lawson, W. B.; Witkop, B.; Gross, E.; Foltz, C. M. *J Am Chem Soc* **1961**, *83*, 1509-1515.

(94) Kramer, J. R.; Deming, T. J. *Biomacromolecules* **2010**, *11*, 3668-3672.

(95) Brzezinska, K. R.; Curtin, S. A.; Deming, T. J. *Macromolecules* **2002**, *35*, 2970-2976.

(96) Yu, M.; Nowak, A. P.; Deming, T. J.; Pochan, D. J. *J Am Chem Soc* **1999**, *121*, 12210-12211.

(97) Pangborn, A. B. G., M.A.; Grubbs, R. H.; Rosen, R.K.; Timmers, F. J. *Organometallics* **1996**, *15*, 1518-1520.

(98) Bianco, A.; Zabel, C.; Walden, P.; Jung, G. *Journal of Peptide Science* **1998**, *4*, 471-478.

(99) Kolb, H. C.; Finn, M. G.; Sharpless, K. B. *Angew. Chem. Int. Ed.* **2001**, *40*, 2004-2010.

(100) Kolb, H. C.; Sharpless, K. B. *Drug Discovery Today* **2003**, *8*, 1128-1137.

(101) Barner-Kowollik, C.; Du Prez, F. E.; Espeel, P.; Hawker, C. J.; Junkers, T.; Schlaad, H.; Van Camp, W. *Angew. Chem. Int. Ed.* **2011**, *50*, 60-62.

(102) Moses, J. E.; Moorhouse, A. D. *Chemical Society Reviews* **2007**, *36*, 1249-1262.

(103) Wu, P.; Feldman, A. K.; Nugent, A. K.; Hawker, C. J.; Scheel, A.; Voit, B.; Pyun, J.; Frechet, J. M. J.; Sharpless, K. B.; Fokin, V. V. *Angew. Chem. Int. Ed.* **2004**, *43*, 3928-3932.

(104) Wu, P.; Malkoch, M.; Hunt, J. N.; Vestberg, R.; Kaltgrad, E.; Finn, M. G.; Fokin, V. V.; Sharpless, K. B.; Hawker, C. J. *Chem. Comm.* **2005**, 5775-5777.

(105) Binder, W. H.; Sachsenhofer, R. *Macromolecular Rapid Communications* **2007**, *28*, 15-54.

(106) Iha, R. K.; Wooley, K. L.; Nystrom, A. M.; Burke, D. J.; Kade, M. J.; Hawker, C. J. *Chem. Rev.* **2009**, *109*, 5620-5686.

(107) Agard, N. J.; Prescher, J. A.; Bertozzi, C. R. *J Am Chem Soc* **2004**, *126*, 15046-15047.

(108) Kiick, K. L.; Saxon, E.; Tirrell, D. A.; Bertozzi, C. R. *Proceedings of the National Academy of Sciences of the United States of America* **2002**, *99*, 19-24.

(109) Bonduelle, C.; Huang, J.; Ibarboure, E.; Heise, A.; Lecommandoux, S. *Chem. Comm.* **2012**, *48*, 8353-8355.

(110) Hansen, M. B.; van Gurp, T. H. M.; van Hest, J. C. M.; Lowik, D. W. P. M. *Org. Lett.* **2012**, *14*, 2330-2333.

(111) Rijkers, D. T. S.; van Vugt, H. H. R.; Jacobs, H. J. F.; Liskamp, R. M. J. *Tetrahedron Letters* **2002**, *43*, 3657-3660.

(112) Tornoe, C. W.; Christensen, C.; Meldal, M. *J. of Org. Chem.* **2002**, *67*, 3057-3064.

(113) Goddard-Borger, E. D.; Stick, R. V. *Org. Lett.* **2011**, *13*, 2514-2514.

(114) Goddard-Borger, E. D.; Stick, R. V. *Org. Lett.* **2007**, *9*, 3797-3800.

(115) Rhodes, A. J.; Deming, T. J. *J Am Chem Soc* **2012**, *134*, 19463-19467.

(116) Kramer, J. R.; Deming, T. J. *Biomacromolecules* **2010**, *11*, 3668-3672.

(117) Gung, B. W.; Fox, R. M. *Tetrahedron* **2004**, *60*, 9405-9415.

(118) Pertici, F.; Pieters, R. J. *Chem. Comm.* **2012**, *48*, 4008-4010.

(119) Aubert, P.; Knott, E. B. *Nature* **1950**, *166*, 4233-4234.

(120) Kricheldorf, H. R. S., M.; Schwarz, G. *Journal of Macromolecular Science, Part A: Pure and Applied Chemistry* **2008**, *45*, 425-430.

(121) Bradbury, J. H.; Leeder, J. D. *Textile Research Journal* **1960**, 118-127.

(122) Kricheld.Hr *Makromolekulare Chemie-Macromolecular Chemistry and Physics* **1974**, *175*, 3325-3342.

(123) Kricheldorf, H. R. B., K. *Makromol. Chem.* **1976**, *177*, 1243-1258.

(124) Wunsch, E. *Angew. Chem. Int. Ed.* **1971**, *10*, 786-790.

(125) Barany, G.; Fulpius, B. W.; King, T. P. *J. Org. Chem.* **1977**, *43*, 2930-2932.

(126) Barany, G.; Schroll, A. L.; Mott, A. W.; Halsrud, D. A. *J. Org. Chem.* **1983**, *48*, 4750-4761.

(127) Poelert, M. A.; Zard, S. Z. *Synlett* **1995**, 325-326.

(128) Forbes, J.; Zard, S. Z. *Tetrahedron* **1993**, *49*, 8257-8266.

(129) Forbes, J. E.; Zard, S. Z. *Tetrahedron Letters* **1989**, *30*, 4367-4370.

(130) Jones, M. H.; Woodcock, J. T. *Analytica Chimica Acta* **1987**, *193*, 41-50.

(131) Woodward, R. B. S., C.H. *J Am Chem Soc* **1947**, *69*, 1551-1552.

(132) Pratt, R. C.; Lohmeijer, B. G.; Hedrick, J. L. *Chem. Rev.* **2007**, *107*, 5813-5840.

(133) Lu, H.; Cheng, J. J. *J Am Chem Soc* **2007**, *129*, 14114-14118.

(134) Seidel, S. W.; Deming, T. J. *Macromolecules* **2003**, *36*, 969-972.

(135) Cotton, F. *Advanced Inorganic Chemistry*, 1988; Vol. 5.

(136) Pandey, L. *Coordination Chemistry Review* **1995**, *140*, 37-114.

(137) Ponnusamy, E. F., U. ; Spisni, A.; Fiat, D. *Synthesis* **1986**, *1986*, 48-49.